2013-04-29

Oxidative Dehydrogenation of Alkanes by O2 and H2S

Premji, Zahra

UNIVERSITY OF CALGARY

Oxidative Dehydrogenation of Alkanes by O_2 and H_2S

by

Zahra Premji

A THESIS

SUBMITTED TO THE FACULTY OF GRADUATE STUDIES

IN PARTIAL FULFILMENT OF THE REQUIREMENTS FOR THE

DEGREE OF DOCTOR OF PHILOSOPHY

DEPARTMENT OF CHEMISTRY

CALGARY, ALBERTA

APRIL, 2013

Abstract

Propylene and other light olefins are an important class of compounds in the petrochemical industry. Currently, the majority of the world's propylene production comes from the cracking of hydrocarbons, where propylene is a co-product of the process. With increasing demand for propylene, interest in developing on-demand processes geared specifically towards propylene production has increased. Oxidative dehydrogenation is a process that has the potential to overcome many of the limitations of catalytic dehydrogenation.

The objective of this work is to study the reaction between propane, butane or mixtures of the two alkanes with O_2 and H_2S to produce propylene with high selectivity and conversion and to obtain an understanding of all aspects of the process. The experiments were carried out using various feeds containing either N_2/HC, N_2/HC/O_2, N_2/HC/H_2S, N_2/HC/O_2/H_2S (Where HC = C_3H_8 or C_4H_{10}) through a tubular reactor at 5-200 ms residence/contact times in the 823-1023 K temperature range. Analysis of the gases was carried out by gas chromatography.

The addition of ~ 5% H_2S to a stream of C_3H_8 (~61% N_2/36% C_3H_8) caused an increase in the conversion of C_3H_8 at 1023 K at a contact time of 35 ms. An increase in C_3H_6 selectivity by 7% and a decrease in C_2H_4 selectivity by 6% were also observed. The overall yield of C_3H_6 more than doubled. Addition of a catalyst enhanced the conversion of C_3H_8 and selectivity to C_3H_6 at 923 K; however, conversions at this temperature range were too low to be of industrial use. At 1023 K, thermal contributions took over and the results obtained were very similar to those obtained for the gas-phase reaction.

Addition of H_2S to the reaction between C_3H_8 and O_2 caused a significant enhancement in the selectivity towards C_3H_6 and a decreased selectivity towards C_2H_4. The presence of

propylene suggested that this reaction was not operating in a thermodynamic regime, as propylene is a partial oxidation product and in a purely thermodynamic regime, solid carbon or carbon oxides would be the most favored carbon products.

Finally, the effect of H_2S on the reactions between C_4H_{10} and O_2 was studied in the gas-phase and over a vanadium catalyst, respectively. Surprisingly, the results showed a significant enhancement in the selectivity to C_3H_6 in the presence of H_2S. In addition, increased conversion of C_4H_{10} was also observed due to the addition of H_2S to the reactant feed gas, and combined with the enhanced selectivity to C_3H_6, it resulted in an increased yield of C_4-C_3 olefins.

The reaction between C_3-C_4 alkanes, O_2 and H_2S has the potential to overcome some of the limitations of ODH by O_2 alone, as reduced selectivity to carbon oxides, increased conversion level of the alkane and improved selectivity to propylene were observed. The gas-phase reactions involving H_2S were observed to be efficient at higher temperatures hence removing the need for the vanadia catalyst from this system. Since all reactant gases are readily available at a Claus plant, this research opens the door to the idea of a small-scale on-demand process for propylene production using cheap raw materials that are already available on-site.

Acknowledgements

This work would not have been possible without the assistance and support of many individuals. In particular, there are a certain few that I would like to recognize by name:

Dr Peter D. Clark, my supervisor, for support and encouragement throughout my graduate degree. Without his unconditional guidance and direction, I would not have been able to achieve my goals.

Dr Norm Dowling and Dr Minming Huang, who sat through many discussions and shared their knowledge and experience regarding experimental design as well as analysis of the results obtained.

Dr John Lo, who carried out the theoretical calculations reported in this thesis and for taking the time to discuss both, theoretical and experimental results, in an effort to understand the mechanistic aspects of this work.

Kevin Lesage, who helped me with all my instrumentation needs and troubleshooting, especially with the GC instrument.

Dr Josephine Hill and her group, for allowing me access to surface area analysis for my catalysts, when our instrument was unavailable.

Bonnie King and other staff at the Chemistry office for their assistance throughout the years.

All other staff at Alberta Sulphur Research Ltd for helping me throughout the process, and welcoming me into their group.

Alberta Sulphur Research Ltd. for funding this project.

And finally, I would like to thank my sweetheart, Karim Lalani, for being the better half during the stressful times and for the endless support, encouragement and love.

I would like to dedicate this thesis to my parents,

Mr Anwar Premji and Mrs Zarina Premji

Table of Contents

List of Tables

List of Figures

List of Symbols

atm	atmospheres
cm	centimeter
K	temperature, Kelvin
EDX	energy dispersive X-ray spectroscopy
GC	Gas Chromatography
BET	Brunauer-Emmett-Teller
mm	millimeters
mL	millilitres
ms	milliseconds
s	seconds
OD	Outer Diameter
ODH	Oxidative Dehydrogenation
PFPD	Pulse Flame Photometric Detector
TCD	Thermal Conductivity Detector
F_{total}	Total Flow
t_c	contact time
t_r	residence time

Chapter 1: Introduction and Literature Review

1.0. General Introduction

Unsaturated hydrocarbons, such as ethylene and propylene, are an important class of feedstocks used in the manufacturing of chemicals and polymers. Specifically, propylene is used in the large-scale manufacture of polypropylene, acrylonitrile and propylene oxide. Polypropylene is a plastic used to make a wide variety of products while acrylonitrile and propylene oxide are monomers used to make other plastics.

The majority of the world's propylene is produced via cracking of hydrocarbons, which includes steam and catalytic cracking.[1] A small amount of the propylene supply also comes from propane dehydrogenation and metathesis. The thermal cracking of alkanes results in methane, ethylene, propylene and other higher olefins. Steam cracking of alkanes is a highly efficient way of producing ethylene with the highest yields being obtained when ethane is used as a feedstock. However, very little propylene is produced when ethane is used. Moreover, the growth in supply of propylene from catalytic cracking is unable to keep up with its continually growing demand hence producers are interested in developing technologies that produce propylene specifically.[2]

Dehydrogenation reactions can also be used to produce olefins from alkane feedstocks however the simple dehydrogenation reaction has many limitations that prevents it from being used extensively. These limitations include side reactions, thermodynamic limitations on selectivity and conversion, its endothermic nature necessitating high energy supply and coke formation resulting in catalyst deactivation.[3] A modification that overcomes many of these limitations is oxidative dehydrogenation (ODH) in which an oxidant is added to the reaction

mixture.[3-5] The significant advantages of ODH are its exothermic nature and the limited amount of coke formed in the process.[6-7] However, the olefin product is more reactive than the feed alkane, hence obtaining good conversions while maintaining reasonable selectivities has been a major obstacle in the development of this method. Many different catalysts have been investigated and were found to be active for ODH, but none have shown product yields that can compare to those obtained by the current industrial methods used for the production of olefins. The development of a suitable catalyst for the production of propylene from propane is still an ongoing topic of interest within the research community.

1.1 Current Industrial Technologies

Much of the world's propylene is produced via cracking of hydrocarbons, specifically by fluid catalytic cracking (FCC) of gas oils in refineries and steam cracking of small alkanes.[1] Cracking product slates and yields depend on the feedstock used. The final yields of propylene from steam cracking of ethane and propane is 2.8% and 16.8% by weight after recycling of the feedstock. If propane is used as the feedstock, a once-through conversion of 90% leads to a molar yield of ethylene and propylene of 45% and 16% respectively. However, a once-through conversion of 75% leads to a slightly higher molar yield of propylene at 26%. As with ODH, higher conversions lead to lower selectivities of propylene.[8]

As shown by the product distributions given above, propylene produced via steam cracking is a co-product. Despite additional cracker capacity, the increase in propylene supply is not enough to satisfy the increased demand of the material. The additional cracker capacity built for ethylene production is insufficient to meet the demand for propylene because these units are usually based on an ethane feedstock, which produce very little propylene. This issue forces

producers to meet the demand for propylene through on-purpose propylene production. On-purpose propylene production is more expensive than co-product propylene production (steam cracking and FCC in refineries), however, high prices of propylene due to the increased demand in the recent years has prompted investment in other technologies for on-purpose propylene production. These developed methods include propane dehydrogenation, metathesis, cracking of higher olefins into propylene, methanol-to-olefin and high severity fluid catalytic cracking (or deep catalytic cracking).[2] Some of these technologies such as metathesis (Total, in Port Arthur, TX) are already in use, however; producers are more likely to invest in cheaper catalyst units that can increase production quickly.

There has been a considerable amount of research effort towards developing a cheaper, more efficient method for the production of propylene using abundant feedstocks. One of the more successful (currently used) methods is the catalytic dehydrogenation of propane.[1] Some of the developed processes based on catalytic dehydrogenation include the Oleflex process developed by UOP, the steam active reforming process of Phillips which uses a supported noble metal catalyst with multiple metal promoters and the Catofin process designed by Air Products which uses a chromium oxide supported alumina catalyst.[9-11]

1.2 Oxidative Dehydrogenation – General Introduction

Thermal steam-promoted dehydrogenation is a process where heat is applied to a hydrocarbon mixture to cause a reaction in which olefins, hydrogen gas and other products such as carbonaceous materials are produced. The process proceeds via a radical mechanism which is outlined in more detail within the next section. Oxidative dehydrogenation refers to a process where an oxidant is added to the reaction feed of a thermal dehydrogenation unit thereby

initiating the reaction via an oxidant rather than the application of high temperatures alone. The presence of an oxidant in the reaction mixture lowers the activation energy of the reaction and results in a relatively high adiabatic temperature (> 973 K).

Compared to a dehydrogenation reaction where H_2 is the co-product, oxidative dehydrogenation using oxygen produces water, which inhibits coke build up. Molecular oxygen is the usual oxidant used due to its low cost and low environmental impact but other oxidants such as halogens, sulfur-compounds and other reagents may be used for this purpose.[6] However, ODH also has several problems associated with it. The most significant challenge with ODH is in controlling further oxidation or steam reforming of olefins to CO and CO_2. There are also other issues with the reaction such as removal of reaction heat, flammability issues brought about by the presence of O_2 and the possibility of reaction runaway.[12] The problem of consecutive oxidation of the olefin can be overcome by development of a catalyst that selectively activates the alkane C-H bond, however, this is easier said than done. Research on developing such a catalyst has met with little success.

Despite the continued interest and research on ODH of light alkanes, only a few industrial processes have been developed. For example, ODH has been developed for ethylene production by Union Carbide (the Ethoxene process[13]) for combined production of ethylene and acetic acid of ~90%. This method has also been applied to the conversion of n-butane to maleic anhydride.[14] Currently, there is no industrial process for the production of propylene by ODH of propane.

The main reason that this method has not been used for the industrial production of propylene is that low selectivities and conversions have been obtained in the laboratory research

conducted to date. As mentioned previously, one of the key reasons for low selectivity is the further oxidation of the olefin produced to form carbon dioxide. Since the formation of carbon oxides is thermodynamically favored, oxidation to carbon oxides is a major competing pathway, influenced to a greater or lesser degree by the reaction conditions.

1.2.1 ODH in the Gas Phase (Homogenous)

In order to overcome the general limitations of ODH, a limited amount of oxygen can be added to the feed. Thermal cracking of propane occurs to a limited extent at 700°C[15] but the presence of some oxygen in the feed promotes exothermic oxidative conversion of propane as well as endothermic dehydrogenation. The increase in conversion due to thermal cracking in the presence of oxygen was higher at lower temperatures but the magnitude of the increase was reduced as the temperatures were increased. This effect is attributed to a radical mechanism which is shown below for reactions in both the presence and absence of oxygen.

In the absence of oxygen, the reaction is initiated by a C-C bond scission yielding a methyl and ethyl radical.

[1.1] $C_3H_8 \rightarrow CH_3\cdot + C_2H_5\cdot$

The formation of propyl radicals is not significant until the propagation stage where a radical can attack a second propane molecule forming the propyl radical (n-propyl or isopropyl radicals).

[1.2] $C_3H_8 + C_2H_5\cdot$ (or $CH_3\cdot$ or $H\cdot$) $\rightarrow C_3H_7\cdot + C_2H_6$ (or CH_4 or H_2)

The propyl and ethyl radicals can then undergo thermal decomposition giving the products shown below

[1.3] $C_3H_7\cdot \rightarrow C_2H_4 + CH_3\cdot$

[1.4] $C_3H_7\cdot \rightarrow C_3H_6 + H\cdot$

[1.5] $C_2H_5\cdot \rightarrow C_2H_4 + H\cdot$

These radicals may undergo further propagation reactions and eventually terminate forming a variety of products including H_2, methane, higher alkanes, alkenes and carbonaceous materials (also known as coke)

Alternatively, in the presence of oxygen, the initiation step is expected to be hydrogen abstraction by oxygen forming propyl radicals and this process may occur at lower temperatures than that of the thermal cracking initiation stage.

[1.6] $C_3H_8 + O_2 \rightarrow C_3H_7\cdot + HO_2\cdot$

The propagation stage is similar to that of the thermal cracking method and some of the other possible reactions that form propyl radicals during propagation are shown below.

[1.7] $C_3H_8 + HO_2\cdot \rightarrow C_3H_7\cdot + H_2O_2$

[1.8] $H_2O_2 \rightarrow 2OH\cdot$

[1.9] $C_3H_8 + OH\cdot \rightarrow C_3H_7\cdot + H_2O$

Propyl radicals can also react with oxygen forming propylene as shown below. A similar reaction can occur for ethyl radicals.

[1.10] $C_3H_7\cdot + O_2 \rightarrow C_3H_6 + HO_2\cdot$

[1.11] $C_2H_5\cdot + O_2 \rightarrow C_2H_4 + HO_2\cdot$

Reactions leading to products occur as described for the thermal mechanism. The products formed are also similar however the ratios in which they are formed differ, as the

initiation reaction using oxygen produces much more of the propyl radical. With oxygen, thermal reaction as well as activation by O_2 occurs simultaneously if the temperature of the system is high enough to cause thermal activation. The final products of the reaction will depend on the temperature of the reaction as well as the amount of O_2 used. The enhancement of yield by O_2 at all temperatures is expected because the presence of O_2 causes the formation of propyl radicals which would not otherwise have formed in the absence of oxygen.

ODH has also been investigated using heterogeneous catalysts, and it has been reported that homogenous gas phase reactions contribute to the alkane conversion.[16-17] The homogenous reactions occur in voids and pores within and between catalyst particles. Hence, the particle size of the catalysts used may affect the degree of the contribution from homogenous oxidation processes. In a study done on two series of catalysts, the catalyst with larger particles was suggested to have a higher contribution of gas-phase reactions on the overall reaction rate.[18] It should be noted that the increased gas phase contributions came as an increase in conversion of the alkane but, in this specific study, this contribution did not result in a loss in selectivity towards the alkene. It was, therefore, concluded that although total conversion increased with catalyst particle size, due to increased gas phase reactions, the product distributions were still determined by the properties of the catalyst.

It has been shown that the selectivity towards propylene decreases as the reaction temperature is increased from 773-973 K. Within the same temperature range, propane conversion increased significantly with increased selectivity to ethylene at the higher temperature.[15] It has also been shown that as the feed ratio of propane/oxygen is increased, the selectivity to propylene increases. The contact times, however, need to be increased slightly to make up for the higher alkane/oxidant ratio compared to an oxidant rich reaction.[19] The amount

of CO compared to CO_2 is also higher for gas phase reactions as the homogenous oxidation reaction proceeds via a peroxy-type radical mechanism.[18] In the presence of catalysts, the product distributions change significantly and dehydrogenation and oxidation products become dominant. In this case, CO_2 becomes the predominant carbon oxide. This result was also observed by Nguyen and Kung in their work on propane oxidation.[20] Based on these observations, it was suggested that the presence of any oxide surface, irrespective of the chemical nature of the material, particle size, catalytic activity and ODH selectivity, terminates the free radical processes. In conclusion, the presence of O_2 or steam increased the propylene/ethylene mole ratio in the products. The presence of oxygen allowed the reaction to occur at milder temperatures and over shorter contact times.

1.2.2 Catalyst-aided ODH (Heterogenous)

The oxidative dehydrogenation of propane over various catalysts has been studied extensively. ODH is an irreversible, exothermic process, however, selectivity to olefins is limited because of the consecutive oxidation of the olefins to CO_x. Improving selectivity while maintaining high conversion levels has been the objective of much of the research done on the topic. The majority of the research is concerned with investigating different catalysts, although some researchers have also looked into changing the oxidant from oxygen to other substances such as CO_2, NO_x and sulfur-compounds. It is important to note that ODH of ethane is different from the ODH of higher alkanes and, therefore, the catalysts used and catalytic behavior in the ODH reaction of ethane cannot be applied to the ODH of propane or higher alkanes.[21] Some factors that affect selectivity within the catalytic systems are the reaction conditions such as feed mixture, temperature of the reaction and contact time between the feed gas and the catalyst. The choice of catalyst for a specific ODH reaction is therefore not only specific to the reactant alkane

in question, but also to the specific reaction conditions to which it will be applied. The literature review on the other types of oxidants investigated is detailed in the next section.

1.2.3 Types of Catalysts Used for the ODH of Light Alkanes

Catalysts investigated in the ODH of light alkanes can be broken down into three types:

1) Redox-type catalysts: Based on reducible metal oxides which operate using a heterogeneous redox-type mechanism. Examples would include oxides of vanadium and iron on inert supports where the active species can oxidize a C-H bond of an alkane and be re-oxidized itself by O_2 to return to the active state. In the case of vanadia-based systems, the activity is due to the ability of vanadium to switch between the +III and +V oxidation states easily, as shown in the simple reaction scheme below.[22]

   [1.12] $C_nH_{2n+2} + V^{V}O \rightarrow C_nH_{2n} + H_2O + V^{III}$ [step 1]

   [1.13] $V^{III} + O_2 \rightarrow V^{IV}O_2$ [step 2]

   [1.14] $V^{IV}O_2 + V^{III} \rightarrow 2V^{V}O$ [step 3]

   where, Z and ZO are a reduced and an oxidized site respectively.

2) Other metal oxide catalysts: Based on non-reducible or difficult to reduce (under reaction conditions) metal oxides. These include alkaline earth metal based oxides such as LiO/MgO and they work based on the activation of molecular oxygen. The mechanism of alkene formation on these catalysts consists of initial alkyl radical formation by surface O^- species of the catalyst followed by desorption of the radicals into the gas-phase where further radicals can be generated or alkene can be formed by reaction of the alkyl radical with oxygen.[23]

A simple reaction scheme for the ODH of ethane is shown below where [1.15] is the initiation step by the catalyst to generate the alkyl radical, which can then desorb into the gas phase and react further with other radicals [1.16] or dissociate [1.17] to form a variety of products including alkenes.[24] A more detailed reaction scheme can be found in the literature.[24]

[1.15] $C_2H_6 + [Li^+O^-]_s \rightarrow C_2H_5^{\cdot} + [Li^+OH^-]_s$

[1.16] $C_2H_5^{\cdot} + O_2 \rightarrow C_2H_4 + HO_2^{\cdot}$

[1.17] $C_2H_5^{\cdot} \rightarrow C_2H_4 + H^{\cdot}$

3) Noble-metal catalysts: Based on noble metals which are typically non-selective for oxidation and are mostly used for combustion reactions. An example is Pt/Al_2O_3 which is known to promote the ODH of light alkanes by providing the initial heat for the reaction, by complete combustion of an alkane, which is then followed by gas-phase dehydrogenation of a second alkane molecule.[25-26]

[1.18] Ignition stage: $C_2H_6 + O_2 \rightarrow 2CO + 3H_2 + Heat$

[1.19] Dehydrogenation stage: $Heat + C_2H_6 \rightarrow C_2H_4 + H_2$

The redox-type catalysts will now be reviewed in more detail.

1.2.3.1 Vanadia-based Catalysts

One of the most studied groups of catalysts for the ODH of propane are vanadium oxide containing catalysts supported on a metal oxide. These include VO_x/Al_2O_3 or TiO_2, V-Mg-O catalysts and other mixed catalysts that contain more than one active species such as V-Sb-Sn oxides supported on alumina or silica. A few examples of vanadia systems investigated for the

ODH of light alkanes and some important findings from these investigations are outlined in the next few paragraphs.

V_2O_5 itself is not a good catalyst for the dehydrogenation of alkanes; however, when supported on alumina or sepiolite a more selective catalyst for the ODH of propane is produced.[27-28] The vanadia-alumina (or sepiolite) systems typically result in low yields (8-9%) and low selectivity (40%) but are active at fairly low temperatures (623-673 K). V-Mg-O systems have also been investigated extensively and were previously considered to be the most promising vanadia-containing system for the reaction.[28-34] These V-Mg-O systems promote higher yields (20%) and selectivities (~60%) but there is no agreement in the literature on which specific phase gives the best results.[27-30,33-34] It is possible that other factors such as the presence of small amounts of dopants (alkali metal or magnesium oxides) or particle size may play a part in determining the performance of the V-Mg-O catalytic systems.

SiO_2 supported vanadia materials have been reported to be selective catalysts for the ODH of methanol and short-chain alkanes. Research done by Parmaliana et al. on different doped and undoped, precipitated and fumed silicas showed that the catalyst that gave the highest yield of propylene was 5.0% V_2O_5 supported SiO_2 (precipitated).[35] The experiments were carried out within the 723-848 K range using a C_3H_8: O_2: N_2: He (2: 1: 1:8) reaction mixture. The selectivity towards propylene and overall conversion of propane for the catalyst mentioned above at 798 K was 54.9% and 13.3% respectively. Another catalyst that had notable activity was a 5.7% V_2O_5 supported silica (fumed) which showed selectivity towards propylene and conversion of propane (at 798 K) of 42% and 13.10% respectively. Over the temperature range investigated, the selectivity decreased as the reaction temperature was increased but the alkane conversion increased to a greater degree resulting in an overall higher yield at the higher temperatures.

Studies on catalysts containing varying amounts of vanadium supported on hexagonal mesoporous silica showed that above a certain amount of vanadia, the selectivity towards the olefin decreases.[36] This effect has been attributed to the dispersion of vanadium and, therefore, the specific VO_x species that are found on the surface of the catalyst. It has been suggested that oligomeric VO_x species as well as oxide-like crystallites (similar to bulk V_2O_5) begin to form in catalysts containing a high amount of vanadia. The amount of vanadia above which oligomeric and oxide-like species begin to form varies with the type of support used and the preparation method. Reports in the literature have shown that, in many cases, this amount ranges from ~ 5 - 8 wt. % though some have reported higher amounts.[37-42] The form of the VO_x species which is dependent on the dispersion of vanadia on the support is, therefore, important within this class of catalysts irrespective of the support used. Thus, it is obvious that higher surface area supports can accommodate a greater amount of vanadia before reaching the point at which the oligomeric and oxide-like species begin to form. It is important to avoid the formation of V_2O_5 crystallites as they favor the further oxidation of the olefin and cause a significant reduction in the selectivity to propylene.

As mentioned above, it was generally found that higher selectivities were obtained for low vanadia-loading catalysts, however the higher selectivities came at the cost of lower yield as low V-loading catalysts have fewer active sites.[43] One way this problem was tackled was by using higher surface area silica supports to obtain higher conversions without loss of selectivity. Mobil researchers reported a new family of siliceous meso-structured materials which can be used as catalyst supports for various reactions. Among this new family of solids, MCM-41 is one of the more widely studied materials. MCM-41 possesses a regular hexagonal array of pores and these pores can be easily customized to sizes between 20 and 100 Å. Additionally, atoms other

than silicon can be incorporated into the matrix including vanadium-substituted mesoporous molecular sieves, V-MCM-41 and V-MCM-48 whose catalytic properties are different from those of the parent MCM solid. V-MCM-41 and vanadium oxide supported on MCM-41 have been reported as selective catalysts for ODH of propane and ethane.[43-45] MCM-41 supported vanadia catalysts have shown selectivities to propylene and conversions of propane at 823 K as high as 61.6% and 14.8% resulting in a yield of 9%. It was also found that MCM-41 supported vanadia catalysts had higher specific catalytic activity than V-substituted MCM-41 materials, especially for vanadium contents of higher than 1 wt%.[44]

Recent work done by Bulanek et al, showed that vanadia supported on hexagonal mesoporous silica catalysts differ in their activity based on the preparation method used.[46] Catalysts (in a wide range of V loadings) were synthesized using one of two routes, direct synthesis or wet impregnation method. Characterization showed that the direct synthesis catalysts had predominantly tetrahedrally co-ordinated VO_x complexes including both monomeric and oligomeric VO_x species. The catalysts made using the wet impregnation method had a broader distribution of vanadia species including square pyramidal and octahedral VO_x units. The results from catalytic tests showed that the catalysts made using the direct synthesis method were three times more productive than the comparable catalyst made using the wet impregnation technique. Based on these results, it was concluded that both monomeric and tetrahedrally coordinated polymeric units containing V-O-V bonds were the active sites responsible for the activity and selectivity of the VOx-HMS catalysts for ODH of propane.

Vanadium oxide supported on mesocellulous silica foams (MCF) was also investigated as a catalyst for the ODH of propane.[47] Unlike the mesoporous supports MCM and SBA, which are two dimensional, MCF is a three-dimensional hydrothermally stable material with large

mesopores (up to 50nm).The larger pore sizes of MCF provides it with an advantage over the more ordered MCM or SBA materials as it allows for improved diffusion of reactants and products, therefore allowing better mass transfer. Catalysts of V-MCF of different vanadium content (1.4-5.6 wt %) were prepared and tested for their catalytic behavior in the ODH of propane. The tests were carried out in the 723-923 K temperature range using a feed of propane/oxygen/nitrogen in a 1:1:8 ratio. The maximum yield of 27.9% was obtained by a 4.2V-MCF catalyst at 823 K. The space time yield was calculated for this result and was determined to be 3.77 kg of propylene $kg^{-1}_{cat}h^{-1}$. This yield is above the 1 kg of product $kg^{-1}_{cat}h^{-1}$ value requirement for industrial operations.[48]

1.2.3.2 Molybdenum-based Catalysts

Molybdates supported on various materials are another class of redox catalysts that have been investigated fairly extensively for ODH of light alkanes. Mazzochia et al investigated the ODH of ethane on α-$NiMoO_4$ and β-$NiMoO_4$ catalysts and found that α-$NiMoO_4$ was the more active phase giving a selectivity of approximately 60% at a 10% conversion.[49] Molybdena supported on various oxides (Nb_2O_5, TiO_2, Al_2O_3, SiO_2, MgO, ZrO_2) were found to be less selective than the mixed metal oxides. Among these catalysts, molybdena supported on titania gave the best yield, however the yield was below 8%.[50]

Single and binary molybdates supported on SiO_2, ternary molybdates, and other molybdenum containing catalysts were used in a broad investigation undertaken by Stern and Grasselli.[51] The best results were obtained with $NiMoO_4/SiO_2$ and $Ni_{0.5}Co_{0.5}MoO_4/SiO_4$ which had yields of about 16% at 27% conversion. These authors also determined that addition of other redox elements increased the activity but with a decrease in selectivity (except Cr). Addition of P

did not affect the catalytic activity; however, Bi and alkali metal oxides caused a significant decrease in activity.

Molybdena catalysts have been investigated mostly for the ODH of ethane, however their activity for the ODH of propane has been investigated.[52-55] More recently, mixed Mo-V systems have been tested for the conversion of ethane and propane. In one study, the authors looked at the effect of adding molybdenum oxide to vanadia catalysts supported on either alumina or titania.[56] Their results showed that at shorter contact times, the molybdena modified catalysts were able to convert the same amount of propane implying no decrease in activity. In addition, selectivities towards propylene at similar conversion levels were higher for the molybdena modified catalysts (92% from 88% for addition of molybdenum oxide to vanadia-alumina catalyst and 77% from 71% for addition of molybdenum oxide to vanadia-titania catalyst), resulting in a higher overall yield of propylene.

1.2.4 Other Oxidants as Gas Dopes

In an attempt to overcome the problem of over-oxidation to CO_x, additives or other oxidants have been investigated for the ODH of light alkanes. These materials include carbon dioxide or sulfur species. Carbon dioxide was considered to be an attractive additive to investigate because it is inexpensive and readily available. Also the product of CO_2 reduction would be carbon monoxide which could be used as a feed in other industrial processes. The problem with CO_2 is its low activity thus requiring use of higher temperatures. The ODH of ethane with CO_2 was investigated using ceria-based catalysts and ethylene selectivities of 58-65% were obtained at 953-1023 K.[57]

The oxidative dehydrogenation of propane over various vanadium-based catalysts in the presence of a mixture of O_2 and N_2O was also investigated, resulting in an increase in selectivity by almost 25% at propane conversions in the range of 1-10%.[58] The authors explained the increased selectivity as an effect of the lower catalyst site re-oxidation capabilities of N_2O, compared to O_2, which causes a decrease in the surface density of oxidizing sites. This decrease is deemed beneficial as propane oxidation to propylene only requires one to two lattice oxygens whereas active sites having more than two lattice oxygen species favor the formation of the carbon oxides.

Some work has also been done on the effect of H_2S or other sulfur species on the ODH to light olefins. Previous work has shown the merit of adding H_2S to an un-catalyzed system for the dehydrogenation of propane.[59-60] Preliminary work on the oxidative dehydrogenation of propane using Al_2O_3 and V/Al_2O_3 catalysts in the presence of H_2S at short contact times has shown yields of propylene of 30.4%.[61] Other research on the oxidative dehydrogenation of ethane in the presence of sulfur also showed high yields of ethylene and improved selectivities over what was obtained for other systems.[62]

1.2.5 The Case for Short Contact Time Reactions

Early research on ODH used contact times in the range of a second, but more recently the focus has shifted to reactions in the millisecond range. When short contact times are used, the reactor size can be reduced by 100-1000 times. The small reactor size combined with the exothermic nature of the reaction results in autothermal operation which can reduce costs further. One of the pioneering works on short contact time ODH was done by Huff and Schmidt using platinum-coated monolith catalysts.[63] Ethylene selectivities of up to 70% at ethane conversions

of more than 80% were observed for a Pt-coated monolith catalyst. More recently, reactions in an empty reactor were compared against reactions over a Pt-coated monolith catalyst and it was found that the ignition temperature for the catalytic reaction was much lower (553 K for the catalytic reaction vs 923 K for the empty reactor), but had a higher selectivity to carbon oxides and H_2.[64] In addition, at higher temperatures (above 1023 K), conversion of ethane was the same in the empty reactor as it was over the catalyst. Ethylene yields were also the same between the empty reactor and the monolith catalyst at temperatures in the 1123-1173 K range. From these observations, it was concluded that catalytic reactions led to the production of carbon oxides, hydrogen gas and heat at low temperatures which elevate the reactor temperature, where-as gas-phase reactions play a major role in the production of olefins at higher temperatures. These conclusions are similar to those obtained in some of the initial work carried out over platinum catalysts.

1.3 Homogeneous Contributions to Heterogeneous Catalytic Reactions

Even in a catalytic system, homogeneous reactions can occur in the void spaces between catalyst particles and in some cases, in micro-pores. In work done by Vislovskiy et al. on the ODH of isobutane, a variety of V-Sb oxide based catalysts on alumina support were studied and contact times in the range of a second were used for their work.[15] The results showed that the conversion of the alkane increased as the particle size of the catalysts used increased. It was suggested that if the reaction proceeded via a radical mechanism where the initially formed radical can undergo further transformations in both the gas-phase and on the catalytic surface, then having larger gaps between particles increases the gas-phase contributions of the observed overall rate. It was also shown that at the operating conditions used, the gas phase reactions in an empty reactor gave a yield of 14.4% which was higher than the yields obtained on some of the

catalysts tested, showing that the gas-phase reactions work well. These results, therefore, bring out two important points. Firstly, there can be a significant gas-phase contribution to the overall rate depending on the particle and pore size of the catalyst used, thus making separation of homogeneous and heterogeneous contributions difficult. Secondly, this observation suggests that addition of a homogeneous component could be beneficial to the overall rate of the reaction. The latter point has already been researched by Nguyen and Kung who showed that higher yields can be obtained by adding a post-catalyst homogeneous reaction zone after the catalyst.[20]

1.4 The ODH of n-Butane

Production of butenes via ODH of butane is considered to be a favorable alternative to the current method for the production of butenes, if a suitable catalyst for the reaction can be found. There are four butenes: 1-butene, cis-2-butene, trans-2-butene and isobutene. Like propylene, butenes are also a co-product of cracking processes in petroleum refineries (steam cracking and fluid catalytic cracking), which is the biggest source of butenes worldwide. Other minor sources of butenes include processes such as catatlytic dehydrogenation and ethylene oligomerization.[65]

The majority of the butenes produced are used in the production of gasoline, either in alkylate production or directly as a gasoline blendstock. Less than 15% of all butenes are used for specific chemical production.[65] In alkylate production, a mixture of olefins are reacted with isobutane over an acid catalyst to produce highly branched paraffins that have high anti-knock properties.[66] Strong acids such as HF and H_2SO_4 have been used to catalyze the process. In recent years however, 70% of processes use H_2SO_4 as their catalyst and when using this catalyst, 2-butenes are considered superior in the feed compared to 1-butene. Isobutene and 2-butenes are

considered to be more valuable as they produce higher quality products during alkylation. Isobutene is also used in the production of methyl tert-butyl ether (MTBE), which is an additive used to increase the octane number of fuels, as well as other chemicals such as methyl methacrylate and methacrylic acid.[66] 1-Butene, while not as effective for alkylate production via the sulphuric acid process, has its use as a co-monomer in the production of linear low density polyethylene and for modifying high density polyethylene.[65]

The catalytic dehydrogenation of C_4 alkanes was developed industrially as a means of producing various butenes. Four of the main processes used to date include:

1. The Oleflex process which uses a platinum - alumina catalyst and operates at higher severity than the Pacol process from which it is derived.[10-11, 67] The more severe conditions were applied to reduce coke formation and decrease skeletal isomerization which results in isobutylene.

2. The Phillips STAR dehydrogenation process which also uses a noble metal catalyst.[68-69]

3. The FBD-4 (Snamprogetti) fluidized bed process employs a promoted chromium oxide catalyst and users of this process are located mostly in the former Soviet Union.[70]

4. The Catofin process which is based on the Houdry Catadiene technology (used to produce 1,3-butadiene from butane), also employs a chromium oxide-alumina catalyst at 773-948 K in vacuo to achieve high conversions of butane to produce isobutene.[71-73]

Despite decades of research on the ODH of butane to form butenes, no industrial processes incorporate the ODH of n-butane to butenes. The reason for this situation is that, as with propane, low selectivities at high conversions lead to low overall yields for the C_4 olefins. The ODH of n-butane and iso-butane has also been investigated using vanadia-based catalysts.

Sulikowski et al studied the ODH of isobutane on MCM-41 catalysts.[74] They studied the catalytic properties of [Si, V]-MCM-41 samples with differing vanadium content with pure [Si]-MCM-41 material being used as a reference. The ODH of isobutane using a helium: isobutane: oxygen feed (82:12:6) was investigated in the 673-873 K temperature range. They found that the reference sample was the least selective. The highest conversion of 36% at 873 K was found for the sample of [Si, V]-MCM-41 that had the higher amount of V. The selectivities, as expected, decreased with increasing conversion levels. At the highest conversion level, the selectivity to isobutene was only 25%. In the case of the butenes, equimolar amounts of the cis and trans-2 butenes were formed on the vanadium containing catalysts whereas an increased amount of the trans-isomer was found when an aluminum containing catalyst was used.

Mesoporous SBA-15 generated by Zhao et al[75] was shown to possess a structure which was more regular and had thicker channel walls than those of MCM-41. Liu et al[39] used this catalyst in tests carried out with a feed gas containing n-butane, oxygen and nitrogen in a 4:8:88 ratio with a flow rate of 100mL/min. The 8.96V-SiO_2 (containing 8.96 weight % V content) catalyst showed a conversion of 47.8% with selectivity to C_4-olefins of 15.6%. In comparison, the 8.96V-SBA-15 (containing 8.96 weight % V content) catalyst gave a conversion level of 54.8% with a selectivity to C_4-olefins of 27.3% resulting in a yield of 15%.

Bronsted acid sites are required for both dehydrogenation and total oxidation. A correlation between Bronsted acid sites and propylene formation was observed[76-77] but it was found that production of CO_x requires a Bronsted acid site as well.[78-79] Therefore, the higher the number of acidic sites, the more prone the surface will be to produce CO_x.[80] The greater the acidity of the site, the less likely the olefin is to desorb and more likely it is to undergo further oxidation. Hence, a careful balance between acidic and basic properties is required for optimal

production of propylene. The higher catalytic activity of VO_x/SBA-15 over V_2O_5/MCM-41 for the ODH of butane was therefore attributed to the larger pore size and lower surface acidity of the support material used in the former.[81] In particular, the increased selectivity towards C_4-olefins by the SBA catalysts can be explained by the lower surface acidity of the material. In addition, the larger pore size allows the alkane molecules to easily diffuse to the inside of the pores and gain access to the VO_x active sites.

More recently, a study on vanadia catalysts supported on different mesoporous silicas (HMS, SBA-15, SBA-16 and MCM-48) for the ODH of propane and butane was carried out by Bulanek et al.[82] The influence of texture of the support material on the speciation of vanadium and how this affected ODH activity was studied. Based on TOF values and selectivities of the various catalysts at iso-conversion conditions, it was concluded that both monomeric and oligomeric tetrahedral species were active and selective for ODH of propane. However, unlike propane ODH, the butane ODH reaction was much more sensitive to the type of vanadia species present on the surface of the catalyst. In this case, monomeric units were much more active and selective as evident in the TOF values obtained for this reaction.

1.5 Mechanism and Kinetics

ODH can take two different paths depending on whether the reaction is in the gas phase or on the surface of a catalyst. In addition, the specific mechanism will differ depending on the catalyst. For this reason, discussion will be limited to the catalytic mechanism relevant to vanadia-based catalysts. The mechanism for gas phase ODH of propane is a radical-based mechanism as described in an earlier part of this introduction.

A basic mechanism for the catalytic ODH has been proposed by several authors. There are some differences between the mechanisms proposed, however they have similarities from which a general stepwise mechanism can be deduced. The following are the general steps of the mechanism of the ODH reaction of alkanes.[83]

1. Adsorption or interaction of the alkane with the surface of the catalyst
2. Breakage of the C-H bond leading to the formation of an alkyl species
3. Reaction of the alkyl species with an adjacent surface oxygen and formation of an alkene via β-elimination
4. Re-oxidation/reduction of the catalyst (regeneration step)

A proposed reaction scheme is presented below.[84] Initially, the alkane adsorbs onto a lattice oxygen site (O^*), followed by hydrogen abstraction from an adjacent lattice oxygen site [1.20 and 1.21]. Formation of propene occurs by H^- elimination and production of a second OH group on the surface[1.22]. The OH groups combine to form H_2O and a reduced V center (*)[1.23]. In the final step [1.24], a molecule of O_2 re-oxidizes the reduced V centers via dissociative chemisorption.

[1.20] $C_3H_8 + O^* \rightleftarrows C_3H_8O^*$

[1.21] $C_3H_8O^* + O^* \rightarrow C_3H_7O^* + OH^*$

[1.22] $C_3H_7O^* \rightarrow C_3H_6 + OH^*$

[1.23] $OH^* + OH^* \rightleftarrows H_2O + O^* + {}^*$

[1.24] $O_2 + {}^* + {}^* \rightarrow O^* + O^*$

The above mechanism is not the only possible reaction pathway for alkanes. Further oxidation via an alkoxide species to aldehydes, carboxylates and eventually carbon oxides are competing pathways.[85-86] The formation of carbon oxides limits selectivity to olefins. Inhibition of the total oxidation pathway leading to these products is one of the challenges of alkane ODH chemistry.

There are many factors that can affect the pathway of the reaction and one of these factors is the co-ordination number of the active species. It was found that the co-ordination number of the active vanadium species affected the pathway of the reaction. Results suggested that vanadium co-ordination numbers higher than four favor the formation of partially oxygenated products or carbon oxides.[87]

In addition to the active catalytic species, the support must also be considered carefully as the rate of formation of the olefinic intermediate and olefin desorption is proposed to depend on the acid /base character of the catalyst.[88] Recent work by Putra et al showed that doping V-Mo catalysts with Sr (oxides) enhanced the selectivity towards propylene formation.[89] It was proposed that the presence of Sr(O) increased the surface basicity of the catalyst which facilitated desorption of the product alkene.[90] In catalytic tests, undoped V-Mo catalysts showed the typical trend of decreasing selectivity towards propylene with an increase in conversion, as a result of increasing the reaction temperature or space time velocity. However, the Sr doped catalysts showed no decrease in selectivity when conversion increased on increasing the reaction temperature from 723 to 823 K.

One of the more investigated aspects of the ODH mechanism is the role of lattice oxygen versus that of gaseous oxygen and which of the two is responsible for the initial C-H abstraction.

The role of lattice oxygen in the C-H bond abstraction has been investigated by many with general agreement that C-H bond activation occurs on lattice oxygen[91] and oxygen-containing ODH products are formed by removal of lattice oxygen. The role of gaseous oxygen in this reaction is to re-oxidize the reduced catalyst. Some evidence for these conclusions is given below.

Research conducted by Kondratenko et al using propane and labeled gaseous oxygen species pulsed over a VOx/γ-alumina catalyst showed that carbon oxide products contained unlabeled oxygen.[92] Since the reactants were pulsed, labeled oxygen incorporated into the lattice by re-oxidation did not appear in the products.

Isotopic tracer studies done by Chen et al on VOx/ZrO_2 using labeled gaseous oxygen ($^{18}O_2$) and $V_2{}^{16}O_5$ for the ODH of propane led to preferential formation of ^{16}O in all the initial oxygen containing products.[84] They also concluded that O_2 chemisorption was not reversible since mixed ^{16}O-^{18}O species were not detected when both gaseous $^{16}O_2$ and $^{18}O_2$ were used in the reaction mixture.

Based on their research, the following mechanism was proposed;

[1.25] $C_3H_8 + O^* \rightarrow C_3H_8O^*$ (adsorption of alkane)

[1.26] $C_3H_8O^* + O^* \rightarrow C_3H_7O^* + O^*H$ (H-abstraction by neighboring oxygen)

[1.27] $C_3H_7O^* \rightarrow C_3H_6 + O^*H$ (H^- elimination)

[1.28] $O^*H + O^*H \rightarrow H_2O + O^*$ (formation of H_2O by combination of two surface OH)

[1.29] $O_2 + {}^* + {}^* \rightarrow O^* + O^*$ (re-oxidation of V centers by dissociation of gaseous O_2)

In addition to the mechanisms proposed from experimental results, computational chemistry has also been used to explain and/or verify conclusions from experimental work. In one study, Goddard et al used quantum mechanical calculations to elucidate the chemical mechanism with propane.[93] The proposed mechanism was the same as that suggested by Chen et al.[84] However, they also assumed that hydrogen transfer was facile on the oxide and therefore V^{III}-OH_2/V^{V}=O sites are in equilibrium with V^{IV}-OH/V^{IV}-OH sites. The results of their calculations suggested that re-oxidation could not occur from a V^{IV}-OH site. In addition, water bound to a V^{III} site was too stable to desorb on its own and that binding of gaseous O_2 molecule to a V^{III}-H_2O site decreased the energy for H_2O desorption. In this mechanism, the initial H-abstraction was proposed to be done by the V^{V}=O site with the resulting iso-propyl radical binding to an adjacent V-O-V site.

Vanadium surfaces can have three types of lattice oxygen. The vanadyl oxygen (V=O) and two and three coordinated oxygen which bridge two and three vanadium ions respectively. The role or involvement of each of these oxygen species was a question that many researchers have tried to answer and various studies have generated differing results as discussed below.

Research by Goddard et al (mentioned previously) proposed that the vanadyl oxygen was responsible for the initial H-abstraction.[93] Mori et al also concluded that the vanadyl oxygen must be responsible for the initial H-abstraction.[94] They measured the rate of the reaction, which is known to be dependent on the rate of initial H-abstraction, and found that it was in proportion to the amount of V=O species in the catalyst at any given oxygen concentration. More recently, Gilardoni et al performed a DFT study and also found that V=O was more active.[95]

However, other work has shown that two coordinated oxygen can also be responsible for initial H-abstraction. Eon et al. studied the ODH of propane on γ-alumina supported V_2O_5 using ESR, NMR and Raman spectroscopies and proposed that the bridging oxygen atoms were the active sites for this reaction.[96] Results from DFT studies conducted by Witko et al. also suggested that the H atoms bond preferentially to two coordinated oxygen.[97] Alexopoulos et al. studied propane oxidation over V_2O_5 and V_2O_5/TiO_2, and concluded that although the vanadyl oxygen was proven to be the most active, the bridging oxygen was more selective towards propane dehydrogenation.[98]

One of the more comprehensive DFT studies on the ODH of propane was carried out by Wang et al who focused on the catalytic role of the different surface oxygen species to determine which site is responsible for the initial H-abstraction.[99] Their results showed that the most stable structure was formed by adsorption at the two-coordinated oxygen however they also showed that propane does not form a molecular adsorption state but only physisorbs weakly on the surface of V_2O_5. Further, considering that the reaction occurs at high temperatures (~1073 K) and, since, contributions from gas phase reactions would be significant at such high temperatures, it suggests that C-H bond breaking of propane over the surface of V_2O_5 is not precursor mediated but is a direct dissociation. Following this result, they studied C-H bond breaking mechanisms over the three types of oxygen and concluded that the most favorable mechanism for vanadyl oxygen is hydrogen abstraction from gas phase propane followed by formation of a V^{IV}-OH and a gas phase propyl radical which then adsorbs onto an adjacent oxygen site. However, the reaction barrier for C-H bond activation is only 3.1 kcal/mol less for vanadyl oxygen compared to two coordinated oxygen. Also, the mechanism of C-H bond breaking on a two coordinated oxygen was proposed to be via oxo-insertion where lattice oxygen

inserts into a C-H bond of propane leading to an alcoholic intermediate followed by proton transfer to a nearby lattice oxygen generating a propyl species bonded to lattice oxygen that can then undergo a second hydrogen abstraction to form propylene.

While the general mechanism for the ODH of propane has been generally accepted, the particulars of the mechanism are still under investigation as evidenced by the above discussion.

1.5.1 Kinetics

Many kinetic studies on the rates of the alkane ODH reactions have been carried out. The basic steps for a gas-solid catalyzed reaction are:

1. Diffusion of the reactants towards the surface of the catalyst.
2. Adsorption of the reactants onto the surface.
3. Reaction of the reactants on the surface.
4. Desorption of the products from the surface.
5. Diffusion of the products away from the surface of the catalyst.

It is expected that the rate of each of these steps varies and is dependent on factors other than the concentration or concentration gradients of the different species present.[100] Steps 1 and 5 depend on the flow characteristics of the system such as the mass velocity of the gas stream, diffusional characteristics of the gases, degree of porosity of the catalyst, the dimensions of the pores and their connectivity. Steps 2 and 4 are determined by the rate of adsorption and desorption of the various species on the surface of the catalysts as well as the character and extent of the catalytic surface. Step 3 is dependent on the nature of the catalytic surface and the activation energy of the reaction on that specific catalytic surface. If the rates of the second, third and fourth stages are slower than the diffusional processes then the kinetic equations will be

representative of the chemical reactivity of the system otherwise it will just describe the diffusion process which will not be very helpful in understanding the reaction itself.

The four main models used to describe the kinetics of the ODH of light alkanes are; 1) Eley-Rideal model, 2) Langmuir-Hinshelwood model, 3) Mars Van Krevelen model (the redox model) and 4) power law model. The complete details of these models can be found in the literature but a brief description of each is given below.[100-109]

1. Eley-Rideal model

This model assumes that one reactant adsorbs on the surface of the catalyst and reacts with a second molecule from the gas phase.[101-102] This is represented as follows:

[1.30] $A_g \leftrightarrow A_{ads}$

[1.31] $A_{ads} + B_g \rightarrow C_{ads} \rightarrow C_g$

Application of Langmuir assumptions for the adsorption of A and assuming a rapid desorption or low coverage of byproducts, the reaction rate is expressed as:

[1.32] $r = (kK_{PA\ PB}) / (1 + K_{PA})$

2. Langmuir-Hinshelwood model

This model assumes that two different reactants will adsorb on the surface of the catalyst and will react at the surface. This mechanism is based on the initial reasoning that chemisorbed molecules remain on the surface of the catalyst for a longer time than molecules in close contact during collision in the homogenous phase and, therefore, the probability of attaining the required activation energy is higher on the surface of a catalyst than for homogenous phase reactions.[110] The model is represented as follows;

[1.33] $A_g + B_g \leftrightarrow A_{ads} + B_{ads}$

[1.34] $A_{ads} + B_{ads} \rightarrow C_{ads}$

[1.35] $C_{ads} \rightarrow C_g$

The mathematical treatment is based on the assumptions that all but the rate-determining step are close to a thermodynamic equilibrium. If the surface reaction is the rate-determining step, then the rate equations are as follows;

[1.36] $r = k\theta_A\theta_B$

where [1.37] $\theta_A = (K_A p_A) / (1 + K_A p_A + K_B p_B + K_C p_C)$

3. Mars Van Krevelen model – The redox model

This mechanism was initially developed for naphthalene oxidation. In this model, the oxygen for the reaction comes from the lattice of the catalyst and the reduced catalyst is later re-oxidized by gaseous oxygen. A steady state adsorption model was developed and applied to the vapor-phase oxidation of o-xylene over vanadium oxide catalyst.[107,111-113] Steady state is assumed to mean that the rate of adsorption of oxygen on the surface of the catalyst equals the rate of consumption of lattice oxygen by the hydrocarbon for the reaction. Unlike the other two models described, the redox model takes into consideration changes to the state of the catalyst. Based on the generally accepted mechanistic information provided in the previous section, it is obvious that this model most accurately describes what is happening on the surface of a vanadium-based ODH catalyst.

4. Power law model

The power law model correlates the rate of reaction with the partial pressures of the reactants and therefore assumes that the reaction can be expressed as follows:[108-109]

[1.38] $r = k_0 P_A^m P_B^n (-E_a/RT)$

where, m and n are the reaction orders found experimentally and are not necessarily equal to the stoichiometric coefficients of A and B respectively. The power law model was developed as a means to simplify the description of complete formal kinetics of a reaction, especially in cases where there is a lack of knowledge on the surface reactions occurring. The power law model is often used as a first approximation in kinetic studies of catalytic reactions.

An exhaustive review on the kinetics of the oxidative dehydrogenation of ethane and propane has been compiled.[83] It can be seen from the mentioned review that all the previously described models have been used to describe the kinetics of the ODH reaction. However, as more new information about the reaction become available, the models used have narrowed to the Mars-van-Krevelen model as it also takes into consideration the redox state of the catalytic species.

In one investigation, Dinse et al carried out a kinetic investigation on the ODH of propane over a VO_x/SBA-15 catalyst.[114] They used a simplified first order rate law to describe the kinetics of the reaction. Despite knowing that the reaction is commonly described using the Mars-van-Krevelen type reaction mechanism, they chose to describe the kinetics of the reaction using simple first order rate expressions. They justified their choice based on the assumption that the rate of re-oxidation of the catalyst was approximately 10^5 times faster than the rate-determining C-H bond activation, as found by Argyle et al.[115] It was stated that if this was true, then the simplified law used would result in the same kinetic description as a Mars-van-Krevelen type model.

1.6 Research Objectives

The overall goal of this research is to examine the chemistry of the conversion of simple refinery alkanes to olefins. The project will examine the catalytic oxidation of C_3 to C_4 alkanes in the presence of H_2S, as individual components, then as a mixture to form olefins. The final goal of this research is to find the appropriate conditions to generate an olefin mixture that can then be used as a reactant mixture in a second stage to produce high octane alkylate. A proposed scheme of the entire process is shown in Figure 1.1 below.

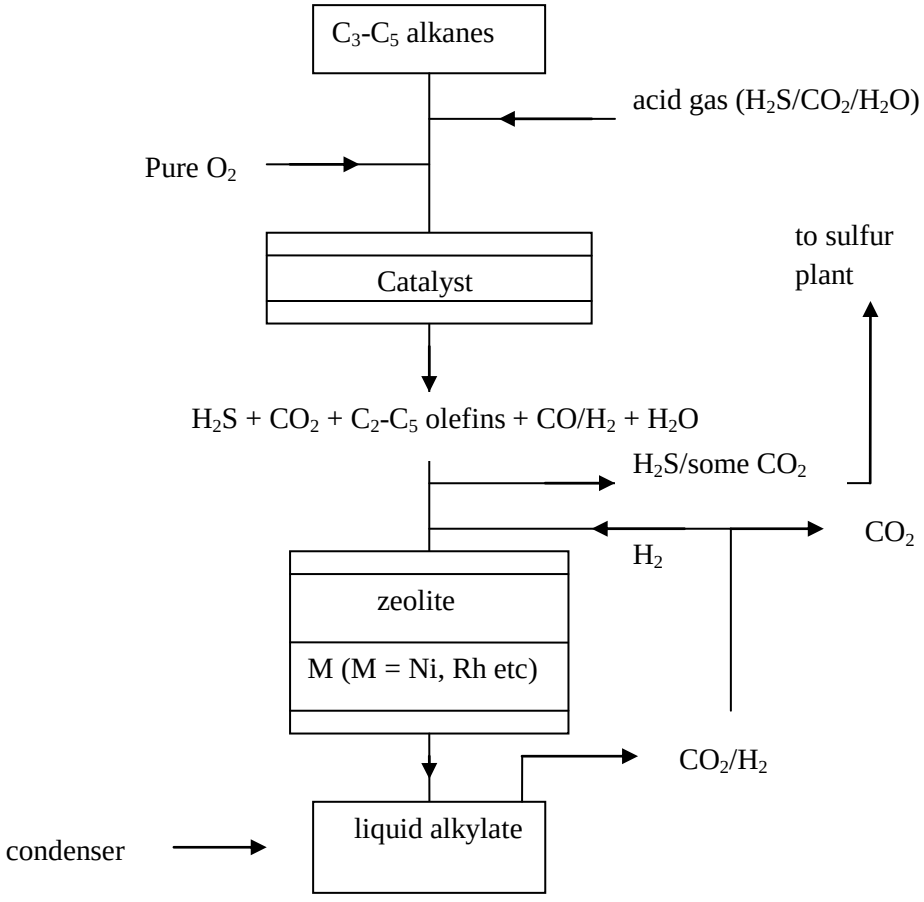

Figure 1.1: Overall process scheme for production of high octane alkylate from simple alkanes

In an industrial setting, the process would be set-up as follows. Light alkanes (C_3-C_5) along with pure O_2 and an acid gas stream would be passed over a catalyst to produce olefins, CO and H_2 along with significant amounts of H_2S, CO_2 and H_2O, some of which would be from the original reactant gas stream. H_2S and some of the CO_2 would then be removed from the product gas using a commercial amine. The H_2S/CO_2 removed could be recycled back to the reactor; however it may be more effective to send it to the sulfur plant and use fresh acid gas instead, which will allow the concentrations of the species in the reactant gas to remain relatively stable. The rest of the gas would be passed through a second reactor containing an acidic zeolite followed by a hydrogenation catalyst such as Ni/Al_2O_3. The product gas stream would then pass through a condenser that would liquefy the hydrocarbon product. The off gas from the condenser would contain mostly CO_2 and H_2, which can be recycled back to the second reactor once it has been separated from the CO_2.

Alternatively, ODH of propane and butane in the presence of H_2S could be used as a source of propylene and butenes for petrochemical syntheses.

Chapter 2: Materials and Methods

2.0. Experimental Procedures

Safety note - All experimental systems and H_2S gas cylinders were contained in ventilated cabinets fitted with gas detectors and automatic shut down systems designed to operate at low level alert and shut down mode (2 and 10 ppmv H_2S), respectively. Further details of safety operations are described in the following sections.

2.0.1 System Description

A tubular quartz reactor with plug flow characteristics, housed in a heated furnace, was used to carry out the experiments. Gases (N_2 (ultra high purity), O_2, H_2S and propane), were purchased from Praxair, and metered to the reactor using mass flow controllers and stainless steel tubing (Figures 2.1 and 2.2). Check valves and pressure relief systems were placed at various points for safety. A pressure gauge was connected to the feed lines to monitor any back pressure caused by solid sulfur accumulation downstream of the reactor. A relief valve, set to 10 psi, was attached to the gauge to allow venting of gases to an aqueous KOH scrubber system.

Catalyst, when used, was housed at the front end of the middle portion of the reactor, within the hot zone, and secured between plugs of quartz wool. A thermocouple was inserted into the front end of the catalyst bed from the front end of the reactor to record catalyst bed temperatures. A sampling tube, inserted from the back end of the reactor, allowed samples to be drawn out from the back end of the catalyst bed. The sampling tube used had a thinner diameter, hence reducing the amount of time spent in the hot zone after the catalytic reaction. The reactor was connected to a sulfur trap operated at ambient temperature followed by a dry trap, a pair of KOH scrubbers and carbon trap to remove moisture, sulfur gases and trace mercaptans, respectively.

The entire reactor system was housed in a ventilated cabinet equipped with H_2S, SO_2 and CO detectors, connected to an alarm system panel, to monitor levels of each of the gases in the area. The detectors were connected to automatic shutdown valves which were set to the gas exposure limits as set out by Alberta Environment for an 8-hour working day. The lines connecting the H_2S and propane gas tanks to the mass flow controllers were also connected via an air-operated valve (AOV) which, for safety reasons, had to be activated prior to each experiment. A flowchart of the experimental set-up is shown in Figure 2.1, below.

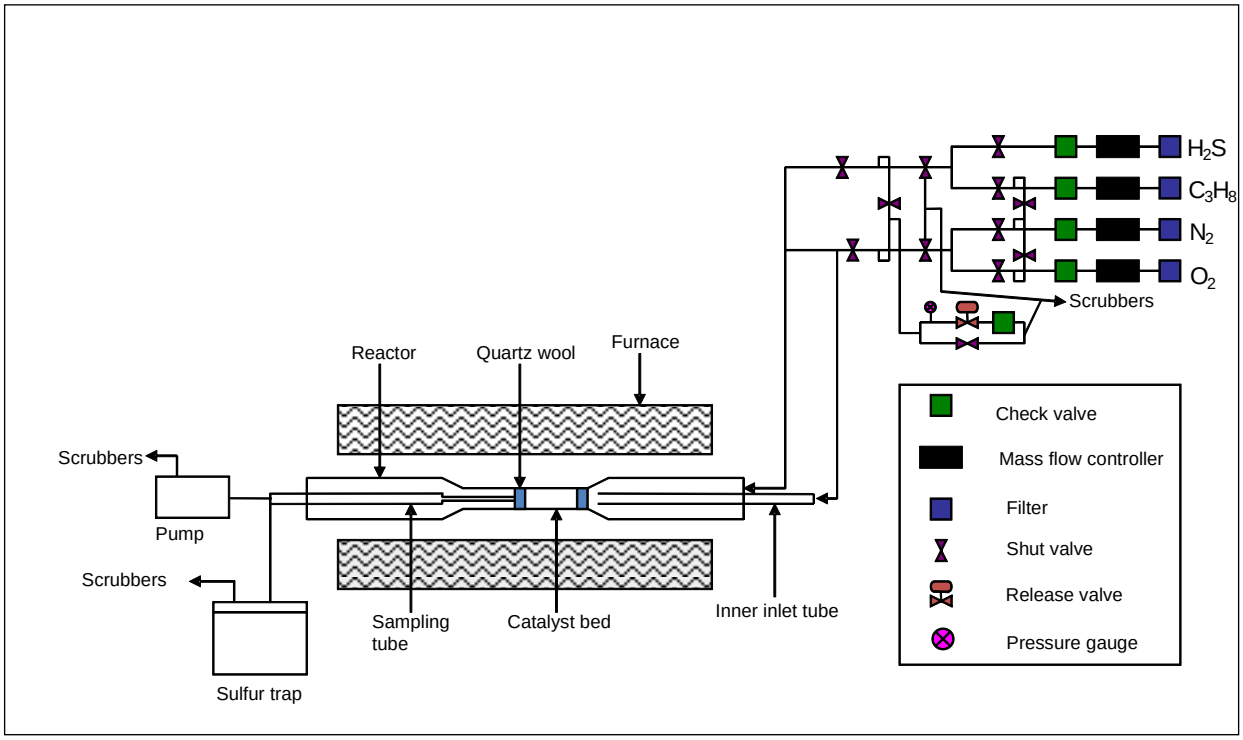

Figure 2.1: Experimental setup flowchart

Prior to commencement of the research, a HAZOP (hazards review process) was performed on the experimental system to confirm the safety of the operation. As well, an H_2S Alive training course run by Enform was attended.

2.0.2 Reactor Design

The tube reactor was made of quartz, which was shown to have a minimal catalytic effect on the reactions under study. It was designed with a wider front and back end, and a narrower middle portion, as shown in Figure 2.2. The outer diameter (OD) and length of the front end were 12.7 mm and 27.5 cm, respectively. The back end of the reactor had the same OD, but had a length of 20 cm. The OD and length of the middle portion were 8.1 mm and 22.5 cm, respectively. The front end of the reactor was designed to be longer, to allow the catalyst bed to be positioned a few centimeters into the hot zone of the furnace, thus avoiding the temperature gradient that can exist at the boundaries of the hot zone in such furnaces. The reactor design was chosen to allow shorter contact times (< 50 ms) for the flow rates available from the mass flow controllers.

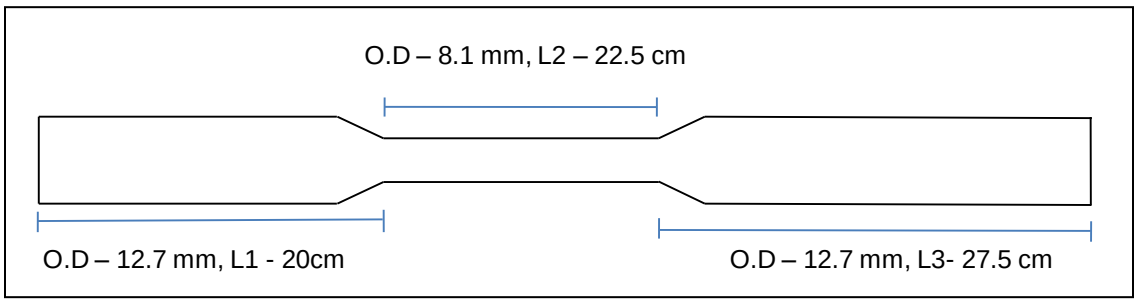

Figure 2.2: Quartz reactor

2.1 Catalyst Preparation

Silica supported vanadia catalysts were prepared using the wet incipient impregnation method. Catalysts with intended vanadia loadings of 1, 2.5, 5 and 10 weight % vanadium atoms supported on grade 40 silica gel were synthesized as follows: Ammonium metavanadate and oxalic acid in a 1:2 ratio were dissolved in de-ionized water to obtain a homogenous solution. The solution was then poured slowly over the pre-crushed (mesh size 16-30) silica, with

continuous stirring of the mixture. The product was then allowed to dry at room temperature for 2 hours, air dried at 373 K for 24 hours, and then calcined at 923 K for 3 hours. Catalysts were analyzed for BET surface area, pore volume and the amount of vanadia.

2.2 Experimental Procedure

Crystalline silica (ALDRICH, grade 40 silica gel) crushed to 16-30 mesh size (595-1190 microns) was used to fill the bed in non-catalytic investigations. Vanadia supported on silica, with a particle size similar to that of the crystalline silica, was used for the catalytic experiments. Catalyst amounts in the range of 0.2 – 2 g were used, depending on the desired contact time. Total flow rates of 300- 1500 mL/min were used, depending on the desired contact time. Nitrogen was used to dilute the feed gas mixture and as the internal standard to correct for condensable products. Fresh catalyst/silica was loaded into the reactor before the start of each experiment. The experimental setup was then connected and sealed, followed by a leak check to ensure no gases could leak out during the experiment. The mass flow controllers were then set up to flow the feed gas at room temperature to verify feed gas concentrations, after which the reactant gases were shut off and only nitrogen was left to flow during the warm-up period of the furnace. Once all checks were complete, the furnace and heating tapes were turned on and set for the desired temperature, and allowed to equilibrate for 1-2 hours. The experiment was then started by initiating reactant gas flow, and after 20-30 minutes of equilibration time, sampling began. After all samples had been obtained at a specific temperature, the reactor temperature was increased to the next condition and the system was allowed to equilibrate (30 min) before sampling.

2.3 Instrumental Analysis

Gas samples were obtained by syringe, with a P_2O_5 trap placed in front of the syringe to dehydrate and remove elemental sulfur from the samples. Analyses were carried out using gas chromatography. A Varian instrument, equipped with 2 columns (a 1.5 mm molecular sieve and an HP Q-PLOT), both of which were connected to thermal conductivity detectors (TCD), was used. A pulsed flame photometric detector (PFPD), in series with the TCD for the second column, was employed for detection of low level sulfur compounds. The HP Q-PLOT column was used for determination of COS, CS_2, CO_2, H_2S, SO_2, C_2H_4, C_2H_6, C_3H_8, C_3H_6, C_4H_{10}, n-C_5H_{12}, methyl-mercaptan, ethyl-mercaptan and propyl-mercaptan, while the molecular sieve column was used for H_2, N_2, O_2, CH_4 and CO.

An SRI GC equipped with a molecular sieve column for H_2 and a T-PLOT column for higher hydrocarbons (H_2S, C_3H_8, C_3H_6, C_4H_{10}, 1-C_4H_8, cis-2-C_4H_8, trans-2-C_4H_8, i-C_4H_{10}) determination was also used. The gas samples were first analyzed as taken, and then diluted with argon (5x dilution) to obtain better resolution of the propane/propylene peaks. For each set of conditions, the outlet gas was sampled 3 times, with each sample being taken after a 30 min time interval. The results of the 3 samples were then averaged to obtain the final numbers reported here.

2.3.1 Gas Chromatograph Calibration

Standard gas mixtures were used to calibrate the gas chromatograph before commencement of the project. Each gaseous component was calibrated using two or more different mixtures. Each mixture was run through the GC three times, and the values used for the calibration curves were an average of the three analyses. Calibrations were carried out for the

following gaseous components: H_2, N_2, O_2, CH_4, CO, COS, CS_2, CO_2, H_2S, SO_2, C_2H_4, C_2H_6, C_3H_8, C_3H_6, C_4H_{10}, 1-C_4H_8, cis-2-C_4H_8, trans-2-C_4H_8, i-C_4H_{10}, n-C_5H_{12}, methyl-mercaptan, ethyl-mercaptan and propyl-mercaptan.

Three of the gas mixtures used were as follows:

1) Hydrocarbon mixture 1 (0.9998% CH_4, 0.9982% C_2H_6, 1.01% C_3H_8, 1.0% C_4H_{10}, 1.02% C_5H_{12} and balance 94.972% N_2)
2) M7036 (1.0% CO, 1.0% CO_2, 1.0% CH_4, 1.0% H_2, 1.0% O_2 and balance 95% N_2)
3) Hydrocarbon mixture 2 (6.98% C_2H_6, 4.0% C_3H_8, 0.401% n-C_4H_{10}, 0.394% i-C_4H_{10}, 0.2% n-C_5H_{12}, 0.201% i-C_5H_{12}, 0.299% N_2, 7.0% CO_2, 0.493% n-C_6H_{14} and balance 80.032% CH_4).

Other gases used were: 500 ppm H_2S in N_2 and 2.5% H_2S in N_2, 500ppm SO_2 in N_2, ultra high purity N_2, propane (instrument grade), n-butane (instrument grade), 1% 1-C_4H_8 in N_2, 1% cis-2-C_4H_8 in N_2, 1% trans-2-C_4H_8 in N_2, 100% C_3H_6 (instrument grade).

2.3.2 Feed Gas Determination

Determination of the feed gas flow rates was based on the contact time desired for each experiment and the limitations of the flow controllers. Mass flow controller set points were calculated based on the desired contact times, using realistic catalyst amounts and total flows achievable by the flow controllers. The following formula was used to determine the total flow (in mL/min) and the amount of catalyst to be used (in grams) for a given contact time experiment:

$$F_{total}(\frac{mL}{min}) = \frac{V_{catalyst}\,(ml) \times 298\,(K) \times 60(\frac{s}{\min})}{T\,(K) \times t_c(s)}$$

For homogenous reactions, the equation used to calculate the total flow and volume of empty reactor was as follows:

$$F_{total}(\frac{mL}{min}) = \frac{V_{reactor}(ml)\times 298\ (K)\times 60(\frac{s}{\text{min}})}{T(K)\times t_c(s)}$$

The flow of each component gas was then calculated from the total flow by the following equation:

$$F_i(\frac{mL}{min}) = F_{total}\left(\frac{mL}{min}\right)\times P_i$$

where F_i is the flow of a given component gas in mL/min and P_i is the volume percent of that component in the feed mixture.

Once the flow rate of each component was determined, correction factors were used to calculate the set point for each component gas based on the mass flow controller assigned to it. Each flow controller is calibrated using a specific gas, and if the gas it is being used for is different than its original calibration gas, then a correction factor needs to be applied when determining set points. Once the approximate set points were calculated, they were then tested by setting the gases to flow through an empty reactor. Samples were drawn at 15 minute intervals using a gas-tight syringe, and analyzed via GC (a minimum of three times each) to obtain an average value for the feed gas. In addition, the feed gas settings being used were validated by GC before the commencement of each experiment.

2.4 Catalyst Characterization

The catalysts were characterized in three ways, namely: BET surface area and pore volume analysis, vanadium content analysis and electron microscopy for imaging. Details of each are provided below.

2.4.1 Surface Area and Vanadium Content Analysis

BET surface area and pore volume were measured using a TriStar 3000 instrument (Micromeritics Instrument Corporation, USA). For the adsorption tests, the samples were degassed at 623 K under vacuum for 1-1.5 h, followed by analysis carried out at 77 K using high purity nitrogen. Vanadium content was measured by crushing the catalyst samples to a fine powder, followed by four-acid digestion and ICP-AES analysis. The results are shown in Table 2.1, below.

Table 2.1: Surface area, pore volume and intended percent vanadia compositions of catalysts vs. actual vanadium content from analysis.

Sample	BET Surface area (m^2/g)	BJH desorption cumulative volume of pores between 10-3000 Å width (cm^3/g)	Vanadium content (atomic %)
Crystalline silica	757	0.480	0
1% VOx/CS	498	0.304	0.86
2.5% VOx/CS	265	0.174	2.28
5% VOx/CS -A	44	0.023	6.2
5% VOx/CS -B	355	0.244	3.97
10% VOx/CS -A	184	0.142	7.62
10% VOx/CS -B	224	0.161	6.52

The general correlation of decreasing BET surface area with increasing vanadium content can be seen from the data in Table 2.1, above. A similar trend was also observed for the pore volume data. The vanadium content analysis showed that in the majority of the cases, the true amount of vanadium was lower than the pre-calculated amount based on the amount used during preparation. This could be because of residual solution left on the sides of the crucibles used during preparation. In addition, the technique of wet incipient impregnation does not provide a

completely homogenous dispersion of the impregnated component, so small variations can be expected among catalyst particles. However, it is assumed that the sample used to carry out the vanadium content analysis is representative of the entire batch of catalyst prepared.

During preparation of the 5% VOx/CS –A catalyst, the sample was left in the calcination furnace for 48 hours instead of the required 3 hours. This may have resulted in the much lower surface area of this sample. For this reason, 5% VOx/CS –B was prepared. However in a few of the catalytic tests, the 5% VOx/CS –A sample was still used. In some tests where this sample was used, the results seemed to be no different than what was expected. However, in other experiments, the results obtained were not in line with what was expected, and hence those experiments were then repeated using the 5% VOx/CS –B sample. Throughout the rest of this written report, information will be provided to indicate which of the two samples was used in a given experiment for which data is reported in the figures/tables.

2.4.2 Scanning Electron Microscopy

Scanning electron microscopy (SEM) was used to obtain images of some fresh, as well as spent, samples of catalyst particles. An FEI XL30 was used to obtain high resolution images and to carry out elemental analysis using the Energy Dispersive X-ray spectroscopy (EDX) technique at various points on a catalyst particle. Images and data from the SEM characterization are shown below.

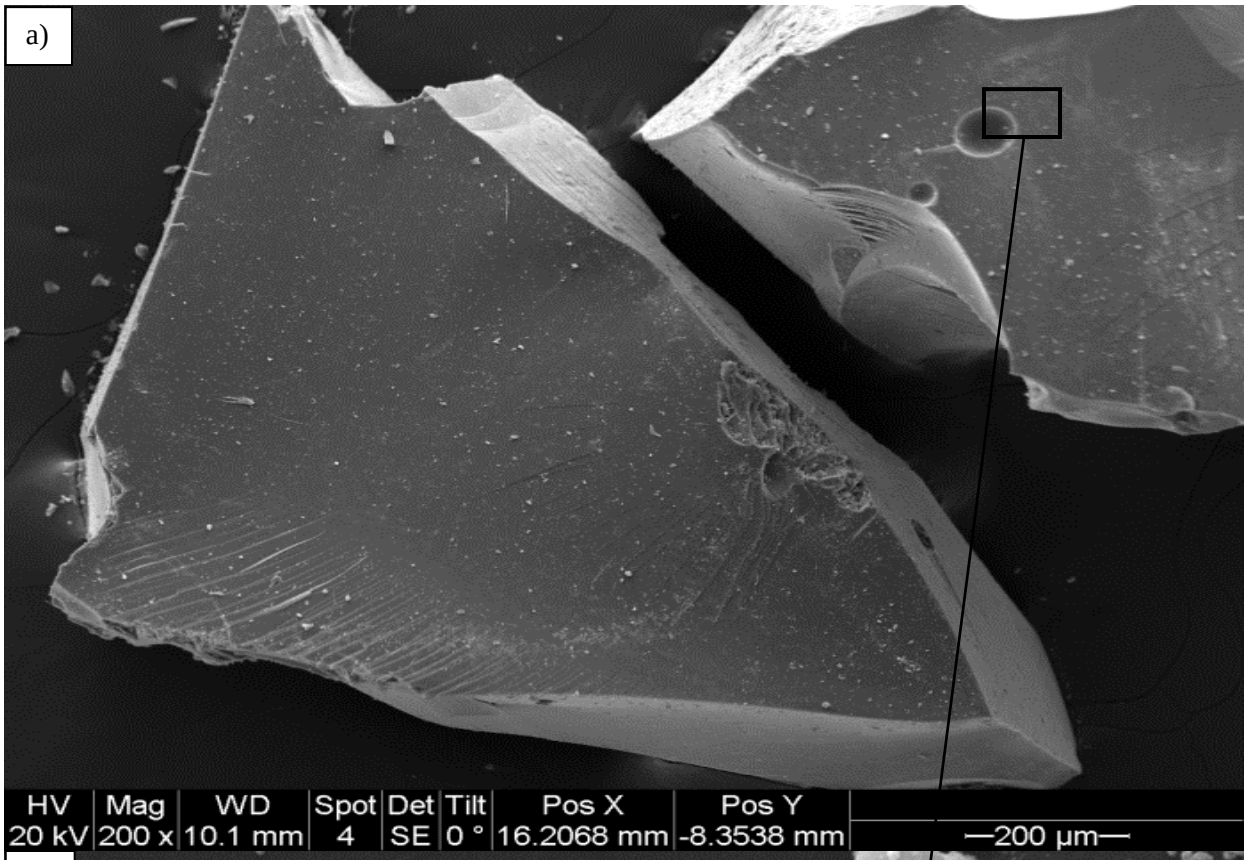
a)
HV
20 kV
Mag
200 x
WD
10.1 mm
Spot
4
Det
SE
Tilt
0 °
Pos X
16.2068 mm
Pos Y
-8.3538 mm
200 µm

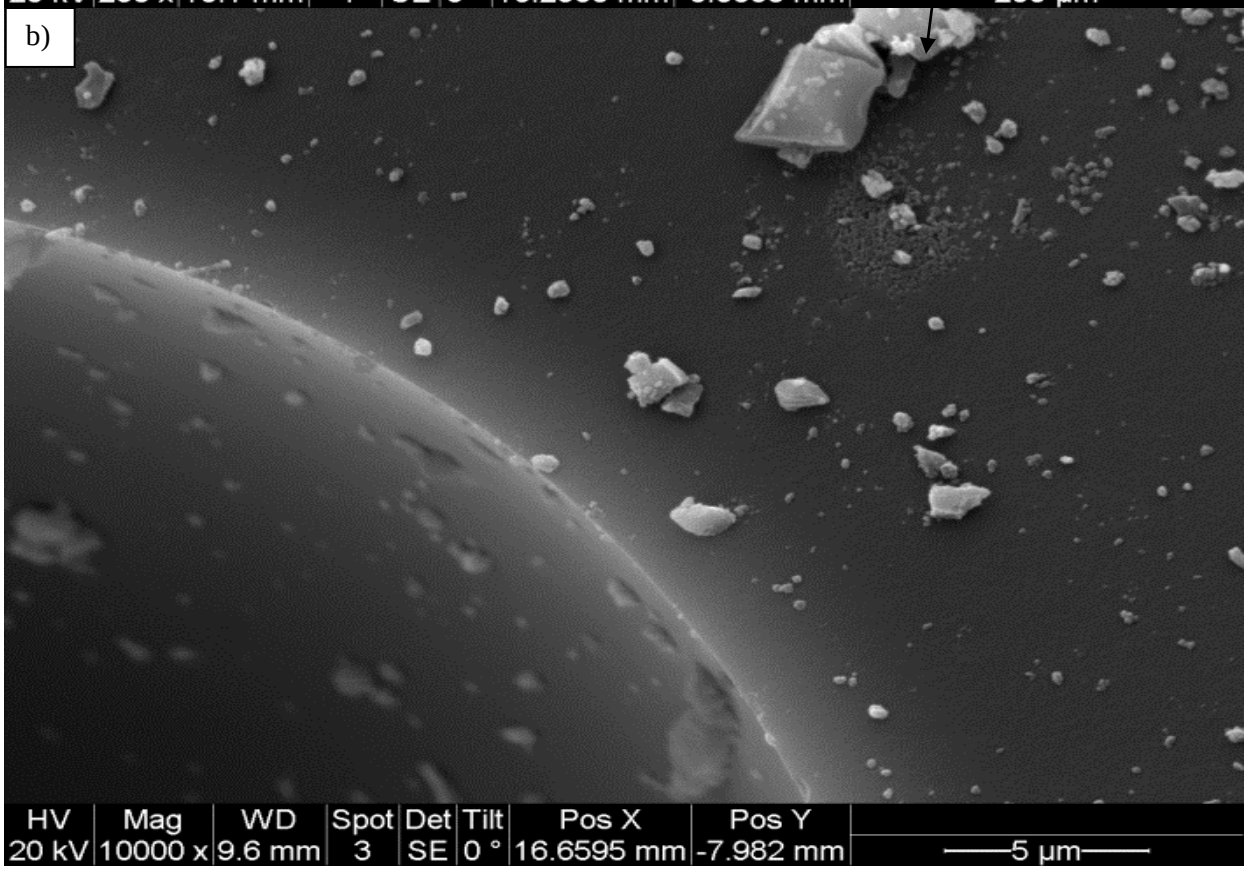
b)
HV
20 kV
Mag
10000 x
WD
9.6 mm
Spot
3
Det
SE
Tilt
0 °
Pos X
16.6595 mm
Pos Y
-7.982 mm
5 µm

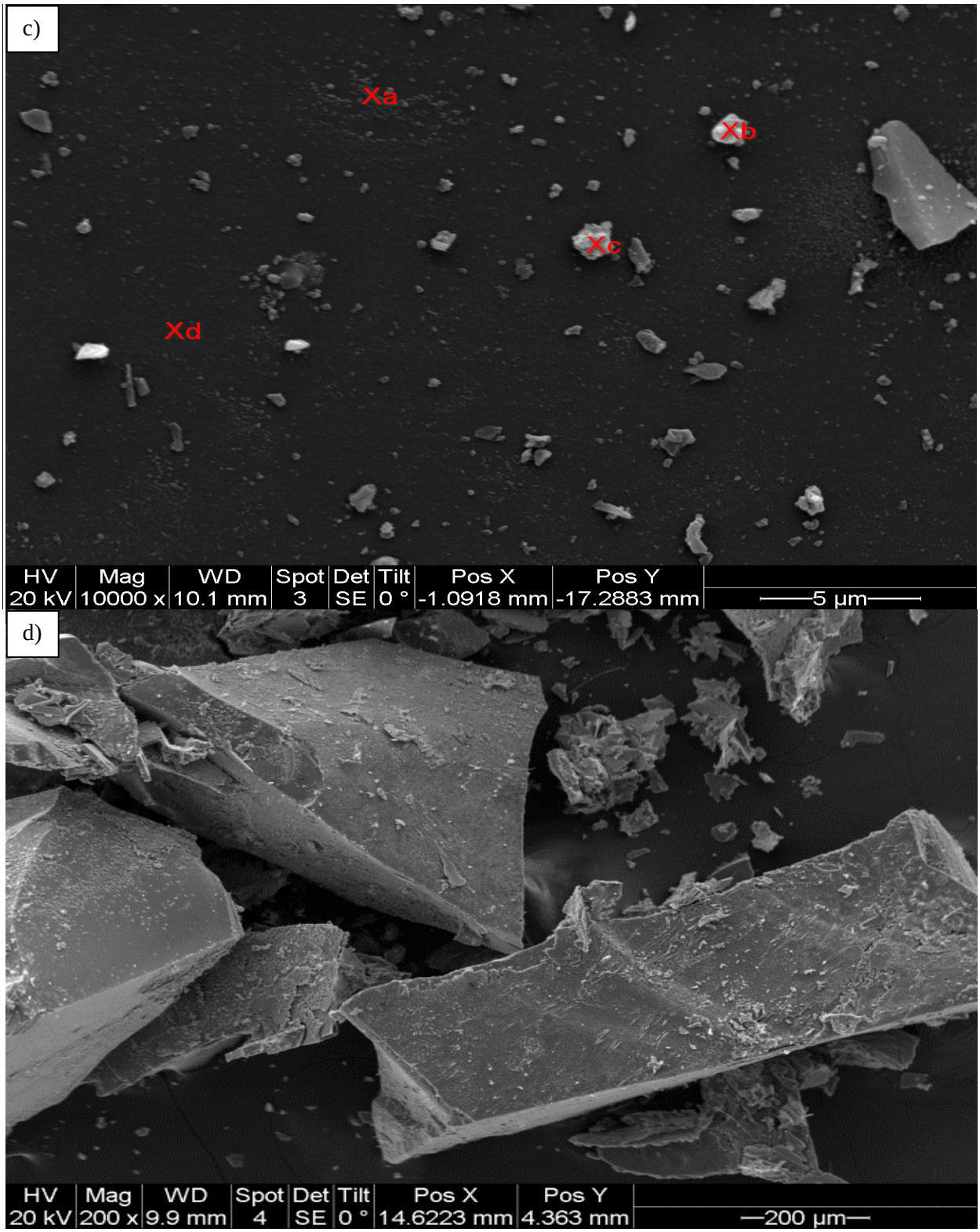

Figure 2.3: SEM images of unused catalysts. a) Full particles of 2.5% VOx/CS, b) Zoomed image of the area shown by the rectangular box in the top left of image 2.3a. c) Surface of a 1% VOx/CS catalyst particle showing areas where EDX was used. d) Low magnification image of an older catalyst.

The images in Figure 2.3 show regular particle structure (2.3a and 2.3d) at low magnifications. SEM images of spent catalyst samples were also taken with the intent to carry out EDX analysis for determination of any sulfur or carbon content on the surface of the spent catalyst. Some of the spent samples looked similar to those of the fresh catalyst in the SEM image. However, in actuality, the fresh samples were yellow or orange crystals (depending on the amount of vanadium in the particular sample), while the spent catalysts were shiny dark grey or black crystals (likely covered in a certain amount of coke and sulfides). On the surface of one of the spent catalyst particles, a rod-like structure was seen during imaging; hence, further magnification was used, for better imaging and for EDX analysis. This is shown in Figure 2.4b, below. EDX analysis carried out on the rod showed that it contained a higher amount of silicon and oxygen and hence was not agglomerated vanadium oxide as initially assumed.

a)

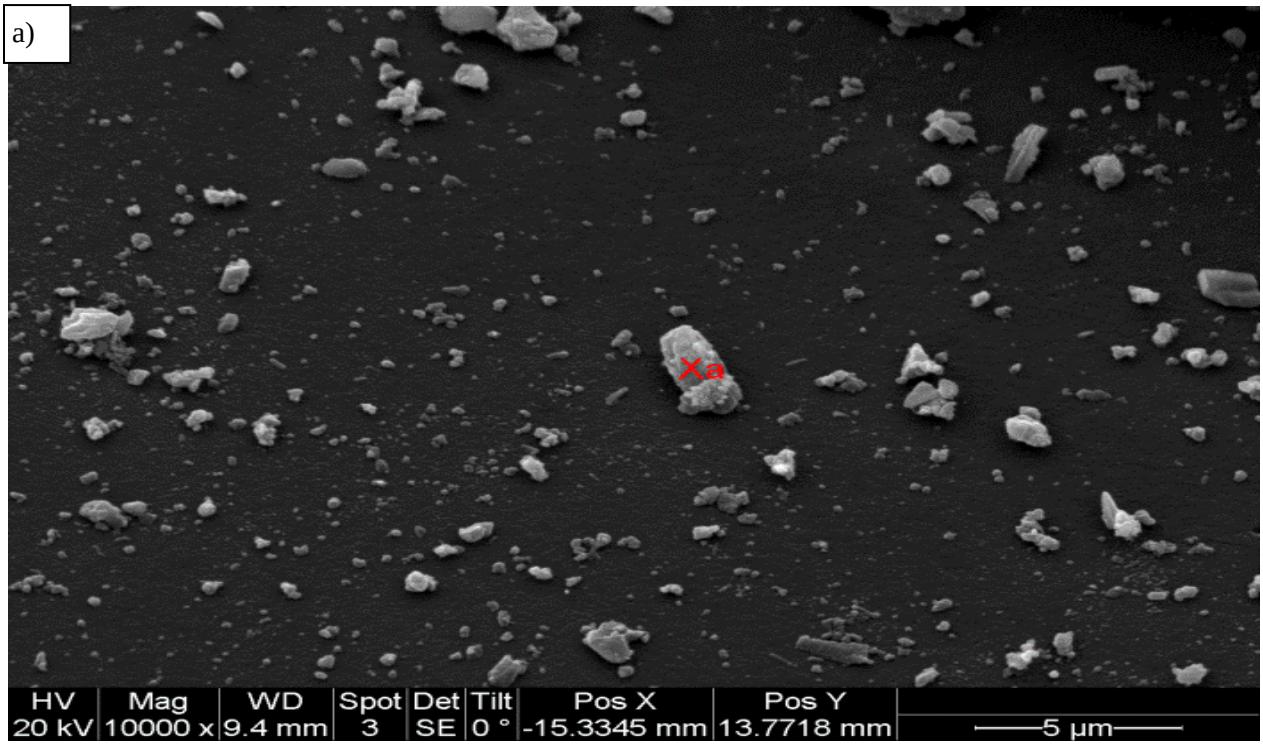

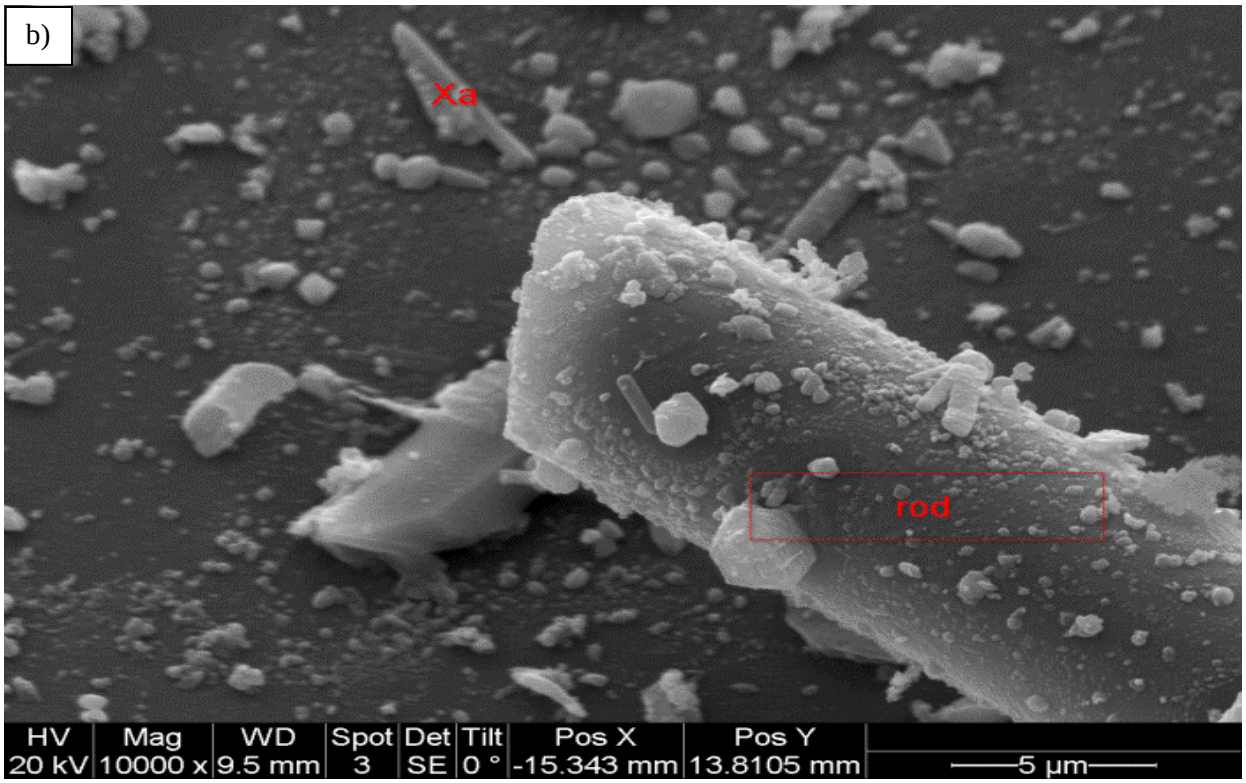

Figure 2.4: SEM images of spent catalyst samples. a) Surface of a spent 5% VOx/CS sample. b) Rod-like structure on the surface of the spent catalyst particle.

The markings on the images show the points or areas were EDX was used, and these data are shown in Table 2.2, below.

Table 2.2: EDX data from images 4a and 4b (above), as well as a fresh 5%VOx/CS sample at positions as labeled in the above images. (Note: n/a means that the element was not analyzed).

Sample	Position	Si (%)	O (%)	V (%)	S (%)	C (%)
3c	Xa	55.52	43.22	1.26	n/a	n/a
3c	Xb	56.67	41.72	1.61	n/a	n/a
3c	Xc	56.76	41.68	1.56	n/a	n/a
3c	Xd	58.20	40.36	1.45	n/a	n/a
4a	Xa	48.99	25.65	11.57	0.98	12.82
4b	Xa	41.05	26.87	24.78	7.30	n/a
4b	rod	62.39	33.33	3.00	1.28	n/a
fresh 5%VOx/CS (SEM image not shown)	Not shown	63.69	26.32	9.99	0.00	n/a

EDX was used on various parts of a catalyst particle to determine if the V content was homogeneously dispersed. The data showed that there was some variation in the amount of vanadium, even for a single catalyst particle. However, such an observation is expected, based on both the method used to impregnate the catalyst (wet incipient impregnation), and the high amount of % vanadium on the catalyst (up to 8% in some cases). It was determined that vanadium was found on the surface, regardless of what the surface looked like during imaging. In the sample imaged in Figure 2.3c, four different spots were picked for EDX, and while the amount of V determined by EDX showed some variation, they all showed the presence of vanadium regardless of whether the surface showed nothing (Xd – 1.45% V), tiny specs (Xa – 1.26% V) or what looked like small crystallites (Xb – 1.61% V and Xc – 1.56% V).

The % V determined for the spent samples showed a significant difference from that of a fresh particle taken from the same initial batch of catalyst. The fresh sample was determined to be 9.99% V at one point, while the spent sample was determined to have 11.57% at one point. In addition, other points on the spent sample had higher amounts of % V as determined by EDX analysis (sample imaged in Figure 4b). It is possible that some agglomeration of the active component may have occurred due to the exposure to high temperatures during the catalytic reaction.

Another reason for using EDX was to determine if coke was present on the spent sample, and the data showed that it was present in a significant amount (12.82% C – sample 4a). Lastly, the EDX was used to determine if any sulfur-containing components were present on the spent catalyst, as vanadium oxide can be sulfided in the presence of H_2S. EDX confirmed the presence of sulfur on the spent samples. The data also showed a correlation between %V and %S for each of the points where EDX was carried out. Points that had higher %V also had higher %S, which

supports the hypothesis that vanadium oxide becomes sulfided in the presence of H_2S. As a control, EDX was also carried out on a fresh catalyst sample to see if any S was present and none was found, proving that the sulfur component came from the catalytic reaction.

The EDX data obtained cannot be used on its own, quantitatively, or be compared to the results obtained from the determination of vanadium content by acid digestion followed by ICP because of differences between the two analysis methods. The EDX method analyzes the surface of a particle to a particular depth, but does not access the entire pore structure, and the results obtained are based on the particular mode used. Different-sized areas can be used for the analysis (spot vs. small area. etc.) and for these samples, mostly spot mode at various points on the particle was used. With the complete digestion method, the amount of vanadium is determined based on the weight of catalyst used, thus the result is an average based on a few particles. The digestion/ICP method therefore gives a better representative of the bulk vanadium content of the catalyst samples.

2.5 Estimation of Errors

To test for analytical accuracy, samples were analyzed multiple times using the same experimental and analysis system that was subsequently used for the reaction studies. The experimental system was set up to flow a certain mixture of gases through an empty reactor; in this case, a mixture of the reactant feed gases were flowed through the reactor, in the specific ratios to be used later for the experiments. The system was kept at room temperature to prevent any chemical changes in the gas compositions. The set-up was left flowing throughout the sample collection and analysis period to prevent any external factors from affecting the results. Samples were drawn from the sample port using a syringe and injected into the GC, similar to

the way it was done in experiments. Three samples, 30 minutes apart, were taken for different gas mixtures. The average and standard deviation of the GC data was calculated and the standard deviation was further converted to relative standard deviation, which is simply the standard deviation divided by the average and expressed as a percentage. The results of two of these trials are shown in Table 2.3 below, along with their standard deviations.

Table 2.3: Results of gas analysis for the purpose of error estimation

	Gas mixture 1			**Gas mixture 2**	
	N_2	C_3H_8	H_2S	N_2	C_3H_8
Sample 1	61.998	36.200	4.697	64.754	36.971
Sample 2	62.055	35.366	4.452	65.625	36.447
Sample 3	62.159	35.387	4.387	65.409	35.613
Average (mol %)	62.070	35.651	4.512	65.262	36.343
Standard deviation (mol %)	0.0816	0.4755	0.1634	0.453	0.684
Relative standard deviation (%)	0.131	1.333	3.623	0.694	1.884

The error calculation shown here is a sum of more than one error. It includes errors due to user sampling and GC instrument errors, as well as fluctuations within the mass flow controllers over the specific time period. From Table 2.3, it can be seen that experimental errors range from 0.13% for components in higher amounts to as high as 3.6% for the components in the lowest amounts. The higher error seen for H_2S in gas mixture 1 is due to the fact that settings in the lower end of the mass controller's range were used to obtain the correct feed ratio. A general error of 1-2% should be acceptable for majority of the components in the system. Based on these results, it may be prudent to include an experimental error of up to 5% of the amount of reactant for this system. Despite this, the data is presented to 1 decimal place. However, it should be kept in mind when comparing values between data sets to obtain trends, that those values that are less than a few percent apart may be a result of experimental error.

One further consideration is that of variation within the experimental data due to experimental factors, an example of which might be coking of the catalyst during catalytic experiments. While the data reported in this work are shown as an average of three samples taken at the same experimental conditions, a table showing the variation within three samples for one of the experiments is shown in Appendix 2.1 to provide an idea of the overall magnitude of variation for such a system. The overall variation shows the sum of both the experimental errors discussed previously as well as variations caused due to the reaction that cannot be controlled.

2.6. Definitions and Data Processing

Contact time and residence time are terms used to describe how long a gas takes to pass through a catalyst bed and empty reactor volume, respectively. They are defined by the following expressions:

$$t_c(s) = \frac{V_{catalyst}(mL) \times 298\ (K) \times 60\ (s/\text{min}\ )}{F_{total}\left(\frac{mL}{min}\right) \times T\ (K)}$$

$$t_r(s)\ = \frac{V_{reactor}(mL) \times 298\ (K) \times 60\ (\frac{s}{\text{min}})}{F_{total}\left(\frac{mL}{min}\right) \times T\ (K)}$$

where, t_c(s) is the contact time in seconds, t_r(s) is the residence time in seconds, $V_{catalyst}$ is the volume of catalyst used, $V_{reactor}$ is the volume of the empty reactor used in mL, T is the temperature in Kelvin and F_{total} is the total flow of all gaseous components in mL/min.

For catalytic reactions, the contact time describes only how long it takes a volume of gas to pass through the catalyst bed and is simply the inverse of the gas hourly space velocity converted to units of seconds, which is a commonly reported industrial parameter. Gas hourly space velocity

is a commonly reported parameter, which allows easy reproduction of reactor conditions, by using the amount of time each volume of gas spends within the reactor. Scaling the reactor size up or down is then easier to carry out and a more appropriate parameter to use for this work.

The data obtained from the GC was used to calculate the conversion, selectivity and yield of the various components according to the following formulae:

$$Conversion\ \%\ (i) = \frac{moles\ of\ reactant\ (i) in\ feed - moles\ of\ reactant\ (i) in\ the\ product}{moles\ of\ reactant\ (i)\ in\ the\ feed} \times 100$$

where, i refers to reactants such as C_3H_8, O_2, H_2S and C_4H_{10}.

$$Selectivity\ \%\ (j) = \frac{moles\ of\ reactant\ converted\ to\ product(j)}{total\ moles\ of\ reactant\ converted} \times 100$$

where, j refers to products such as CO, CO_2, CH_4, C_2H_4, C_2H_6, C_3H_6 etc.

$$Yield\ \%\ (j) = Conversion\ (i) \times Selectivity\ (j)$$

2.7. Computational Calculation Procedures

In the first part of the computation work shown in this thesis, potential energy surfaces were computed for reaction pathways between the n-propyl and i-propyl radicals with either O_2 or S_2. Similar reaction profiles were also computed for the reactions of both n-butyl and i-butyl radicals with either O_2 or S_2. In this work, the CBS-QB3 model,[116] which is a variant of the CBS-Q model[117] where the MP2 geometry optimization is replaced by B3LYP geometry optimization and the high-level correlation energy calculation is carried out at CCSD(T) level, was employed. This method is well suited for the studies of transition states for chemical reactions,[116] and its applicability has been verified in numerous thermochemical and reaction kinetic

investigations.[118-122] All electronic structure calculations were performed with Gaussian 09 suite of programs.[123]

In the second part, the potential energy profile for the sulfidation of the vanadyl O as well as the potential energy profiles for the vanadyl mechanism on V_2O_5 and V_2O_4S were shown. These were generated using the Vienna Ab initio Simulation Package (VASP)[124-127] in which the spin-polarized density functional methodology at generalized gradient approximation with the Perdew-Burke-Ernzerhof (PBE) functional[128] was employed. Full details of the computational methods used has already been reported.[129]

Chapter 3: Reaction between C_3H_8 and H_2S

3.0 Reaction of Propane with H_2S (Sulfided Catalyst Work)

In most of the ODH studies reported in the literature, O_2 has been the oxidant used. Oxygen aids the process from an industrial viewpoint, as no external heat source should be required; also, it has been shown that less coke is formed.[130] The high selectivity and conversion required for an industrial process is difficult to attain, because as conversion increases, selectivity to the olefin decreases. This co-relation is described extensively by Cavani,[131] where a plot of conversion of alkane versus selectivity to olefin is compiled for the many catalytic systems that were used in studies between 2000-2006.[131] The plots were divided into two groups, one showing the conversion of propane versus the selectivity to propylene for vanadium-containing catalytic systems and another plot showing other catalysts. For vanadium-containing catalytic systems, the majority of the studies reported propylene yields that were below 20% (0.20 as shown in the plot) and only 3 studies showed yields that were between 20% and 30%, with the highest yield being just below 30%. One reason for loss of selectivity is that partial oxidation products, such as propylene, are more reactive than the corresponding alkane,[131] and hence, can undergo further reaction to CO and CO_2 via steam reforming with product H_2O.[130,132] In addition, since the ODH reaction is exothermic, poor heat removal from the catalyst bed can cause excessive temperatures, thus promoting undesirable side-reactions.

Addition of a co-reactant/oxidant other than oxygen has been used to improve the selectivity/yield for conversion of alkanes to olefins. Kondratenko investigated the ODH of C_2-C_4 alkanes using N_2O and compared it to experiments using oxygen,[133] and reported improvements in selectivity, but at the cost of lower conversions. The increase in selectivity

observed using N_2O was due to suppressed CO_x formation. Carbon dioxide in combination with CrO_x/silica catalysts has been shown to be effective for conversion of small alkanes to olefins, but the high selectivity (~85%) observed initially decreased with time on stream.[134] The same system, but using oxygen, displayed lower selectivity/conversion initially but resulted in higher olefin yields after prolonged time on stream in comparison to CO_2.[134] The decrease in conversion using CO_2 was shown to be due to conversion of chromate species into α-Cr_2O_3 and accumulation of coke.

3.1 Effect of H_2S on the Pyrolysis of Propane

Sulfur compounds have also been used as co-reactants/oxidants for the ODH of ethylene, with one report on the catalytic dehydrogenation of propane.[61] The effectiveness of elemental sulfur was shown in the oxidative dehydrogenation of ethane to form ethylene.[62] When a feed composition of $C_2H_6/S_2/H_2S/N_2$ at a ratio of 60/5/22/13 was used to carry out gas-phase oxidative dehydrogenation of ethane, ethylene selectivity of up to 89% was obtained at 84% conversion of ethane using a contact time of 0.6 seconds and a reaction temperature of 1123 K. In the above work, H_2S was used only as a diluent, with the added advantage of possibly inhibiting coke formation.

In the current research, the use of H_2S in combination with O_2 for the oxidative dehydrogenation of propane to form propylene in the gas-phase and over supported vanadia catalysts is reported (Chapter 4). Since H_2S is readily available at natural gas plants as well as in oil refineries, its use in propylene manufacture using propane by-product from various units may offer a commercial advantage. The choice of H_2S as a reactant is based on two reasons. Research has shown that H_2S can dissociate thermally at high temperatures (873-1273 K) to form sulfur,

H_2, SH radicals and other sulfur components, although equilibrium conversion is low < 973 K.[135-137] Both sulfur and the SH radical should theoretically be able to initiate H-abstraction from a propane molecule. Also, it has been reported that supported vanadium oxide catalysts promote dissociation of H_2S on vanadyl sites, forming sulfides, which then act as a catalyst for further dissociation of H_2S.[138,139] This process would allow for the continuous catalytic generation of S_2 which would then carry out the ODH of propane. Although the overall process is endothermic, the formation of carbon sulfides is not favorable above 873 K because of the weakness of the C-S bond. In comparison, the C-O bond strength is a key driver for production of CO_x in the oxygen-driven system. The main competing side reactions in the sulfur system would then be cracking of propane as well as coking, but these processes are known to be inhibited by H_2S and other sulfur species.

All of these points suggest that H_2S, without O_2, can play a role in the conversion of C_3H_8, so a variety of studies were performed to examine that role.

3.1.1 Thermal Reaction

In the overall reaction involving propane and H_2S, one of the first reactions of importance is the thermal dissociation of H_2S, which has already been studied for its potential in hydrogen production.[140] This reaction can be described by the following equation:

[3.1] $$H_2S_{(g)} \leftrightarrow H_{2(g)} + \tfrac{1}{2} S_{2(g)} \qquad \Delta H_{rxn}\,(25°C) = 84.9\ kJ/mol$$

The reaction is endothermic and yields are limited by equilibrium conversion at low temperatures. As an example, conversion of H_2S at 1133 K is expected to be approximately 10%. It has also been shown that at temperatures above 1023 K, diatomic sulfur (S_2) is the primary sulfur species produced.[135,141] In addition, the advantages of using a catalyst decrease rapidly at

temperatures above 1073 K, since the thermal reaction proceeds quite rapidly to the equilibrium.[135,141]

The second step of the reaction is the oxidative dehydrogenation of propane by S_2 to produce propylene and H_2S as a by-product, as shown by the following:

[3.2] $C_3H_8 + ½ S_2 \rightarrow C_3H_6 + H_2S$

In many of the experiments reported here, the conversion of H_2S appeared to be negligible. It is possible that H_2 and S_2 recombine while in the hot zone to re-produce H_2S, but also, S_2 will re-form H_2S via oxidation of C_3H_8. The net reaction is, then, the dehydrogenation of C_3H_8 to produce propylene and $H_{2(g)}$ along with some cracking products, coking products and any unused diatomic sulfur. Without participation of S_2, the accepted mechanism for the formation of C_3H_6 and C_2H_4 is as follows:[142,143]

[3.3] $C_3H_8 \rightarrow CH_3\cdot + C_2H_5\cdot$

[3.4] $C_3H_8 + C_2H_5\cdot$ (or $CH_3\cdot$ or $H\cdot$) $\rightarrow C_3H_7\cdot + C_2H_6$ (or CH_4 or H_2)

[3.5] n-$C_3H_7\cdot \rightarrow C_2H_4 + CH_3\cdot$

[3.6] i-$C_3H_7\cdot \rightarrow C_3H_6 + H\cdot$

[3.7] $C_2H_5\cdot \rightarrow C_2H_4 + H\cdot$

Overall, the reaction mechanism in the presence of H_2S is predicted to be similar to that of the reaction of oxygen with propane, as S_2 is expected to have a similar reactivity to oxygen. The mechanism for the reaction of propane with oxygen is described in the literature. [144,145]

In the presence of H_2S and S_2, the following mechanism can be written:

[3.8] $C_3H_8 + S_2 \rightarrow C_3H_7\cdot + HS_2\cdot$

[3.9] $C_3H_8 + HS_2\cdot \rightarrow C_3H_7\cdot + H_2S_2$

[3.10] $H_2S_2 \rightarrow 2SH\cdot$

[3.11] $C_3H_8 + SH\cdot \rightarrow C_3H_7\cdot + H_2S$

[3.12] $C_3H_7\cdot + S_2 \rightarrow C_3H_6 + HS_2\cdot$

[3.13] $C_2H_5\cdot + S_2 \rightarrow C_2H_4 + HS_2\cdot$

[3.14] $C_2H_5\cdot$ or $CH_3\cdot$ or $H\cdot + H_2S \rightarrow C_2H_6$ or CH_4 or H_2) + $HS\cdot$

Overall, the main hydrocarbon products obtained were dehydrogenation products (C_3H_6 and H_2), cracking products (C_2H_4, CH_4 and C_2H_6) and coking products (carbon). Elemental sulfur and H_2S were the only major sulfur products quantified. Carbon was not measured directly, but calculated from the carbon mass balance; likewise, elemental sulfur was calculated from the sulfur mass balance. CS_2 was observed in the product stream at times, but in negligible quantities below the quantifiable limit of the TCD used in the GC instrument for analysis.

The first set of experiments compared the gas-phase reaction of propane, in the presence and absence of H_2S, through an empty reactor at 923 K and 1023 K. The results are shown in Table 3.1, below. From the results, it can be seen that the main (and perhaps only) advantage of using H_2S in an empty reactor at these conditions and residence times is the increase in conversion that is observed. Selectivity to C_3H_6 is higher for the pyrolysis reaction, and the selectivity to C_2H_4 is only slightly lower at 923 K and significantly higher at 1023 K for the pyrolysis reaction. The overall yields of both the olefins are higher for the H_2S-containing reaction due to the significant increase in conversion.

Table 3.1: Effect of H_2S on the pyrolysis of C_3H_8 in an empty reactor, at 36 ms residence time.

	Temperature °K	Conversion %		Products, mole/100 moles of feed [Selectivity %]							Yield %	
		C_3H_8	H_2S	C_3H_6	C_2H_4	C_2H_6	CH_4	$C_{(s)}$	S_2	H_2	C_3H_6	C_2H_4
No H_2S	923	4	0	0.3 [24]	0.2 [10]	0.0 [0]	0.3 [7]	2.5 [59]	0.0	0.5	1	0
with H2S	923	8	4	0.4 [15]	0.5 [13]	0.0 [0]	0.5 [7]	5.1 [65]	0.1	0.5	1	1
No H_2S	1023	26	0	3.5 [39]	4.8 [35]	0.0 [0]	4.6 [17.1]	2.5 [9]	0.0	4.1	10	9
with H_2S	1023	46	2	5.2 [33]	6.1 [26]	0.4 [2]	6.6 [14]	12.5 [26]	0.1	5.4	15	12

Note: No H_2S feed= 66.7% N_2 and 34.2% C_3H_8 and with H_2S feed= 60.3% N_2, 34.9% C_3H_8 and 4.9% H_2S. See Appendix 3.1 for complete data table.

Equilibrium calculations were carried out to determine the predicted product distributions for the pyrolysis of propane, and the reaction with H_2S. The results of these calculations are shown in Table 3.2 and Table 3.3 below. The calculations were carried out with $C_{(s)}$ in the products in Table 3.2 and without $C_{(s)}$ in the products in Table 3.3. Calculations could not be completed for the pyrolysis reaction without $C_{(s)}$ in the products because the calculation requires all major products to be included in order for a solution to be found, and since $C_{(s)}$ is a major product of the pyrolysis reaction, excluding it from the set of products prevented the calculation from converging. In addition, the calculations look for solutions where the free energy of the system is minimized, and without carbon as an allowed product, a viable solution would not be available because no combination of the products would lead to a system with lower free energy than that of the original. Therefore, only the reaction of propane and H_2S is shown.

Table 3.2: Results of equilibrium calculations carried out to determine product distribution from the pyrolysis of C_3H_8 as well as the reaction between C_3H_8 and H_2S, with $C_{(s)}$ as an allowed product.

	Temperature °K	Products, mole/100 moles of feed								Conversion %		Yield % [Selectivity %]						
		H_2	C_3H_6	C_2H_4	C_2H_6	CH_4	CS_2	$C_{(s)}$	S_2	C_3H_8	H_2S	C_3H_6	C_2H_4	C_2H_6	CH_4	CS_2	$C_{(s)}$	S_2
no H2S	923	61.28	8.2E-10	3.9E-06	3.8E-04	3.8E+01	0.0E+00	6.5E+01	0.0E+00	100	0	0.00 [2E-09]	0.00 [8E-06]	0.00 [7E-04]	36.78 [36.78]	0.00 [0]	63.22 [63.22]	0.00
with H2S	923	62.35	8.6E-10	4.0E-06	3.9E-04	3.9E+01	1.9E-06	6.6E+01	1.7E-07	100	0	0.00 [2E-09]	0.00 [8E-06]	0.00 [8E-04]	36.88 [36.88]	0.00 [2E-06]	63.12 [63.12]	7.0E-06
no H2S	1023	74.05	1.4E-09	6.9E-06	3.4E-04	3.1E+01	0.0E+00	7.1E+01	0.0E+00	100	0	0.00 [4E-09]	0.00 [1E-05]	0.00 [7E-04]	30.56 [30.56]	0.00 [0]	69.44 [69.44]	0.00
with H2S	1023	75.35	1.4E-09	7.2E-06	3.5E-04	3.2E+01	3.7E-06	7.3E+01	3.6E-07	100	0	0.00 [4E-09]	0.00 [1E-05]	0.00 [7E-04]	30.67 [30.67]	0.00 [3E-06]	69.33 [69.33]	1.5E-05

Note: no H_2S feed = 66.65% N_2 and 34.18% C_3H_8 and with H_2S feed = 60.26% N_2, 34.89% C_3H_8 and 4.86% H_2S.

Table 3.3: Results of equilibrium calculations carried out to determine product distribution from the reaction of C_3H_8 with H_2S, without allowing $C_{(s)}$ as a potential product.

	Temperature °K	Products, mole/100 moles of feed										Conversion %		Yield % [Selectivity %]					
		N_2	C_3H_8	H_2S	H_2	C_3H_6	C_2H_4	C_2H_6	CH_4	CS_2	S_2	C_3H_8	H_2S	C_3H_6	C_2H_4	C_2H_6	CH_4	CS_2	S_2
Feed		60.26	34.89	4.86															
Product	923	60.26	0.18	0.00	0.01	7.47	9.76	1.14	40.81	2.43	0.00	99.48	100	21.41 [21.52]	18.65 [18.75]	2.17 [2.18]	38.99 [39.19]	2.32 [2.33]	0.00
Product	1023	60.26	0.09	0.00	0.04	6.32	15.68	0.85	41.19	2.43	0.00	99.75	100	18.11 [18.16]	29.96 [30.03]	1.62 [1.62]	39.35 [39.45]	2.32 [2.33]	0.00

The equilibrium calculations in Table 3.2 show that coke ($C_{(s)}$) and CH_4 should be the two major carbon products. Olefins are expected in trace quantities only, and conversion of C_3H_8 is expected to be complete (~100%). When H_2S is added to the reactant mixture, no significant difference was observed in the results. The product distributions of the reaction with and without H_2S were almost identical. Conversion of H_2S was less than 0.01% and only trace amounts of S_2 and CS_2 are expected. This differs considerably from what was seen experimentally, showing that the system might be manipulated usefully using kinetic control.

The calculations were carried out without $C_{(s)}$ in the products after the results (Table 3.2) showed that $C_{(s)}$ was the most thermodynamically favoured carbon product. Excluding carbon from the calculation allowed the system to be examined in a pseudo-kinetic manner. The data in Table 3.3, carried out without allowing $C_{(s)}$ in the products, shows that in the absence of coke, dehydrogenation and cracking will occur. At both temperatures, the amount of cracking is higher than the amount of dehydrogenation; however, the difference is greater at 1023 K. At both temperatures, near complete conversion of C_3H_8 is expected, and 100% conversion of H_2S is expected to occur. CS_2 is expected to be the only sulfur product obtained in meaningful quantities.

In the second set of experiments, the reaction was repeated with the reactor filled with a bed containing crystalline silica, a material that is expected to have no catalytic effect on the reactions taking place. The results of these experiments, which compare the gas-phase reaction of propane with and without H_2S over a bed of crystalline silica at 923 K and 1023 K, are shown in Table 3.4 and Figure 3.1 below.

Table 3.4: Effect of adding H_2S on the pyrolysis of propane over a silica bed at 35 ms contact time.

	Temp °K	Conversion %		Products, mole/100 moles of feed [Selectivity %]							Yield %	
		C_3H_8	H_2S	C_3H_6	C_2H_4	C_2H_6	CH_4	$C_{(s)}$	S_2	H_2	C_3H_6	C_2H_4
without H_2S	923	5	n/a	0.4 [22]	0.4 [14]	0.0 [0]	0.4 [7]	3.1 [57]	0.0	0.5	1	1
with H_2S	923	5	-1	0.9 [50]	1.2 [42]	0.0 [0]	1.2 [22]	-0.7 -[13]	-0.1	1.0	3	2
without H2S	1023	26	n/a	3.5 [37]	5.3 [37]	0.2 [2]	5.3 [18]	1.7 [6]	0.0	4.5	10	10
with H2S	1023	46	-2	7.1 [44]	7.5 [31]	0.8 [3]	8.2 [17]	2.8 [6]	-0.1	6.0	20	14

Note: H_2S feed= 65.3% N_2 and 36.6% C_3H_8 and with H_2S feed= 60.6% N_2, 35.6% C_3H_8 and 4.9% H_2S. See Appendix 3.2 for complete data table.

Note: The conversion of H_2S obtained from the experimental data after calculations show a negative value even though true conversion can never be negative. These data show that the amount of H_2S in the outlet stream was higher than that in the inlet (as calculated from inlet samples taken at the beginning of the experiment). H_2S, being the feed component in the lowest amount, is expected to have a greater amount of error (as shown in section 2.5). As well, in general, H_2S as a component seemed to have the greatest amount of error in its measurement and therefore when conversion was close to zero, the data sometimes showed more H_2S in the outlet than the inlet leading to negative H_2S conversions.

Additionally, $C_{(s)}$ values as calculated from the mass balance of all carbon products also suffered from negative values at times. A negative value for the amount of $C_{(s)}$ implied that more carbon was found in the outlet than was measured in the inlet and is a consequence of the errors in the system, more so at lower conversions where the products are produced in lower amounts and therefore may have a greater amount of error attached to the measurement of these

components. In general, the amount of negative $C_{(s)}$ was within 5% of the amount of alkane in the system for any given experiment.

The advantage of adding H_2S to the reaction mixture was evident in the data obtained. The propylene yield increased from 1% to 3% and from 10% to 20% at 923 K and 1023 K, respectively. An increase in conversion from 26% to 46% was observed at 1023 K due to the addition of H_2S to the reaction.

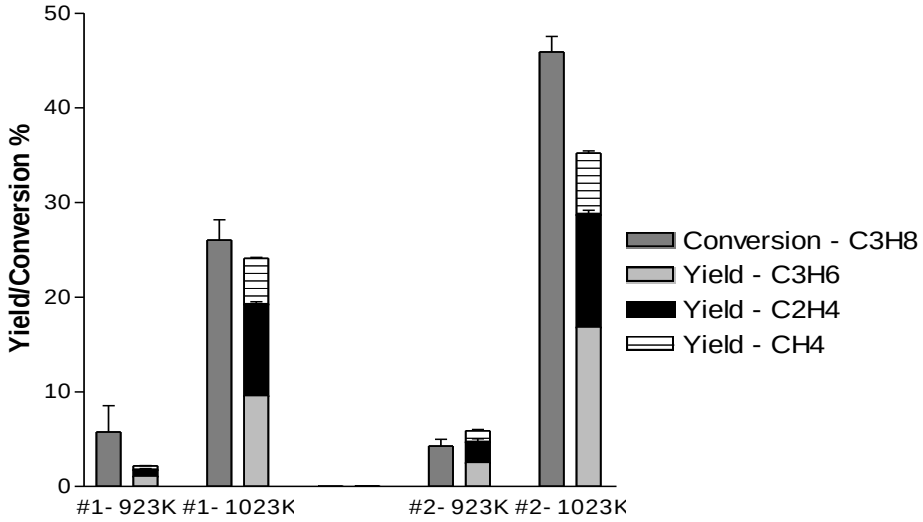

Figure 3.1: Comparison of the product distributions between the reaction of propane without H_2S (Exp #1) and with H_2S (Exp #2) using an inert silica bed. (based on data from Table 3.4)

If it is assumed that there are no catalytic contributions from silica, then the increase in conversion of propane/yield of propylene must be attributed to the addition of H_2S to the reactant mixture. At 1023 K, a greater amount of H_2S dissociation is expected to occur, producing a greater amount of S_2 for the reaction, hence explaining the significant increase in conversion at the higher temperature. In addition, this result also suggests that the presence of H_2S affects the initiation step of the reaction.

An interesting observation noted was the change in product distribution. More specifically, a disproportionate increase in the yield of cracking products such as ethylene and methane was observed, compared to the increase in propylene at 923 K. While the yield of propylene increased by 200% when H_2S was added to the reaction mixture, the yield of ethylene only increased by 100%. This suggests that the addition of H_2S to the reaction causes one pathway (dehydrogenation) to be favored more than another (cracking). If H_2S played no role in the actual reaction pathway, then the product distribution between dehydrogenation products and cracking products would be the same for both the experiment with, and the one without H_2S; however, the results showed that this was not the case. In previous work reported in the literature on the pyrolysis of propane, the authors showed that at low conversions (10% or less), the dehydrogenation and cracking products were produced in equimolar quantities, and when the conversion was increased, cracking products were produced in greater quantities.[146] Those results fit the experimental reaction carried out without H_2S, where at 923 K, conversion was ~5% and C_3H_6 and C_2H_4 were produced in approximately equimolar quantities, and at 1023 K when conversion of C_3H_8 increased to 26%, the mole % of C_2H_4 obtained was 5.3% while that of C_3H_6 was only 3.5%. However, when H_2S was added to the reaction, a higher conversion was obtained, ~46% at 1023 K, and yet the mole % of C_3H_6 and C_2H_4 were 7.1% and 7.5% respectively, which is close to equimolar. At such high conversions, the amount of C_2H_4 produced is expected to be significantly higher than that of C_3H_6, and this may imply that cracking reactions were somewhat inhibited and dehydrogenation processes were somewhat favored in exchange, due to the addition of H_2S.

The addition of H_2S to the reaction enhanced the selectivity to propylene at both reaction temperatures. The selectivity is expected to decrease when the reaction temperature is increased

from 923 K to 1023 K — similar to that for a typical ODH reaction, where selectivity decreases as conversion increases. This trend was indeed observed by the drop in selectivity from 50% at 923 K to 44% at 1023 K. The results shown in Table 3.4 are also for a homogeneous reaction; however, the presence of crystalline silica (compared to an empty reactor in Table 3.1) seemed to benefit the reaction with H_2S significantly. However, the results for the pyrolysis reaction remained similar for both the experiment carried out in an empty reactor and for the experiment carried out using a silica bed. It has been suggested in the literature that inert silica, as a material, quenches free radical reactions,[20] which in this case was shown to be beneficial to the reaction. However, it should be stated that silica is not known to have any catalytic effect on the reaction otherwise.

Details on the reaction between propane and sulfur and its comparison to the reaction between propane and oxygen could not be found in the literature. One report that may be relevant is that done by Savchenko et al. who carried out thermodynamic calculations on the reaction of methane and sulfur, and looked at the formation of partial oxidation and oxidative coupling products.[147] Calculations for the reaction using oxidants other than oxygen were also carried out. The results showed that conversion of methane was expected to be higher when O_2 was used as an oxidant compared to S_2.

3.1.2 The Catalytic Reaction

Similar experiments were then carried out using a 5% VO_x/silica catalyst (Table 3.5, Figure 3.2). Cross comparison to the data in Table 3.4 allows determination of the effect of H_2S, as well as the true effect of the catalyst.

Table 3.5: Effect of adding H_2S on the pyrolysis of propane over a 5% VOx/Silica bed at 35 ms contact time.

	Temp °K	Conversion %		Products, mole/100 moles of feed [Selectivity %]							Yield %	
		C_3H_8	H_2S	C_3H_6	C_2H_4	C_2H_6	CH_4	$C_{(s)}$	S_2	H_2	C_3H_6	C_2H_4
Without H_2S #3	923	4	0	0.9 [58]	0.6 [25]	0.0 [0]	0.6 [13]	0.2 [5]	0.0	1.3	2	1
With H_2S #4	923	8	-7	2.3 [79]	1.1 [24]	0.0 [0]	1.1 [13]	-1.4 -[16]	-0.1	2.9	6	2
Without H_2S #4	1023	28	0	3.8 [37]	5.6 [36]	0.0 [0]	5.3 [16.97]	3.1 [10]	0.0	4.5	11	10
With H_2S #4	1023	48	-9	7.4 [43]	8.0 [31]	0.7 [3]	9.5 [19]	2.5 [5]	-0.1	6.7	21	15

Note: H_2S feed= 65.26% N_2 and 36.34% C_3H_8 and with H_2S feed= 62.07% N_2, 35.65% C_3H_8 and 4.70% H_2S. See Appendix 3.3 for complete data table.

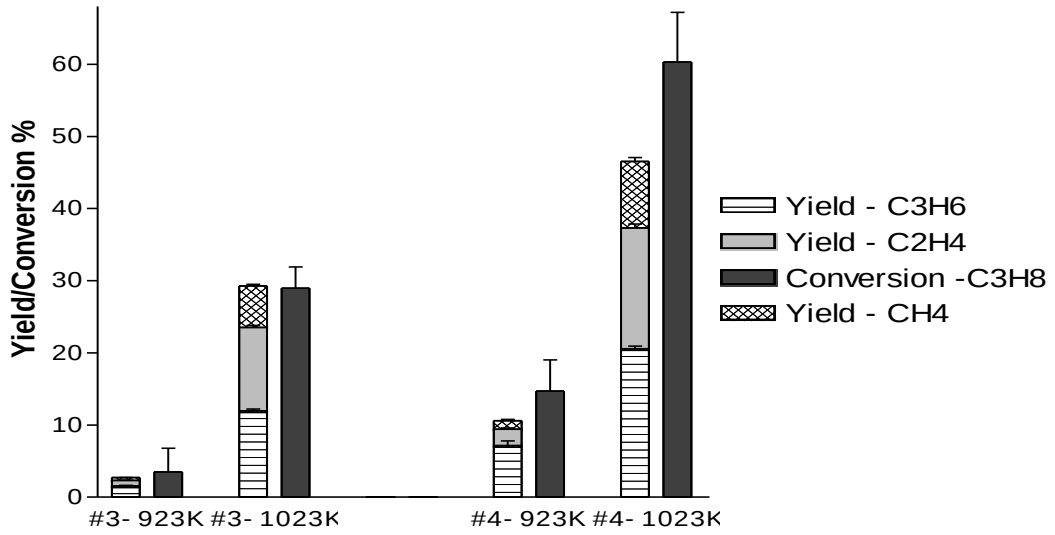

Figure 3.2: Comparison of the product distributions between the reaction of propane without H_2S (Exp #3) and with H_2S (Exp #4) on a 5%VOx/silica catalyst. (based on data from Table 3.5)

The data presented in Table 3.5 shows that the activity of the catalyst increased when H_2S was added to the reaction mixture, as shown by the increase in conversion of C_3H_8 from 4% to 8%. The true contribution from the catalyst itself can only be found by comparing the data from the H_2S-containing experiments in Tables 3.4 and 3.5, as both have the same reactant

components, but one is carried out over crystalline silica (inert) (Table 3.4), and the other is carried out over the vanadium catalyst (Table 3.5). The conversion of C_3H_8 increased from 5% to 8% by the addition of the catalyst at 923 K. The difference in conversion at 1023 K is much smaller and only increased from 46% to 48%.

Addition of H_2S to the catalytic reaction (Table 3.5) caused an increase in the selectivity towards C_3H_6. The ratio between the propylene to ethylene yields was found to be higher for the reactions with H_2S present. Since the main difference between the two experiments is H_2S, this suggests that the dehydrogenation pathway may be favored to a greater extent than the cracking pathway, when a catalyst is used in the presence of H_2S. Since this trend was also seen for the reaction over a crystalline silica (inert) bed, it is likely that the true cause of the effect is the addition of H_2S and not the catalyst; however, it can be said that the catalyst does not interfere with the trend reported.

Reports on the dissociation of H_2S on a silica supported-vanadium oxide surface were not found in the literature, but the catalytic dissociation of H_2S on pure vanadium oxide, as well as alumina-supported vanadia catalysts, has been reported.[138,148] In the case of pure vanadium oxide, H_2S reacts initially to sulfide the vanadia according to equation [3.15].[138]

[3.15] $5H_2S + V_2O_5 \rightarrow V_2S_3 + 5H_2O + 2S^0$

The resulting vanadium sulfide species acts as a catalyst for continuous dissociation of H_2S according to equations [3.16]-[3.17] below:

[3.16] $V_2S_3 + 5H_2S \rightarrow 2VS_4 + 5H_2$

[3.17] $2VS_4 \rightarrow V_2S_3 + 5S^0$

The formation of sulfur and V_2S_3 was detected by the authors using X-ray analysis. The activity of the vanadia and alumina-supported vanadia catalysts was measured by monitoring the production of H_2 by gas chromatography over time. Sulfiding of alumina-supported vanadia was reported to occur in a similar manner as that of the bulk vanadia. At 673 K, sulfidation results in the reduction of supported (micro) crystalline V_2O_5 to V_2O_3.[148] It was reported that the surface of the vanadia crystallites is sulfided to a greater extent, unlike highly dispersed vanadium oxide species, which are sulfided and reduced only partially.

The above reactions [3.15-3.17] are a viable pathway for the continuous generation of the oxidant (S_2) used for reaction with propane, but the exact contribution of this pathway is unknown, as two possible pathways exist for production of S_2, thermal or catalytic dissociation of H_2S, especially at higher temperatures. In a typical ODH reaction using oxygen as the oxidant, the first step is generally accepted as hydrogen abstraction by vanadyl oxygen.[132,6] At this point, the propyl radical may desorb into the gas phase for further homogeneous reaction.[20] Alternatively, this species may react at the surface via a second hydrogen abstraction (on the same or adjacent site), leading to formation of H_2O on a reduced vanadia site and propylene. The H_2O is then desorbed into the gas phase either independently, leaving a reduced site that needs to be oxidized, or in a concerted manner with desorption of H_2O and re-oxidation of the reduced site by another oxidant molecule occurring in the same step. Either way, it is this final step that requires an oxidant for the catalytic cycle to continue. In the case of the reaction between H_2S and propane on the catalyst, H_2S itself cannot carry out the re-oxidation of the reduced site, as it is already a reduced species. However, if some of the vanadium oxide centers on the catalyst are sulfided in the initial stages of the reaction to form vanadium sulfide sites, those sites can

continuously produce sulfur and hydrogen via catalytic dissociation of H_2S[138] hence providing an oxidant (sulfur) for the regeneration step of the catalyzed surface reaction.

Alternatively, the S_2 produced by the sulfided vanadia can desorb into the gas phase and react homogenously with propane to produce propylene and H_2S. In this situation, although the oxidative reaction does not occur heterogeneously, the production of an oxidant (S_2) requires a catalyst. Hence, the generation of S_2, whether thermally or by the catalyst, is key for continuation of the oxidative dehydrogenation reaction. However, the true role of S_2 once it is generated is ambiguous, as it can play a role in both gas-phase and surface-catalyzed mechanisms. And similarly, the true role of the active sites on the catalyst is also ambiguous, as they can be used to generate the oxidant (S_2) or participate directly in a surface catalyzed reaction — and which of these processes is dominant at the reaction conditions is unknown.

3.2 Effect of the Amount of H_2S

The amount of H_2S used in the reaction should play a significant role, since it is the only source of oxidant. The amount of H_2S in the reactant gas stream is therefore directly related to the amount of oxidant (sulfur) available for reaction with propane. In the case of vanadia catalysts supported on alumina, the authors reported the H_2S decomposition reaction as being first order with respect to H_2S concentration.[138] As previously stated, the amount of conversion expected at 1023 K is less than 10%, which in turn means that the true conversion amount given an inlet percentage of 3.4% is approximately 0.3% or less. Therefore, it can be expected that the true contribution from increasing the inlet H_2S amount from 3.4% to 6.8% will be approximately 10% of the difference, or less than 0.34%. At 923 K, the actual conversion of H_2S will be well lower than 10% of the inlet amount. However, at the lower temperature of 923 K, there is also

less thermal dissociation of H_2S in the gas phase; hence the effects observed as a result of doubling the amount of inlet H_2S will be to a greater extent from catalytic dissociation of H_2S (rather than thermal processes). At 823 K, it can be expected that thermal dissociation of H_2S will be even less, and hence the effect observed will be mostly due to the catalytic reactions. For this reason, experiments were carried out using feeds with varying amounts of H_2S to observe how changing the amount of H_2S influences the reaction. The results are shown in Table 3.6, below.

Table 3.6: Conversion of propane and yield of olefins as a function of the amount of H_2S in the reactant gas stream (40 ms contact time)

C_3H_8 : H_2S ratio	Temp °K	Conversion %		Products, mole/100 moles of feed [Selectivity %]							Yield %	
		C_3H_8	H_2S	C_3H_6	C_2H_4	C_2H_6	CH_4	$C_{(s)}$	S_2	H_2	C_3H_6	C_2H_4
10.41	823	3	-10	0.9 [76]	0.0 [0]	0.0 [0]	0.0 [1]	0.8 [23]	-0.1	1.2	2	0
4.96	823	4	-10	0.9 [58]	0.0 [0]	0.0 [0]	0.0 [0]	1.9 [42]	-0.2	1.1	2	0
3.64	823	10	0	1.0 [27]	0.0 [0]	0.0 [0]	0.0 [<1]	8.2 [73]	0.5	1.2	3	0
10.41	923	14	-5	2.0 [42]	0.7 [10]	0.0 [0]	0.7 [5]	8.3 [44]	0.0	2.3	6	1
4.96	923	14	-10	2.5 [51]	0.8 [11]	0.0 [0]	0.9 [6]	4.8 [32]	-0.1	2.9	7	2
3.64	923	15	-4	2.9 [50]	0.9 [11]	0.0 [0]	1.0 [6]	5.9 [34]	-0.3	3.5	8	2
10.41	1023	51	-11	6.4 [36]	7.8 [29]	0.9 [3]	8.8 [16]	8.3 [15]	-0.1	6.0	18	15
4.96	1023	55	-11	7.1 [37]	8.8 [31]	0.9 [3]	9.4 [16]	7.2 [13]	-0.1	6.0	20	17
3.64	1023	55	-6	8.5 [41]	9.6 [30]	0.8 [2]	11.1 [18]	5.7 [9]	-0.3	7.6	22	17

Note: Detailed feed amounts can be found in the full data table in Appendix 3.4.

The results at 823 K show that conversion of C_3H_8 increased as the amount of H_2S was increased. It can be expected that the greater the initial amount of H_2S, the greater the amount of oxidant generated (if the catalytic reaction is first order or higher with respect to the

concentration of H_2S), and the greater the amount of oxidant in the system, the higher will be the conversion of C_3H_8. At 923 K, the amount of C_3H_8 converted will be a result of thermal initiation via pyrolysis of C_3H_8, as well as initiation by any oxidant generated due to H_2S dissociation (thermal and catalytic). The increased contributions from thermal processes overshadow the trends more and more as temperature is increased.

The trends observed in C_3H_6 selectivity were different at the lowest reaction temperature compared to the other two reaction temperatures. At 823 K, the selectivity to C_3H_6 decreased significantly as the amount of H_2S increased, from 75.5% at a 10.4 C_3H_8: H_2S ratio to 27.0% at a 3.6 C_3H_8: H_2S ratio. In exchange, the lost carbon content went towards increased selectivity to $C_{(s)}$, which increased from 23.1% to 72.5% as the feed ratio was changed from 10.4 to 3.6 C_3H_8: H_2S ratio. C_3H_6 and $C_{(s)}$ were the only two major carbon products obtained at 823 K.

At 923 K, cracking products such as C_2H_4 and CH_4 were observed, and the selectivity towards these products showed a general increasing trend as the amount of H_2S was increased. The selectivity to C_3H_6 also increased with increasing amounts of H_2S, which is opposite to the trend observed at 823 K. In return, the selectivity to $C_{(s)}$ decreased as the amount of H_2S increased. At 1023 K, the same increasing trend is observed for C_3H_6 and C_2H_4 selectivity, but with a smaller magnitude. At this temperature, the effects of increasing H_2S are reduced to a ~5% increase in C_3H_8 conversion and C_3H_6 selectivity. Since cracking and other thermal processes occur at these temperatures and these reactions cannot be completely inhibited at the reaction conditions used, it thereby reduces any gains obtained from varying the amount of H_2S. This might make increasing the amount of H_2S, as an optimization strategy, uneconomical at higher temperatures.

3.3 Effect of Contact Time

Contact time as a parameter should make a difference in this reaction, since the initial reaction (dissociation of H_2S to form SH• radicals or S_2) may be significantly affected by contact time. In addition to the dissociation of H_2S, initiation of the reaction may occur via pyrolysis and this may also be affected by contact time; therefore, it is possible that the effects seen in the data below are a combination of the effect of contact time on both types of initiation steps possible in this reaction mixture. The reaction was investigated at various contact times ranging from 18 ms to 158 ms, and the data are shown in Table 3.7 below.

Table 3.7: Conversion of propane and yield of olefins as a function of contact time of the reactant gas stream.

Contact time (ms)	Temp °K	Conversion %		Products, mole/100 moles of feed [Selectivity %]							Yield %	
		C_3H_8	H_2S	C_3H_6	C_2H_4	C_2H_6	CH_4	$C_{(s)}$	S_2	H_2	C_3H_6	C_2H_4
18	823	4	-1	0.5 [34]	0.0 [0]	0.0 [0]	0.0 [0]	2.9 [66]	0.1	0.7	1	0
35	823	4	-6	0.5 [34]	0.0 [0]	0.0 [0]	0.1 [3]	2.6 [63]	-0.1	0.7	1	0
158	823	13	-7	4.4 [55]	0.0 [0]	0.0 [0]	0.2 [<1]	10.8 [45]	-0.1	5.5	7	0
18	923	12	-3	1.6 [40]	1.0 [17]	0.0 [0]	1.0 [9]	4.1 [34]	0.1	1.7	5	2
35	923	15	-7	2.5 [48]	1.2 [15]	0.0 [0]	1.3 [8]	4.4 [28]	0.0	3.0	7	2
158	923	24	-9	9.3 [60]	1.8 [8]	0.3 [1]	2.3 [5]	12.0 [26]	-0.2	7.4	14	2
18	1023	54	1	6.3 [34]	7.7 [27]	0.9 [3]	9.8 [17]	10.6 [19]	0.3	6.0	18	15
35	1023	55	-8	7.1 [38]	8.7 [31]	1.0 [3]	9.6 [17]	6.5 [11]	0.1	6.9	21	17
158	1023	60	-9	14.7 [38]	17.5 [30]	4.3 [7]	20.2 [17]	8.2 [7]	-0.3	8.2	23	18

Note: 18, 35 ms experiments feed = 61.3% N_2, 34.8% C_3H_8 and 4.9% H_2S and 158 ms experiment feed = 32.3% N_2, 64.0% C_3H_8 and 8.3% H_2S. See Appendix 3.5 for complete data table.

The data in the table above show that conversion of C_3H_8 generally increased with contact time. At 823 K, the conversion tripled from 4% to 13% due to the contact time increase from 18 ms to 158 ms. This increase is only double (from 12% to 24%) at 923 K, and at 1023 K the conversion increased by 6%, which is only an 10% relative increase (from 54% to 60%). The increases were greater at lower temperatures, where there is a lower contribution from thermal processes. More interestingly, the selectivity to C_3H_6 at all temperatures increased as contact time was increased, which is abnormal, since selectivity is expected to decrease at higher contact times and higher conversions. This shows that contact time can be used to optimize the yield of C_3H_6, especially at the lower temperatures. The selectivity towards C_3H_6 as a function of temperature increases initially and then drops as temperature is increased further. For example, for the reaction at 35 ms, the selectivity increased from 34% to 48% when the temperature increased from 823 to 923 K, but then dropped to 38% when the temperature was increased further to 1023 K. The same trend would be expected for contact time as well; therefore, contact time will eventually cause a decrease in selectivity towards C_3H_6 if it is increased further. However, at 158 ms the maximum selectivity seemed not to have passed its peak yet.

Another interesting observation is in regards to selectivity towards coke ($C_{(s)}$), which showed a decrease as contact time was increased. This trend was observed at all three reaction temperatures tested. It would be expected that as contact time is increased, the system would move closer and closer to equilibrium conditions, and at equilibrium conditions carbon is the most favorable product; however, this was not found to be the case experimentally. It has been reported previously that sulfur compounds (including H_2S) catalyze decomposition of saturated hydrocarbons and increase the yield of primary products such as light olefins, and also act on radical propagation reactions, which results in reduced coke formation.[149]

The overall yield of C_3H_6 increased as a function of contact time due to the increased conversion of C_3H_8 as well as increased selectivity towards C_3H_6, and this trend was the same at all three reaction temperatures. The best combination of reaction conditions of those in Table 3.7 was a temperature of 1023 K using a contact time of 158 ms, where C_3H_6 and C_2H_4 selectivity was 38% and 30% respectively (for a combined olefin selectivity of 68%), resulting in a yield for C_3H_6 and C_2H_4 of 23% and 18% respectively, at a conversion of 60%.

3.4 Effect of % Vanadia in the Catalyst

The amount of vanadia available in the catalyst for reaction pertains to its dispersion. It has been reported that for a well dispersed catalyst, monomeric and dimeric units of vanadium oxide are present on the surface.[150] As the percentage of vanadia increases, the monomeric units begin to coalesce resulting in polymeric units. The monomeric and polymeric units of vanadia are reported as being active and selective for the oxidative dehydrogenation of light alkanes.[132,30] The crystallites, however, have been reported to be active but not selective to the desired partial oxidation products (propylene), and instead lead to total oxidation in the presence of oxygen, producing CO_x. The reaction of propane with H_2S or S_2 on these catalysts has not previously been reported.

The reaction of C_3H_8 with H_2S was carried out over catalysts containing different amounts of vanadium oxide ranging from 1 to 10 weight percent (see Table 2.1 for actual %V values), and the results of these experiments are shown in Table 3.8, below. The first trend observed in the data was the decrease in conversion when the amount of vanadia on the catalyst was increased, and this was observed at all the reaction temperatures investigated. This trend could be due to the dispersion of vanadia sites on the surface of the catalyst, as more active sites

may be readily accessible on highly dispersed catalysts compared to catalysts that have a higher amount of the active component but lower dispersion, where some of the active component is not readily accessible for catalytic reactions. Additionally, the surface area of these catalysts may also play a role, as the surface area was found to decrease as a function of the amount of vanadia deposited on the surface of the catalyst. With a lower surface area, a smaller number of molecules can interact with a catalyst particle at any given time, and this may affect the activity of the catalyst.

Table 3.8: Effect of the amount of vanadium content (40 ms, feed ratio of C_3H_8: H_2S: N_2 = 35%: 5%: 60%).

Catalyst	Temp °K	Conversion %		Products, mole/100 moles of feed [Selectivity %]							Yield %	
		C_3H_8	H_2S	C_3H_6	C_2H_4	C_2H_6	CH_4	$C_{(s)}$	S_2	H_2	C_3H_6	C_2H_4
1%VOx/CS	823	7	3	0.9 [36]	0.0 [0]	0.0 [0]	0.2 [2]	4.4 [61]	0.1	1.1	2	0
2.5% VOx/CS	823	3	7	0.3 [29]	0.0 [0]	0.0 [0]	0.0 [0]	2.2 [71]	0.2	0.5	1	0
10% VOx/CS	823	3	7	0.2 [19]	0.0 [0]	0.0 [0]	0.0 [1]	2.5 [80]	0.2	0.5	1	0
1%VOx/CS	923	17	2	3.0 [49]	1.3 [13]	0.0 [0]	1.4 [8]	5.4 [29]	0.1	3.5	8	2
2.5% VOx/CS	923	8	6	1.5 [57]	0.8 [20]	0.0 [0]	0.9 [11]	0.9 [11]	0.2	2.3	4	2
10% VOx/CS	923	5	4	1.0 [51]	0.7 [23]	0.0 [0]	0.7 [12]	0.8 [14]	0.1	1.4	3	1
1%VOx/CS	1023	56	9	6.6 [33]	8.1 [27]	0.9 [3]	8.9 [15]	13.6 [23]	0.2	6.2	18	15
2.5% VOx/CS	1023	51	4	7.2 [40]	7.7 [28]	0.7 [3]	8.6 [16]	7.5 [14]	0.1	7.0	20	14
10% VOx/CS	1023	47	4	6.8 [41]	7.3 [29]	0.6 [2]	8.3 [17]	5.5 [11]	0.1	6.7	19	14

Note: Feed was composed of 62.3% N_2, 35.8% C_3H_8 and 5.1% H_2S. See Appendix 3.6 for complete data table.

The trends in selectivity towards C_3H_6 were plotted in Figure 3.3 below as a function of the amount of vanadia on the catalyst, for all three reaction temperatures.

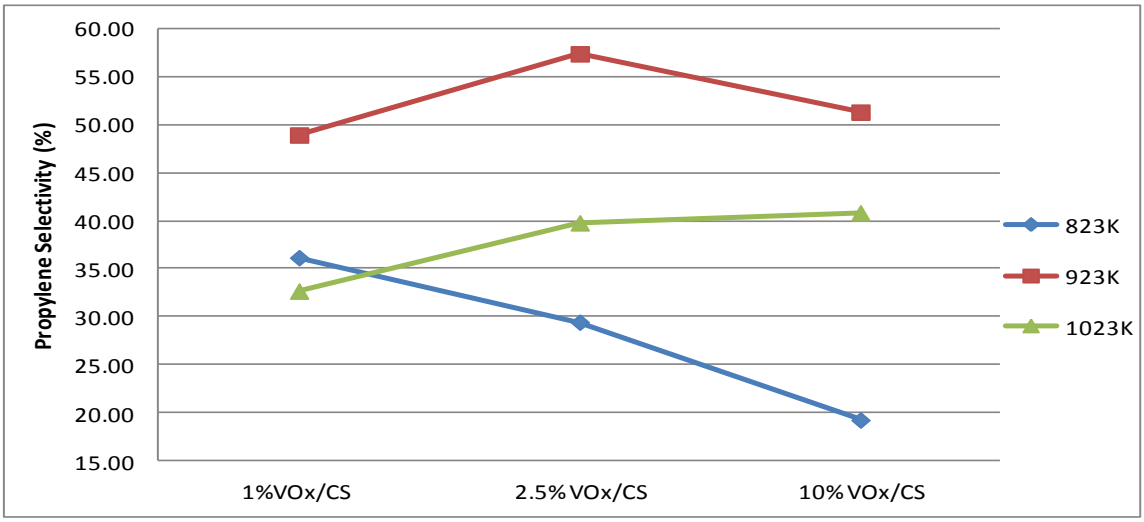

Figure 3.3: Plot of selectivity as a function of the amount of vanadia on the catalyst for all three reaction temperatures. Data is taken from Table 3.8, above.

From this figure, the change in trends at the different temperatures can be observed. The selectivity to propylene at 823 K shows a decreasing trend as the % vanadia in the catalysts is increased. When the temperature is increased to 923 K, the selectivity towards C_3H_6 increases first and then decreases, and at 1023 K, the selectivity increases as the amount of vanadia on the catalyst is increased. The trends are different at different temperatures; however, an analysis of the contributing factors at each of these reaction temperatures can offer a possible explanation. At the lowest temperature, the majority of the activity (conversion of C_3H_8) can be attributed to the effect of the catalyst, as initiation of the reaction by thermal processes is very low. It is at this temperature that the effect of the catalyst is expected to be seen, and what is observed is that the catalyst containing the lowest amount of vanadia has the highest selectivity. This effect may be related to the nature of the active sites on each of these catalysts. When the reaction temperature is increased, a greater contribution from thermal processes (which consists of both thermal dissociation of H_2S and the pyrolysis of C_3H_8 itself) is expected. Another point of consideration is also the relationship between conversion and selectivity. The difference in conversion between

the 1% VO_x/CS catalyst and the 2.5% VO_x/CS catalyst is significant, so it can be expected that if the catalyst played no role, the selectivity towards C_3H_6 would be lower for the 1% VO_x/CS catalyst, due to its higher conversion. Therefore the change in the selectivity trend is likely because of the thermal contributions to this reaction, which can start to overshadow some of the catalytic effects, and the resulting trend observed is a combination of effects from changing the amount of vanadium as well as the effect of temperature on the pyrolysis reaction.

3.5 Other Mechanistic Inferences

Some studies were later conducted to determine the role of surface sites. In these experiments, a stream of H_2S diluted with N_2 was passed over the catalyst at 823 K for approximately 5 hours, after which the system was purged with N_2 overnight. After confirming that no residual H_2S was present in the gas stream, and that the outlet gas stream contained nothing other than N_2 (by gas chromatography), a stream of propane diluted by nitrogen was passed over the catalyst, and the outlet stream was analyzed by gas chromatography at various times after the propane stream was initiated. Two products, C_3H_6 and H_2S, were found in the outlet stream in addition to the reactant gases (C_3H_8 and N_2). The presence of H_2S confirms that vanadium oxide does indeed get sulfided when H_2S is passed over it at high enough temperatures, such as the ones used in this work. A partially sulfided monomeric site might look something like the one shown below.

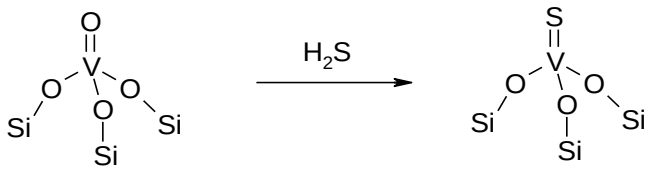

These sulfided sites are then used in the oxidative dehydrogenation of propane liberating H_2S. A suggested reaction scheme is shown below.

[3.18] $H_2S + V_2O_5 \rightarrow H_2O + V_2O_4S$

[3.19] $V_2O_4S + C_3H_8 \rightarrow C_3H_6 + H_2S + [V_2O_4]$

For the re-oxidation of the spent active site, O_2 is known to carry out this process according to equation [3.20], so it is hypothesized that S_2 could probably do so in a similar way as shown in equation [3.21].

[3.20] $[V_2O_4] + ½\ O_2 \rightarrow V_2O_5$

[3.21] $V_2O_4 + ½S_2 \rightarrow V_2O_4S$

In addition, the amount of H_2S liberated decreased with time on stream, as did the amount of C_3H_6 produced. The amount of H_2S decreased to zero, and the amount of C_3H_6 obtained decreased to a steady state amount significantly lower than the initial amount. This showed that as the sulfided sites were consumed, C_3H_6 formed, and once these sites were depleted, only C_3H_6 from the pyrolysis reaction was observed. These observations are similar to those of vanadyl oxygen that are present on the surface of supported vanadia catalysts and are used in the oxidative dehydrogenation of propane with O_2, then are eventually liberated as H_2O. To confirm that this effect only occurred for the catalytic reaction, the same experiment was carried out over a crystalline silica bed, and no H_2S was observed in the product stream when propane flow was initiated.

3.6 Conclusions

The study of oxidative dehydrogenation of propane in the presence of H_2S was carried out. The reaction was compared to the thermal pyrolysis of propane under similar conditions, for

both the homogenous and catalytic reaction. For the homogenous reaction using a filled inert bed, addition of H_2S to the reactant stream increased the conversion of propane, selectivity to propylene and the overall yield of propylene. In the gas phase, the reaction is likely to be initial thermal decomposition of H_2S to produce S_2 and H_2, followed by reaction of propane with the S_2 produced. The resulting products are propylene and H_2S, which is regenerated and may be recycled in an industrial process. For the catalytic reaction, the exact nature of the contribution from the catalyst is unknown; however, at least two possibilities exist. What is known is that partial or complete sulfidation of the vanadia on the surface of the catalyst occurs. Whether this sulfided site participates directly by reaction with propane (similar to the mechanism proposed for the reaction of propane with O_2 on a vanadia catalyst) or whether the sulfided sites are only sites for further decomposition of H_2S (to produce S_2 which is then desorbed into the gas phase for use in a homogenous reaction) is unknown, as in-situ analysis was not carried out.

Additionally, the decomposition of H_2S step has a low conversion rate (~ 10% at 1133 K), so increasing the amount of H_2S as a way to increase the overall conversion/selectivity requires significantly more H_2S to be added to the gas stream for a noticeable effect when the reaction is carried out at lower temperatures.

The amount of vanadia and hence its dispersion on the support also plays a role in the activity and selectivity of the reaction. It was observed at 823 K, where catalytic contributions are more significant, that increasing the vanadium content from 1% to 10% resulted in a lowering of the selectivity to propylene. This effect is similar to that seen for other vanadia systems for the oxidative dehydrogenation of alkanes using oxygen as the oxidant, and is attributed to the type of surface vanadia site (monomeric, polymeric or crystallite) that is present on the catalyst surface.

For this work, the reactions were carried out at 823 K, 923 K and 1023 K, each being chosen for a different reason. At 823 K and 923 K, the effects of changing reaction parameters can be seen more readily, as contributions from thermal processes are lower. However, for industrial processes, higher conversions are required; hence, carrying out the experiments at the higher temperature of 1023 K provides data that may be important in evaluating the reaction's industrial potential. Of course, contributions from thermal versus catalytic processes will be significantly different at the two temperatures. The general observation was that contributions from thermal processes overshadow the differences in catalytic activity from changing various parameters at 1023 K. Also, at this temperature, the thermal processes themselves (notably the decomposition of H_2S) are quite efficient on a comparative scale, hence begging the question, "Is a catalyst even required?"

Chapter 4: H_2S-assisted Oxidative Dehydrogenation of Propane

4.0 Introduction to Concept and Explanation of Proposed Chemistry

The reaction of C_3H_8 with O_2 and H_2S was investigated and the details of this work are presented in this chapter. In comparison to the ODH of propane with O_2, the addition of H_2S allows for a different reaction pathway to occur; reaction of O_2 with H_2S to produce sulfur which can then react as a less potent oxidant with C_3H_8 to produce propylene. The reaction between O_2 and H_2S can be expected to proceed at a faster rate than that between O_2 and C_3H_8 (or another saturated hydrocarbon), as the S-H bond (BDE - 89 kcal/mol) is weaker and, most probably, easier to break than a C-H bond (BDE 104 kcal/mol in CH_4). A thermodynamically favored process during oxidative dehydrogenation of propane is the formation of carbon oxides and H_2O. This occurs when O_2 is used as the sole oxidant. Although the stability of carbon-oxygen bonds is the driving force for the reaction with O_2, the carbon-sulfur single bond is considerably weaker and, for this reason, the formation of carbon sulfides at the reaction temperatures > 850 K is not as favorable and will, therefore, limit production of organosulfur compounds such as propanethiol.

H_2S is a highly flammable gas with lower and upper flammability limits for H_2S-air of 4.3% H_2S and approximately 45% H_2S, respectively.[151] The oxidation of H_2S in the gas phase is an important part of the Claus sulfur recovery plant.[152-153] The original Claus process was established in the late 1800's and later modified in 1936 by I.G. Farben to the two-step oxidation that is still being used today. [153-155] The basic technology has not been modified in over 70 years, apart from the introduction of advanced tail gas treatment add-ons. As an important industrial reaction, the oxidation of H_2S and the Claus reaction has been well studied, including the

fundamental reactions occurring in these processes; reports, as well as review articles, can be found in the literature.[156-157] When the reaction is carried out in the gas phase, products can include SO_2, S_2 (or other forms of elemental sulfur, depending on the reaction temperature), H_2, H_2O. When the reaction is carried out with an excess of O_2, such as those of the Claus furnace, SO_2 and H_2O are the major products. However, at lower O_2 ratios, elemental sulfur and H_2O are the major products, as shown in the equations below.

[4.1] $H_2S + (3/2)O_2 \rightarrow SO_2 + H_2O$

[4.2] $H_2S + (1/2)O_2 \rightarrow H_2O + (1/n)S_n$

Other equations of importance are the Claus reaction itself [4.3], as well as the decomposition of H_2S [4.4, 4.5] to produce H_2, S_2 or SH radicals, as shown below.

[4.3] $SO_2 + 2H_2S \rightarrow 2H_2O + (3/n)S_n$

[4.4] $H_2S \rightarrow H_2 + (1/2)S_2$

[4.5] $H_2S \rightarrow SH\bullet + H\bullet$

As the system is a chemical equilibrium, the various amounts of each of the products will depend on the pressure, temperature, residence time and feed ratio of the reactants within the reaction.

4.0.1 Oxidation of H_2S and Influence of the H_2S:O_2 Ratio

The ratio of H_2S to O_2 in the feed can have a significant influence on the products obtained. As would be expected, the higher the amount of O_2 present, the greater the percentage of SO_2 produced and the lower the amount of O_2 present, the greater would be the amount of S_2. The equilibrium product for the reaction of H_2S and O_2 in different ratios is shown in Figure 4.1, below. The corresponding data table is available in Appendix 4.1.

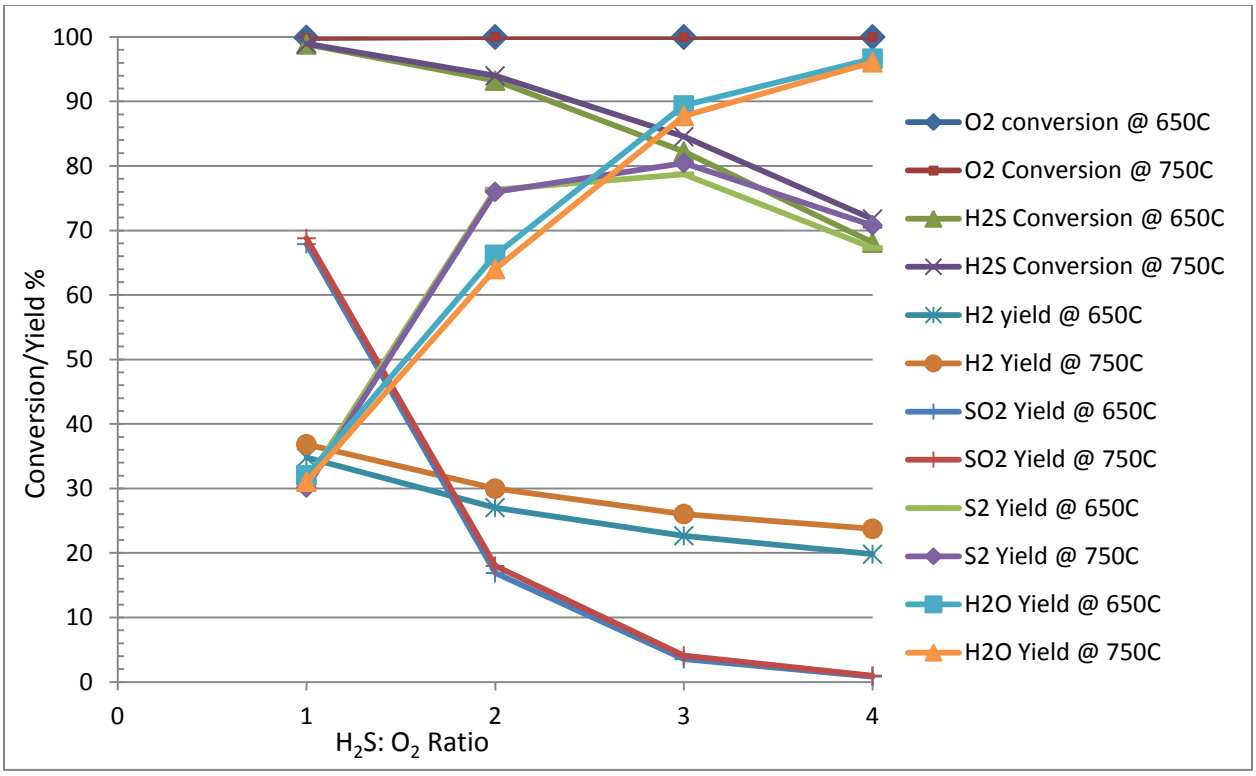

Figure 4.1: Equilibrium conversions of reactants and yields of products for the reaction between H_2S and O_2 as calculated by GASEQ.[158]

The results from equilibrium calculations show that with higher O_2 amounts, SO_2 is the preferred product. As the quantity of O_2 relative to H_2S decreases, S_2 becomes the preferred product and the O_2 is used up to produce H_2O, which in turn leads to the decrease in H_2 production at higher H_2S:O_2 ratios. For the purpose of this work, S_2 is the desired product; hence, ratios of H_2S:O_2 of 2 or higher should be used.

4.0.2 Equilibrium Calculations for Determination of Adiabatic Temperatures

The reaction of O_2 with H_2S is highly exothermic, leading to specific adiabatic temperatures from the oxidation of H_2S at different feed ratios (Figure 4.2, complete data table can be found in Appendix 4.1).

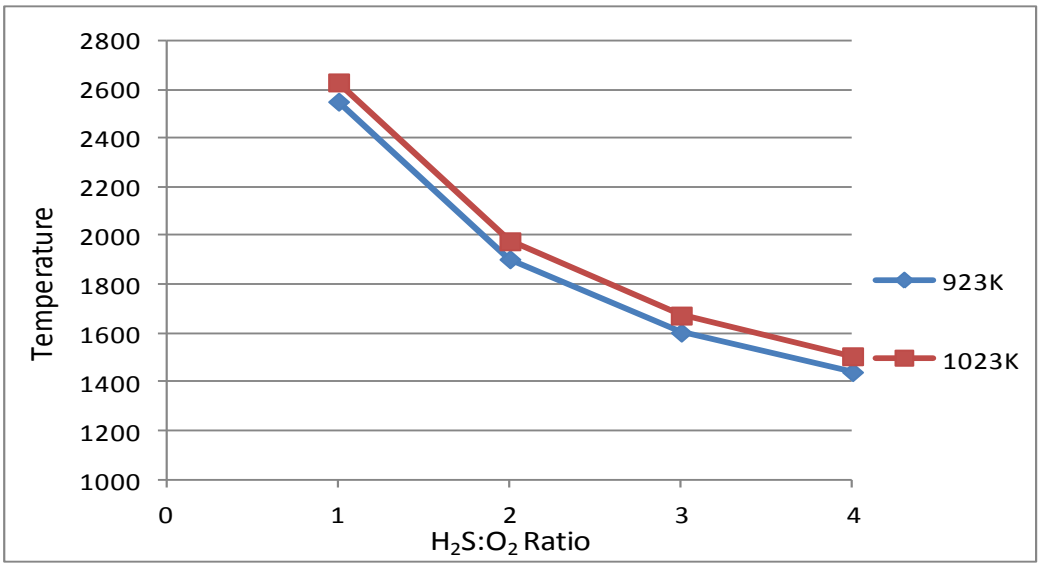

Figure 4.2: Adiabatic temperatures of the reaction between H_2S and O_2 at various feed ratios as calculated by GASEQ[8] at 923 and 1023 K.

Even at leaner H_2S: O_2 ratios such as 4:1, the adiabatic temperature of the reaction at equilibrium is in excess of 1400 K, and this value increases as a greater amount of oxygen is present in the system. This exothermic reaction is beneficial, as it provides thermal energy for the dehydrogenation of propane, as well as supplying the chemical oxidant, S_2. Some of the energy liberated in the process can also be recovered from the product gases in a heat exchanger and used to pre-heat the inlet propane and air or oxygen, if pure O_2 is used.

4.1 Gas-phase Reactions using an Empty Catalyst Bed (Homogeneous Reaction)

As previously mentioned, gas-phase reactions may make significant contributions to catalytic reactions, so the gas-phase reactions were examined to provide this reference information. In the initial work, the reaction between C_3H_8 and O_2 was studied; in later experiments, H_2S was added to the reactant gas mixture to study its contribution and effect on the ODH reaction. In addition, the gas-phase reactions were first studied using an unfilled

reactor, and later using a reactor filled with an inert material such as quartz chips or crystalline silica.

4.1.1 Gibbs Free Energy Calculations for Expected Product Distributions

To determine if the reaction was in a kinetically controlled regime, free energy minimization calculations were carried out to determine expected equilibrium products for the reaction between C_3H_8 and O_2 in the gas phase. The products selected for these calculations were chosen based on major products expected and seen in preliminary experimental observations. In addition, the calculations were carried out twice, once allowing coke ($C_{(s)}$) as a possible product and once without it. The reactant feed ratios and initial temperatures were chosen to match some of the experimental feed ratios and furnace temperatures used. The results are shown in Tables 4.1 and 4.2, below.

Table 4.1: Equilibrium products of the reaction of C_3H_8 and O_2 at different ratios, calculated without allowing $C_{(s)}$ as a product.

C_3H_8:O_2 ratio	Temperature °K	Feed (moles/100 moles)			Conversion %		Product (moles/100 moles) [Selectivity %]							
		N_2	C_3H_8	O_2	C_3H_8	O_2	C_3H_6	C_2H_4	C_2H_6	CH_4	CO	CO_2	H_2O	H_2
2:1	923	33.00	44.66	22.33	100	100	0.22 [0.49]	16.09 [24]	0.14 [0.21]	56.20 [41.9]	44.66 [33.3]	0.00 [3E-05]	0.00	32.98
4:1	923	33.00	53.10	13.30	99.98	100	1.29 [2.43]	26.55 [33.3]	0.45 [0.56]	74.48 [46.8]	26.60 [16.7]	0.00 [2E-05]	0.00	4.77
2:1	1023	33.00	44.66	22.33	100	100	0.23 [0.52]	18.58 [27.7]	0.12 [0.18]	51.19 [38.2]	44.66 [33.3]	0.00 [2E-05]	0.00	38.00
4:1	1023	33.00	53.10	13.30	99.99	100	1.04 [1.96]	28.79 [36.1]	0.36 [0.46]	71.03 [44.6]	26.60 [16.7]	0.00 [1E-05]	0.00	8.30

Note: selectivities are based on carbon and therefore show the product distribution according to % of overall carbon used to make that product. See Appendix 4.2a for complete data table.

The results show that C_2H_4, CO and CH_4 would be the major carbon products when coke is not an allowed product. Propylene is a minor product the selectivity of which increases when less oxygen is available. However, lower amounts of oxygen also translate to lower conversion of the alkane. Slightly less than 100% conversion is obtained at a 4:1 C_3H_8:O_2 ratio compared to

the 100% conversion obtained for the higher oxygen ratio. It can be expected that at experimental reaction conditions (which have short contact times), the conversion could be lower than the equilibrium levels. The selectivity to CH_4 and C_2H_4 increases as the amount of oxygen is reduced, while the selectivity to CO decreases when less oxygen is used. Other interesting observations include the fact that neither CO_2 nor H_2O is expected to be a significant product, a consequence of having sub-stoichiometric levels of O_2 in the feed mixtures. The effects of temperature can also be seen in the data above. As expected, C_2H_4 selectivity increases with increasing temperature, as cracking occurs to a greater extent at higher temperatures. The same can be seen for the amount of H_2 produced as the initial temperature of the reaction is increased.

The results of the same calculations, while allowing carbon to be product, are significantly different, as shown in Table 4.2, below.

Table 4.2: Equilibrium products of the reaction of C_3H_8 and O_2 at different ratios, calculated with $C_{(s)}$ in the product list.

C_3H_8: O_2 ratio	Temperature °K	Feed (moles/100 moles)			Conversion %		Products (moles/100 moles) [Selectivity %]								
		N_2	C_3H_8	O_2	C_3H_8	O_2	C_3H_6	C_2H_4	C_2H_6	CH_4	CO	CO_2	$C_{(s)}$	H_2O	H_2
2-1	923	33.00	44.66	22.33	100	100	0.00 [2E-08]	0.00 [1E-04]	0.00 [0]	7.51 [5.6]	35.23 [26.3]	1.73 [1.29]	89.52 [66.82]	5.98	157.64
4-1	923	33.00	53.10	13.30	100	100	0.00 [1E-08]	0.00 [5E-05]	0.00 [0]	23.13 [14.5]	11.79 [7.4]	1.74 [1.09]	122.63 [76.98]	11.33	154.81
2-1	1023	33.00	44.66	22.33	100	100	0.00 [2E-08]	0.00 [1E-04]	0.00 [0]	5.51 [4.11]	38.75 [28.9]	1.03 [0.77]	88.70 [66.2]	3.86	163.77
4-1	1023	33.00	53.10	13.30	100	100	0.00 [2E-08]	0.00 [7E-05]	0.00 [0]	18.64 [11.7]	14.78 [9.28]	1.42 [0.89]	124.46 [78.13]	8.98	166.13

Note: selectivities are based on carbon and therefore show the product distribution according to % of overall carbon used to make that product. See Appendix 4.2b for complete data table.

These data show that when carbon (coke) is an allowed product, it becomes the major carbon-containing species. From the selectivity values, it can be seen that the amount of carbon produced increases as oxygen is reduced, as evidenced by the increase in carbon selectivity when going from a 2:1 to a 4:1 C_3H_8:O_2 ratio. In addition, olefins are expected only in negligible

quantities. The other major products are H_2, H_2O, CO, CH_4 and small amounts of CO_2; the amounts of each vary depending on how much oxygen is put into the system. Increasing the amount of oxygen resulted in an increased amount of CO and a decrease in the amount of CH_4, $H_2O$and $C_{(s)}$. The effect of temperature can also be seen in the changes in selectivity for CH_4, CO and CO_2. The data show that higher temperatures favor the production of CO, while lower temperatures favor the production of CH_4 and CO_2. In addition, high temperature seems to favor H_2 production at the cost of H_2O production. One possibility to explain this is steam reforming of carbon to produce CO and H_2.

Similar calculations were also carried out for the reaction between C_3H_8, H_2S and O_2 to determine the equilibrium product distributions when H_2S is added to the reaction. Feed ratios similar to those used in the experiments at reaction temperatures of 923 K and 1023 K, were used as the input parameters for the calculations. Tables 4.3 and 4.4 show the results of the calculations when carbon was not allowed and allowed as products, respectively.

The data in Table 4.3 show that increased amounts of oxygen lower the amount of olefins (C_3H_6 and C_2H_4) in the products. CS_2 is also the major sulfur product, and COS, SO_2 and S_2 are all predicted to be minor products. CO is the major oxygenated product, and CO_2 and H_2O are very minor products. Finally, CH_4, CO, C_2H_4 and CS_2 are the major carbon products, while CO_2, C_2H_6, COS and C_3H_6 are minor carbon products. Conversion of all reactants occurs to an appreciable extent. O_2 is converted fully in all feed mixtures. C_3H_8 is converted fully, except in the mixture with the lowest alkane:oxidant ratio (8:3:1 feed) but, even then, the conversion was at 99%.

Table 4.3: Equilibrium products of the reaction of C_3H_8, H_2S and O_2 at different ratios, calculated without $C_{(s)}$ in the product list. (Note: selectivities are based on carbon and therefore show the product distribution according to % of overall carbon used to make that product).

Feed ratio C_3H_8:H_2S:O_2	Temperature (°K)		Feed, mole/100 moles of feed				Conversion %			Products, mole/100 moles of feed [Selectivity %]											
	Initial	Adiabatic	N_2	C_3H_8	H_2S	O_2	C_3H_8	O_2	H_2S	C_3H_6	C_2H_4	C_2H_6	CH_4	CO	CO_2	CS_2	COS	SO_2	S_2	H_2	H_2O
4:2:1	923	1133.3	33.00	38.29	19.14	9.57	100	100	95.27	0.15 [0.39]	6.96 [12.11]	0.20 [0.36]	71.85 [62.55]	19.10 [16.6]	4.89E-05 [4E-05]	9.10 [31.67]	0.04 [0.15]	1.4E-16	5.6E-04	12.71	4.3E-02
4:2:2	923	1247.9	33.00	33.50	16.75	16.75	100	100	87.52	0.03 [0.1]	3.89 [7.75]	0.08 [0.15]	51.66 [51.4]	33.44 [33.3]	1.18E-04 [1E-04]	7.30 [29.05]	0.06 [0.24]	4.1E-15	2.1E-03	37.22	2.0E-04
8:3:1	923	945.3	13.42	60.56	18.58	6.76	99.93	100	99.63	2.90 [4.79]	23.33 [25.71]	1.03 [1.14]	99.76 [54.95]	13.49 [7.43]	2.30E-05 [1E-05]	9.24 [20.36]	0.03 [0.07]	1.4E-19	1.2E-05	1.00	9.2E-07
4:2:1	1023	1180.7	33.00	38.29	19.14	9.57	100	100	95.15	0.17 [0.45]	9.03 [15.72]	0.19 [0.33]	67.67 [58.91]	19.11 [16.6]	2.94E-05 [3E-05]	9.09 [31.65]	0.03 [0.12]	1.4E-16	7.2E-04	16.87	3.4E-02
4:2:2	1023	1292.2	33.00	33.50	16.75	16.75	100	100	89.58	0.05 [0.15]	5.65 [11.25]	0.08 [0.15]	47.92 [47.68]	33.45 [33.3]	6.55E-05 [7E-05]	7.48 [29.76]	0.05 [0.18]	2.5E-15	2.2E-03	41.49	1.4E-04
8:3:1	1023	1025.2	13.42	60.56	18.58	6.76	99.96	100	99.23	1.96 [3.24]	26.27 [28.93]	0.76 [0.84]	98.20 [54.07]	13.50 [7.43]	1.31E-05 [7E-06]	9.21 [20.28]	0.02 [0.05]	6.1E-19	4.1E-05	2.73	2.0E-06

Table 4.4: Equilibrium products of the reaction of C_3H_8, H_2S and O_2 at different ratios, calculated with $C_{(s)}$ in the product list. (Note: selectivities are based on carbon and therefore show the product distribution according to % of overall carbon used to make that product).

Feed Ratio C_3H_8:H_2S:O_2	Temperature (°K)		Feed, mole/100 moles of feed				Conversion %			Products, mole/100 moles of feed [Selectivity %]													
	Initial	Adiabatic	N_2	C_3H_8	H_2S	O_2	C_3H_8	O_2	H_2S	C_3H_6	C_2H_4	C_2H_6	CH_4	CO	CO_2	CS_2	COS	$C_{(s)}$	SO_2	S_2	H_2	H_2O
4:2:1	923	919	33.00	38.29	19.14	9.57	100	100	0.24	0.00 [9.9E-09]	0.00 [4E-05]	0.00 [0.0003]	16.07 [13.99]	8.44 [7.35]	1.27 [1.11]	0.00 [0.001]	0.05 [0.16]	89.05 [77.52]	1.1E-09	4.4E-05	113.0	8.11
4:2:2	923	1016.8	33.00	33.50	16.75	16.75	100	100	0.72	0.00 [1.2E-08]	0.00 [9E-05]	0.00 [0.0001]	5.54 [5.514]	26.06 [25.9]	1.36 [1.36]	0.00 [0.009]	0.12 [0.46]	67.42 [67.08]	4.4E-09	3.0E-04	118.4	4.60
8:3:1	923	860.5	13.42	60.56	18.58	6.76	100	100	0.06	0.00 [8.6E-09]	0.00 [3E-05]	0.00 [0.0007]	46.50 [25.59]	2.80 [1.54]	0.56 [0.31]	0.00 [1E-04]	0.01 [0.03]	131.81 [72.55]	1.2E-10	6.5E-06	139.7	9.60
4:2:1	1023	949.2	33.00	38.29	19.14	9.57	100	100	0.29	0.00 [1.2E-08]	0.00 [6E-05]	0.00 [0.0002]	12.55 [10.93]	10.86 [9.45]	1.00 [0.87]	0.00 [0.002]	0.05 [0.19]	90.40 [78.7]	1.3E-09	3.0E-04	121.9	6.22
4:2:2	1023	1056.6	33.00	33.50	16.75	16.75	100	100	0.80	0.00 [1.3E-08]	0.00 [0.0001]	0.00 [7E-05]	3.95 [3.93]	28.97 [28.8]	0.77 [0.77]	0.00 [0.019]	0.12 [0.49]	66.67 [66.34]	4.2E-09	6.3E-04	123.4	2.85
8:3:1	1023	887.9	13.42	60.56	18.58	6.76	100	100	0.09	0.00 [1.1E-08]	0.00 [4E-05]	0.00 [0.0006]	38.54 [21.21]	4.06 [2.23]	0.54 [0.29]	0.00 [2E-04]	0.02 [0.03]	138.53 [76.25]	1.8E-10	1.2E-05	156.8	8.37

Conversion of H_2S ranged from 87-99.9%, showing that a significant amount of H_2S will be consumed at equilibrium.

The data in Table 4.4, however, show a different picture. When carbon is allowed as a potential product (as could be the case in experiments), overall conversion of H_2S is not expected to occur to any significant degree. In all reactant mixtures, conversion of H_2S was less than 1%, but complete conversion of C_3H_8 and O_2 is predicted. The major carbon product is coke ($C_{(s)}$), and CO, CO_2 and CH_4 are minor products. C_3H_6, C_2H_4, C_2H_6, COS and CS_2 are expected only in negligible quantities. The major oxygen-containing product is CO, followed by H_2O, with small amounts of CO_2 and negligible amounts of COS and SO_2 also being produced. An overall conclusion from the calculations is that production of large yields of olefins would have to occur under kinetically controlled conditions, as only limited quantities will be seen at equilibrium.

4.1.2 Experimental Product Distributions

The ODH of propane by O_2 was studied first, to understand the behavior of the experimental system for this reaction and to provide a means of comparison. The experimentally obtained product distributions for the reaction between C_3H_8 and O_2 through an empty reactor at ~ 20 ms residence time are shown in Table 4.5, below.

The experimental product distributions show that carbon is, indeed, a major carbon product. However, the values for selectivity to CO are lower than those seen in the equilibrium calculations, except for the reaction using a 2:1 feed ratio at 1023 K. Selectivity to CO increased at higher temperatures, similar to the trend predicted in the equilibrium calculations.

Table 4.5: Experimental product distributions, reactant conversions and product selectivities for the homogeneous reaction between C_3H_8 and O_2, at different feed ratios.

Feed ratio C_3H_8:O_2	Temperature °K	Feed, mole/100 moles			Conversion %		Products, mole/100 moles of feed [Selectivity %]								
		N_2	C_3H_8	O_2	C_3H_8	O_2	C_3H_6	C_2H_4	C_2H_6	CH_4	CO	CO_2	$C_{(s)}$	H_2O	H_2
4:1	923	33.0	53.1	13.3	19	23	1.3 [13]	2.4 [17]	0.0 [<1]	1.6 [5]	0.4 [1]	0.5 [2]	18.6 [63]	4.7	0.7
2:1	923	33.0	44.7	22.3	36	30	3.5 [21]	5.1 [20]	0.2 [1]	3.7 [7]	1.7 [3]	0.4 [1]	21.7 [47]	10.9	1.7
4:1	1023	33.0	53.1	13.3	50	83	5.4 [21]	10.6 [27]	0.7 [2]	9.0 [11]	5.1 [6]	1.5 [2]	25.0 [32]	13.9	5.7
2:1	1023	33.0	44.7	22.3	72	82	5.8 [18]	13.9 [29]	0.9 [2]	11.5 [12]	10.1 [11]	2.2 [2]	25.6 [27]	22.2	6.7

See Appendix 4.4 for complete data table.

Other major carbon products are CH_4, C_2H_4 and C_3H_6, while CO_2 and C_2H_6 were minor products (less than 2.5% selectivity). Formation of significant quantities of C_3H_6 indicates that it is a kinetically controlled product, as it was not expected in any of the equilibrium calculations (with and without $C_{(s)}$).

When comparing the trends seen between the equilibrium calculations and the experimental results, the following observations were noted. The selectivity to $C_{(s)}$ and CO_2 increased when the feed ratio was increased from 2:1 to 4:1 C_3H_8: O_2. In contrast, the selectivity to CH_4, C_2H_6, C_2H_4 and C_3H_6, obtained experimentally at 923 K, all decreased when the feed ratio was increased from 2:1 to 4:1. This trend is a marked departure from the distributions predicted by the equilibrium calculations.

Variations in temperature at this residence time also produced different product distributions in comparison to equilibrium calculations for certain products. Thus, selectivity to CO_2, CH_4 and C_2H_6 all increased in going from 923 to 1023 K, whereas at equilibrium, amounts decreased as temperature was increased. Overall, these trends illustrate kinetic control. At higher temperatures, a greater amount of cracking is expected to occur; hence yields of C_2H_4 and

CH_4 are expected to be higher. Since C_2H_6 can be formed from the further reaction of products from cracking reactions (ethyl and methyl radicals), such as collision between 2 CH_3• or collision between C_2H_5• and H•, it can be expected that as temperature is increased, a greater amount of these cracking intermediate products would be available, thus resulting in an increased amount of C_2H_6. Since these products have a limited amount of time defined by the remaining residence time in the reactor, further reactions are limited, and therefore, these species are observed in the products.

The trends in selectivity to C_3H_6 depended on the feed ratio used. Selectivity decreased with increasing temperature for the 2:1 feed ratio, but increased with increasing temperature for the 4:1 feed ratio. Dehydrogenation and cracking are both endothermic reactions, so it is expected that as temperature is increased, a greater amount of both reactions will occur. Dehydrogenation increases the amount of C_3H_6 produced, while cracking decreases the amount of C_3H_6 still remaining in the products. The results obtained for the given reaction conditions suggest that at a 4:1 feed ratio, the amount of dehydrogenation (which produces C_3H_6) is higher than the amount of cracking (which reduces C_3H_6), leading to an overall increase in the selectivity to C_3H_6. However, at the 2:1 feed ratio, a slight decrease in selectivity to C_3H_6 is observed at the higher temperature conditions. In this case, the larger amount of O_2 enhances complete oxidation. Hence, a feed with a higher amount of O_2 (such as the 2:1 feed ratio) is expected to have a greater amount of total oxidation products than a feed with a lower amount of O_2 (such as the 4:1 feed ratio). The increase in total oxidation products (CO and CO_2) is higher at the 2:1 feed ratio and could be the reason for the slightly lower selectivity to C_3H_6. In fact, this is the main limitation of ODH reactions that use O_2 as the oxidant. Loss of C_3H_6 is likely related to bond strengths, as the C-H bond in C_3H_6 (BDE = 85 kcal/mol)[159] is lower than the C-H bond

in C_3H_8 (BDE = 97 kcal/mol)[160]. Therefore, loss of C_3H_6, especially at longer residence time, can be expected, presumably via steam reforming type reactions and overall oxidation to CO_2. This trend of decreasing selectivity with increasing conversion has been reported many times before.[6]

4.1.3 The Effect of Adding H_2S to the Reactant Feed Mixture

When H_2S was added to the feed, the product distribution obtained experimentally changed significantly. The product distributions for a reaction of C_3H_8 and O_2 compared to the reaction of C_3H_8, O_2 and H_2S are shown in Table 4.6 and Table 4.7, using different feed ratios.

Table 4.6: Comparison of product distributions between the ODH of propane with and without H_2S at 20 ms residence time using an unfilled reactor.

Feed Ratio	Temp °K	Conversion %			Products, (mole/100 moles of feed) [Selectivity %]									
		C_3H_8	O_2	H_2S	C_3H_6	C_2H_4	C_2H_6	CH_4	CO	CO_2	$C_{(s)}$	S_2	H_2O	H_2
4:1	923	19	23	0	1.3 [13]	2.4 [17]	0.0 [<1]	1.6 [5]	0.4 [1]	0.5 [2]	18.6 [63]	0.0	4.7	0.7
4:2:1	923	38	80	59	5.1 [35]	4.5 [21]	0.2 [1]	5.0 [11]	1.2 [3]	0.0 [0]	12.4 [29]	5.6	14.2	1.9
4:1	973	37	58	0	4.2 [22]	7.0 [24]	0.3 [1]	5.6 [10]	2.2 [4]	0.8 [1]	22.9 [39]	0.0	11.7	2.9
4:2:1	973	50	85	58	6.7 [35]	6.8 [24]	0.3 [1]	7.5 [13]	1.6 [3]	0.0 [0]	13.5 [24]	5.6	14.6	3.2
4:1	1023	50	83	0	5.4 [21]	10.6 [27]	0.7 [2]	9.0 [11]	5.1 [6]	1.5 [2]	25.0 [32]	0.0	13.9	5.7
4:2:1	1023	62	92	60	8.9 [37]	8.9 [25]	0.5 [1]	9.8 [14]	1.8 [3]	0.1 [<1]	14.2 [20]	5.7	15.7	4.6

Note: 4:1 Feed = N_2- 33.0%, C_3H_8- 53.1% and O_2- 13.3% and 4:2:1 Feed = N_2- 33.0%, C_3H_8- 38.3%, H_2S- 19.1% and O_2- 9.6%. See Appendix 4.5 for complete data table

The data in Tables 4.6 and 4.7 show similar trends when compared to the reactions without H_2S, but at all temperatures, the selectivity to C_3H_6 is higher for the reactions containing H_2S: nearly double in most experiments.

Table 4.7: Comparison of product distributions between the ODH of propane in an unfilled reactor with and without H_2S at 20 ms residence time.

Feed ratio	Temp °K	Conversion %			Products, mole/100 moles of feed [Selectivity %]									
		C_3H_8	O_2	H_2S	C_3H_6	C_2H_4	C_2H_6	CH_4	CO	CO_2	$C_{(s)}$	S_2	H_2O	H_2
2:1	923	36	30	0	3.5 [21]	5.1 [20]	0.2 [1]	3.7 [7]	1.7 [3]	0.4 [1]	21.7 [47]	0.0	10.9	1.7
4:2:2	923	50	91	84	8.4 [51]	5.6 [22]	0.3 [1]	5.8 [12]	2.3 [5]	0.2 [<1]	4.5 [9]	7.0	27.7	2.2
2:1	973	58	70	0	5.4 [21]	9.6 [25]	0.5 [1]	7.6 [10]	7.7 [10]	1.8 [2]	23.8 [31]	0.0	19.7	5.6
4:2:2	973	60	93	83	9.7 [48]	7.3 [24]	0.4 [1]	7.8 [13]	2.9 [5]	0.2 [<1]	5.1 [8]	6.9	27.9	3.2
2:1	1023	72	82	0	5.8 [18]	13.9 [29]	0.9 [2]	11.5 [12]	10.1 [10]	2.2 [2]	25.6 [27]	0.0	22.2	6.7
4:2:2	1023	68	95	86	11.0 [49]	8.7 [25]	0.5 [2]	9.3 [14]	2.7 [4]	0.2 [<1]	4.6 [7]	7.2	28.6	4.3

Note: 2:1 Feed = N_2- 33.0%, C_3H_8- 44.7% and O_2- 22.3% and 4:2:2 Feed = N_2- 33.0%, C_3H_8- 33.5%, H_2S- 16.8% and O_2- 16.8%. See Appendix 4.6 for complete data table

Notably, CO_2 production was lower for the reaction containing H_2S at all temperatures and did not exceed 0.5% of the consumed propane. The selectivity to CO was higher at 923 K for both H_2S containing feeds (4:2:1 and 4:2:2). However, as the temperature increased, some selectivity when using H_2S was lost, eventually resulting in higher selectivity to CO for the non-H_2S containing reaction at 973 K and 1023 K. A similar trend was seen for C_2H_4 selectivity, where, at 923 K the selectivity to C_2H_4 was higher for the H_2S containing reactions but lower than that for the non-H_2S reaction at temperatures above this value. This trend resulted in a higher selectivity to C_2H_4 for the non-H_2S reactions at 973 and 1023 K. The selectivity to $C_{(s)}$ was lower for the H_2S-containing reactions at all temperatures. This effect is not unexpected, as H_2S and other sulfur compounds are known to inhibit coke.[149,161-162]

In comparison to the equilibrium calculations for the H_2S containing reactions, the following observations were made: C_3H_8 and C_2H_4 selectivities were much higher than predicted. COS and CS_2 were obtained, however, only at quantities below the limit of

quantification for the GC instrument, implying that the amounts formed were negligible. The conversion of H_2S was supposed to be less than 1% according to the results in Table 4.4 (equilibrium calculations including $C_{(s)}$ in the products); however, the experimental results showed H_2S conversion in the 58-86% range. Finally, S_2 was not expected to be present in any significant amount according to both sets of equilibrium calculations; however, S_2 was calculated as being present in appreciable quantities (5.6-7.2 mole %) based on the sulfur mass balance calculated from the experimental data. The trends in conversion and selectivity of major components from Tables 4.6 and 4.7 are shown in Figures 4.3 and 4.4, respectively.

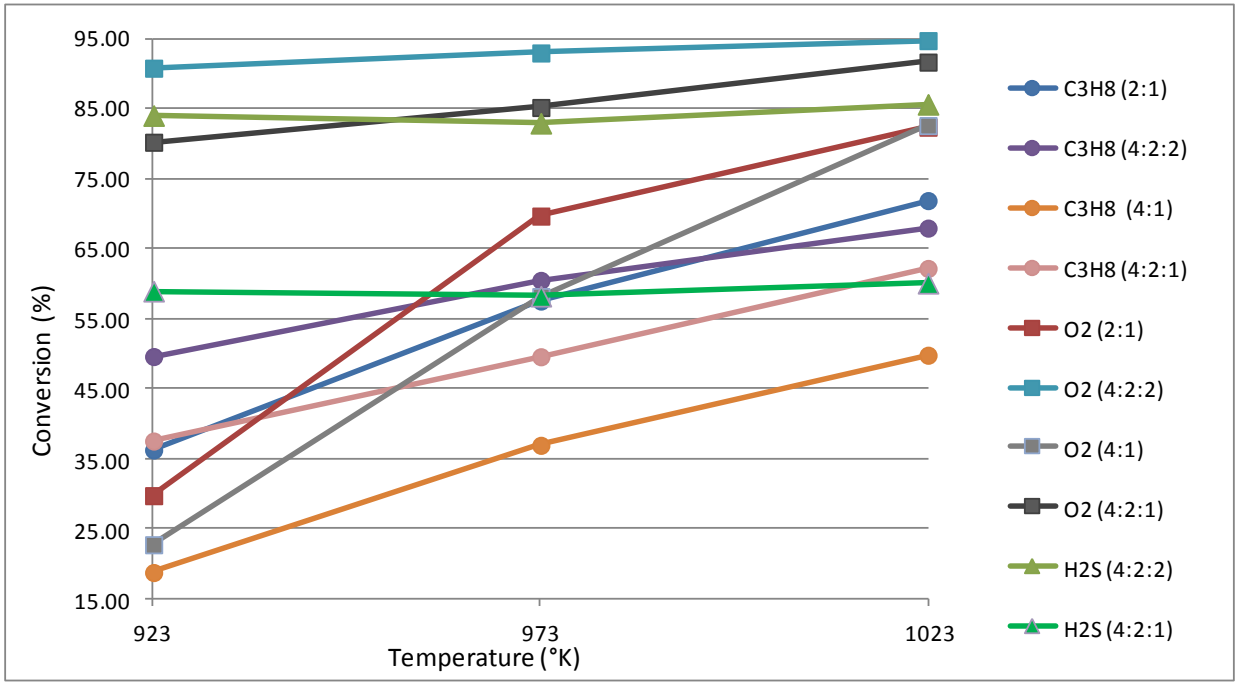

Figure 4.3: Trends in conversion of C_3H_8, O_2 and H_2S for various feed ratios.

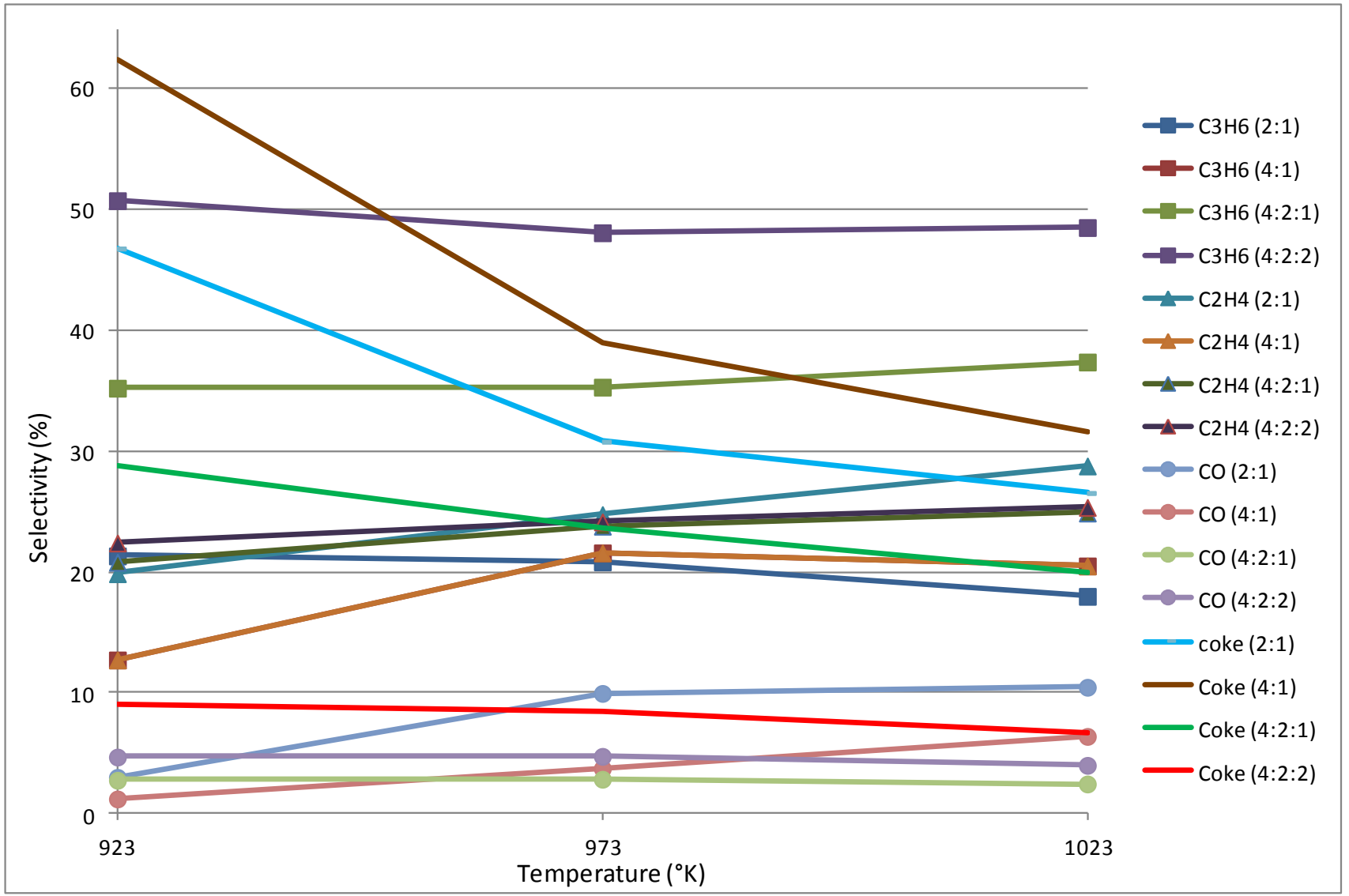

Figure 4.4: Trends in selectivity of C_3H_6, C_2H_4, CO and $C_{(s)}$ (coke) for various feed ratios.

4.2 Gas-phase Reactions using an Inert Packed Bed

Crystalline silica or quartz chips were used to fill the reactor to approximate flow conditions in a catalyst bed. These materials are known to be inert in the Claus process and are made of similar components to the reactor itself (quartz). However, it should be noted that a packed bed does have some effect compared to a non-packed (empty) reactor. Research found in the literature reported that packed beds, especially those filled with silica/quartz-like materials, can terminate free radical reactions and so, overall, can affect the overall reaction in comparison to gas phase processes.[20] Thus, it was of interest to compare the ODH reaction in the presence of H_2S for an empty reactor versus a quartz chips-filled reactor.

Table 4.8: Comparison between empty tube and quartz chips for the ODH of C_3H_8 in the presence of O_2 and H_2S using a 4:2:2 C_3H_8: H_2S: O_2 feed at 20 ms contact time.

	Temp °K	Conversion %			Products, mole/100 moles of feed [Selectivity %]									
		C_3H_8	O_2	H_2S	C_3H_6	C_2H_4	C_2H_6	CH_4	CO	CO_2	$C_{(s)}$	S_2	H_2O	H_2
Empty tube	923	50	91	84	8.4 [51]	5.6 [22]	0.3 [1]	5.8 [12]	2.3 [5]	0.2 [<1]	4.5 [9]	7.0	27.7	2.2
Quartz chips	923	57	80	77	9.1 [48]	7.0 [24]	0.4 [1]	7.8 [14]	2.8 [5]	0.2 [<1]	4.3 [7]	6.4	23.8	3.3
Empty tube	1023	68	95	86	11.0 [49]	8.7 [25]	0.5 [2]	9.3 [14]	2.7 [4]	0.2 [<1]	4.6 [7]	7.2	28.6	4.3
Quartz chips	1023	74	89	76	11.3 [46]	9.5 [26]	0.6 [2]	10.3 [14]	3.3 [4]	0.4 [1]	6.3 [8]	6.4	25.7	5.2

Note: 4:2:2 Feed = N_2- 33.0%, C_3H_8- 33.5%, H_2S- 16.8% and O_2- 16.8%. See Appendix 4.7 for complete data table.

While there was some enhancement in conversion of C_3H_8 when the reaction was carried out over a packed bed, the product selectivity values obtained were within ± 3% to gas phase experiments. The effect of adding H_2S to the conventional ODH reaction of C_3H_8 and O_2 was re-examined over an inert packed bed to be sure that the addition of a packed bed did not distort the trends previously observed. The results from those experiments are shown in Tables 4.9 and 4.10 below.

Table 4.9: Effect of adding H_2S to the reaction between C_3H_8 and O_2 over an inert quartz chips bed at a 5 ms residence time.

Feed ratio	Temp °K	Conversion %			Products, mole/100 moles of feed [Selectivity %]									
		C_3H_8	O_2	H_2S	C_3H_6	C_2H_4	C_2H_6	CH_4	CO	CO_2	$C_{(s)}$	S_2	H_2O	H_2
4:1	923	66	80	0	5.5	10.0	0.7	7.3	4.6	0.2	54.8	0.0	16.5	3.5
					[16]	[19]	[1]	[7]	[4]	[<1]	[52]			
4:2:1	923	45	79	55	5.9	6.2	0.3	6.9	1.4	0.0	12.3	5.2	13.6	2.8
					[34]	[24]	[1]	[13]	[3]	[<1]	[24]			
4:1	973	72	87	0	6.1	12.4	1.0	9.5	5.7	0.1	55.2	0.0	17.3	4.7
					[16]	[21]	[2]	[8]	[5]	[<1]	[48]			
4:2:1	973	57	82	54	7.6	8.2	0.5	9.2	1.8	0.0	14.7	5.1	13.8	4.2
					[35]	[25]	[1]	[14]	[3]	[<1]	[22]			
4:1	1023	75	87	0	6.6	15.1	1.0	12.3	6.3	0.2	49.0	0.0	16.4	6.1
					[17]	[25]	[2]	[10]	[5]	[<1]	[41]			
4:2:1	1023	71	86	54	9.9	10.7	0.7	12.1	2.1	0.2	14.5	5.2	13.8	5.8
					[37]	[26]	[2]	[15]	[3]	[<1]	[18]			

Note: 4:1 Feed = N_2- 33.0%, C_3H_8- 53.1% and O_2- 13.3% and 4:2:1 Feed = N_2- 33.0%, C_3H_8- 38.3%, H_2S- 19.1% and O_2- 9.6%. See Appendix 4.8 for complete data table.

The data in both tables shows that the selectivity to C_3H_6 increases to double or more of what it was by the addition of H_2S to the reaction. This is similar to what was observed for the reactions in the empty reactor. An overall conclusion is that gas-phase reactions with H_2S show better selectivity to C_3H_6 compared to ODH of C_3H_8 by O_2 alone, indicating that S_2 could be a preferred oxidant for the commercial synthesis of C_3H_6.

Table 4.10: Effect of adding H_2S to the reaction between C_3H_8 and O_2 over an inert quartz chips bed at a 10 ms residence time.

Feed ratio	Temp °K	Conversion %			Products, mole/100 moles of feed [Selectivity %]										Yield %
		C_3H_8	O_2	H_2S	C_3H_6	C_2H_4	C_2H_6	CH_4	CO	CO_2	$C_{(s)}$	S_2	H_2O	H_2	C_3H_6
2:1	923	62	71	0	6.6	13.5	0.9	9.7	7.4	0.3	17.2	0.0	23.8	4.8	15
					[24]	[32]	[2]	[12]	[9]	[<1]	[1]				
4:2:2	923	60	83	75	10.0	6.9	0.3	7.5	2.5	0.1	-3.0	6.3	25.2	3.5	30
					[50]	[23]	[1]	[13]	[4]	[<1]	-[5]				
2:1	1023	80	81	0	6.5	18.7	1.1	15.9	10.9	0.6	20.9	0.0	24.1	7.2	15
					[18]	[35]	[2]	[15]	[10]	[1]	[19]				
4:2:2	1023	77	91	61	12.1	9.4	0.6	10.1	2.9	0.5	-2.6	5.1	26.5	5.1	36
					[47]	[24]	[1]	[13]	[4]	[1]	-[3]				

Note: 2:1 Feed = N_2- 33.0%, C_3H_8- 44.7% and O_2- 22.2% and 4:2:2 Feed = N_2- 33.0%, C_3H_8- 33.5%, H_2S- 16.8% and O_2- 16.8%. See Appendix 4.9 for complete data table.

Data shown in Table 4.10 also illustrate a reduction in selectivity towards C_2H_4. This effect was not seen in the data recorded in Table 4.9, most probably due to the lower amount of O_2 in the 4:1 feed ratio. Also, less C_2H_4 was obtained at the 4:1 ratio than at the 2:1 ratio (Table 4.5). CO selectivity for the reaction with H_2S was almost half that of the reaction with only O_2. The selectivity to CO_2 is lower for the reaction with H_2S at 923 K but higher for the reaction with H_2S at 1023 K, showing that selectivity to CO_2 increases at a faster rate above 973 K when both H_2S and O_2 are present. However, the overall production of CO_2 was negligible in both cases (1% selectivity).

C_3H_8 conversion was higher for the reaction without H_2S, but O_2 conversion was higher for the reaction with H_2S. This result is due to the rapid reaction of O_2 with H_2S in comparison to the rate of O_2 with C_3H_8. Finally, the yield of C_3H_6 remained the same on increasing the temperature from 923 K to 1023 K for the 2:1 feed ratio. Even though the conversion of C_3H_8 increased by 18% (from 62% to 80%), the selectivity dropped by 6%, leading to an overall similar yield as a consequence of by-product formation at the increased temperature. While the overall trends remained the same for the 4:2:2 feed ratio, the proportions were different, and in turn led to an overall increase in yield of C_3H_6 due to the temperature increase. The conversion of C_3H_8 also increased by 17% (from 60 to 77%) and the selectivity to C_3H_6 decreased from 50% to 47%, leading to an overall increase in yield by 6% (from 30 to 36%). It should be noted that even at 923 K, the yield obtained for the 4:2:2 feed ratio under these reaction conditions was close to 30%, which is high compared to many of the reports found in the literature.

4.2.1 Effect of Contact Time

The effect of contact time was examined for a feed ratio that included H_2S. The results are shown in Table 4.11, below. The effect of contact time is important because increasing contact time should lead to equilibrium-like product distributions, hence moving away from kinetically controlled processes. Since C_3H_6 is not a significant equilibrium product, it would be important to know what the ideal contact times would be for optimal C_3H_6 production.

Table 4.11: Effect of contact time on the ODH reaction of C_3H_8 and O_2 in the presence of H_2S over a crystalline silica bed.

Contact time	Temp °K	Conversion %			Products, mole/100 moles of feed [Selectivity %]										Yield %
		C_3H_8	O_2	H_2S	C_3H_6	C_2H_4	C_2H_6	CH_4	CO	CO_2	$C_{(s)}$	S_2	H_2O	H_2	C_3H_6
12ms	923	11	95	7	3.4 [56]	3.7 [40]	0.0 [0]	3.8 [21]	0.8 [5]	1.5 [8]	-3.8	0.4	12.2	2.2	6
60ms	923	20	92	6	4.9 [42]	4.3 [25]	0.0 [0]	4.5 [13]	0.6 [2]	1.3 [5]	4.9	0.5	12.1	2.6	8
120ms	923	22	98	5	5.4 [42]	4.1 [21]	0.0 [0]	4.3 [11]	0.6 [2]	0.7 [2]	8.9	0.4	14.4	2.3	9
12ms	1023	75	93	4	16.4 [38]	20.9 [32]	2.2 [3]	24.3 [19]	0.5 [<1]	1.9 [2]	8.3	0.2	11.4	7.7	28
60ms	1023	75	90	5	14.8 [34]	18.8 [29]	2.0 [3]	21.7 [17]	0.4 [<1]	1.7 [1]	21.2	0.6	11.3	7.3	26
120ms	1023	75	98	14	13.8 [32]	16.4 [25]	1.8 [3]	19.0 [15]	0.5 [<1]	0.5 [<1]	32.7	1.2	14.4	7.9	24

Note: Feed = 20.5% N_2, 58.1% C_3H_8, 16.3% H_2S and 8.5% O_2. (~ 7:2:1 C_3H_8: H_2S: O_2). See Appendix 4.10 for complete data table.

The first and obvious effect of increasing residence time expected will be the conversion of C_3H_8, which should increase with increased residence time. This prediction is based on radical pathways, as C_3H_8 molecules can enter the reaction sequences either via C-C bond scission or by collision with another radical as a propagation step. Both of these pathways will increase the amount of C_3H_8 converted with increasing time, especially the propagation step which relies on bimolecular collisions. In addition, it is expected that the product distributions will change as

well, as further reaction of some products will occur during the extra time the molecules are in the reaction hot zone.

The experimental data show that conversion of C_3H_8 increases significantly at 923 K. But, in the experiments reported here (Table 4.11), the conversion did not change significantly at 1023 K when residence time was varied. C_3H_6 selectivity decreased with increasing residence time at both reaction temperatures. This was expected, as it is already known that C_3H_6 is prone to further oxidation (steam reforming); so the higher the residence time, the greater the chance for further oxidation and therefore, the lower the selectivity to C_3H_6.

It is possible that an increase in selectivity to C_2H_4 would be seen when the residence time was increased, but this was not the case. In fact, the trend observed was a decrease in C_2H_4 selectivity, and this trend was much greater at 923 K than at 1023 K. This result can be explained by considering how much cracking occurs at each of these temperatures. The amount of cracking at 923 K is expected to be much lower, and therefore, increasing contact time allows a significant portion of the cracking products to react further. However, at 1023 K an appreciable amount of cracking is expected to occur, and since there is a greater amount to begin with, whatever is converted due to the extra reaction time will have a smaller effect on the total. In addition, a decrease in selectivity towards all carbon-containing products was observed, except for carbon ($C_{(s)}$), which increased in yield as residence time was increased. This result fits with the equilibrium position when carbon was allowed as a product.

4.3 Catalytic Reactions

The catalytic reactions were studied next, and the results are presented below. To get an accurate picture for comparison purposes, the catalysts were first tested for the ODH reaction

between C_3H_8 and O_2, in the absence of any H_2S. As the class of vanadia catalysts has already been investigated extensively for the ODH of C_3H_8 by O_2, the mechanism of the catalytic reaction has already been reported and was shown in the introduction. It is generally accepted that the main role of O_2 for the ODH reaction is in the re-oxidation of the vanadia sites that get reduced as part of the catalytic reaction. This step re-oxidizes the reduced V-O site. It should be remembered that above 873 K, homogenous processes may occur in the voids between particles of the catalyst.[15] The data presented in the previous sections have already shown the effect of the homogenous reaction in the presence and absence of H_2S, and at various feed ratios and contact times. The following data will show the results of experiments carried out over various catalysts of vanadia-supported on crystalline silica, a generally inert support for oxidative reactions.

4.3.1 Catalytic Oxidation of H_2S

The first aspect of the reaction that was studied was the reaction of H_2S with O_2 over a vanadia catalyst bed. While the catalytic oxidation of H_2S was not studied for every catalyst within the group of catalysts that was synthesized for this research, it was assumed that the trends observed would be representative of this class of catalysts (VO_x/CS). The catalytic oxidation of H_2S by vanadia catalysts has been previously studied and reports can be found in the literature. Marshneva and Mokrinskii compared 21 metal oxides and found that V_2O_5 was the most selective towards sulfur.[163] Despite it being the most selective, the catalysts most commonly used in the Claus process are alumina and titania, due to their stability and low cost. Most of the research in the literature focuses on conditions similar to the Claus process conditions, so reaction temperatures are low (473-673 K range), and may include excess water or small amounts of ammonia in the reactant feed. No reports of higher temperature H_2S oxidation using V_2O_5 or silica/alumina supported V_2O_5 catalysts were found.

In one report on the oxidation of H_2S over VO_x/SiO_2 and V_2O_5 catalysts at 473-623 K, the effect of V loading, temperature, H_2S/O_2 ratio, space velocity and reaction time were investigated.[164] Results showed that conversion increased and selectivity decreased as the O_2/H_2S ratio was increased from 0.4 to 1.0. It was also found that for low loading catalysts (1.0 wt% V), selectivity to sulfur increased from 91% at 498 K to 95.2% at 573 K, and then decreased thereafter. For the higher loading catalysts (5 wt% V and higher), the selectivity decreased as temperature was increased; however, even at 598 K the selectivity did not drop below 92.1%. Since data for higher temperatures are not available, it can be assumed that the trend for selectivity as a function of temperature may continue, and that a lower selectivity may be expected at higher temperatures such as the ones used in our research. The authors later concluded that the reaction must use a redox type mechanism, where H_2S consumes oxygen from the vanadium oxide, and gas-phase oxygen regenerates the reduced sites. The faster deactivation observed at low vanadium loadings or at higher space velocities supported the conclusion.

In order to obtain some experimental data on the oxidation of H_2S over a VO_x/CS catalyst at conditions similar to the ones to be used in this investigation, a few experiments were conducted at different H_2S/O_2 ratios. Table 4.12 below shows the reaction of H_2S and O_2 in different feed ratios over a catalyst bed containing 5% VO_x/CS at a contact time of 35 ms.

Table 4.12: Effect of feed ratio on the reaction between H_2S and O_2 over 5% VO_x/CS.

Feed ratio	Temperature (K)		Feed (mole /100 moles)			Conversion %		Yield %		Selectivity %	
(H_2S:O_2)	Furnace	Reactor	N_2	O_2	H_2S	O_2	H_2S	SO_2	H_2	SO_2	H_2
3:1	823	913.4	86.5	3.4	10.9	88	46	0	0	0	0
2:1	823	930.5	87.4	4.3	9.3	91	52	1	0	1	0
1:1	823	956.8	85.9	7.6	6.9	96	86	22	3	25	4
3:1	923	998.4	86.5	3.4	10.9	92	46	0	0	0	0
2:1	923	1000.9	87.4	4.3	9.3	94	53	<1	0	1	0
1:1	923	1014.3	85.9	7.6	6.9	97	87	20	4	23	5

Note: The table shows only the two products analyzed/detected by GC. Components such as S_2 and H_2O, which are liquid at room temperature, were not quantified directly but can be calculated by calculating the remaining mass balance of sulfur atoms and oxygen atoms from the data above.

The data obtained show trends similar to those seen in the equilibrium calculations presented earlier, which were calculated as a gas-phase reaction with no catalyst. It is known that oxidation of H_2S by oxygen proceeds rapidly over vanadia-based catalysts to yield a high proportion of S_2 and either H_2 or H_2O, depending on the amount of O_2 in the system. The trends noted were: increased yield of SO_2 and increased selectivity towards H_2 at higher amounts of O_2, as well as, increased reactor bed temperature and increased conversion of all reactants with increased amount of O_2. The effect of initial furnace temperature on the conversion of H_2S is very small (less than 1% increase in H_2S conversion when the furnace temperature was increased by 100 K, regardless of the feed ratio) therefore, the increase in temperature to 923 K made no significant difference in the conversion of H_2S. However, there is a significant effect of feed ratio on the conversion of H_2S, as seen from the data above. The conversion increased from 46% to 86% when the feed ratio was changed from 3:1 to ~1:1 H_2S: O_2, which is entirely expected, since O_2 is the oxidant in the reaction. Both H_2 and SO_2 production were only observed in significant amounts when high O_2 levels were present, such as in the 1:1 H_2S: O_2 feed ratio. O_2 reacts preferentially to produce H_2O, and only at high O_2 amounts is SO_2 seen in the gas phase. It should be noted that at the 2:1 H_2S:O_2 ratio, H_2 was seen as a very small peak on the GC; however, the level was below the limit quantifiable by TCD.

4.3.2 Catalytic ODH Reactions

Catalysts ranging from 0.86% to 7.62% vanadium oxide supported on silica were used in these experiments. It was expected that catalysts containing higher amounts of vanadia will have lower dispersion of the active components, and therefore will have a higher proportion of polymeric or crystallite vanadia species on the surface of the support material. These species are already known to have lower selectivity towards partial oxidation products, as they promote total

oxidation pathways.[36] The first catalyst tested was therefore 1% vanadium oxide supported on crystalline silica. The results are shown in the figures below. Figure 4.5 shows the yields of all carbon products totaling 100% of all the carbon in the system.

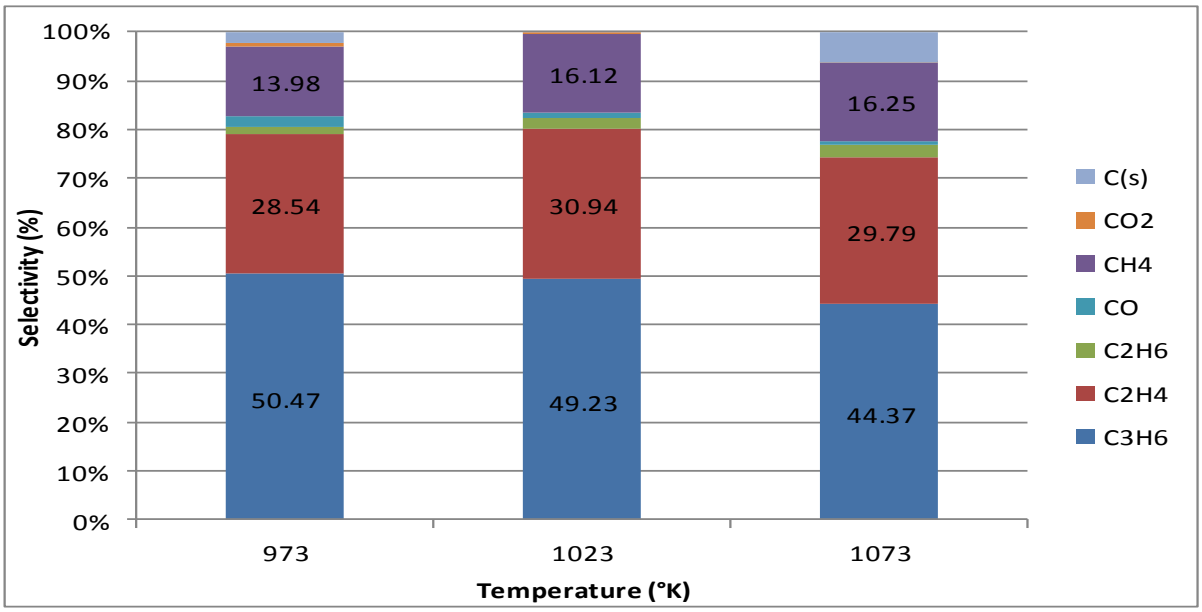

Figure 4.5: Column graph showing all carbon product selectivities as a function of reaction temperature for a 1% VO_x/CS catalyst. (36 ms contact time, feed: 11.6% N_2, 12.9% O_2, 17.7% H_2S and 58.5% C_3H_8). See Appendix 4.11 for complete data table.

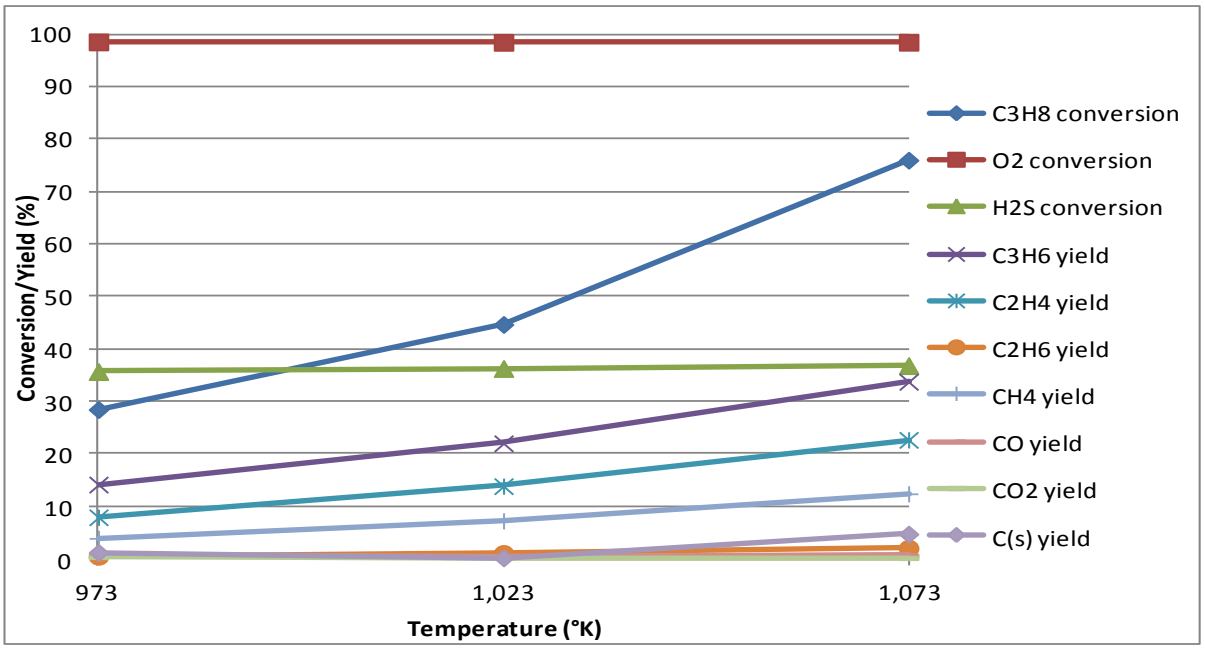

Figure 4.6: Conversion and yield of carbon containing products for the reaction of C_3H_8, O_2 and H_2S over a 1% VO_x/CS catalyst.

Figure 4.5 shows that C_3H_6 is the major product at both reaction temperatures tested, followed by C_2H_4 and CH_4. The rest of the products such as C_2H_6, CO, CO_2 and $C_{(s)}$ are all minor products. The total combined selectivity to olefins was 79%, 80% and 74% at 973, 1023 and 1073 K reaction temperatures, respectively. Figure 4.6 shows the conversion of all reactants and yield percent of all carbon-containing products. The conversion of O_2 and H_2S did not change significantly with increased temperature, whereas the conversion of C_3H_8 increased from 28% at 973 K to 76% at 1073 K. Due to the large increase in conversion as a function of increasing temperature, the yield of C_3H_6 still increased despite the decrease in selectivity.

The homogeneous contributions to the catalytic reaction increase with temperature, since gas-phase reactions occur to a greater extent at temperatures above 873 or 923 K. The homogeneous reaction is mediated through radical pathways, and this includes both the oxidation of H_2S by O_2 and the reaction of S_2 (or O_2 or SO_2 or other oxidant species) with C_3H_8. The catalytic reaction is surface-based, and likely consists of two hydrogen abstractions from C_3H_8 to produce C_3H_6 and a reduced vanadia site that gets re-oxidized by O_2 (or in this case S_2). The results obtained from the catalytic experiments are therefore a combination of both these types of reactions, and the amount of each is not easily differentiated. Reducing the particle size of the catalyst would likely reduce the amount of gas-phase reactions that occur in the void spaces between the particles, but would lead to other issues such as pressure drop through the catalyst bed, and back-pressure issues in trying to flow high volumes of gases through the reactor.

While the low conversions and yields obtained for reactions carried out at 923 K may seem uninteresting from a commercial viewpoint, the trends observed at this reaction temperature are important to discern the effect brought about by changing reaction parameters, and this information will be ultimately valuable in designing the optimal conditions. However,

for industrial viability, higher conversions (which sometimes require high temperatures) may be required; so the reactions are also carried out at 1023 K, despite the larger contribution from gas-phase reactions.

To isolate the effects of the catalyst on the ODH reaction, the initial reactions were studied at lower temperatures such as 823 K and 873 K, where conversion of reactants is expected to be low but the effects of the catalyst can be seen with less interference from gas-phase contributions. Data in Table 4.13 shows the comparison between the reaction of C_3H_8 and O_2 in a 2:1 feed ratio at 20 ms contact time over a crystalline silica bed and a 1% VO_x/CS catalyst bed. The fifth row of the table shows the reaction with H_2S in a 4:2:2 (C_3H_8: H_2S: O_2) feed ratio.

Table 4.13: Comparison of the reaction between C_3H_8 and O_2 over an inert (CS) or catalyst (1% VO_x/CS) bed and the effect of adding H_2S to the catalytic reaction (20 ms contact time).

Catalyst	Temp K	Feed Ratio	Conversion %			Products, mole/100 moles of feed [Selectivity %]										Yield %	
			C_3H_8	O_2	H_2S	C_3H_6	C_2H_4	C_2H_6	CH_4	CO	CO_2	$C_{(s)}$	S_2	H_2O	H_2	C_3H_6	C_2H_4
CS	823	2:1	7	2	0	0.0 [0]	0.02 [<1]	0.0 [0]	0.05 [<1]	0.0 [0]	0.0 [0]	9.9 [99]	0.0	1.1	0.2	0	<1
1%	823	2:1	12	3	0	0.3 [6]	0.02 [<1]	0.0 [0]	0.04 [<1]	0.0 [0]	0.1 [1]	15.1 [93]	0.0	1.1	0.4	1	<1
CS	873	2:1	13	12	0	1.1 [19]	1.1 [13]	0.0 [0]	0.7 [4]	0.3 [2]	0.0 [0.04]	10.7 [63]	0.0	3.2	0.3	2	2
1%	873	2:1	22	18	0	2.4 [24]	1.5 [10]	0.0 [<1]	0.9 [3]	0.7 [2]	0.4 [1]	17.4 [59]	0.0	4.4	0.2	5	2
1%	823	4:2:2	16	85	65	4.7 [88]	0.7 [9]	0.0 [0]	0.4 [2]	0.7 [4]	0.1 [1]	-0.6 -[4]	5.5	18.4	0.3	14	1

Note: 2:1 feed = 33.0% N_2, 44.7% C_3H_8 and 22.3% O_2. 4:2:2 feed = 33.0% N_2, 33.5% C_3H_8, 16.8% H_2S and 16.8% O_2. See Appendix 4.12 for complete data table.

The data in rows 1-4 in Table 4.13 show that the presence of the catalyst increases the conversion of C_3H_8 as well as O_2. This effect is more pronounced at higher temperatures, and therefore the amount of the increase is higher at 873 K. It also increases the selectivity to C_3H_6 by around 5-6% at each reaction temperature. The selectivity to C_2H_4 is slightly higher for the

inert bed reaction compared to the catalyst bed reaction. The overall yield of C_2H_4 at 873 K is the same for both the catalytic and inert bed reaction because the increase in conversion more than compensates for the slight decrease in selectivity.

Looking at the reaction with H_2S (row 5), it can be seen that the conversion of O_2 is significantly higher than that observed for the non-H_2S reaction. This trend likely occurs because the reaction between H_2S and O_2 initiates at a much lower temperature and is highly exothermic. This oxidation increases the temperature in the catalytic bed region of the reactor, which enhances the ODH and other gas-phase reactions to a much greater extent. The selectivity to C_3H_6 is much greater than that for the reaction without H_2S, and at these lower temperatures, it is the major carbon product. The selectivity to C_2H_4 is also significantly higher for the H_2S-containing reaction when compared to the reaction without H_2S at the same temperature. However, it is close to the selectivity obtained for the catalytic reaction without H_2S at 873 K (which is 50 K higher). This is because even at lower temperatures, the initial oxidation of H_2S is already occurring to a significant extent (due to its low temperature ignition) and, as it is an exothermic reaction, the temperature in the catalyst bed is likely higher than the set temperature, facilitating a greater amount of cracking. Even though the reaction between C_3H_8 and O_2 is exothermic, the reaction requires temperatures above 823 K to proceed at a significant rate. Therefore, at 823 K the amount of reaction that is occurring is low, and subsequently the amount of heat obtained from the exothermic reaction is low, so the amount of cracking that occurs is also low. When the two reactions are compared at higher temperatures where both reactions are occurring in significant amounts, the amount of cracking is much more comparable.

To examine the effect of adding H_2S at higher temperatures where conversions are also higher, the reaction with and without H_2S was compared over a 1% catalyst bed at 923 K and

1023 K. These results are presented in Table 4.14, below. At comparable reaction temperatures (Table 4.15), the conversion of C_3H_8 is higher for the reaction without H_2S. The selectivity to the partial oxidation product, C_3H_6, is significantly higher for the reaction containing H_2S, which has been seen in all the results so far. The overall yield of C_3H_6 is also higher for the reaction containing H_2S because the significantly higher selectivity compensates for the lower conversion.

Table 4.14: Effect of adding H_2S to the reaction between C_3H_8 and O_2, over a 1% VO_x/CS catalyst bed at 35 ms contact time.

Feed ratio	Temp (°K)	Conversion %			Products, mole/100 moles of feed [Selectivity %]										Yield %	
		C_3H_8	O_2	H_2S	C_3H_6	C_2H_4	C_2H_6	CH_4	CO	CO_2	$C_{(s)}$	S_2	H_2O	H_2	C_3H_6	C_2H_4
4:1	923	27	97	0	3.9 [20]	6.0 [20]	0.4 [1]	5.9 [10]	4.9 [9]	7.5 [13]	16.7 [27]	0.0	19.3	6.1	5	6
4:1	1023	56	98	0	8.9 [22]	16.9 [28]	1.1 [2]	17.9 [15]	9.8 [8]	4.6 [4]	28.2 [23]	0.0	19.5	7.3	12	15
4:2:1	1023	45	98	36	12.9 [49]	12.1 [31]	0.9 [2]	12.6 [16]	0.8 [1]	0.2 [<1]	0.2 [<1]	3.2	24.1	6.4	22	14
4:2:1	1073	76	98	37	19.7 [44]	19.9 [30]	1.7 [3]	21.7 [16]	1.0 [1]	0.2 [<1]	8.2 [6]	3.3	24.0	9.3	34	23

Note: 4:1 feed = 10.7% N_2, 72.8% C_3H_8 and 20.4% O_2 and ~ 4:1.5:1 feed = 11.6% N_2, 58.5% C_3H_8, 17.7% H_2S and 12.9% O_2. See Appendix 4.13 for complete data table.

The opposite trend was observed for C_2H_4 as the selectivity was only slightly higher for the reaction with H_2S, but the lower conversion is enough to produce a slightly lower yield of C_2H_4 when H_2S is present in the reaction. Other results, such as lower selectivity to CO, CO_2 and $C_{(s)}$ when H_2S is present in the reaction, were also observed here, and trends are similar to the purely gas-phase reactions described in earlier sections of this chapter.

4.3.3 Effect of Changing Catalyst Vanadium Content

The next aspect of the reaction that was investigated was the effect of changing the amount of vanadia on the support. This translates to the number of active sites, as well as the type of active sites present on the catalyst. As previously mentioned in the introduction, the

higher the amount of vanadium oxide on the support, the lower the dispersion will be, and dispersion has been linked to the nature of active sites. Catalysts containing vanadium oxide amounts lower than one monolayer coverage of the support are known to have mostly monomeric VO_x units spread out on the support surface. When the amount of vanadium oxide is above one monolayer, polymeric VO_x sites or V_2O_5 crystallites can be produced. It has been noted from the literature that polymeric or crystallite V_2O_5 are not selective towards partial oxidation products such as C_3H_6, and instead favor total oxidation products such as CO and CO_2.[18] The results from the reaction between C_3H_8 and O_2 over VO_x/CS catalysts containing varying amounts of vanadium oxide are shown in Table 4.15 below. While it is understood that at 1023 K the contributions from gas-phase reactions may be significant enough to overshadow the effects of the catalysts, this work is carried out from an industrial perspective where high conversions are necessary for optimal operation, and therefore the studies were carried out at a higher temperature (1023 K) as well as a lower temperature (923 K).

The results show that conversion of C_3H_8 increased as the amount of vanadium oxide on the support increased. This result may be due to the greater number of active sites available for initiation of the reaction when a greater amount of vanadium oxide is present in the catalyst. However, the selectivity towards the desired product, C_3H_6, decreased with increasing VO_x amounts. The drop in selectivity to C_3H_6 between the 1% and 2.5% VO_x/CS catalysts is very small (20% to 19%), but is much more significant in going from the 2.5% to 5%VO_x/CS catalysts (19% to 14%).

Table 4.15: Comparison of different catalysts for the ODH of C_3H_8 with only O_2 using a 4:1 C_3H_8: O_2 feed at ~ 25-30 ms contact time.

Catalyst	Temp			Products, mole/100 moles of feed									Yield %	
	°K	Conversion %		[Selectivity %]										
		C_3H_8	O_2	C_3H_6	C_2H_4	C_2H_6	CH_4	CO	CO_2	$C_{(s)}$	H_2O	H_2	C_3H_6	C_2H_4
1% VOx/CS	923	27	97	3.9	6.0	0.4	5.9	4.9	7.5	16.7	19.3	6.1	5	6
				[20]	[20]	[1]	[10]	[9]	[13]					
2.5%Vox/CS	923	40	95	4.9	8.7	0.5	7.5	2.6	5.8	28.6	20.5	4.3	8	9
				[19]	[22]	[1]	[10]	[3]	[7]					
5%Vox/CS	923	49	80	4.9	10.4	0.6	9.1	3.9	3.6	51.3	19.2	4.3	7	10
				[14]	[20]	[1]	[9]	[4]	[3]					
1% VOx/CS	1023	56	98	8.9	16.9	1.1	17.9	9.8	4.6	28.2	19.5	7.3	12	15
				[22]	[28]	[2]	[15]	[8]	[4]					
2.5%Vox/CS	1023	66	99	7.2	19.8	1.5	18.4	6.1	3.9	36.7	22.2	7.4	11	20
				[17]	[31]	[2]	[14]	[5]	[3]					
5%Vox/CS	1023	68	95	10.2	22.8	1.4	21.0	6.7	4.2	33.1	21.0	8.6	14	21
				[21]	[32]	[2]	[15]	[5]	[3]					

Note: 4:1 feed = 11-2% N_2 with the remaining gas split to approximately a 3.6:1 ratio between C_3H_8 and O_2. See Appendix 4.14 for complete data table

Decreased selectivity to CO and CO_2 was also observed for the catalyst with the highest amount of vanadium oxide, which is an effect opposite to what was expected. To explain this, one just needs to look at the selectivity of $C_{(s)}$, which increased as the amount of vanadium oxide in the catalyst increased. This implies that instead of total oxidation products such as CO_x, coke is the favored product at these reaction conditions.

Similar sets of experiments were conducted, but including H_2S in the feed gas, and the results are shown in Table 4.16 below.

The data in Table 4.16 show some similar trends to the non-H_2S reaction. The conversion of C_3H_8 increased with an increased amount of vanadium oxide on the catalyst. The conversion of H_2S also increased. However, conversion of O_2 remained about the same at 98-99% regardless of the amount of vanadium oxide on the catalyst. The selectivity towards C_3H_6 showed an interesting trend.

Table 4.16: Comparison of different catalysts for the ODH of C_3H_8 in the presence of O_2 and H_2S using a 4:2:1 C_3H_8: H_2S: O_2 feed and ~ 25-30 ms contact time.

Catalyst	Temp °K	Conversion %			Products, mole/100 moles of feed [Selectivity %]										Yield %	
		C_3H_8	O_2	H_2S	C_3H_6	C_2H_4	C_2H_6	CH_4	CO	CO_2	$C_{(s)}$	S_2	H_2O	H_2	C_3H_6	C_2H_4
1% Vox/NS	923	13	99	5	3.8 [53]	2.3 [20]	0.1 [1]	1.8 [8]	1.9 [9]	4.2 [20]	-0.9	0.5	15.2	1.4	7	3
5% Vox/CS	923	31	98	6	3.6 [23]	5.4 [23]	0.1 [<1]	5.9 [13]	2.6 [5]	4.1 [9]	14.2	1.2	17.9	5.6	7	7
10% Vox/CS	923	32	99	8	3.8 [22]	5.0 [20]	0.1 [<1]	5.1 [10]	2.0 [4]	4.0 [8]	18.6	1.3	17.9	4.9	7	6
1% Vox/NS	1023	43	99	10	11.9 [47]	10.5 [28]	0.6 [2]	10.2 [14]	2.2 [3]	1.5 [2]	3.5	0.9	20.3	5.6	20	12
5% Vox/CS	1023	54	99	10	9.9 [35]	13.6 [33]	1.1 [3]	13.5 [16]	2.1 [2]	2.2 [3]	6.9	0.8	19.4	7.0	19	17
10% Vox/CS	1023	79	98	14	13.7 [32]	17.7 [28]	1.7 [3]	19.9 [16]	1.6 [1]	3.5 [3]	21.5	1.0	19.3	7.4	26	22

Note: 4:1 feed = 12-20% N_2 with remaining gas split to approximately a 4:1.5:1 ratio between C_3H_8, H_2S and O_2. See Appendix 4.15 for complete data table.

At both temperatures, the selectivity to C_3H_6 decreased as the amount of vanadium oxide on the catalyst increased, which is in line with what was previously expected. However, looking at the reaction on each catalyst separately, it can be seen that selectivity decreased as temperature was increased on the 1% VO_x/CS catalyst but not on the other two catalysts. A possible explanation may be that on the 1% catalyst, the selectivity towards C_3H_6 is higher for the catalytic reaction than if the reaction were to occur in the gas phase, hence when the temperature is increased and gas-phase contributions become more significant, a drop in selectivity is observed. In the case of the catalysts containing higher amounts of vanadium oxide, the selectivity to C_3H_6 is lower, and may in fact be lower than the purely gas-phase reaction selectivity to C_3H_6. This observation could explain why, when the temperature is increased to 1023 K and gas-phase contributions are more significant, the selectivity to C_3H_6 increases compared to the lower temperature reaction where catalytic contributions play a more significant role.

The general trend observed for C_2H_4 selectivity is an increase as the amount of vanadium oxide is increased from 1% to 2.5%, but then a decrease when it is increased further, probably because higher amounts of vanadium oxide favor the production of $C_{(s)}$. This explanation is supported by the data for $C_{(s)}$, which increases steadily as the amount of vanadium oxide is increased.

In addition to studying the effect of varying the amount of vanadium oxide on the support, the effect of changing the feed ratio while keeping the catalyst the same was also studied. The results of this study are shown in Table 4.17 below.

Table 4.17: Effect of varying the feed gas concentration for the ODH of C_3H_8 in the presence of H_2S and O_2 over a 2.5% VO_x/CS catalyst bed using a 22 ms contact time.

Feed ratio	Temp °K	Conversion %			Products, mole/100 moles of feed [Selectivity %]										Yield %	
		C_3H_8	O_2	H_2S	C_3H_6	C_2H_4	C_2H_6	CH_4	CO	CO_2	$C_{(s)}$	S_2	H_2O	H_2	C_3H_6	C_2H_4
7:2:1	923	28	96	4	4.3 [27]	1.6 [6]	0.0 [0]	1.5 [3]	0.3 [1]	0.0 [0]	31.1	0.3	14.2	0.8	7	2
4:1:1	923	45	97	22	5.7 [25]	4.7 [14]	0.2 [1]	4.2 [6]	1.4 [2]	1.0 [1]	36.3	1.6	21.9	2.1	11	6
7:2:1	1023	47	95	4	11.0 [40]	11.0 [27]	0.8 [2]	11.8 [14]	0.4 [<1]	0.0 [0]	13.8	0.3	14.0	6.2	19	13
4:1:1	1023	54	99	10	9.9 [35]	13.6 [33]	1.1 [3]	13.5 [16]	2.1 [3]	2.2 [3]	6.9	0.8	19.4	7.0	19	17

Note: 7:2:1 feed = 20.9% N_2, 58.5% C_3H_8, 16.2% H_2S and 7.5% O_2. 4:1:1 feed = 21.1% N_2, 52.1% C_3H_8, 15.3% H_2S and 13.1% O_2. See Appendix 4.16 for complete data table.

In addition to the overall changes in C_3H_8:O_2 ratio, the more important variable is the H_2S:O_2 ratio, which increases from 1:1 (in the 4:1:1 feed ratio) to 2:1 (in the 7:2:1 feed ratio). It has already been shown that a higher H_2S:O_2 ratio will lead to lower conversion of both reactants. This change will lead to lower S_2 quantities being produced, and since this is the preferred oxidant for reaction with C_3H_8, that will affect the selectivity towards C_3H_6. The other consideration is the overall ratio of alkane to O_2 and also alkane to H_2S + O_2 and both are higher

for the 7:2:1 feed ratio, which translates to a lower amount of O_2 or $H_2S + O_2$ for a given amount of the alkane. Again, lower activity would be expected based on these ratios.

The results in Table 4.17 showed that conversion of C_3H_8 was lower for the 7:2:1 feed ratio, as expected. The conversion of O_2 was comparable at 923 K and slightly higher for the 4:1:1 ratio at 1023 K. The conversion of H_2S was higher for the 4:1:1 ratio, also as expected based on the feed conditions. The selectivity to C_3H_6 was only slightly higher for the 7:2:1 ratio (2% higher) at 923 K, but the difference increased at 1023 K (5% higher). The selectivity to C_2H_4 was lower for the feed ratio with the lower amount of O_2 (7:2:1 feed ratio). In gas-phase reactions without H_2S (Tables 4.5, 4.6 and 4.7), it was found that the feed ratio with the lower amount of oxygen (4:1 C_3H_8: O_2) had a lower selectivity to C_2H_4 compared to the feed ratio with a higher amount of O_2 (2:1 C_3H_8: O_2). The same result had been found for H_2S reactions shown earlier (Tables 4.6 and 4.7), where different amounts of O_2 were used (4:2:1 vs 4:2:2 C_3H_8: H_2S: O_2 ratio). Since C_2H_4 is a product of cracking reactions, the results imply that cracking is favored by feed conditions containing higher amounts of O_2, whereas dehydrogenation is favored by feed conditions containing lower amounts of O_2

4.3.4 Effect of Contact Time on the Catalytic Reaction

The effect of contact time on the H_2S-containing reaction over a vanadia catalyst was also investigated, and the results are presented in Table 4.18, below. The data in the table showed some additional error as the conversion of oxygen cannot be lower at 1023 K than at 923 K, yet the data for 60 ms and 100 ms show this. The error was likely introduced while sampling, since a double syringe system is used for sampling streams which contain moisture and, therefore, air may sometimes be accidentally drawn into the syringe. By comparing the O_2 amounts between

the two reaction temperatures data and assuming that the O_2 conversion at 1023 K has to be at least as much as that found at 923 K, the amount of air (which represents the amount of error within the sample) can be estimated. For the experiment carried out at 60 ms, the difference in O_2 amount explicitly found by the GC was 0.41%. Since air contains ~20% O_2, the total amount of air drawn into the syringe during sampling was 2.04%.

This sampling error affects the overall data in two ways. Firstly, the true gas sample makes up only 98% of the total volume in the syringe sample and so each of the components (except N_2 and O_2) will be understated. Secondly, because air is made up of ~80% N_2, the amount of N_2 in the sample is now higher than it would otherwise be and since N_2 is the internal standard which is used to correct for condensed components in the system, this will cause a second error. A higher amount of N_2 will reduce the amount of the correction and again will cause the rest of the components in the system to be understated. The total error is a product of the two contributions and in this particular case adds up to about 6% for the values obtained via GC for each of the components. The final effect after data analysis would be that the true values for yield and selectivity of the products should have been higher and the conversion of propane should have been lower. The magnitude of the sampling error here should not affect the trends observed from the data set; however the occurrence of the error and discussion of its consequences needed to be mentioned. An online sampling system between the experimental set-up and the GC would easily solve the problem in future studies; however, that option was not available at the time of these studies.

Table 4.18: Effect of contact time on the ODH reaction between C_3H_8, H_2S and O_2 over a 2.5% VO_x/CS catalyst bed using a 7:2:1 C_3H_8: H_2S: O_2 ratio.

Contact time (ms)	Temp (°K)	Conversion %			Products, mole/100 moles of feed [Selectivity %]										Yield %	
		C_3H_8	O_2	H_2S	C_3H_6	C_2H_4	C_2H_6	CH_4	CO	CO_2	$C_{(s)}$	S_2	H_2O	H_2	C_3H_6	C_2H_4
12	923	16	97	4	4.1 [46]	4.5 [33]	0.2 [1]	4.5 [17]	0.7 [2]	0.2 [1]	-1.2 -[7]	0.3	13.7	2.7	7	5
60	923	35	93	0	4.6 [23]	4.4 [15]	0.2 [1]	4.5 [8]	1.2 [2]	0.4 [1]	30.5 [48]	0.0	12.3	4.0	8	5
100	923	53	88	2	5.2 [18]	3.9 [9]	0.4 [1]	4.4 [5]	1.8 [2]	0.5 [1]	49.5 [58]	0.2	10.6	5.1	10	5
12	1023	76	96	-5	15.7 [36]	22.4 [34]	2.4 [4]	30.9 [23]	0.3 [<1]	2.1 [2]	4.3 [3]	-0.4	10.2	8.5	27	25
60	1023	84	83	-2	14.5 [30]	20.5 [28]	2.1 [3]	23.4 [16]	0.4 [<1]	2.2 [2]	31.5 [22]	-0.1	8.0	8.3	25	24
100	1023	84	82	7	8.4 [19]	18.3 [27]	1.9 [3]	21.1 [16]	0.3 [<1]	1.6 [1]	44.3 [33]	0.6	9.1	7.4	16	23

Note: 7:2:1 feed = 22.6% N_2, 56.6% C_3H_8, 16.1% H_2S and 7.7% O_2. See Appendix 4.17 for complete data table.

The trends observed in the data are similar to what was seen for the gas-phase reactions containing H_2S. Conversion of C_3H_8 increased with increased contact time, and the increases were higher at the lower temperature. A greater effect from catalytic reaction is expected at 923 K compared to 1023 K, as catalytic contributions are higher at 923 K, whereas gas-phase contributions become more significant at the higher temperature. The magnitude of the increase also implies that at lower temperatures, the catalyst can increase its activity significantly by a change in contact time. Contact time becomes less crucial as a parameter for control of activity at higher temperatures. The conversion of H_2S also seemed to decrease with increased contact time at 923 K. However, since the values themselves are so low (4% conversion or less), it is difficult to state the trend with confidence. What is more interesting is the fact that conversion was very low for H_2S. It is expected that the reaction between H_2S and O_2 over the catalyst would yield S_2 and H_2O as the major products, and with the O_2 being mostly used up in this reaction, the only oxidant left for reaction with C_3H_8 is S_2. The product of oxidative dehydrogenation of C_3H_8 by S_2 would yield C_3H_6 and H_2S. This would make the total conversion of H_2S seem very low, and if this is indeed what is happening, then it means that the reaction is efficient at using up all the

O_2 for production of H_2O, which is exothermic and provides heat of reaction and also produces S_2 for ODH of C_3H_8, in turn regenerating one of the reactants (H_2S) for re-use. There is also the added advantage of lower CO_x production if most of the O_2 is consumed in the oxidation of H_2S.

The selectivity towards C_3H_6 decreased with increased contact time at both temperatures and this is expected, as it is well known that the longer C_3H_6 remains in the catalyst bed, the higher the probability that it will react further. It is expected that the active site on the catalyst does not differentiate between a C-H bond on a saturated or a non-saturated hydrocarbon, and so it will cause hydrogen abstraction from either propane or propylene, given the opportunity. The similar trend of decreasing selectivity is observed for all other carbon-containing products, even C_2H_4, which is a product of cracking. Cracking occurs to a greater extent at higher temperatures, and this is observed experimentally by the selectivity and yield of C_2H_4, which is typically higher at 1023 K than at 923 K. The results above show that the effect of contact time on the selectivity of C_2H_4 is more sensitive at 923 K, dropping from 33.4% to 9.09% when contact time increased from 12 ms to 100 ms, as compared to a drop from 33.7% to 27.3% at 1023 K for the same increase in contact time. At the lower temperature, catalytic processes play a greater role, and since it is apparent in the data from the 12 ms contact time experiment that a significant amount of C_2H_4 is already formed, a longer contact time will simply allow time for the C_2H_4 already produced to react further to produce CO_x or $C_{(s)}$, depending on the reaction path and availability of oxygen or reaction with water. Additionally, since no significant increase in the selectivity to CO_x was observed in the data, it can be concluded that further reaction leads to $C_{(s)}$ as is seen from the mass balance data.

Indeed, the data show that higher contact times over the catalyst at all temperatures lead to increased $C_{(s)}$ formation. Especially at the lower reaction temperature (923 K), the selectivity

to $C_{(s)}$ increased significantly with increased contact time — showing that if the contact time were increased to the point where the system is at equilibrium-like conditions, $C_{(s)}$ would be the most favored product, similar to that predicted by the gas-phase equilibrium calculations.

4.4 Conclusions

The ODH reaction between C_3H_8 and O_2 in the presence of H_2S shows significant improvement due to the presence of H_2S, especially in terms of selectivity towards C_3H_6, without a great loss of C_2H_4 selectivity. The improvement in selectivity is thought to arise from the early reaction of O_2 with H_2S, which not only produces S_2 but also uses up a significant amount of the O_2, hence limiting production of CO_x, which can be a result of direct combustion of C_3H_8 by O_2. S_2 is a milder oxidant than O_2 and the overall reaction of C_3H_8 and O_2 is much more exothermic, so a drop in conversion is observed. However, in the majority of the experiments carried out, the overall yield of C_3H_6 (which is of greater industrial importance) is higher for the H_2S reactions. This is because the higher selectivity to C_3H_6 more than compensates for any reduction in conversion. A significant conversion of H_2S is observed in the gas-phase reaction, which was different from that observed for catalytic reactions.

The catalytic ODH reaction showed similar improvement when H_2S was added to the reaction between C_3H_8 and O_2. However, this improvement was very similar to that seen in the gas-phase reaction showing very little, if any improvement to the selectivities observed in the gas-phase reaction, especially at higher temperatures. The biggest potential improvement comes in the form of C_3H_8 conversion. The conversion of C_3H_8 also improved significantly at higher contact times, especially at 923 K where conversions are generally on the lower side. However, the selectivity towards the desired product, C_3H_6, suffered considerably in that the overall

outcome (yield) was comparable between the two cases (gas phase vs catalyst). In terms of the overall goal of the reaction, which is production of olefins and in particular C_3H_6, the catalytic reaction offers no significant improvement, if any.

However, one of its major advantages was the low conversion of H_2S while obtaining similar yields of C_3H_6 at certain reaction conditions. This may be industrially useful, as a lower amount of H_2S would be needed to maintain the feed amounts, since most of it still remains in the product gas after the reaction. H_2S separation technologies are already available, and it would not pose a significant challenge to add such a process in order to recycle the H_2S to the front end of the process. While S_2 and H_2O were both observed visibly in the product stream, the experimental system used in this research was not set up to quantify these amounts. If the amount of S_2 produced in these reactions could be quantified and recovered separately, the information obtained from it would be beneficial in drafting up a true cost analysis for the process, and would help to decide whether the catalyst is worth the extra cost or not. As S_2 is a valuable product, its production/separation from within the gas-phase process could make the non-catalytic process seem more cost effective.

Chapter 5: The ODH of n-Butane

5.0 The ODH of n-Butane

The reaction between C_4H_{10} and O_2 and H_2S is expected to follow a similar pattern to that of C_3H_8 with H_2S and O_2. However, the presence of the extra carbon atom in the alkane chain will expand the number of products possible. Compared to the case of the three carbon alkane chain where there was only one main dehydrogenation product, namely C_3H_6, the four carbon chain alkane has three main dehydrogenation products (not including the isomer, iso-butene or 1,3-butadiene): 1-C_4H_8, cis -2-C_4H_8 and trans-2-C_4H_8, the structures of which are shown below.

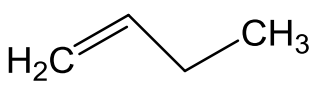

1-C_4H_8

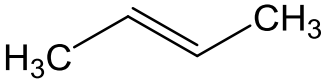

trans-2-C_4H_8

cis-2-C_4H_8

In addition, cracking can occur at two different parts of the carbon chain: between the first and second carbon or between the second and third carbon, and each of these will result in different products. Cracking between carbon 1 and 2 will lead to a C_3 and a C_1 product [5.1], while cracking between carbon 2 and 3 will lead to two C_2 products [5.2], according to the equations below.

[5.1] $C_4H_9\bullet \rightarrow CH_3\bullet + C_3H_6$

[5.2] $C_4H_9\bullet \rightarrow C_2H_5\bullet + C_2H_4$

From a commercial viewpoint, the use of C_4H_{10} as a feedstock offers the possibility of making C_2 – C_4 alkenes from a single feedstock, a process which, if controlled to produce propene and butenes, may offer significant economic advantage.

5.0.1 Gibbs Free Energy Calculations for Expected Product Distributions

Expected product distributions for the pyrolysis of C_4H_{10}, the reaction of C_4H_{10} with O_2, the reaction between C_4H_{10} and S_2 as well as the reaction between C_4H_{10}, O_2 and H_2S as calculated by equilibrium calculations are shown in Table 5.1a-d, below.

The equilibrium calculations show trends which are very similar to those seen in the calculations carried out for propane. For calculations that allowed carbon in the products, $C_{(s)}$ will almost always be the major carbon product along with H_2 and CH_4, regardless of whether an oxidant such as S_2 or O_2 is present. When O_2 is included in the reactants, the major oxygen product is H_2O, with the minor product being CO along with a very small amount of CO_2. When S_2 is present in the reactants, the major sulphur product is H_2S. When both O_2 and H_2S are present, the final products look similar to the reaction of C_4H_{10} and O_2 (as if H_2S is absent).

When $C_{(s)}$ is not allowed in the products, the product distributions determined by the calculations are significantly different, and include dehydrogenation as well as cracking products. For the reaction between C_4H_{10} and O_2, the main products are C_4H_8, C_3H_6, C_2H_4 and CH_4. At 923 K, the selectivity to C_3H_6 and C_2H_4 is approximately the same (~22%) and the selectivity to C_4H_8 is about 16%, thus showing that cracking processes will occur to a greater extent compared to dehydrogenation processes. When the temperature was increased to 1023 K, the selectivity to C_4H_8 dropped by 6.9%, the selectivity to C_3H_6 dropped by 3.4% and the selectivity to C_2H_4 increased by 10.7%, showing that cracking is favoured even more at higher temperatures and in particular, the cracking pathway that leads to ethylene formation. The selectivity towards CH_4 remained approximately the same at both temperatures. The major oxygen-containing product in this reaction is CO.

Table 5.1a: Expected product distributions for the pyrolysis of C_4H_{10} based on Gibbs free energy equilibrium calculations with $C_{(S)}$ in the products.

	Temp °K	Products, mole/100 moles of feed										Conversion %	Yield % [Selectivity %]						
		N_2	n-C_4H_{10}	H_2	1-C_4H_8	C_3H_6	C_3H_8	C_2H_4	C_2H_6	CH_4	$C_{(s)}$	C_4H_{10}	1-C_4H_8	C_3H_6	C_3H_8	C_2H_4	C_2H_6	CH_4	$C_{(s)}$
Feed		79.00	23.50																
Product	923	79.00	8.0E-13	55.41	9.7E-14	6.1E-10	1.3E-08	3.2E-06	2.8E-04	31.05	62.95	100	4.1E-13	1.9E-09	4.2E-08	6.7E-06	6.0E-04	33.03	66.97
													[4E-13]	[2E-09]	[0]	[7E-06]	[6E-04]	[33]	[67]
Product	1023	79.00	6.6E-13	67.47	1.7E-13	1.0E-09	1.1E-08	5.9E-06	2.4E-04	25.02	68.98	100	7.1E-13	3.3E-09	3.6E-08	1.3E-05	5.2E-04	26.61	73.39
													[7E-13]	[3E-09]	[0]	[1E-05]	[5E-04]	[26.6]	[73.4]

Table 5.1b: Expected product distributions for the reactions between C_4H_{10} and S_2 and C_4H_{10} and O_2 calculated without $C_{(s)}$ in the products.

	Temp °K	Products, mole/100 moles of feed											Conversion %		Yield % [Selectivity %]						
		N_2	n-C_4H_{10}	S_2	H_2	1-C_4H_8	C_3H_6	C_3H_8	C_2H_4	C_2H_6	CH_4	CS_2	C_4H_{10}	S_2	1-C_4H_8	C_3H_6	C_3H_8	C_2H_4	C_2H_6	CH_4	CS_2
Feed		27.97	50.25	6.45																	
$C_4H_{10}+S_2$	923	27.97	0.38	7.1E-09	2.4E-03	17.18	15.60	0.75	8.45	2.44	53.05	6.45	99.24	100	34.20	23.29	1.12	8.41	2.43	26.39	3.21
															[34.5]	[23.5]	[1.13]	[8.47]	[2.4]	[26.59]	[3.23]
	1023	27.97	0.11	3.8E-08	1.1E-02	11.97	17.12	0.38	17.77	1.92	54.26	6.45	99.78	100	23.82	25.55	0.57	17.68	1.91	26.99	3.21
															[23.9]	[25.6]	[0.57]	[17.7]	[1.9]	[27.05]	[3.22]
		N_2	n-C_4H_{10}	O_2	H_2	1-C_4H_8	C_3H_6	C_3H_8	C_2H_4	C_2H_6	CH_4	CO	C_4H_{10}	O_2	1-C_4H_8	C_3H_6	C_3H_8	C_2H_4	C_2H_6	CH_4	CO
$C_4H_{10}+O_2$	923	27.97	0.06	1.4E-38	0.03	7.99	15.09	0.27	22.61	1.78	61.01	12.90	99.89	100	15.90	22.53	0.41	22.50	1.77	30.35	6.42
															[15.9]	[22.6]	[0.41]	[22.5]	[1.8]	[30.39]	[6.43]
	1023	27.97	0.02	2.8E-36	0.09	4.53	12.83	0.14	33.37	1.37	61.53	12.90	99.96	100	9.01	19.14	0.21	33.20	1.37	30.61	6.42
															[9.01]	[19.2]	[0.21]	[33.2]	[1.4]	[30.62]	[6.42]

See Appendix 5.1a and 5.1b for full data table.

Table 5.1c: Expected product distributions for the reactions between C_4H_{10} and S_2, and C_4H_{10} and O_2 calculated with $C_{(s)}$ in the products.

	Temp °K	Products, mole/100 moles of feed									Conversion %		Yield % [Selectivity %]								
		N_2	n-C_4H_{10}	O_2	H_2	CH_4	CO	CO_2	H_2O	$C_{(s)}$	C_4H_{10}	O_2	1-C_4H_8	C_3H_6	C_3H_8	C_2H_4	C_2H_6	CH_4	CO	CO_2	$C_{(s)}$
Feed		27.97	50.25	6.45																	
$C_4H_{10} + O_2$	923	27.97	0.00	3.7E-25	141.66	50.09	2.52	0.49	9.40	147.90	100.00	100.00	2.3E-12	8.0E-09	6.6E-08	2.4E-05	6.9E-04	24.92	1.25	2.4E-01	7.4E+01
													[2E-12]	[8E-09]	[7E-08]	[2E-05]	[7E-04]	[24.92]	[1.251]	[0.24]	[73.58]
	1023	27.97	0.00	2.1E-24	159.96	41.52	3.70	0.48	8.24	155.30	100.00	100.00	3.0E-12	1.1E-08	5.4E-08	3.5E-05	5.8E-04	20.66	1.84	2.4E-01	7.7E+01
													[3E-12]	[1E-08]	[5E-08]	[3E-05]	[6E-04]	[20.66]	[1.842]	[0.24]	[77.26]
		N_2	n-C_4H_{10}	H_2S	S_2	H_2	C_2H_4	C_2H_6	CH_4	$C_{(s)}$	C_4H_{10}	S_2	1-C_4H_8	C_3H_6	C_3H_8	C_2H_4	C_2H_6	CH_4	CS	CS_2	$C_{(s)}$
$C_4H_{10} + S_2$	923	27.97	0.00	12.90	1.1E-06	111.97	1.2E-05	8.3E-04	63.19	137.81	100.00	100.00	1.3E-12	4.5E-09	7.9E-08	1.2E-05	8.3E-04	31.44	6.5E-12	5.9E-06	6.9E+01
													[1E-12]	[4E-09]	[8E-08]	[1E-05]	[8E-04]	[31.44]	[7E-12]	[0]	[68.56]
	1023	27.97	0.00	12.90	2.2E-06	132.41	2.0E-05	7.3E-04	52.97	148.03	100.00	100.00	2.0E-12	6.9E-09	6.9E-08	2.0E-05	7.2E-04	26.35	2.9E-11	1.1E-05	7.4E+01
													[2E-12]	[7E-09]	[7E-08]	[2E-05]	[7E-04]	[26.35]	[3E-11]	[0]	[73.65]

See Appendix 5.2 for complete data table.

Table 5.1d: Expected product distributions for the reactions between C_4H_{10}, H_2S and O_2 calculated with and without $C_{(s)}$ in the products.

	Temp °K	moles/100 moles					Conversion %			Yield % [Selectivity %]													
		N_2	C_4H_{10}	H_2S	O_2	H_2	C_4H_{10}	O_2	H_2S	C_4H_8	C_3H_6	C_3H_8	C_2H_4	C_2H_6	CH_4	CO	CO_2	CS_2	COS	SO_2	S_2	H_2O	$C_{(s)}$
Feed		27.97	50.25	15.53	6.45																		
With $C_{(s)}$	923	27.97	2.8E-12	15.52	3.3E-25	143.24	100.00	100.00	0.06	2.0E-12	7.2E-09	5.8E-08	2.2E-05	6.5E-04	24.54	1.26	0.25	7.6E-05	0.02	5.2E-10	5.0E-05	72.64	73.95
										[2E-12]	[7E-09]	[6E-08]	[2E-05]	[6E-04]	[24.5]	[1.26]	[0.25]	[8E-05]	[0.018]				[74]
	1023	27.97	2.1E-12	15.52	2.0E-24	162.23	100.00	100.00	0.08	2.6E-12	9.8E-09	4.7E-08	3.3E-05	5.4E-04	20.12	1.88	0.24	1.3E-04	0.02	7.8E-10	9.3E-05	63.14	77.75
										[3E-12]	[1E-08]	[5E-08]	[3E-05]	[5E-04]	[20.1]	[1.88]	[0.24]	[1E-04]	[0.023]				[77.8]
Without $C_{(s)}$	923	27.97	0.02	0.01	0.01	0.11	99.96	100.00	99.94	6.15	14.08	0.24	25.52	1.70	42.00	6.40	0.00	15.41	0.07	1.1E-20	7.6E-06	6.4E-07	n/a
										[6.155]	[14.08]	[0.245]	[25.53]	[1.697]	[42]	[6.4]	[0]	[15.42]	[0.067]				
	1023	27.97	0.01	0.02	0.00	0.39	99.99	100.00	99.87	2.75	10.00	0.11	33.48	1.23	42.13	6.41	0.00	15.41	0.04	6.1E-20	3.5E-05	1.5E-06	n/a
										[2.75]	[10.01]	[0.114]	[33.49]	[1.233]	[42.1]	[6.41]	[0]	[15.41]	[0.043]				

See Appendix 5.3 for complete data table.

The expected products for the reaction between C_4H_{10} and S_2 are the same as that for C_4H_{10} and O_2, but in different proportions. C_4H_8 had the highest selectivity (34.5%) followed by CH_4 (26.9%), C_3H_6 (23.5%) and then C_2H_4 (8.47%). The combined yield to C_2-C_3 olefins was 31.70%, which is lower than the yield of C_4H_8, showing that dehydrogenation is favoured over cracking, though only slightly. When the temperature was increased to 1023 K, the selectivity to C_4H_8 dropped by 10.6%, while that towards C_3H_6 and C_2H_4 increased by 2.1% and 9.25%, respectively. In the presence of S_2, C_3H_6 is the favoured cracking product, over C_2H_4, which is the opposite of what was seen for the reaction of C_4H_{10} with O_2. The major sulphur product is CS_2. Although S_2 was not added directly to C_4H_{10} in the experimental studies (it is produced in-situ via the oxidation of H_2S), the comparison between equilibrium product distributions of the reaction between the reaction with S_2 versus the reaction with O_2 helps to show the differences between the two oxidants. O_2 favours a higher proportion of cracking leading to C_2H_4, while S_2 seems to promote dehydrogenation, and when cracking occurs, the favored cracking product is C_3H_6 over C_2H_4 even at the higher temperature of 1023 K.

Finally, the results of the reaction between $C_4H_{10,}$ H_2S and O_2 (without $C_{(s)}$ in the products) at 923 K looks more like the reaction of C_4H_{10} with O_2 rather than S_2, where CH_4 and C_2H_4 are the major carbon products followed by CS_2 and C_3H_6 and only ~6% of the carbon in the system goes towards dehydrogenation products. The major oxygen-containing product is CO and the major sulphur-containing product is CS_2, both of which would be to near 100% selectivities for their respective (non-carbon) elements. H_2O is not calculated to be produced in more than negligible quantities. Finally, all the reactants were shown to have near-complete conversions (~99% or higher).

5.0.2 Gas-phase ODH of n-Butane with H_2S

Experimentally, the reaction was first studied in the gas phase by using an inert crystalline silica bed to ensure good mixing of the reagents. The reaction of C_4H_{10} with O_2 was first carried out, followed by the same reaction with H_2S as co-reactant (Table 5.2). Reaction between C_4H_{10} and O_2 at short contact times led to C_4H_{10} conversion in the range of 19% to 31% at 923 K and 1023 K, respectively. The selectivity towards dehydrogenation products was approximately 11%, while the selectivity towards cracking products such as C_3H_6 and C_2H_4 was 18% for both products at 923 K. When the temperature was increased to 1023 K, selectivity to both dehydrogenation products and cracking products increased. As well, selectivity to CO and CO_2 decreased slightly at the higher temperature. The proportion of C_2H_6 relative to the amount of C_2H_4 produced was found to be relatively low. The main observation is that in gas-phase reactions the selectivity towards C_3H_6 and C_2H_4 is very similar, and this trend was seen at both temperatures.

When H_2S was added to the reaction at 923 K, the selectivity to dehydrogenation products increased and the proportion of 1-C_4H_8 to 2-C_4H_8 was different from that seen for the reaction without H_2S. In addition, the selectivity to C_3H_6 was significantly higher quantitatively as well as relative to that of C_2H_4, thus showing that reaction pathways leading to C_3H_6 are more favourable than those leading to C_2H_4. The amount of C_2H_6 relative to the amount of C_2H_4 was significantly higher than it was in the reaction without H_2S. The selectivity to 2-C_4H_8 was higher for the reaction containing H_2S at both temperatures.

Table 5.2: The reaction between C_4H_{10} and O_2 and the effect of adding H_2S, over an inert silica bed at a 6-8 ms contact time.

	Temp °K	Conversion %			Products, mole/100 moles of feed [Selectivity %]													Yield %			
		C_4H_{10}	O_2	H_2S	1-C_4H_8	2-C_4H_8	C_3H_6	C_3H_8	C_2H_4	C_2H_6	CH_4	CO	CO_2	$C_{(s)}$	S_2	H_2O	H_2	1-C_4H_8	2-C_4H_8	C_3H_6	C_2H_4
No H_2S	923	19	99	0	1.5	0.2	3.5	0.1	5.1	1.1	4.6	1.7	5.6	15.6	0.0	20.3	3.1	2	0	4	3
					[10]	[1]	[18]	[<1]	[18]	[4]	[8]	[3]	[10]	[27]							
With H_2S	923	25	90	29	2.4	1.0	5.2	0.0	2.2	1.3	5.2	0.1	0.1	8.0	2.3	11.3	0.3	5	2	8	2
					[20]	[8]	[32]	[0]	[9]	[5]	[10]	[<1]	[<1]	[16]							
No H_2S	1023	31	99	0	3.5	0.3	7.7	0.2	10.8	2.0	10.2	2.0	6.0	7.6	0.0	6.4	5.1	5	0	8	7
					[16]	[<1]	[25]	[1]	[24]	[5]	[11]	[2]	[7]	[8]							
With H_2S	1023	76	95	24	3.7	1.1	20.5	0.0	9.4	6.7	23.8	0.3	0.8	15.7	1.9	10.3	3.4	7	2	31	9
					[10]	[3]	[40]	[0]	[12]	[9]	[15]	[<1]	[1]	[10]							

Note: No H_2S feed = 17.8% N_2, 73.5% C_4H_{10} and 16.7% O_2. With H_2S feed = 28.0% N_2, 50.3% C_4H_{10}, 15.5% H_2S and 6.5% O_2. See Appendix 5.4 for complete data table.

Table 5.3: Effect of residence time on the reaction of ~4:2:1 C_4H_{10}: H_2S: O_2 over an inert silica bed.

Contact time	Temp °K	Conversion %			Products, mole/100 moles of feed [Selectivity %]													Yield %			
		C_4H_{10}	O_2	H_2S	1-C_4H_8	2-C_4H_8	C_3H_6	C_3H_8	C_2H_4	C_2H_6	CH_4	CO	CO_2	$C_{(s)}$	H_2O	H_2	S_2	1-C_4H_8	2-C_4H_8	C_3H_6	C_2H_4
8 ms	923	25	90	29	2.4	1.0	5.2	0.0	2.2	1.3	5.2	0.1	0.1	8.0	11.3	0.3	2.3	5	2	8	2
					[20]	[8]	[32]	[0]	[9]	[5]	[11]	[<1]	[<1]	[16]							
27 ms	923	35	93	14	5.3	0.5	8.7	0.0	3.5	2.6	9.2	0.5	0.6	1.3	9.2	0.6	0.8	10	1	12	3
					[29]	[3]	[36]	[0]	[10]	[7]	[13]	[1]	[1]	[2]							
8 ms	1023	76	95	24	3.7	1.1	20.5	0.0	9.4	6.7	23.8	0.3	0.8	15.7	10.3	3.4	1.9	7	2	31	9
					[10]	[3]	[40]	[0]	[12]	[9]	[16]	[<1]	[1]	[10]							
27 ms	1023	80	90	10	4.1	0.9	23.9	0.3	11.3	7.9	28.4	0.6	1.0	7.9	8.0	3.1	0.7	8	2	34	11
					[10]	[2]	[42]	[1]	[13]	[9]	[17]	[<1]	[1]	[5]							

Note: 8 ms experiment feed = 28.0% N_2, 50.3% C_4H_{10}, 15.5% H_2S and 6.5% O_2. 27 ms experiment feed = 30.0% N_2, 52.5% C_4H_{10}, 13.6% H_2S and 6.0% O_2. See Appendix 5.5 for complete data table.

The selectivity to CO and CO_2 was very low (1% or less) at both reaction temperatures compared to the reaction without H_2S, which had close to 10% selectivity towards CO_2 at 923 K and 7% at 1023 K. When the temperature was increased to 1023 K, the selectivity towards dehydrogenation products decreased and the selectivity towards cracking products increased. However, the ratio of C_3H_6 to C_2H_4 was still greater than 3 at the higher temperature. The combined C_2-C_4 olefin yields were 49% for the reaction containing H_2S, and 20% for the reaction without H_2S.

Next, the effect of contact time on the gas-phase reaction was also studied to confirm if the trends seen earlier in the ODH of propane would apply to the reaction with butane as well. The experiments were performed by studying the reaction at two different residence times (8 and 27 ms, Table 5.3).

The data from these reactions (C_4H_{10}, O_2 and H_2S) followed expected trends, i.e., C_4H_{10} conversion should increase, more so at the lower of the two reaction temperatures, and higher yields of cracking products (C_3H_6, C_2H_4, C_2H_6 and CH_4) should be observed. Experimentally, the conversion of C_4H_{10} increased with contact time, and the increase was greater at 923 K than at 1023 K. The selectivity to C_4H_8 increased when contact time was increased at 923 K, but at 1023 K, the selectivities remained approximately the same at both contact times. The selectivity towards C_3H_6 and C_2H_4 increased as a function of contact time. At 923 K, the selectivity increased by 4% and 1% for C_3H_6 and C_2H_4 respectively. At 1023 K, the selectivity increased by 2% and 1% for C_3H_6 and C_2H_4 respectively. One more important observation from these data is in regard to conversion of H_2S, which decreased with increased contact time at both reaction temperatures. Of course, this effect may not be due to lower conversion itself, but rather more effective recycling of sulphur or sulphur-containing products back to H_2S, which is the most favourable sulphur product at these temperatures.

5.0.3 The Catalytic ODH of n-Butane with H_2S

The catalytic reaction is expected to be similar to the gas-phase reaction; however, at lower temperatures the catalyst may aid the reaction in both activity and selectivity. The vanadium oxide sites on the surface are capable of participating in the ODH reaction, and either unreacted O_2 or the S_2 that is produced from the oxidation of H_2S can be used for completing the catalyst cycle to regenerate the reduced spent catalytic site to its oxidized form for further reaction. This surface mechanism is expected to be similar to that of the reaction containing C_3H_8, H_2S and O_2.

Data in Table 5.4a shows the reaction between C_4H_{10}, O_2 and H_2S at a relatively short contact time (8 ms) over an inert bed containing crystalline silica and a catalyst bed containing 5% VO_x/CS. At 923 K, where catalytic contributions are expected to be most visible, the catalyst does provide some additional selectivity to highly desirable products. Selectivity to 1-C_4H_8 and 2-C_4H_8 increased from 30% and 4% to 47% and 7% respectively, thus showing that the catalytic reaction is more selective towards dehydrogenation than the gas-phase reaction. Selectivity to cracking products also increased from 22% to 30% and 6% to 9% for C_3H_6 and C_2H_4 respectively. The C_2-C_4 olefin yield was 29% for the catalytic reaction, at 31% conversion of C_4H_{10}. Comparatively, the C_2-C_4 olefin yield was 19% for the non-catalytic reaction at 31% conversion of C_4H_{10}.

Table 5.4a: Comparison of reaction products when an 8:2.5:1 C_3H_8: H_2S: O_2 feed is passed over an inert bed or catalyst bed at 8 ms.

	Temp °K	Conversion %			Products, mole/100 moles of feed [Selectivity %]													Yield %			
		C_4H_{10}	O_2	H_2S	1-C_4H_8	2-C_4H_8	C_3H_6	C_3H_8	C_2H_4	C_2H_6	CH_4	CO	CO_2	$C_{(s)}$	S_2	H_2O	H_2	1-C_4H_8	2-C_4H_8	C_3H_6	C_2H_4
CS	923	31	91	37	4.7	0.6	4.7	0.0	1.9	1.1	4.6	0.1	0.0	16.4	2.9	11.6	0.3	9	1	7	2
					[30]	[4]	[22]	[0]	[6]	[4]	[7]	[<1]	[<1]	[26]							
5% VOx/CS	923	31	87	13	4.6	0.7	4.0	0.0	1.8	0.9	3.9	0.2	0.1	-3.3	0.5	5.6	0.1	14	2	9	3
					[47]	[7]	[30]	[0]	[9]	[5]	[10]	[1]	[<1]	-[9]							
CS	1023	75	96	32	3.4	0.8	18.4	0.0	8.4	6.2	21.3	0.3	0.8	29.7	2.5	10.5	3.0	7	2	27	8
					[9]	[2]	[36]	[0]	[11]	[8]	[14]	[<1]	[<1]	[19]							
5% VOx/CS	1023	76	89	2	2.6	0.6	13.3	0.0	6.6	4.2	15.3	0.3	1.0	6.2	0.1	4.2	2.1	8	2	31	10
					[11]	[3]	[41]	[0]	[14]	[9]	[16]	[<1]	[1]	[6]							

Note: CS feed = 26.0% N_2, 50.8% C_4H_{10}, 15.5% H_2S and 6.5% O_2. 5% VO_x/CS feed = 60.7% N_2, 32.0% C_4H_{10},7.8% H_2S and 3.8% O_2. See Appendix 5.6 for complete data table.

Table 5.4b: Comparison of reaction products when an 8:2:1 C_3H_8: H_2S: O_2 feed is passed over an inert bed or catalyst bed at 27 ms.

Catalyst	Temp °K	Conversion %			Products, mole/100 moles of feed [Selectivity %]													Yield %			
		C_4H_{10}	O_2	H_2S	1-C_4H_8	2-C_4H_8	C_3H_6	C_3H_8	C_2H_4	C_2H_6	CH_4	CO	CO_2	$C_{(s)}$	S_2	H_2O	H_2	1-C_4H_8	2-C_4H_8	C_3H_6	C_2H_4
CS	923	35	93	14	5.3	0.5	8.7	0.0	3.5	2.6	9.2	0.5	0.6	1.3	0.8	9.2	0.6	10	1	12	3
					[29]	[3]	[36]	[0]	[10]	[7]	[13]	[1]	[1]	[2]							
2.5% VOx/CS	923	39	87	15	5.7	0.8	9.7	0.0	4.1	2.6	10.9	0.5	0.9	0.0	1.0	8.1	0.7	11	2	14	4
					[28]	[4]	[36]	[0]	[10]	[6]	[13]	[1]	[1]	[<1]							
CS	1023	80	90	10	4.1	0.9	23.9	0.3	11.3	7.9	28.4	0.6	1.0	7.9	0.7	8.0	3.1	8	2	34	11
					[10]	[2]	[42]	[1]	[13]	[9]	[17]	[<1]	[1]	[5]							
2.5% VOx/CS	1023	86	93	5	3.7	1.3	26.8	0.1	12.8	8.6	31.5	0.5	1.9	4.3	0.4	6.9	3.6	7	2	38	12
					[8]	[3]	[44]	[<1]	[14]	[10]	[17]	[<1]	[1]	[2]							

Note: feed for both experiments =30.0% N_2, 52.5% C_4H_{10},13.6% H_2S and 6.0% O_2. See Appendix 5.7 for complete data table.

At 1023 K, the selectivity to dehydrogenation products dropped; however, the catalytic reaction still had a slightly higher selectivity towards C_4 olefins. The selectivity to cracking products increased for both the gas-phase and the catalytic reaction, as would be expected. However, the difference in selectivities towards C_3H_6 and C_2H_4 between the two reactions is slightly lower, showing that at high temperatures gas-phase contributions increase, thereby limiting the advantages of using a catalyst. The overall C_2-C_4 olefin yield was 51% and 44% for the catalytic and gas-phase reaction, respectively.

Table 5.4b shows the reaction between C_4H_{10}, O_2 and H_2S at a higher contact time (27 ms) than Table 5.4a (8 ms), over an inert silica bed and over a 2.5% VO_x/CS catalyst bed. The catalytic reaction had approximately 4-6% higher C_4H_{10} conversion at both reaction temperatures. The selectivity towards 1-C_4H_8 was slightly lower (1-2%) for the catalytic reaction at both temperatures. However, the selectivity for 2-C_4H_8 was higher for the catalytic reaction at both temperatures, with the magnitude of the increase being higher for the reaction at 923 K compared to that at 1023 K. This trend of 2-C_4H_8 having a higher selectivity when a catalyst is used was also seen for the shorter contact time reaction (shown in Table 5.4a). The selectivities to C_3H_6 and C_2H_4 were both less than 2% different between the catalytic and non-catalytic reaction, regardless of the reaction temperature used. These results show that at this contact time, the amount of cracking and the resulting product distribution is not affected by the catalyst. However, due to the 4-6% higher conversion of C_4H_{10} for the catalytic reaction, the overall yield of C_2-C_4 olefins will be slightly higher for the catalytic reaction. The C_2-C_4 olefin yields for the catalytic and non-catalytic reactions were 59% and 55% respectively. The selectivity to CO was very similar for both reactions; however, the selectivity to CO_2 was slightly higher for the catalytic reaction. The higher selectivity to CO_2 was also seen in the shorter contact time

reactions in Table 5.4a. However, the combined selectivities to carbon oxides was never higher than 2%, showing that these are minor products and well below the 8-13% observed for the non-H_2S reactions (Table 5.2).

The data summarized in Tables 5.4a and 5.4b show that, for the most part, selectivities towards desirable products such as olefins are not significantly different between the gas-phase and catalytic reactions, at least at temperatures where conversion of C_4H_{10} is high. This observation leads one to question whether the slight enhancement in overall yield is worth the cost of having a catalyst in an industrial application. To further highlight that the best enhancement to the ODH reaction comes from the addition of H_2S to the reaction and not the presence of a catalyst, the reaction was carried out with and without H_2S over a catalyst bed. The product distribution from the addition of H_2S to the ODH reaction between C_4H_{10} and O_2 over a catalyst bed is compared to that of the catalytic reaction without H_2S in Table 5.5 below. Table 5.6 shows the comparison between the 2.5% VO_x/CS and 5% VO_x/CS catalysts for the reaction between C_4H_{10}, O_2 and H_2S.

The data in Table 5.5 illustrates the effect of adding H_2S to the reaction between C_4H_{10} and O_2 over a 5% VO_x/CS catalyst. In the absence of H_2S, the reaction at 923 K showed a combined selectivity of 32% towards olefins produced by dehydrogenation, and a combined selectivity of 44% towards olefins from cracking (C_3H_6 and C_2H_4). Production of carbon oxides was negligible. At 1023 K, the selectivity towards C_4H_8 (combined C_4 olefins) decreased slightly to 30%. The selectivity towards C_3H_6 decreased to 23% from 27%, while that for C_2H_4 increased to 22% from 17%, showing that at higher temperatures, cracking starts to favour production of C_2H_4 over C_3H_6.

Table 5.5: Effect of H_2S on the reaction between C_4H_{10} and O_2 over a 5% VO_x/CS catalyst bed at 14 ms contact time.

	Temp °K	Conversion %			Products, mole/100 moles of feed [Selectivity %]												Yield %			
		C_4H_{10}	O_2	H_2S	1-C_4H_8	2-C_4H_8	C_3H_6	C_3H_8	C_2H_4	C_2H_6	CH_4	CO	CO_2	$C_{(s)}$	S_2	H_2O	H_2	1-C_4H_8	2-C_4H_8	C_3H_6	C_2H_4
No H_2S	923	29	74	0	5.5	0.3	6.5	0.3	5.9	1.4	7.5	0.3	0.2	5.8	0.0	22.5	2.5	9	1	8	5
					[30]	[2]	[27]	[1]	[17]	[4]	[11]	[<1]	[<1]	[8]							
With H_2S	923	34	80	26	8.9	1.2	6.6	0.0	4.3	2.0	9.0	0.3	0.0	-7.0	2.5	15.4	0.9	16	2	9	4
					[47]	[6]	[26]	[0]	[11]	[5]	[12]	[<1]	[0]	-[9]							
No H_2S	1023	57	88	0	9.9	0.7	10.8	0.2	15.4	2.8	15.2	0.8	0.9	11.3	0.0	23.2	9.6	16	1	13	12
					[28]	[2]	[23]	[1]	[22]	[4]	[11]	[1]	[1]	[8]							
With H_2S	1023	90	78	14	4.2	1.2	23.9	0.1	16.2	8.8	34.6	1.1	2.5	13.2	1.1	9.9	5.1	8	2	33	15
					[9]	[3]	[36]	[<1]	[16]	[9]	[18]	[1]	[1]	[7]							

Note: No H_2S Feed = 19.5% N_2, 61.9% C_4H_{10} and 15.9% O_2. With H_2S feed = 19.9% N_2, 54.9% C_4H_{10}, 11.1% H_2S and 10.1% O_2. See Appendix 5.8 for complete data table.

Table 5.6: Comparison of 2.5% and 5% VO_x/CS catalysts for the reaction between C_4H_{10}, O_2 and H_2S at 8 ms contact time.

	Temp °K	Conversion %			Products, mole/100 moles of feed [Selectivity %]												Yield %			
		C_4H_{10}	O_2	H_2S	1-C_4H_8	2-C_4H_8	C_3H_6	C_3H_8	C_2H_4	C_2H_6	CH_4	CO	CO_2	$C_{(s)}$	S_2	H_2O	H_2	1-C_4H_8	2-C_4H_8	C_3H_6	C_2H_4
2.5% Vox/CS	923	32	90	13	3.6	0.4	4.3	0.0	1.9	0.9	4.0	0.2	0.2	-2.8	0.5	5.6	0.4	13	1	11	3
					[40]	[4]	[36]	[0]	[11]	[5]	[11]	[1]	[<1]	-[8]							
5% VOx/CS	923	31	87	13	4.6	0.7	4.0	0.0	1.8	0.9	3.9	0.2	0.1	-3.3	0.5	5.6	0.1	14	2	9	3
					[47]	[7]	[30]	[0]	[9]	[5]	[10]	[1]	[<1]	-[9]							
2.5% Vox/CS	1023	82	91	2	1.9	0.5	13.4	0.0	7.0	4.1	15.8	0.2	0.8	3.8	0.1	4.4	2.0	7	2	36	12
					[8]	[2]	[43]	[<1]	[15]	[9]	[17]	[<1]	[1]	[4]							
5% VOx/CS	1023	76	89	2	2.6	0.6	13.3	0.0	6.6	4.2	15.3	0.3	1.0	6.2	0.1	4.2	2.1	8	2	31	10
					[11]	[3]	[41]	[0]	[14]	[9]	[16]	[<1]	[1]	[6]							

Note: 5% VO_x/CS feed = 60.7% N_2, 32.0% C_4H_{10}, 7.8% H_2S and 3.8% O_2. 2.5% VO_x/CS feed = 61.1% N_2, 28.2% C_4H_{10}, 7.8% H_2S and 3.4% O_2. See Appendix 5.9 for complete data table.

In comparison, when the reaction feed contained H_2S, selectivity to dehydrogenation products was found to be 53% at 923 K. However, at 1023 K, this value drops significantly to only 12%. The selectivity to cracking products was observed to be 37% at 923 K, but increased significantly to 52% at 1023 K. The majority of this increase is for C_3H_6, the selectivity of which increased from 26% to 36% when the temperature was increased from 923 K to 1023 K. In addition, conversion of C_4H_{10} was found to be higher for the H_2S-containing reaction at both temperatures. At 1023 K, the difference in conversion is significant and leads to a total olefin yield that is much higher for the H_2S-containing reaction. Overall, the C_2-C_4 olefin yield at 1023 K was 42% for the non-H_2S reaction, while that for the H_2S-containing reaction was 58%.

While it may look like the non-H_2S reaction has a higher selectivity for C_4 olefins at 1023 K and may therefore be the better reaction, this is not the case at all. The H_2S-containing reaction had the highest selectivity towards dehydrogenation products at 923 K, and by looking at the yields of C_4 olefins, it can be seen that the yield of C_4 olefins for the H_2S-containing reaction at 923 K was similar in magnitude to the C_4 olefin yield for the non-H_2S reaction at 1023 K. This result shows that the H_2S-containing reaction can produce the same yield of C_4H_8 as the non-H_2S reaction, but at a lower C_4H_{10} conversion level and at a temperature that is 100 K lower. In an industrial setting, reaction conditions are chosen based on the end product desired. If C_4 olefins are the desired product, then running the H_2S-containing reaction at 923 K would give the best yield. However, at that conversion level, recycling of un-reacted C_4H_{10} would be a requirement. If both, C_3 and C_4, olefins are desired, then the reaction can be carried out at the higher temperature of 1023 K, where conversion is approximately 90% (and could perhaps be increased to 100% with further increase in temperature or contact time) and therefore no recycling of reactants would be required, while good yields of the desired products would still be provided.

Table 5.6 shows the comparison between two catalysts with differing amounts of vanadium oxide impregnated on a silica support. The effect of the catalyst was studied in Chapter 3/4 earlier and, therefore, is touched on here only very briefly. The results in Table 5.6 show that at short contact times (8 ms), the catalyst with the lower amount of vanadium oxide has a slightly lower selectivity to dehydrogenation products and a slightly higher selectivity towards cracking products. The 2.5% VO_x/CS promoted reactions also had slightly higher C_4H_{10} conversions, with the difference being greater at the higher temperature. At 923 K, with only slightly differing conversions of C_4H_{10}, the overall C_2-C_4 olefins yields were comparable at 28% for both the 2.5% VO_x/CS catalyst and the 5% VO_x/CS catalyst, although differing in the proportions of each type of olefin. At 1023 K, the difference in conversion is a little more significant (6%), and this leads to slightly higher yields for the 2.5% VO_x/CS catalyst at 57% compared to that for 5% VO_x/CS, which was 51%.

5.1 The Reaction between n-Butane and H_2S

The pyrolysis of n-butane and the effect of adding H_2S to this reaction was studied, first over an inert bed and then over a catalyst, to determine the effects of H_2S for both the homogeneous and the catalytic reaction. Because O_2 was not used in this reaction, loss of carbon due to total oxidation to undesirable carbon oxides was eliminated. While the lack of O_2 may reduce the temperature of the reaction, there is another factor to consider: even though it is the reaction of O_2 with H_2S that provides heat due to its exothermic nature, the lack of O_2 may still prove beneficial if side reactions are reduced and if the catalyst is found to be capable of keeping the reaction going with just H_2S and no O_2. Earlier, in Chapter 3, it was shown that selectivities to desirable products, such as olefins, were good; however, conversion of the alkane was lower compared to a reaction containing O_2. Table 5.7 below shows the changes in product distribution

due to the addition of H_2S to the pyrolysis of n-butane over an inert silica bed, at 36 ms contact time.

The results show that when butane undergoes pyrolysis in the gas phase at 923 K, almost equimolar quantities of the two major cracking products (C_3H_6 and C_2H_4) are obtained, as well as some dehydrogenation product (1-C_4H_8). When the temperature is increased to 1023 K, the amount of C_2H_4 increased relative to the amount of C_3H_6. Compared to the reaction with H_2S, the conversion of C_4H_{10} in the pyrolysis reaction is significantly lower.

Table 5.7: Pyrolysis of n-butane and effect of adding H_2S to the reaction carried out over an inert crystalline silica bed at a contact time of 36 ms.

	Temp °K	Conversion %		Products, mole/100 moles of feed [Selectivity %]										Yield %			
		C_4H_{10}	H_2S	1-C_4H_8	2-C_4H_8	C_3H_6	C_3H_8	C_2H_4	C_2H_6	CH_4	$C_{(s)}$	S_2	H_2	1-C_4H_8	2-C_4H_8	C_3H_6	C_2H_4
No H_2S	923	13	0	0.3 [10]	0.0 [0]	0.8 [20]	0.0 [0]	0.7 [12]	0.2 [3]	0.8 [7]	5.7 [48]	0.0	0.4	1	0	2	2
With H_2S	923	25	1	0.6 [9]	0.1 [1]	4.0 [42]	0.0 [0]	1.4 [10]	1.3 [9]	4.3 [15]	1.3 [5]	0.0	0.4	2	0	10	2
No H_2S	1023	47	0	3.2 [29]	0.0 [2]	4.4 [30]	0.1 [1]	6.6 [30]	0.8 [4]	6.0 [14]	-4.1 -[9]	0.0	3.0	14	1	14	14
With H_2S	1023	74	-1	2.5 [12]	0.5 [2]	13.7 [48]	0.0 [<1]	7.8 [18]	4.2 [10]	16.8 [20]	-3.8 -[5]	0.0	2.8	9	2	35	13

Note: No H_2S feed = 79.0% N_2 and 23.5% C_4H_{10}. With H_2S feed = 67.1% N_2, 29.2% C_4H_{10} and 5.0% H_2S. See Appendix 5.10 for complete data table.

When H_2S is added to the reaction, a greater amount of C_4H_{10} is converted, even though the H_2S looks to be unreacted (but in actuality, it might simply be regenerated at the end of the reaction instead). The selectivity to dehydrogenation products was similar to the pyrolysis reaction at 923 K; however, the selectivity to cracking products was quite different. Quantitatively, the selectivity to C_3H_6 increased from 20% to 42% when H_2S was added to the reaction. The ratio of selectivity of C_3H_6 to C_2H_4 increased to 4 (42% for C_3H_6 vs 10% for C_2H_4) when H_2S was present in the reaction, compared to 1.6 for the pyrolysis reaction. When the

temperature was increased to 1023 K, the selectivity towards C_2H_4 did increase; however, C_3H_6 remained the dominant cracking product with a selectivity of 48%. The reaction with H_2S at 1023 K gave a total C_2-C_4 olefin yield of 59% versus the pyrolysis reaction, which gave a total C_2-C_4 olefin yield of 43%.

5.1.1 The Catalytic Reaction between n-Butane and H_2S

Similar experiments were then carried out using a catalyst in place of the inert silica bed, and the results from these experiments are shown in Table 5.8, below.

Table 5.8: Pyrolysis of n-butane and effect of adding H_2S to the reaction carried out over a 5% VO_x/CS bed at a contact time of 36 ms.

	Temp °K	Conversion %		Products, mole/100 moles of feed [Selectivity %]										Yield %			
		C_4H_{10}	H_2S	1-C_4H_8	2-C_4H_8	C_3H_6	C_3H_8	C_2H_4	C_2H_6	CH_4	$C_{(s)}$	S_2	H_2	1-C_4H_8	2-C_4H_8	C_3H_6	C_2H_4
No H_2S	923	12	0	1.5	0.2	0.7	0.5	0.6	0.0	0.7	1.5	0.0	1.4	6	0	2	1
				[43]	[7]	[15]	[10]	[9]	[0]	[5]	[11]						
With H_2S	923	24	3	0.6	0.0	2.6	0.0	0.8	0.9	2.7	7.1	0.1	0.1	2	0	8	2
				[10]	[0]	[33]	[0]	[7]	[7]	[12]	[31]						
No H_2S	1023	48	0	3.5	0.0	5.6	0.0	8.0	1.1	7.5	-2.2	0.0	3.8	12	0	15	14
				[26]	[0]	[31]	[0]	[30]	[4]	[14]	-[4]						
With H_2S	1023	74	1	2.1	0.4	10.4	0.0	5.3	3.3	12.1	1.2	0.1	1.7	9	2	32	11
				[12]	[2]	[44]	[0]	[15]	[9]	[17]	[2]						

Note: No H_2S feed = 72.1% N_2 and 28.2% C_4H_{10}. With H_2S feed = 69.2% N_2, 24.2% C_4H_{10} and 5.7% H_2S. See Appendix 5.11 for complete data table.

The pyrolysis reaction on the catalyst showed high selectivity for 1-C_4H_8 at 923 K. When the temperature was increased to 1023 K, the selectivity to C_4H_8 dropped from 43% to 26%. In exchange, at 1023 K the selectivity to C_3H_6 and C_2H_4 increased to 2-3 times its value at the lower temperature. This result is expected, as cracking should occur in higher amounts at 1023 K. Conversion of C_4H_{10} almost doubled when H_2S was added to the reaction; however, the product distribution was also very different compared to the pyrolysis reaction. Selectivity to dehydrogenation products (C_4H_8) dropped to 10% and in exchange, the selectivity to propylene increased to 33%, showing that cracking between the first and second carbon is favoured over

cracking between the second and third carbon, which would have led to a greater amount of C_2H_4 and C_2H_6. At the higher temperature of 1023 K, the amount of cracking increased even more and selectivity to all cracking products increased. The selectivity towards C_3H_6 increased from 33% to 44%, while the selectivity towards C_2H_4 increased from 7% to 15%. Another difference between the product distributions of the two reactions (with and without H_2S) is the amount of C_2H_6 produced relative the amount of C_2H_4 produced. In the pyrolysis reaction, the ratio of C_2H_4 relative to C_2H_6 is significantly greater than the value of the same ratio for the reaction containing H_2S.

5.2 Conclusions from the Reactions using C_4H_{10}

When the oxidative dehydrogenation of C_4H_{10} was first studied, the intent was to investigate and confirm if the trends seen for the ODH of C_3H_8 would be repeated. If that were found to be the case, then it would seem feasible to put a mixture of C_3H_8 and C_4H_{10} in the reactant stream and expect a significant amount of C_4 and C_3 olefins, with each one being produced from its corresponding starting alkane. However, what was observed from experiments was that when C_4H_{10} was the reactant alkane, oxidative cracking to produce C_3H_6 was favoured quite significantly, in addition to some dehydrogenation (producing C_4H_8) and cracking (to produce C_2H_4). These observations showed that for the production of propylene, n-butane may be the better starting material, as the selectivity and yield observed for C_3H_6 were higher than those observed for the ODH of C_3H_8. While dehydrogenation was the original objective of this work, one goal was actually to produce a mixture of C_3 and C_4 olefins in high yields from a C_3/C_4 alkane reactant mixture.

5.3 Reactions using a C_3H_8/C_4H_{10} Mixture

The final step of this work was to investigate what would happen when the two alkanes were put in the same reaction mixture and reacted with O_2 and H_2S. Would the two alkanes work in a complementary manner, as C_4H_{10} is easier to activate and, therefore, would have the potential to increase the conversion of C_3H_8? Would the selectivities observed for the individual alkane reactions still be observed when the two alkanes are put together?

The results from the gas-phase and catalytic reactions between C_3H_8/C_4H_{10}, H_2S and O_2 (in a ~ 8:1:0.7 feed ratio of total alkane: H_2S: O_2) are shown in Table 5.9, below. Before going into a discussion of the results, it must be remembered that propane is a product in the ODH of butane, but is also a reactant in this reaction. This means that the values for conversion of propane may be a bit misleading, as it is impossible to differentiate the propane in the reactant feed from propane produced in the reaction. The table therefore shows conversion of propane and butane separately, and also a value for the total conversion of both reactant alkanes, which represents the total carbon % converted. However, this value will include some of the propane produced from the reaction and so the conversion amounts may be slightly understated. But the data tables in the preceding parts of this chapter give a general idea of how much propane is produced in the ODH of butane, and assuming no significant change in product distribution, the selectivity to propane as a product of the ODH of butane will only be in the 0-5% range at most.

Table 5.9: Reaction of C_3H_8/C_4H_{10}, O_2 and H_2S over an inert silica bed and over a 2.5% VO_x/CS catalyst bed at 12 ms.

	Temp °K	Conversion %					Products, mole/100 moles of feed [Selectivity %]													Yield %			
		C_3H_8	C_4H_{10}	C_3+C_4	O_2	H_2S	1-C_4H_8	2-C_4H_8	C_3H_6	C_2H_4	C_2H_6	CH_4	CO	CO_2	$C_{(s)}$	SO_2	S_2	H_2O	H_2	1-C_4H_8	2-C_4H_8	C_3H_6	C_2H_4
CS	923	25	21	21	73	20	4.3	0.5	5.3	2.6	1.1	5.3	0.2	0.0	11.8	1.2	0.4	8.9	0.5	6	1	6	2
							[29]	[4]	[27]	[9]	[4]	[9]	[<1]	[0]	[20]								
2.5% VO_x/CS	923	14	30	29	87	40	5.2	0.5	5.2	2.4	1.2	5.5	0.4	1.8	27.0	0.0	1.9	8.8	1.0	7	1	6	2
							[26]	[3]	[19]	[6]	[3]	[7]	[<1]	[2]	[34]								
CS	1023	53	68	66	84	1	5.2	0.9	25.4	16.0	8.6	33.0	0.4	1.9	-0.5	1.1	-0.5	6.3	5.5	7	1	27	11
							[11]	[2]	[41]	[17]	[9]	[18]	[<1]	[1]	[<-1]								
2.5% VO_x/CS	1023	70	72	72	83	54	5.2	0.9	24.2	16.1	8.4	33.2	0.5	2.0	20.3	0.0	2.5	7.6	6.0	7	1	26	12
							[10]	[2]	[36]	[16]	[8]	[16]	[<1]	[1]	[10]								

Note: CS feed = 12.7% N_2, 14.1% C_3H_8, 59.7% C_4H_{10}, 9.6% H_2S & 6.2% O_2. 2.5% VO_x/CS feed = 12.9% N_2, 14.3% C_3H_8, 58.0% C_4H_{10}, 9.3% H_2S & 7.4% O_2. See Appendix 5.12 for complete data table.

The results show that conversion of the hydrocarbons is higher when the catalyst is used compared to an inert silica bed. It should be noted that the feed ratio is approximately 20:3:2 for C_3H_8 + C_4H_{10} : H_2S: O_2, which contains a lower amount of the oxidant/oxidant generating components (H_2S + O_2) compared to some of the feeds used in experiments described in earlier parts of this chapter. Despite this, the conversions obtained were within the same range of values as those seen in some of the experiments in this and the previous chapter. The data at 923 K for the catalyst reaction shows that there is a preference for C_4H_{10} conversion over C_3H_8 conversion, and this may simply have to do with the amount of C_4H_{10} in the reactant feed compared to the amount of C_3H_8 (4:1 C_4H_{10}: C_3H_8 ratio). At 1023 K, the percentage of C_4H_{10} and C_3H_8 converted is similar.

5.4 Conclusions

The use of n-C_4H_{10} as a reactant for the ODH reaction leads to overall higher conversions of the alkane compared to the reaction using propane. In addition, a mixture of olefins is obtained as a major portion of the products, all of which are valuable. Perhaps the most interesting and unexpected observation from the experimental results was the preference towards C_3H_6 when H_2S was also included in the reactant gas stream. This trend was observed for gas-phase as well as catalytic reactions. Alternatively, in the absence of H_2S, propylene and ethylene were produced in almost equal quantities at 923 K, with ethylene being favoured more when the temperature was increased to 1023 K. C_4H_8 selectivity of almost 50% were obtained in some of the experiments at 923 K, but these were not sustainable and dropped significantly when the reaction temperature was increased to 1023 K. Finally, the reaction between n-C_4H_{10} and H_2S (in the absence of O_2) showed good selectivities towards olefin products (similar trends to those

observed in the reaction between C_4H_{10}, O_2 and H_2S) but at lower conversions. This was expected as the similar trend was seen for the reaction between propane and H_2S in chapter 3.

More interestingly, although one would expect that C_4H_{10} conversion would be higher than that of C_3H_8 since butane is easier to activate, it seems that at higher temperatures the C_3H_8 conversion likely benefits from initiation by butane, which may generate radicals that can then initiate the conversion of C_3H_8 as well.

Comparatively, for the pure gas-phase reaction, the conversion of C_3H_8 was slightly higher than the conversion of C_4H_{10} at 923 K. In the gas phase, all reactions are radical-controlled, and since C_4H_{10} initiates more easily and generates radicals, these can then initiate C_3H_8. However, at 1023 K, the conversion trends go back to the expected trend, which is a slightly higher C_4H_{10} conversion compared to the conversion of C_3H_8.

In terms of selectivity, the gas-phase reaction had selectivities that were slightly better for each olefin product than those seen for the catalytic reaction, leading to a total olefin selectivity that was higher for the gas-phase reaction. The combined selectivity towards C_2-C_4 olefins was 68% and 54% for the gas-phase and catalytic reactions respectively, at 923 K. At 1023 K, the C_2-C_4 olefin selectivities were 72% and 64% for the gas-phase and catalytic reaction respectively. Since the catalytic reaction had a higher conversion at both reaction temperatures, the overall total C_2-C_4 olefin yields were more comparable at 14% and 15% for the gas- phase and catalytic reaction at 923 K respectively, and 47% and 46% for the gas-phase reaction and catalytic reaction at 1023 K respectively. Again, the results from Table 5.9 above show that there is no need for a catalyst at these reaction conditions, and that the gas-phase reaction is just as efficient, mostly due to the influence of H_2S on the ODH of C_3H_8 or C_4H_{10} with O_2.

Chapter 6: Mechanistic Insights gained from Experimental and Theoretical Data

6.0 Homogeneous Reaction between C_3H_8, O_2 and H_2S

The oxidative dehydrogenation reaction in the gas phase is a process that follows a typical radical mechanism, involving an initiation step, some propagation steps and finally a termination step. Radical reactions are hard to control and many by-products are often produced. However, trends in the product distribution can be controlled to some extent by varying a given parameter.

As previously shown in the introduction chapter, the initiation step for this reaction may consist of C-C bond cleavage from a propane molecule (in the absence of any other component) or could be hydrogen abstraction from propane by an oxidant (in this case either O_2 or S_2 or other species such as SH• etc). C-C bond cleavage would lead to two alkyl radical products as shown by the reaction below.

[6.1] $C_3H_8 \rightarrow C_2H_5\bullet + CH_3\bullet$

Alternatively, hydrogen abstraction from a propane molecule can also lead to two different alkyl radical products as shown by the two reactions below.

[6.2] $C_3H_8 + O_2 \rightarrow n\text{-}C_3H_7\bullet + OOH\bullet$

[6.3] $C_3H_8 + O_2 \rightarrow i\text{-}C_3H_7\bullet + OOH\bullet$

In the next series of steps, these radicals can react with more C_3H_8 or can, themselves, undergo cracking via β-scission to produce an olefin and another radical. The reaction paths possible depend on the type of propyl radical formed initially.

For an n-propyl radical, a second hydrogen abstraction by species such as OOH•, OH•, CH_3• would lead to formation of propylene [6.4-6.6] whereas β-scission leads to production of ethylene and a methyl radical [6.7].

[6.4] $n\text{-}C_3H_7\bullet + OH\bullet \rightarrow H_2O + C_3H_6$

[6.5] $n\text{-}C_3H_7\bullet + OOH\bullet \rightarrow C_3H_6 + H_2O_2$

[6.6] $n\text{-}C_3H_7\bullet + CH_3\bullet \rightarrow C_3H_6 + CH_4$

[6.7] $n\text{-}C_3H_7\bullet \rightarrow C_2H_4 + CH_3\bullet$

For the i-propyl radical, C-C bond β-scission cannot occur because the radical is already at carbon number 2, however a second hydrogen abstraction (again, by any number of species) will also lead to formation of C_3H_6.

It was previously established that oxidation of H_2S by O_2 is a fast process that leads to S_2 (as well as H_2O and H_2) and other sulfur radicals (e.g. HS•). At high H_2S:O_2 ratios, S_2 is the likely oxidant in the gas-phase ODH of propane. S_2 is expected to react similarly to O_2 in terms of mechanism, but, of course, cannot yield stable carbon sulfides initially. While the mechanism and some of the overall products might be similar or the same between the reaction of C_3H_8 with O_2 or S_2, the energy barriers and energies of each of the reaction's intermediate steps may be different. Calculation of these parameters may, therefore, provide insight into the activity and selectivity patterns observed for the reactions by each of these oxidants.

To support these results, potential energy surface diagrams were constructed for the reactions between each of the propyl radicals (n-propyl and i-propyl) and each of the oxidants (O_2 and S_2) and these are shown in Figures 6.1-6.4. These diagrams represent some of the major pathways and products for the reaction of either the n- or i-propyl radical with O_2 and S_2 and show the relative stabilities of the products as well as intermediates. The diagrams show two

important things, relative stabilities of the final products and activation barriers (indicated by the energy of the transition state of the rate determining step) for each reaction path, therefore allowing a comparison of the relative activation barriers for all of the different processes. The rate determining step is defined as the part of a given pathway that has the highest energy transition state.

Figure 6.1 and 6.2 show, respectively, the reaction co-ordinate for the n-propyl radical reacting with O_2 and S_2. The relative stabilities of the products illustrate the selectivity at equilibrium. Therefore, when multiple reaction paths exist (and if there are no differences in activation barriers) the product with the lowest energy (and therefore greatest stability) will be produced in a greater amount in the final product distribution.

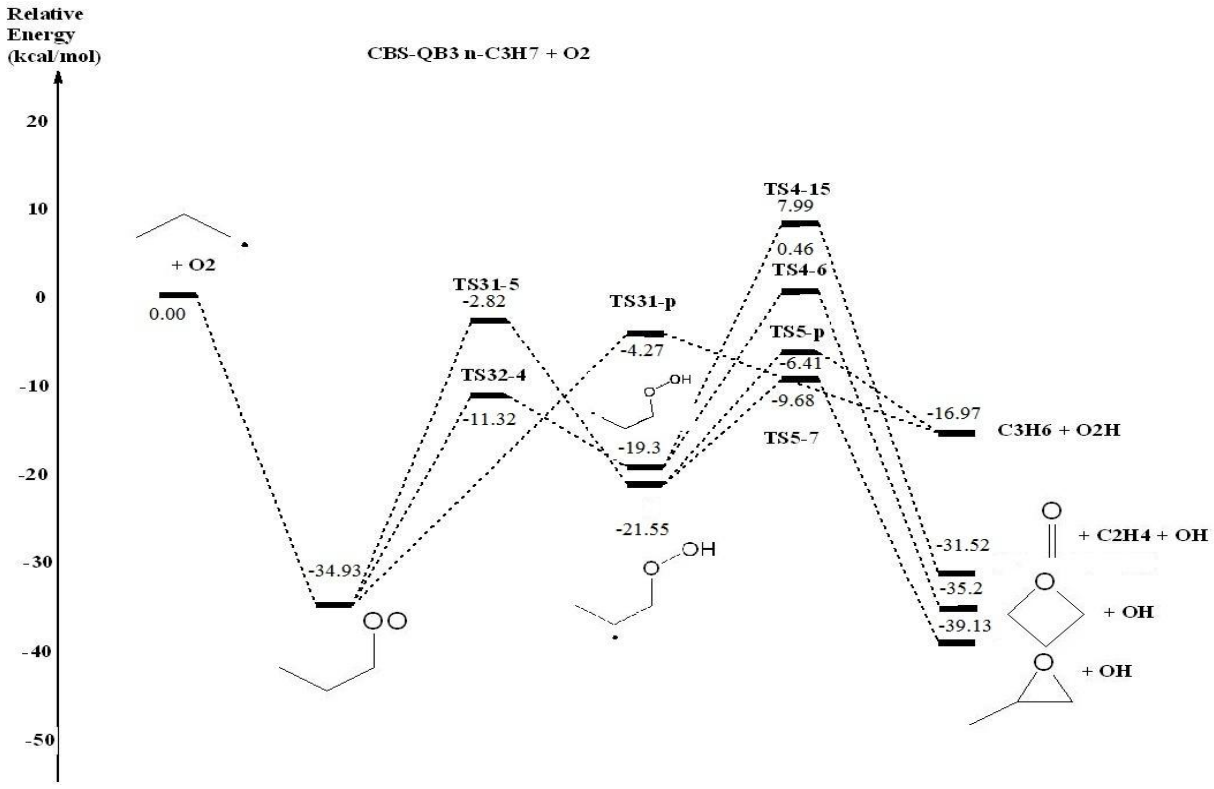

Figure 6.1: Reaction co-ordinate diagram for the reaction between an n-propyl radical and O_2 (Plots of Electronic Energy + Zero Point Energy at 298 K, 1 atm.

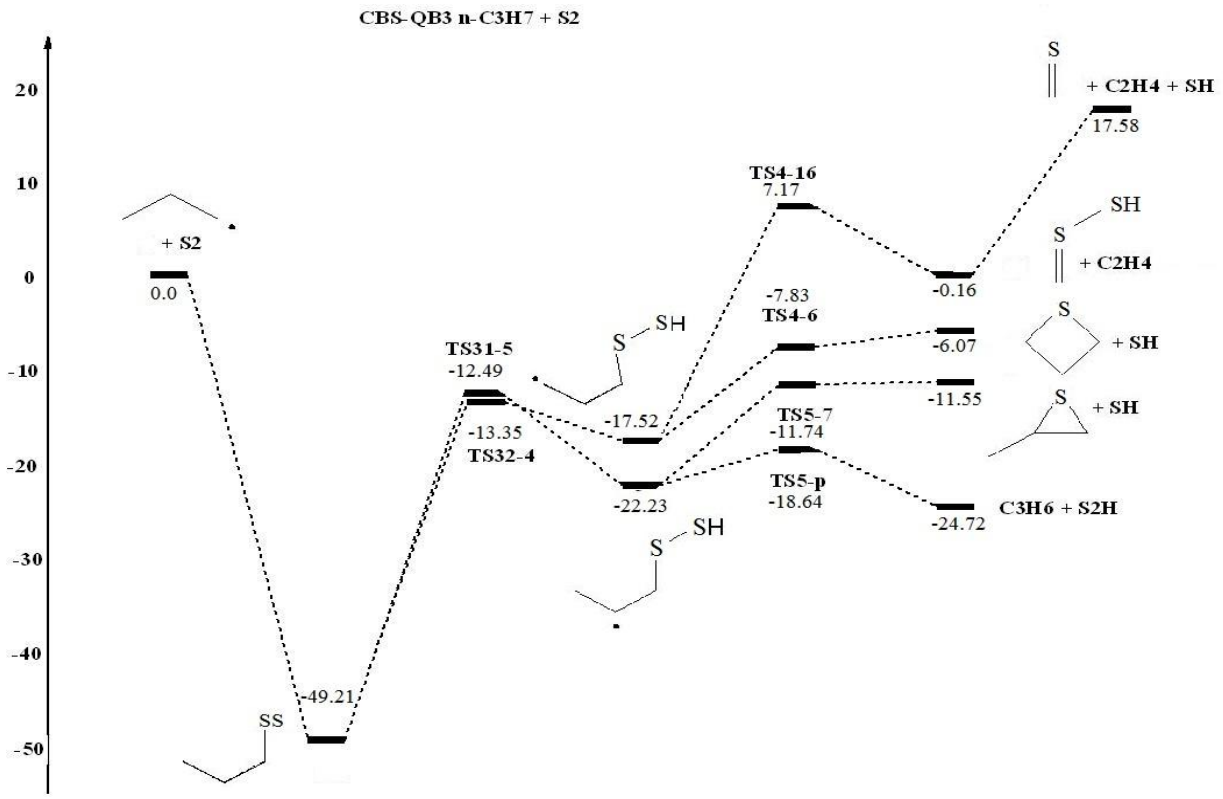

Figure 6.2: Reaction co-ordinate diagram for the reaction between an n-propyl radical and S_2

Looking at the relative stabilities of the products from the two diagrams above, it can be seen that the desired product C_3H_6 is produced with either HS_2 or HO_2 and the combination of C_3H_6 + S_2H has an energy of -24.72 kcal/mol whereas that of C_3H_6 + O_2H has an energy of -16.97 kcal/mol. In comparison, the energies of C_2H_4 + 15 (H_2C=O) +SH and C_2H_4 + 15 + OH are 17.58 and -31.52 kcal/mol respectively. Two observations can be made from comparison of these values. Firstly, production of C_2H_4 + 15 + OH is thermodynamically favoured over the production of C_3H_6 + O_2H for the system containing O_2 as the oxidant. This observation is opposite to the trend observed for the S_2 containing system, where production of C_3H_6 + S_2H is more thermodynamically favoured compared to production of C_2H_4 + 15 + SH. The second observation is that production of C_3H_6 is more thermodynamically favourable in the S_2 reaction compared to the O_2 reaction as deduced by comparing the energy of the products for that

particular pathway between the two reactions. Likewise, production of C_2H_4 is more thermodynamically favourable for the O_2 system compared to the S_2 system when the starting radical is the n-propyl radical.

Comparison of the energy barriers for the rate determining steps of each pathway shows that for the reaction between n-C_3H_7• and S_2, the pathway leading to C_3H_6 has the lowest activation barrier compared to all other paths shown in that figure. Additionally, the pathway leading to C_2H_4 has the highest activation barrier. This shows that C_3H_6 is the kinetic product and C_2H_4 production is kinetically less favourable. The final product observed will be dependent either, on the ratio between the activation energies of each pathway, if the reaction is in a kinetically controlled region, or on the ratio between the energies of the final products of each of the pathways, if the reaction is controlled by stability of the products (thermodynamic regime). Both kinetic and thermodynamic controls should lead to a higher amount of C_3H_6 relative to C_2H_4 for the reaction between n-C_3H_7• and S_2. However, for the reaction between n-C_3H_7• and O_2, the pathway with the lowest activation energy is that leading to C_3H_6 and the pathway with the highest activation barrier is that leading to C_2H_4, so in a purely kinetically controlled region the reaction should lead to production of a greater amount of C_3H_6 compared to C_2H_4. However, as the reaction shifts from kinetic to thermodynamic regime, the reaction will change to favour C_2H_4 production relative to that of C_3H_6.

Since n-C_3H_7• is only one of two radicals that are formed via hydrogen abstraction from C_3H_8, a look at the reaction co-ordinate diagram for the i-C_3H_7 must also be considered to provide a more complete picture (see Figures 6.3 and 6.4).

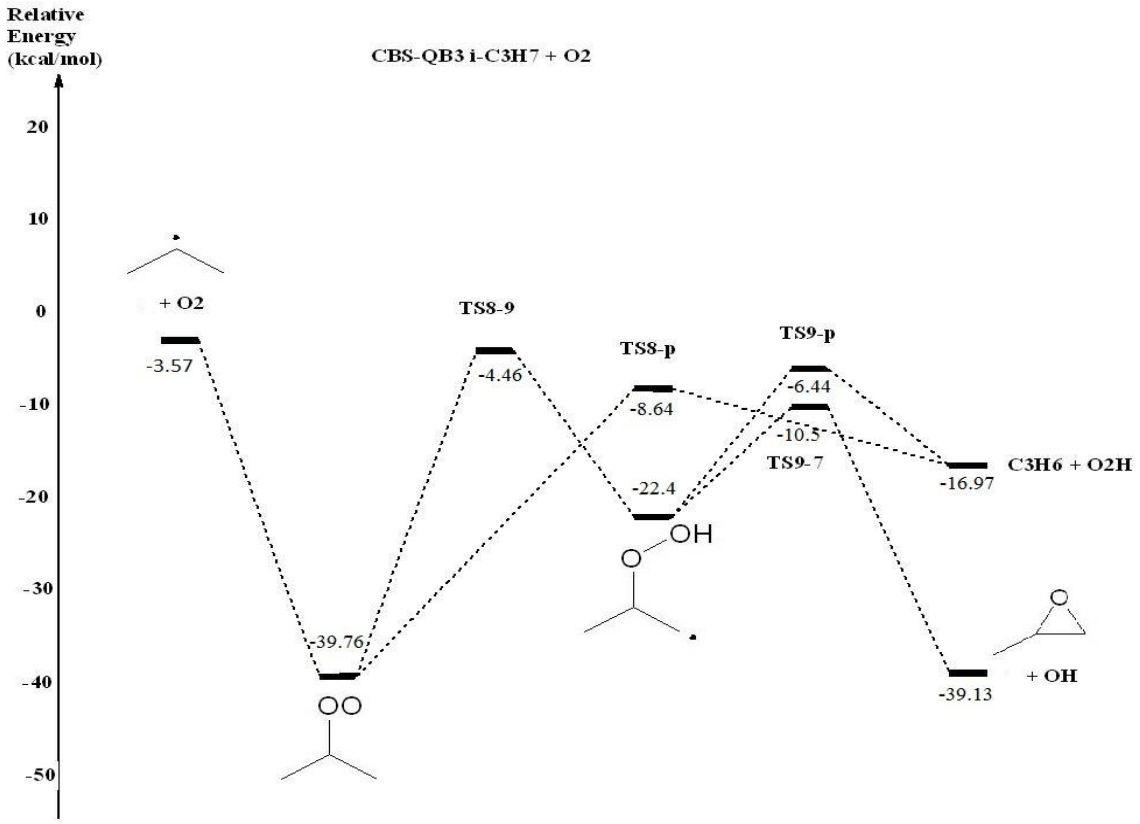

Figure 6.3: Reaction co-ordinate diagram for the reaction between an i-propyl radical and O_2

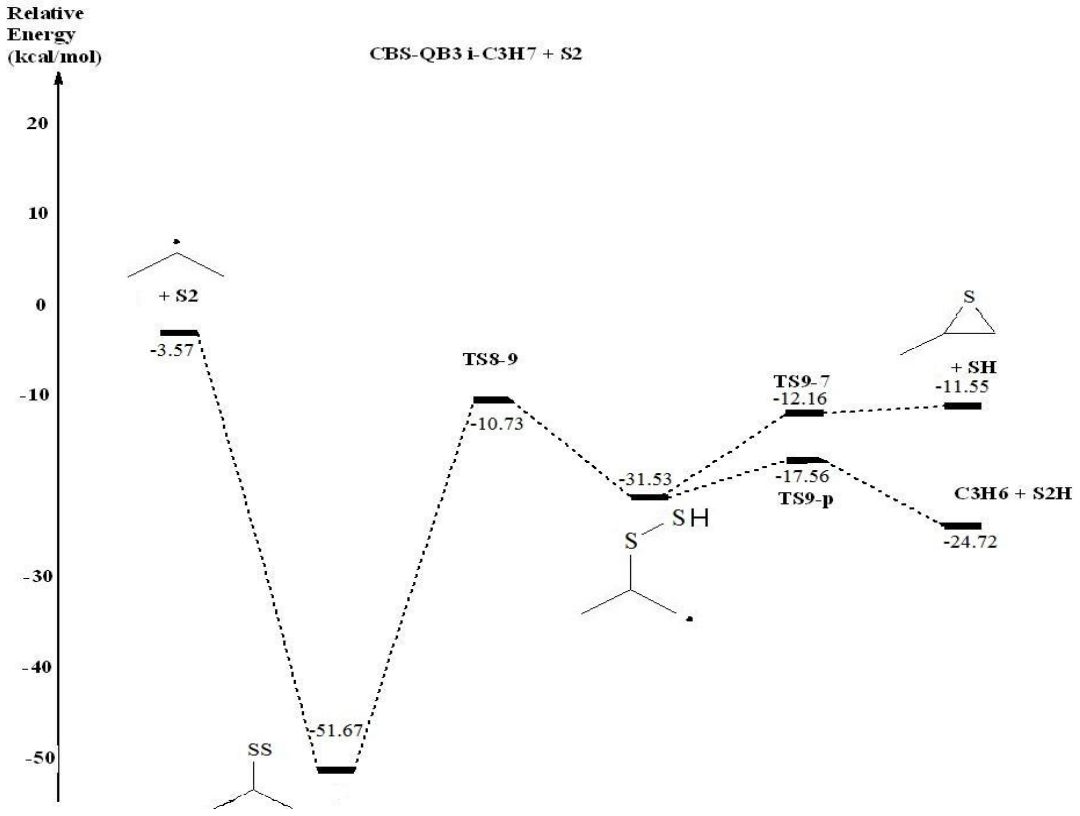

Figure 6.4: Reaction co-ordinate diagram for the reaction between an n-propyl radical and S_2

There are fewer reaction pathways possible for i-C_3H_7•, and, as observed from the figures above, C_2H_4 formation is not possible as β-scission is precluded. As was seen for the reaction of the n-propyl radical, C_3H_6 is the thermodynamic product when reaction occurs with S_2, while it is not in the reaction between i-C_3H_7• and O_2. This observation can be made from analyzing the energy profile of each system separately. Production of C_3H_6 is also thermodynamically less favoured when O_2 is the oxidant compared to when S_2 is the oxidant used, as determined by comparing the relative stabilities of the propylene containing products from each system. Kinetically, C_3H_6 is favoured for both reactions with O_2 and S_2, which is similar to the case for the n-propyl radical. Again, the true product distribution will be a ratio between the thermodynamic products if the reaction is under thermodynamic control, or a ratio between the kinetic products if the reaction is in a kinetically controlled regime.

Comparison of the reaction between n-propyl or i-propyl radicals and O_2 or S_2 highlights some important trends (Table 6.1) for the pathways leading to formation of either C_3H_6 or C_2H_4.

Table 6.1: Comparison of activation barriers and overall energy of the reaction pathways leading to C_3H_6 and C_2H_4 for the reactions between C_3H_7• and either S_2 or O_2. (*with respect to propyl + O_2/S_2)

	Transition state energy* for rate limiting step leading to C_3H_6	Transition state energy* for rate limiting step leading to C_2H_4	$E_{(products - reactants)}$ for the pathway leading to C_3H_6	$E_{(products - reactants)}$ for the pathway leading to C_2H_4
n-C_3H_7• + O_2	-4.27	7.99	-16.97	-31.52
n-C_3H_7• + S_2	-12.49	7.17	-24.72	-0.16
i-C_3H_7• + O_2	-8.64	n/a	-13.4	n/a
i-C_3H_7• + S_2	-10.73	n/a	-21.15	n/a

Note: Units = kcal/mol for all columns as the data was taken from the energy profiles in Figures 6.1-6.4.

C_3H_6 is the thermodynamic product when S_2 is used whereas C_2H_4 is the thermodynamic product when O_2 is reacted with the n-propyl radical. Additionally, C_3H_6 should be the kinetic product for all the above reactions based on activation energy of each of the reaction pathways.

Finally, the reaction with S_2 has lower activation energy and a more stable intermediate product for the C_3H_6 pathway compared to the reaction with O_2.

The above trends match the experimental results quite well. In the reactions between C_3H_8 and O_2 (Table 4.6) and C_3H_8, H_2S and O_2 (Table 4.7) carried out in an empty tube, the amount of C_2H_4 produced was higher than the amount of C_3H_6 produced for the reaction between C_3H_8 and O_2 at all three reaction temperatures. This trend is the opposite for the reaction containing C_3H_8, H_2S and O_2 which is expected to produce S_2 in situ for reaction with C_3H_8. Also, the conversion of C_3H_8 was found to be higher when both O_2 and H_2S were used compared to the reaction of C_3H_8 with only O_2 and this also agrees with the predictions from the reaction co-ordinate diagrams above. The energy profile diagrams do not show all possible pathways such as those leading to solid carbon or carbon oxide formation. They simply provide a comparison between the reaction pathways that lead to formation of C_3H_6 and C_2H_4 for each of the propyl radicals/oxidants to help understand why one reaction leads to a greater amount of C_3H_6 while another leads to a greater amount of C_2H_4.

6.1 Homogeneous Reaction between C_4H_{10}, O_2 and H_2S

Similar to the reaction between C_3H_7• and each of the oxidants, the energy diagrams for the reaction between each of the C_4H_9• and each of the oxidants was also examined. The reaction between the butyl radicals and either S_2 or O_2 are more complicated and have a greater number of possible pathways. The entire set of energy profiles are shown in Appendix 6.1-6.4. Instead, the reaction energy (defined as $E_{products} - E_{reactants}$) of each of the pathways leading to products observed experimentally (such as butylenes, propylene, ethylene etc) as well as the energy of highest transition state for those pathways are given in Table 6.2 and 6.3 below.

Table 6.2: Reaction energy and highest energy transition state for reaction pathways leading to desirable products starting from the i-C_4H_9• (* with respect to butyl + O_2/S_2)

	Reaction with O_2		Reaction with S_2	
	Highest energy transition state*	Energy of reaction ($E_{product} - E_{reactant}$)	Highest energy transition state*	Energy of reaction ($E_{product} - E_{reactant}$)
1-C_4H_8 via TS1-5	-1.38	-13.29	-7.96	-21.03
2-C_4H_8 via TS2-11	-4.26	-16.16	-12.2	-23.87
C_2H_4 via TS3-9	4.56	-36.16	6.46	0.3

Note: Units = kcal/mol for all column as shown in the reaction profiles in Appendix 6.1-6.4.

Three main products are predicted to form from i-butyl radicals: 1-butene, trans-2-butene and ethylene (and all are observed experimentally). Results from calculations for the reaction with O_2 (Table 6.2) show that C_2H_4 is thermodynamically more favourable as a product than either of the butenes. However the pathway leading to C_2H_4 also has the highest transition state energy of the three pathways but the transition state energy was only 4.56 kcal/mol with respect to the reactants, which, at 923 or 1023 K should be easily surmountable. The results for the reaction with S_2 suggest a completely different trend. C_2H_4 is the least thermodynamically favourable product and 2-C_4H_8 is the most favourable with 1-C_4H_8 being only slightly less favourable than 2-C_4H_8. So, at equilibrium (if only these three pathways were possible), a greater amount of C_4H_8 would be expected compared to the amount of C_2H_4. The energy of the highest energy transition states of each of these pathways follows the same trends as the reaction energies with the pathway to 2-C_4H_8 having the lowest value followed by the pathway that leads to 1-C_4H_8 and finally the pathway leading to C_2H_4 which has the greatest value and the only positive value of the three.

Table 6.3: Energy of reaction and highest energy transition state for reaction pathways leading to desirable products starting from the n-C_4H_9•

	Reaction with O_2		Reaction with S_2	
	Highest energy transition state	Energy of reaction ($E_{product} - E_{reactant}$)	Highest energy transition state	Energy of reaction ($E_{product} - E_{reactant}$)
1-C_4H_8 via TS3-17	-2.82	-16.41	-13.08	-24.16
C_3H_6 via TS3-11	17.22	-36.96	17.2	-2.38
C_3H_6 via TS4-10	6.09	-36.96	16.34	-2.38
C_3H_6 via TS2-10	4.69	-36.96	3.83	-2.38
C_2H_4 via TS1-7	9.42	3.81	8.69	3.63

Note: Units = kcal/mol for all column as shown in the reaction profiles in Appendix 6.1-6.4

The reactions starting from n-C_4H_9 have five pathways that are important to this discussion, 1 pathway leads to 1-C_4H_8, 3 pathways result in C_3H_6 and one pathway gives C_2H_4. When the reaction is carried out with O_2, the thermodynamic product distribution should include a greater amount of C_3H_6, followed by some 1-C_4H_8 and a much smaller amount of C_2H_4. Based on energies of the highest transition states, kinetics should favour production of 1-C_4H_8 as this path has the lowest reaction barrier. C_3H_6 should be the next kinetic product as two of the pathways have transition state energies lower than that for the pathway leading to C_2H_4. When the reaction is carried out with S_2, the thermodynamic product distribution should have the greatest amount of 1-C_4H_8 followed by C_3H_6 and finally the product in the lowest amount should be C_2H_4. The kinetics based on activation energies follows the same trend, as the pathway leading to 1-C_4H_8 has the lowest value followed by one of the pathways leading to C_3H_6 and finally C_2H_4.

In addition, a second scheme of reactions that yield only the cracking products (C_3H_6 and C_2H_4) was generated. The energy profiles comparing the reactions using O_2 and S_2 are illustrated in Figures 6.5 and 6.6 below. The cracking reactions considered are as follows:

[6.8] n-C_4H_9• → C_2H_4 + C_2H_5•

[6.9] i-C_4H_9• → C_3H_6 + CH_3•

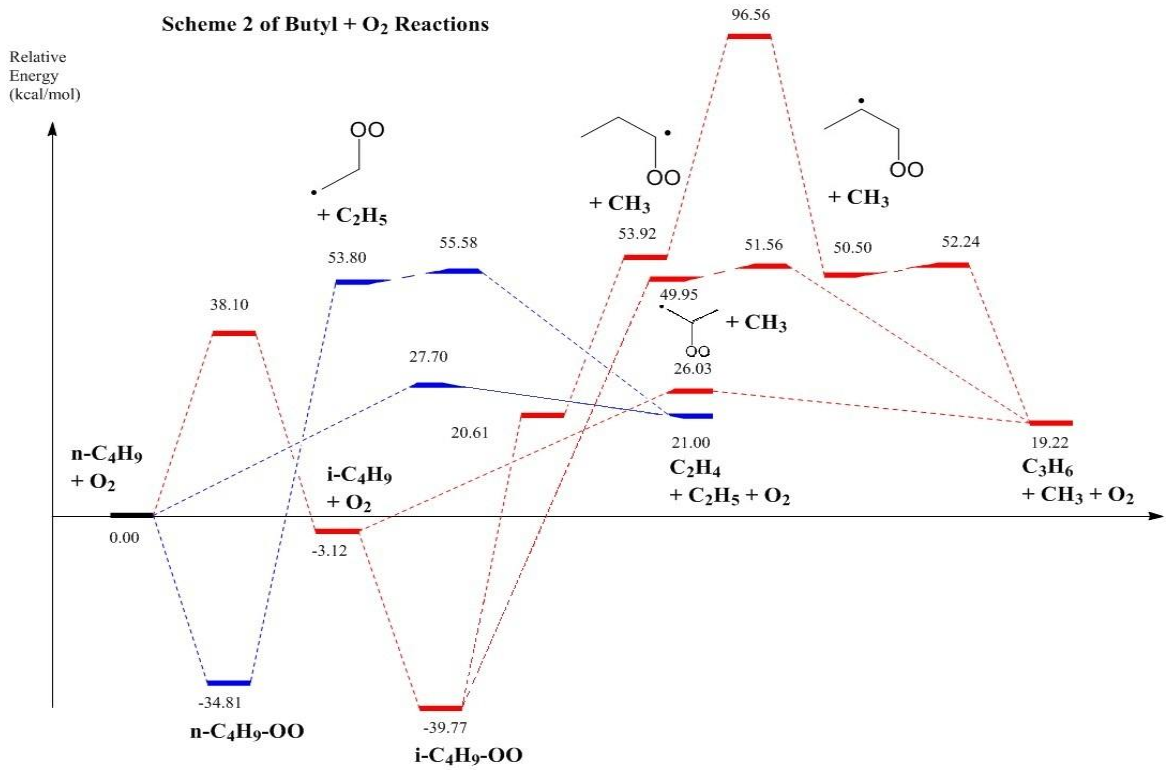

Figure 6.5: Energy profile for scheme 2 of reaction between n and i-butyl radical and O_2 leading to cracking products.

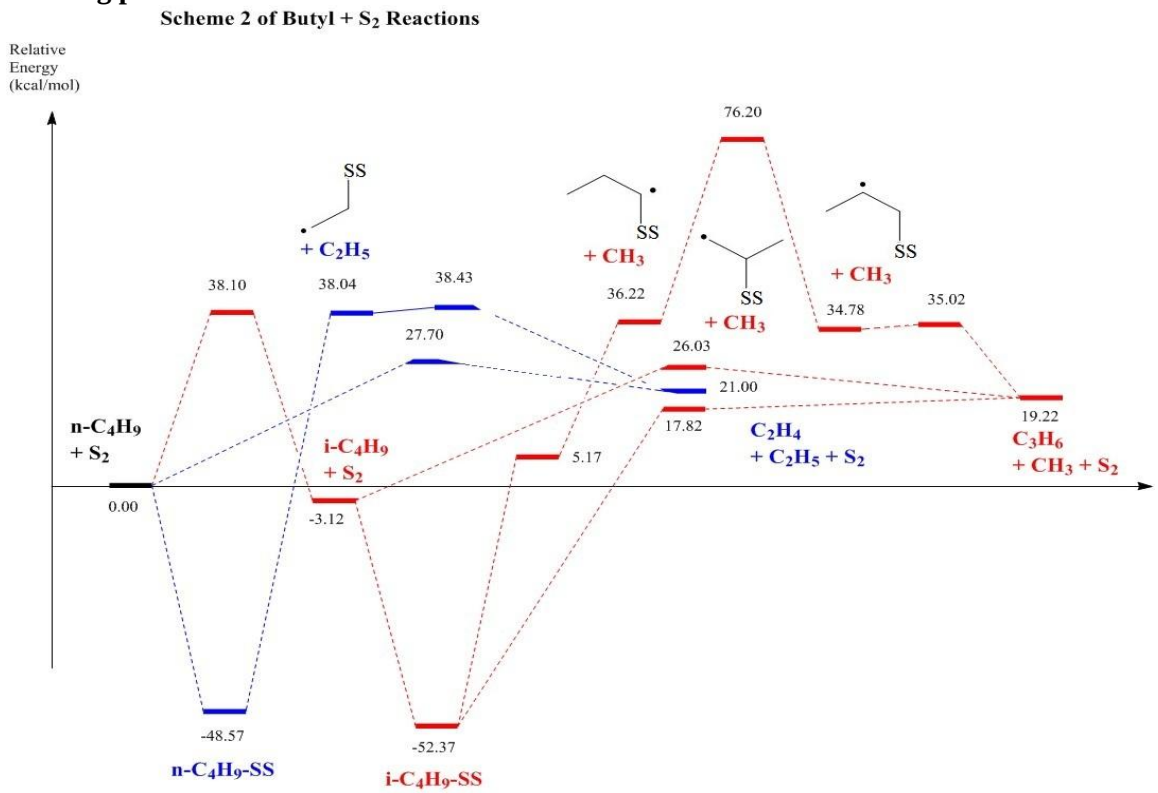

Figure 6.6: Energy profile for scheme 2 of reaction between n and i-butyl radical and S_2 leading to cracking products.

Scheme 2 highlights one main point, which is, the rate of reaction of pathways involving intermediates containing S_2 bonded to the butyl radical (or a fragment of the original radical) should be faster than that of O_2 as shown by the lower activation energies of these pathways. Obviously, all pathways that don't involve the oxidant (O_2 or S_2) bonded in some way to the original fragment have the same energy in both Figures 6.5 and 6.6. However, all of the paths that do have the oxidant bonded to the original radical have lower energy transition states when S_2 is used compared to O_2. The results of these calculations infer that the reaction pathways not involving an oxidant will proceed at the same rate regardless of which oxidant is present. However, those pathways that do involve the oxidant will be faster when S_2 is used compared to when O_2 is used. In general, the pathways that do not involve an oxidant have lower activation energies than the ones involving the oxidant, so in a kinetic regime the pathways involving the oxidants would contribute very little to the overall reaction. The one exception is the reaction path starting from i-C_4H_9• and reacting with S_2 that leads to C_3H_6, CH_3• and S_2 that goes via a transition state whose energy is 17.82 kcal/mol which is the lowest barrier pathway on the energy profile. In addition, when n-C_4H_9• is the starting point, the pathway not involving any oxidant leads to C_2H_5• and C_2H_4 and the activation barrier is 27.70 kcal/mol. When i-C_4H_9• is the starting point, the pathway not involving any oxidant leads to C_3H_6 and CH_3• and activation barrier is 26.03 kcal/mol. With the activation barriers being close in value, one can expect the product selectivities towards C_3H_6 and C_2H_4 to be quite similar if n-propyl and i-propyl radicals are present in equal amounts and if no oxidants are involved in the cracking process. The presence of the lower energy pathway leading to C_3H_6, due to reaction with S_2, may help in explaining why production of C_3H_6 is significantly favoured in the reaction containing H_2S and O_2 (which can generate S_2 in-situ) and not as favoured when the reaction is carried out with O_2 alone.

Combining the results from schemes 1 and 2, it can be seen that in general the products of the pure cracking processes shown in scheme 2 have a positive reaction energy making them less favourable. In addition, they have high activation barriers compared to some of the other pathways shown in scheme 1 that involve an oxidant. The conclusions are tabulated below, showing the order in which products are favoured, based on either the pathway's reaction energy (labelled as Equilibrium) or the value of the transition state energy (labelled as Kinetic). The first row shows the most favoured product, second row shows the next most favoured product and the third row shows the least favoured of the three products. This table is based on the pathways leading to olefin products observed during experimental analysis of the product stream and doesn't consider all the possible pathways shown in the energy profiles.

Table 6.4: Order in which the olefins, observed experimentally, are favoured according to the energy profiles calculated for the reactions between n-C_4H_9• and i-C_4H_9• and either O_2 or S_2.

Reactions starting with n-C_4H_9•				Reactions starting with i-C_4H_9•			
Carried out by O_2		Carried out by S_2		Carried out by O_2		Carried out by S_2	
Kinetic	Equilibrium	Kinetic	Equilibrium	Kinetic	Equilibrium	Kinetic	Equilibrium
1-C_4H_8	C_3H_6	1-C_4H_8	1-C_4H_8	2-C_4H_8	C_2H_4	2-C_4H_8	2-C_4H_8
C_3H_6	1-C_4H_8	C_3H_6	C_3H_6	1-C_4H_8	2-C_4H_8	1-C_4H_8	1-C_4H_8
C_2H_4	C_2H_4	C_2H_4	C_2H_4	C_2H_4	1-C_4H_8	C_2H_4	C_2H_4

In addition to the trends given above, ΔG(1023 K) values were also calculated for certain reaction pathways to consider how temperature may impact each of these pathways. The results of these calculations are shown in Table 6.5 below.

The table below highlights two key pieces of information. Firstly, the effect of temperature on the ΔG for the selected reaction pathways can be obtained by comparing the ΔG values at 298 K and 1023 K.

Table 6.5: ΔG calculations for reaction pathways leading to olefins using either S_2 or O_2 as the oxidant.

	E + ZPE (CBS-QB3 electronic Energy + zero-point Energy)	ΔG @298K (Gibbs free energy change)	ΔG @1023K (Gibbs free energy change)
i-C_4H_9 + O_2	0.00	0.00	0.00
1-C_4H_8 + O_2H	-13.29	-13.24	-11.62
2-C_4H_8 + O_2H	-16.13	-16.03	-14.76
C_2H_4 + CH_3CHO + OH	-36.17	-44.71	-67.44
i-C_4H_9 + S_2	0.00	0.00	0.00
1-C_4H_8 + S_2H	-21.03	-21.12	-20.18
2-C_4H_8 + S_2H	-23.87	-23.91	-23.32
C_2H_4 + CH_3CHS + SH	15.09	6.47	-16.39
n-C_4H_9 + O_2	0.00	0.00	0.00
C_2H_4 + CH_3CHO + OH	-39.29	-48.02	-71.17
C_3H_6 + CH_2O + OH	-33.83	-42.28	-64.74
1-C_4H_8 + O_2H	-16.41	-16.55	-15.36
2-C_4H_8 + O_2H	7.42	-2.45	-27.04
n-C_4H_9 + S_2	0.00	0.00	0.00
C_2H_4 + CH_3CHS + SH	11.96	3.17	-20.13
C_3H_6 + CH_2S + SH	15.27	6.61	-16.37
1-C_4H_8 + S_2H	-24.16	-24.43	-23.92
2-C_4H_8 + S_2H	-0.32	-10.33	-35.60
n-C_4H_9 + O_2/S_2	0.00	0.00	0.00
i-C_4H_9 + O_2/S_2	-3.13	-3.30	-3.74
C_2H_4 + C_2H_5 + O_2/S_2	20.99	10.82	-15.93
C_3H_6 + CH_3 + O_2/S_2	19.21	10.26	-14.22

Note: All values reported in this table are in units of kcal/mol

The values in the table for the reaction of n-C_4H_9 with either O_2 or S_2 show that dehydrogenation processes are favoured less by increasing the temperature of the reaction (indicated by the slight reduction in magnitude of the negative value in going from 298 K to 1023 K), while cracking processes are favoured greatly by the increase in reaction temperature (indicated by the increase in magnitude of the negative value or decrease in value for the positive values of ΔG). For the reaction between n-C_4H_9 and O_2/S_2, the similar trend is seen for the cracking processes, which exhibits an increase in magnitude for the negative values of ΔG in going from 298 K to 1023 K, but the dehydrogenation processes do not follow the same trend as before. In the case of 1-C_4H_8 production, the reaction follows the same trend as before, showing

a decrease in (the magnitude of) ΔG in going from 298 K to 1023 K however, the process leading to 2-C_4H_8 production shows an increase in the magnitude of the negative value of ΔG when the reaction temperature is increased, illustrating that this pathway is favoured at higher temperatures. Finally, the last row of the table shows pathways that lead to cracking products and leave the oxidant intact. The ΔG values of these pathways go from being positive valued at 298 K to negative valued at 1023 K suggesting that these process are favoured by the increase in temperature, which should be expected.

Secondly, comparing the values for ΔG at 1023 K for the different pathways will show to which extent each one will be favoured at equilibrium and whether the processes will be spontaneous or not. At 298 K, some of the processes (mainly cracking processes) have a positive value for the ΔG, showing that triggering these processes requires an additional input of energy and are therefore non-spontaneous. However, at 1023 K, all the ΔG values are negative and these reactions will therefore occur spontaneously. Of course, the overall distribution of products at equilibrium will still depend on the magnitude of the ΔG values for each of the pathways. For the reaction between i-C_4H_9 and O_2, the system will favour production of C_2H_4 > 2-C_4H_8 > 1-C_4H_8 at equilibrium and all these pathways have negative ΔG at 298 K showing the reactions will occur spontaneously even at room temperature. Comparatively, when the reaction is between i-C_4H_9 and S_2, the system will favour production of 2-C_4H_8 > 1-C_4H_8 > C_2H_4. For the reaction starting with n-C_4H_9 radical and O_2, the system favours production of C_2H_4 > C_3H_6 > 2-C_4H_8 > 1-C_4H_8 at equilibrium whereas, when S_2 is used, the system favours production of 2-C_4H_8 > 1-C_4H_8 > C_2H_4 > C_3H_6. Finally, the two cracking processes that leave the oxidant intact in the products have negative values for ΔG showing that they are spontaneous and C_2H_4 production is favoured slightly over that of C_3H_6.

Now, looking at the data obtained experimentally, results from the gas-phase reaction between C_4H_{10} and O_2 show that at shorter contact times and a reaction temperature of 923 K, the major products are C_3H_6 and C_2H_4 (with C_2H_4 being produced in a higher amount compared to C_3H_6) and 1-C_4H_8 being produced in a significantly lower amount. Alternatively, in the presence of H_2S, the product distribution highly favours production of C_3H_6 followed by 1-C_4H_8, and the olefin produced with the lowest selectivity is C_2H_4 (although, looking at the actual mol % will show that 1-C_4H_8 and C_2H_4 are produced in approximately the same amount).When the temperature is increased to 1023 K, the amount of 1-C_4H_8 drops and C_3H_6 becomes even more dominant in the product distribution.

Reconciling the trends seen experimentally with what the theoretical calculations suggest is easy for the reaction using O_2 as the oxidant but not quite as easy when S_2 is used. For the reaction where O_2 is the oxidant, both the experimental results and the theoretical calculations (especially the ΔG values) show that the product distribution favours $C_2H_4 > C_3H_6 > C_4H_8$. However in the case of the reaction with S_2, experimental results at 923 K show that $C_3H_6 > C_4H_8 > C_2H_4$ and when the temperature is raised to 1023 K the system favours production of $C_3H_6 > C_2H_4 > C_4H_8$. Neither the kinetic information obtained, nor the thermodynamic insight obtained from the theoretical calculations suggested that C_3H_6 should be highly favoured when S_2 is used as the oxidant.

6.2 Interaction between Vanadium Oxide and H_2S

The dissociative adsorption of H_2S on V_2O_5 has previously been reported in the literature.[138- 139] These reports have shown that vanadyl sites can be sulfided and these sites then become catalysts for further dissociation of H_2S to generate S_2. Another report has also shown that H_2S uptake occurs even at 293 K out and a noticeable color change of a V_2O_5 sample was

observed.[148] The potential energy profile for the sulfidation of the vanadyl O is depicted in Figure 6.7.[129]

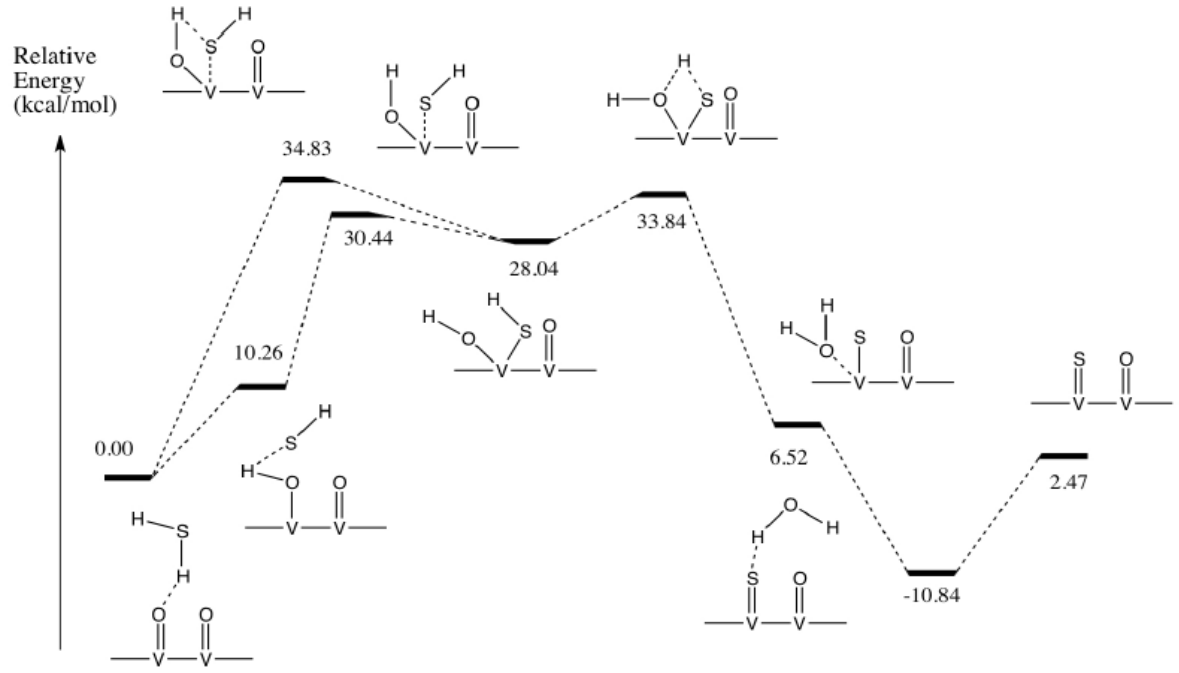

Figure 6.7: The energy profile for the substation of O by S at the vanadyl site on V_2O_5

The figure shows that the reaction energy for the substitution of O by S at the vanadyl position of V_2O_5 is 2.47 kcal/mol. The figure also shows that there are two different paths available and the activation barrier for each of these pathways is different as is the rate determining step. In one pathway, the rate determining step is H abstraction from H_2S by V=O with the corresponding SH remaining partially co-ordinated to the H and also being partially co-ordinated to the V as well, and the energy of this transition state is 34.83 kcal/mol. The second pathway occurs in a stepwise fashion where the first H abstraction occurs with the SH remaining partially co-ordinated to the H and in the second step, the SH breaks off from the H and partially co-ordinates to the V. The initial H abstraction in this second path has a lower energy (10.26 and 30.44 kcal/mol for each step in this first H abstraction). In this second pathway, the rate

determining step (part of the mechanism with the highest energy transition state) is therefore the hydrogen abstraction from SH which has an activation energy of 33.84 kcal/mol. Since the difference between the activation barriers of the two pathways is only 0.99 kcal/mol, both pathways should be occurring to almost the same degree and either were to be favoured, it would likely not be due to the activation barrier.

6.3 Catalytic Reaction on a Partially Sulfided Surface

To compare the reaction of C_3H_8 on a pure V_2O_5 surface to that on a partially sulfided V_2O_4S surface, the potential energy profiles for phase 1 of the reaction occurring on a vanadyl site are shown below. The mechanism for phase 1 is shown in appendix 6.6c and refers to the ODH of one molecule of propane over a vanadyl site resulting in the formation of propylene and H_2O. Adsorption of O_2 on the reduced vanadium site initiates the regeneration of the reduced site. In order to complete the regeneration of the vanadium site, a second molecule of propane must undergo ODH liberating a second molecule of propylene and H_2O.

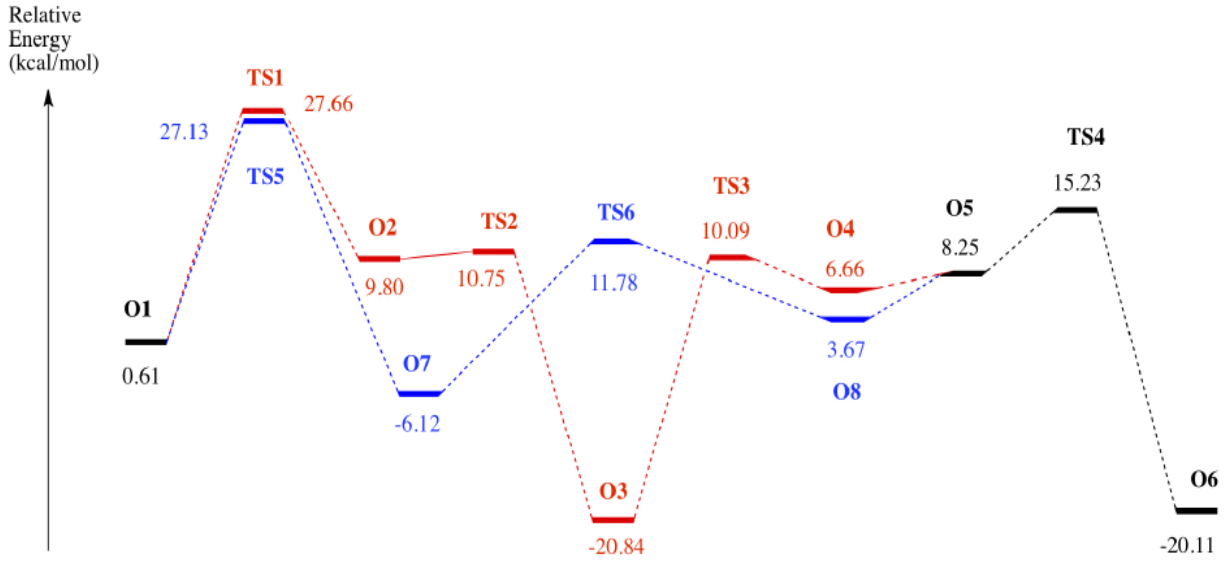

Figure 6.8: Potential energy profiles for phase 1 of the vanadyl mechanism on V_2O_5. (Red) Reaction channel involving multiple vanadyl sites. (Blue) Reaction channel involving isopropanol intermediate.[129] Structures of the transition states are shown in appendix 6.6.

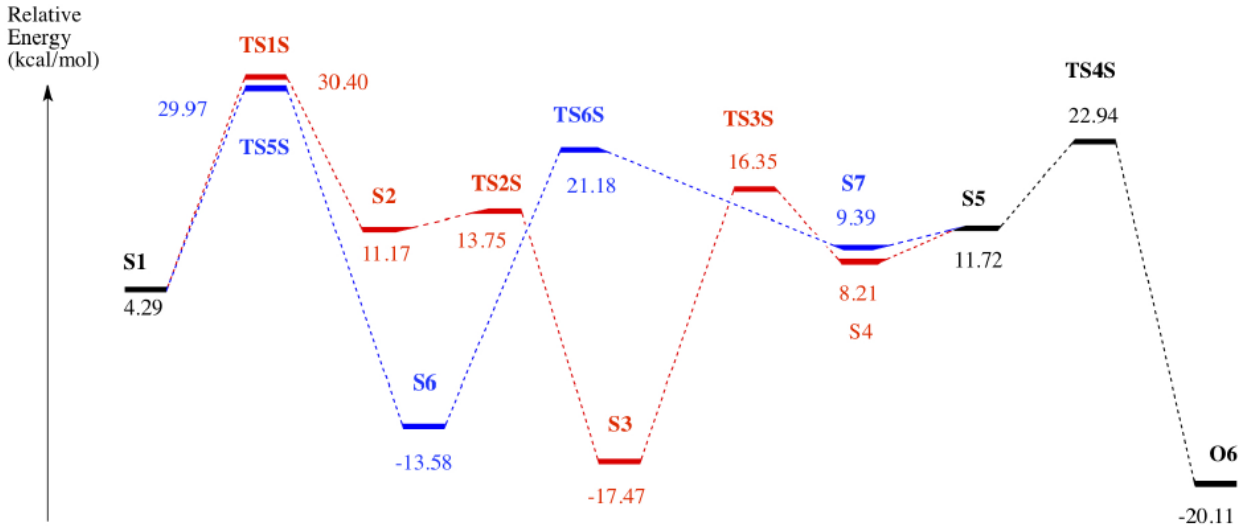

Figure 6.9: Potential energy profiles for phase 1 of the vanadyl mechanism on V_2O_4S. (Red) Reaction channel involving multiple vanadyl sites. (Blue) Reaction channel involving isopropy thiol intermediate.[129]

Comparison of the Figures 6.8 and 6.9 shows that the activation barrier of the pathway involving multiple vanadyl sites (Red) on V_2O_5 is 27.66 kcal/mol and on V_2O_4S is 30.40 kcal/mol. Similarly, the activation barrier for the reaction channel involving isopropanol on a V_2O_5 surface is 27.13 kcal/mol while that involving an isopropyl thiol intermediate on a V_2O_4S surface is 29.97 kcal/mol. If these were competing reactions, kinetics would favour the reaction on a V_2O_5 surface over the same reaction on a V_2O_4S surface. The final energies of the product are the same, but the energies of the reactants are not since V_2O_4S is at a higher energy compared to V_2O_5; therefore the reaction energy for the V_2O_5 system is -20.72 kcal/mol while that for the V_2O_4S system is -24.4 kcal/mol.

6.4 Discussion of other Mechanistic Aspects

In the initial gas-phase reaction, H_2S reacts with O_2 to form mostly S_2, H_2O and H_2 with some SO_2 observed at higher O_2:H_2S ratios. Complete oxidation of H_2S would lead to SO_2 and H_2O being the main products, however SO_2 can react with unreacted H_2S to produce S_2 and H_2O. In addition, pyrolysis of H_2S to produce H_2 and S_2 can also occur if the temperature is high

enough. The final product of the reaction between H_2S and O_2 is a function of the reaction temperature, reactant feed ratio and contact time. The S_2 (produced in situ) then functions very similarly to O_2 for the oxidative dehydrogenation of propane but produces H_2S as the second product, whereas O_2 would produce H_2O as the second product. The typical radical mechanism for the oxidation of C_3H_8 and n-C_4H_{10} by either O_2 or S_2 leads to products such as C_2-C_4 olefins, C_3-C_1 alkanes, CO, CO_2, H_2, H_2O, H_2S and S_2 and the mechanism for the formation of these products is well known.

However, because H_2S is also a reactant, the amount of H_2S obtained in the product stream is a combination of unreacted H_2S as well as H_2S formed as a product by reaction of S_2 with propane or butane. H_2S can also be formed via many other routes and two that may be of significant importance are noted below.

[6.10] $SH\bullet + H_2 \rightarrow H_2S + H\bullet$

The major routes from which SH• (which is a key intermediate in a radical reaction containing either H_2S or S_2) can be produced are: initial abstraction of hydrogen from H_2S by another radical (such as $CH_3\bullet$), dissociation of the H-S bond in H_2S (during initiation of the radical reaction) or splitting of H_2S_2 to produce two SH•.

The other potentially significant route that H_2S can come from is hydrolysis of CS_2. According to the equilibrium calculations, when coke was not allowed in the product list, CS_2 should have been the major sulphur product and conversion of H_2S was expected to be greater than 87% (up to 99% depending on the amount of O_2 in the system). However, when coke was an allowed product, conversion of H_2S was less than 1% suggesting that H_2S is the thermodynamic sulphur product. Experimentally, CS_2 was not observed in any significant

amount. In most experiments, a peak for CS_2 was observable, but below the quantifiable limit, therefore suggesting it was produced in only negligible amounts.

When elemental carbon is formed during these high temperature oxidation reactions, S_2 may react with it to form CS_2. However, at the reaction temperatures used and in the presence of H_2O (which is formed during initial oxidation of H_2S), CS_2 will hydrolyze according to the two step reaction shown below.

[6.11] $CS_2 + H_2O \rightarrow COS + H_2S$

[6.12] $COS + H_2O \rightarrow CO_2 + H_2S$

The driving force of these two reactions is the stability of the products formed. The strength of the carbon-oxygen bonds in CO_2, compared to that of carbon-sulfur in CS_2, drives the reaction.

In the absence of sulphur compounds, steam reforming of coke may occur according to the equation below.

[6.13] $C + H_2O \rightarrow CO + H_2$

Additionally, the water-gas shift reaction shown below may also occur to further convert some of the CO formed from steam reforming of coke.

[6.14] $CO + H_2O \rightarrow CO_2 + H_2$

The experimental results, for short contact time reactions (5-10 ms) showed greater amounts of CO than CO_2 for both H_2S-containing reactions and reactions performed without H_2S. At higher contact times, for the H_2S containing reactions, CO_2 became the dominant carbon oxide at 923 K, but at higher temperatures the amount of CO produced increased while the amount of CO_2 generally decreased. This would be expected as the water-gas shift reaction is slightly

exothermic hence the forward reaction is expected to be suppressed as temperature is increased and the reverse water-gas shift reaction may come into play which decreases the amount of CO_2.

6.5 Conclusions

In the presence of a catalyst, additional pathways for S_2 generation become available. As previously mentioned in the literature and the reaction profiles shown above, the vanadia catalyst can sulphide upon exposure to H_2S, and the sulfided vanadia site is then able to catalyze further H_2S dissociation to produce S_2. The sulfided site is also able to react directly with an alkane molecule to produce an olefin and H_2S, leaving a spent site that can be re-oxidized by a new O_2 molecule (and presumably S_2 as well). From the experiments where a supported vanadium oxide catalyst was first exposed to H_2S followed by propane, it became apparent that the active site on V_2O_5 can be sulfided, as evidenced by the presence of H_2S in the product stream of the alkane exposure step. Those results also provided evidence that the surface reaction between a partially sulfided vanadium oxide site and an alkane resulting in C_3H_6 and H_2S does occur. However in a system where S_2, H_2S, O_2 and the alkane are all present, it is unknown to which extent the surface sites will contribute to H_2S dissociation as opposed to direct oxidative dehydrogenation with the hydrocarbon. In addition, there is no evidence on whether the re-oxidation step will be carried out by O_2 or S_2, should both be available and present in the gas-phase.

As pointed out by the reaction profiles in Figures 6.8 and 6.9, there is no theoretical evidence that the direct reaction involving a sulfided catalyst is more efficient than the reaction over a vanadium oxide catalyst. However, the presence of S_2 in the gas-phase reactions made a huge difference in both theoretical calculations and in experimental results. The biggest enhancement to the reaction (experimentally) in terms of both activity and selectivity to C_3H_6 came from the addition of H_2S to the reactant mixture containing C_3H_8 or C_4H_{10} and O_2. The

reactions containing only the alkane and O_2 showed a higher selectivity towards C_2H_4 for both C_3 and C_4 alkane reactions, and some supporting evidence was found from the reaction profiles in Figures 6.1-6.4 as well as the computed ΔG at 1023 K shown in Table 6.5. On the other hand, the reactions containing H_2S had a higher selectivity to dehydrogenation products and certain cracking products over others. In the reaction between C_3H_8, O_2 and H_2S, the experimental results showed a higher selectivity towards C_3H_6 and a lower selectivity towards C_2H_4, which was supported by the theoretical calculations as shown in Figures 6.1-6.4.

When the reactant alkane was C_4H_{10}, experimental results again showed a high selectivity towards C_3H_6 (especially at 1023 K) and a lower selectivity towards C_2H_4. This trend was seen in all the reactions containing C_4H_{10}, O_2 and H_2S but theoretical calculations could not provide sufficient evidence for why this was the case. While the energy profiles showed that C_3H_6 would be favoured over C_2H_4, it also suggested that C_4H_8 should be favoured more and hence did not provide enough support for why C_3H_6 was the dominant product when the reaction contains S_2. One of the pathways from the reaction between C_4H_9• and S_2 (Figure 6.6) did have a lower energy transition state pathway leading to C_3H_6 compared to the corresponding pathway involving O_2 (Figure 6.5) which does help the case for C_3H_6. However, the ΔG calculations did not suggest the same trend either so the calculations were not able to provide support for why C_3H_6 is the dominant product for the reaction containing both O_2 and H_2S. It must be pointed out that the calculated ΔG values as well as the reaction energies are equilibrium values and therefore the trends obtained from using these values should not be expected to occur concomitantly for a reaction that is under kinetic control.

Chapter 7: Concluding Remarks

This research was carried out with the overall objective of finding a suitable oxidant for the oxidative dehydrogenation of propane and butane that will allow for high conversions while maintaining high selectivities to produce olefins, which can subsequently be used in the production of other petrochemicals, as well as high octane gasoline. One of the main problems of ODH is complete oxidation, which produces carbon oxides and H_2O as products. Sulfur was chosen in this work, because it is considered to be a softer oxidant and additionally, the production of carbon sulfides was not expected to be favourable at the ODH reaction temperature. However, S_2 was not added directly, but produced in-situ by oxidation of H_2S by O_2, which is expected to be a fast reaction with high S_2 selectivity at high H_2S:O_2 ratios at 900-1000 K. This in situ production of S_2 also has an added advantage of providing some heat for the reaction as the oxidation of H_2S is a highly exothermic reaction, as shown by the equilibrium calculations in Chapter 4. The reactions were studied first in the gas-phase and then over various silica-supported vanadium oxide catalysts.

Chapter 3 reported the study of reactions between propane and H_2S. The first few experiments showed the effects of H_2S on the gas phase pyrolysis of propane. The experimental data revealed that addition of H_2S enhanced the conversion of propane significantly. In addition, the product distribution in terms of product selectivities was also affected. The enhancement in the conversion of propane was noticeable at the higher reaction temperature as a greater amount of H_2S is expected to dissociate at that temperature. Table 3.4 showed that at 1023 K, conversion increased from 26% to 46% when H_2S was added to a propane stream (diluted by nitrogen) over an inert silica bed at 36 ms contact time. The addition of H_2S also increased the selectivity towards C_3H_6 and this effect was greater at 923 K. At 1023 K, the amount of cracking leading to

C_2H_4 production was higher for the reaction without H_2S, showing that propane pyrolysis favours cracking to a greater extent compared to the reaction with H_2S, which favours dehydrogenation to a greater extent.

The catalytic experiments carried out using similar reactants and conditions showed similar results. Experiments where the catalyst was first exposed to H_2S followed by C_3H_6 showed that sulfidation of the active sites on the catalyst surface did occur, and in the absence of any gas-phase oxidant these sites can participate in the ODH reaction. However, re-oxidation of these sites would require an oxidant that could be obtained from thermal (or catalytic) dissociation of H_2S. The surface sites can therefore participate either directly in the ODH reaction or to generate the oxidant (S_2 via catalytic dissociation of H_2S), but which process dominates at the reaction conditions is unknown. It was observed that the catalytic reaction provided no significant enhancement to the ODH reaction, especially at high temperatures where conversions are already generally high.

In Chapter 4, the results of the reactions between propane, H_2S and O_2 are described, first for gas-phase experiments and then over catalysts. In the gas-phase, addition of H_2S to the reaction between propane and O_2 resulted in a huge improvement in the selectivity towards C_3H_6. The reaction with H_2S also led to less cracking products compared to the reaction between propane and O_2. Slightly lower conversions were observed for the H_2S-containing reactions, yet the yield of C_3H_6 was significantly higher (36% for the H_2S-containing reaction vs 15% for the reaction without H_2S at 1023 K – Table 4.11). The catalytic reactions led to similar conclusions as those seen in Chapter 3, where improvements due to the addition of the catalyst were more significant at lower temperatures (where conversions are relatively low). Varying the amount of vanadium on the silica support caused changes in both conversion and selectivity to desired products. Increasing the amount of vanadium increased the conversion of propane but at the cost

of selectivity towards C_3H_6. The effect of contact time on the catalytic reaction was also studied; it was found that at higher contact times, conversion was improved (as would be expected) but at the cost of selectivity towards C_3H_6 and C_2H_4. Since all olefins are partial oxidation products and carbon oxides as well as solid carbon are the thermodynamic products, it should have been expected that selectivities towards olefinic products would suffer when contact time was increased. The trends observed were supported by the equilibrium calculations as well as the DFT calculations which unravelled why C_3H_6 was favoured to a greater extent in the presence of S_2 compared to C_2H_4 which is more favoured in the presence of O_2.

The most interesting results from this research project, regarding the oxidative dehydrogenation of n-butane with and without H_2S, and the effect of H_2S on the pyrolysis of n-butane, were described in Chapter 5. When the reaction was carried out with only n-butane and O_2, the product distribution contained the greatest amount of C_2H_4, followed by C_3H_6 and finally C_4H_8. When H_2S was added to the ODH reaction, the selectivity to C_3H_6 increased significantly, at the cost of C_2H_4 production. In Table 5.2, the results showed that in the absence of H_2S, the selectivity to C_2H_4 and C_3H_6 was 18% each at 923 K, whereas, in the presence of H_2S, the selectivity to C_2H_4 and C_3H_6 was 9% and 32% respectively. At 1023 K, the selectivity to C_3H_6 increased for both reactions to 25.5% and 40% for the reaction without H_2S and with H_2S respectively. The selectivity to C_2H_4 also increased for both reactions to 24% and 12% for the reaction without H_2S and with H_2S respectively. In addition, the conversion of n-butane was higher for the reaction containing H_2S. The effect of increasing the contact time from 8 ms to 27 ms was beneficial on the H_2S containing reaction at 923 K as conversion of n-butane increased from 25% to 35% and selectivity to desirable compounds such as olefins also increased. At 1023 K, the selectivity to C_4H_8 was approximately the same at both contact times, while the selectivity to C_2H_4 and C_3H_6 increased only slightly (1% and 2% respectively) due to the increased contact

time. The catalytic reaction was also tested and the results showed that at lower contact times (eg. 8 ms), the improvement to the reaction, in terms of selectivity to olefins, is observed and the effect is greater at the lower temperature. At the relatively longer contact time of 27 ms, the effects of the catalyst are essentially cancelled out and no significant difference in activity or selectivity was observed. This is likely because thermal reactions, which have previously been shown to be quite efficient for the production of olefins from n-butane, predominate.

The final conclusions obtained from the experimental work were that, if propane were to be used as the reactant, addition of H_2S favours the dehydrogenation pathways and leads to a higher selectivity for C_3H_6; and if butane is used as the reactant, addition of H_2S also leads to a higher selectivity to C_3H_6 albeit via cracking. When the reactions are carried out with only the alkane and O_2, cracking is favoured and leads to C_2H_4 production being favoured over C_3H_6 production. Conversion of reactants also proceeds in the absence of O_2 (i.e. containing only the alkane and H_2S), but consumption of the alkane is much lower and, therefore, may not be as attractive for industrial purposes. The best combination is to use both H_2S and O_2 together with the alkane to obtain a high conversion and high selectivity to C_3H_6. Use of a vanadia-based catalyst is apparently not necessary as the enhancement of the reaction due to the catalyst is seen only at lower temperatures where conversion is also low. Moreover, additional separation and recycling of unreacted alkane (which translates to extra costs) is required, that may end up negating the benefits of the catalyst.

References

1. G.A. Olah, A. Molnar, Hydrocarbon Chemistry 2nd Ed., Wiley-Interscience, Hoboken, NJ, 2003

2. Peck Hwee Sim. Chemical Week. New York: 168 (May 17th, 2006) 23.

3. F. Cavani and F. Trifiro, Appl. Catal. A, 88 (1992) 115.

4. L.M. Welch, L.J. Croce and H.F. Christmann, Hydrocarb. Process., 57 (11) (1978) 131.

5. T.G. Alkhazov and A.E. Lisovskii, Oxidative Dehydrogenation of Hydrocarbons (in Russian), Khimia, Moscow, 1980.

6. E.A. Mamedov, V. Corte´s Corberan, Appl. Catal. A 127 (1995) 1

7. Y. Moro-oka, W. Ueda, Partial Oxidation and Ammoxidation of Propane: Catalysts and Processes. Catalysis; Specialist Periodical Report; Royal Society of Chemistry: Cambridge (1994) Vol. 11, 223–245.

8. A. Chauvel, G. Lefebvre, L. Castex, Petrochemical Processes: Technical and economic characteristics, second ed., Paris Éditions Technip, 1989. Ch 2.

9. R.C. Berg, B.V. Vora, J.R. Mowry, Oil Gas J. 78 (1980) 191.

10. B.V. Vora, T. Imai, Hydrocarbon Process., Int. Ed. 61 (1982) 171.

11. P.R. Pujado, B.V. Vora, Energy Prog. 4 (1984) 186; Hydrocarbon Process., Int. Ed. 69 (1990) 65.

12. G. Centi, F. Cavani, F. Trifiro, Selective oxidation by heterogenous catalysis, in: Fundamental and Applied Catalysis; Kluver Academic/ Plenum Publishers., New York, 2000

13. K. Brooks, Chem. Week 137(4), (1985) 36.

14. G. Emig and F. Martin, Catal. Today 1 (1987) 477.

15. R. Burch, E.M. Crabb, Appl. Catal. A 100 (1993) 111.

16. D.J. Driscoll, K.D. Campbell, J.H. Lunsford, Adv. Catal. 35 (1987) 139.

17. M.Yu. Sinev, L.Ya. Margolis, V.N. Korchak, Uspekhi Khimii (Russ. Chem. Rev.) 64 (1995) 373.

18. V.P. Vislovskiy, T.E. Suleimanov, M.Yu. Sinev, Yu.P. Tulenin, L.Ya. Margolis, V. Cortés Corberán, Catal. Today 61 (2000) 287.

19. M. Fathi, R. Lødeng, E.S. Nilsen, B. Silberova, A. Holmena, Catal. Today 64 (2001) 113.

20. K.T. Nguyen, H.H. Kung, J. Catal. 122 (1990) 415.

21. A. Galli, J.M. Lopez Nieto, A. Dejoz, M.I. Vasquez, Catal. Lett. 34 (1995) 51.

22. E.A. Mamedov, V. Corte´s Corberan, Appl. Catal. A 127 (1995) 1**.**

23. E. Morales, J.H. Lunsford, J. Catal. 118 (1989) 255.

24. S. Gaab, J. Find, T.E. Muller, J.A. Lercher, Top. Catal. 46 (2007) 101.

25. A. Beretta, E. Ranzi, P. Forzatti, Catal. Today 64 (2001) 103.

26. F. Donsi, K.A. Williams, L.D. Schmidt, Ind. Eng. Chem. Res. 44 (2005) 3453.

27. A. Corma, J.M. Lopez Nieto, N. Parades, A. Dejoz, I. Vasquez, In: V. Cortez Corberan, S. Vic Bellon, (Eds.), Proceedings of the 2nd World Congress & European Workshop Meeting on New Developments in Selective Oxidations, 1993. Paper B4

28. O.S. Owen, H.H. Kung, J. Mol. Catal. 79 (1993) 265.

29. M.C. Kung, H.H. Kung, J. Catal., 134 (1992) 668.

30. M.D. Chaar, D. Patel, M.C. Kung, H.H. Kung, J. Catal., 105 (1987) 483.

31. D. Sew Hew Sam, V. Soenen, J.C. Volta, J. Catal. 123 (1990) 417.

32. X. Gao, P. Ruiz, Q. Xin, X. Guo, B. Delmon, Catal. Lett. 23 (1994) 321.

33. P.M. Michalakos, M.C. Kung, I. Jahan, H.H. Kung, J. Catal., 140 (1993) 226.

34. M.D. Chaar, D. Patel, M.C. Kung, H.H. Kung, J. Catal., 109 (1988) 463.

35. A. Parmaliana, V. Sokolovskii, F. Arena, F. Frusteri, D. Miceli Catal. Letters 40 (1996) 105.

36. P. Knotek, L. Capek, R. Bulanek, J. Adam, Top. Catal. 45 (2007) 51

37. S.A. Karakoulia, K.S. Triantafyllidis, A.A. Lemonidou, Micropor. Mesopor. Mater. 110 (2008) 157.

38. R. Zhou, Y. Cao, S.R. Yan, J.F. Deng, Y.Y. Liao, B.F. Hong, Catal. Lett. 75 (2001) 107.

39. W. Liu, S. Y. Lai, H. Dai, S. Wang, H. Sun, C. T. Au, Catal. Lett. 113, (February 2007) 147.

40. C. Hess, J.D. Hoefelmeyer, T.D. Tilley, J. Phys. Chem. B 108 (2004) 9703.

41. E.V. Kondratenko, M. Cherian, M. Baerns, D.S. Su, R. Schlogl, X. Wang, I.E. Wachs, J. Catal. 234 (2005) 131.

42. J. Santamaria-Gonzalez, J. Luque-Zambrana, J. Merida-Robles, P. Maireles-Torres, E. Rodriguez-Castellon, A. Jimenez-Lopez, Catal. Lett. 68 (2000) 67.

43. B. Solsona, T. Blasco, J. M. Lo´pez Nieto,1 M. L. Pen˜ a, F. Rey, A. Vidal-Moya, J. Catal. 203 (2001) 443

44. M.L. Pena, A. Dejoz, V. Fornes, F. Rey, M.I. Vazquez, J.M Lopez Nieto, Appl. Catal. A 209 (2001) 155.

45. J.M. Lopez Nieto, M.L. Pena, F. Rey, A. Dejoz, M.I. Vazquez, Abstract of 217th ACS National Meeting, Anaheim,. Am. Chem. Soc.,Washington, D.C., 1999, CATL-012.

46. R. Bulanek, P. Cicmanec, H. Sheng-Yang, P. Knotek, L. Capek, M. Setnicka, Appl. Catal. A 415-416 (2012) 29.

47. Y.M. Liu, W.L. Feng, T.C. Li, H.Y. He, W.L. Dai, W. Huang, Y. Cao, K.N. Fan, J. Catal. 239 (2006) 125.

48. J.B. Stelzer, J. Caro, M. Fait, Catal. Commun. 6 (2005) 1.

49. A. Kaddouri, R. Anouchinsky, C. Mazzocchia, L.M. Maderia, M.F. Portela, Catal. Today, 40 (1998) 201**.**

50. F.C. Meunier, A. Yasmeen, and J.R.H. Ross, Catal. Today, 37 (1997) 33.

51. D.L. Stern, R K. Grasselli, J. Catal. 167 (1997) 550.

52. R.B. Watson, S.L. Lashbrook, U.S. Ozkan. J. Mol. Catal A 208 (2004) 233.

53. E. Heracleous, M. Machli, A.A. Lemonidou, I.A. Vasalos, J. Mol. Catal A 232 (2005) 29.

54. B**.** Solsona, A. Dejoz, T. Garcia, P. Concepcion, J.M. Lopez Nieto, M.I. Vazquez, M.T. Navarro, Catal. Today 117 (2006) 228.

55. A. Christodoulakis, S.J. Boghosian, Catal. 260 (2008) 178.

56. S.C. Nayak, D. Shee, G. Deo, Catal. Lett. 136 (2010) 271.

57. V.C. Corberan, Catal. Today 99 (2005) 33.

58. E.V. Kondratenko, M. Cherian, M. Baerns, Catal.Today 112 (2006) 60.

59. L.G. Tischler, M.S. Wing, U.S. Patent 3,773,850 (1973).

60. D.V. Porchey, D.J. Royer, U.S. Patent 3,803,260 (1974**).**

61. P.D. Clark, N.I. Dowling, X. Long, Y. Li, J. Sulfur Chem. 25 (2004) 381**.**

62. S. Liu, ODH of Ethane to Ethylene with H_2S and Sulfur. Ph.D. Thesis. (2007**)** Calgary, AB: University of Calgary.

63. M. Huff, L.D. Schmidt, J. Phys. Chem. 97 (1993) 11815.

64. B. Silberova, M. Fathi, A. Holmen, Appl. Catal. A, 276 (2004) 17.

65. F. Obenaus, W. Droste, J. Neumeister, Butenes (2011), Ullmann's Encyclopedia of Industrial Chemistry.

66. N. Calamur, M.E. Carrera, R.A. Wilsak, Butylenes (2003), Kirk-Othmer Encyclopedia of Chemical Technology.

67. R.C. Berg, B.V. Vora, J.R. Mowry, Oil Gas J. 78 (1980) 191.

68. F.M. Brinkmeyer, D.F. Rohr, M.E. Olbrich, L.E. Drehman, Oil Gas J. 81 (1983) 75.

69. P.R. Sarathy, G.S. Suffridge, Hydrocarbon Process., Int. Ed. 72 (1993), 89; 72 (1993), 43.

70. D. Sanfilippo, Chemtech. 23 (1993) 35.

71. Hydrocarbon Process., Int. Ed. 59 (1980), 210.

72. S. Gussow, D. C. Spence, E. A. White, Oil Gas J. 78 (1980) 96.

73. R. G. Craig, E. A. White, Hydrocarbon Process., Int. Ed. 59 (1980) 111.

74. B. Sulikowski, Z. Olejniczak, E. Włocha, J. Rakoczy, R.X. Valenzuela, V. Cortés Corberán (2002) Appl. Catal. A, 232 (2002) 189.

75. D.Y. Zhao, J.L. Feng, Q.S. Huo, N. Melosh, G.H. Fredrickson, B.F. Chmelka, G.D. Stucky, Science 279 (1998) 548.

76. Y.S. Yoon, W. Ueda and Y. Moro-oka, Catal. Lett., 35 (1995) 57.

77. L. Savary, G. Costentin, M.M. Bettahar, J.C. Lavalley, M. Gubelmann-Bonneau, Catal. Lett., 38 (1992) 197.

78. J. Buiten, J. Catal., 10 (1968) 188.

79. Y. Moro-Oka, S. Tan and A. Osaki, J. Catal., 12 (1968) 241.

80. M. M. Bettahar, G. Costentin, L. Savary, J.C. Lavalley, Appl. Catal. A 145 (1996) 1.

81. Y.M. Liu, Y. Cao, S.R. Yan, W.L. Dai and K.N. Fan, Catal. Lett. 88 (2003) 61.

82. R. Bulanek, A. Kaluzova, P. Cicmanec, M. Setnicka, A. Zukal, J. Mayerova, Catal. Today 179 (2012) 149.

83. R. Grabowski, Catal. Rev. 48 (2006) 199.

84. K. Chen, A. Khodakov, J. Yang, A.T. Bell, E. Iglesia, J. Catal. 186 (1999) 325.

85. E. Finocchio, G. Busca, V. Lorenzelli, R.J. Willey, J. Catal., 151 (1995) 204.

86. H.H. Kung, Ind. Eng. Chem. Prod. Res. Dev., 25 (1995) 171.

87. P. Conception, J.M. Lopez Nieto, J. Perez Pariente, Catal. Lett. 19 (1993) 333.

88. J.M. Lopez Nieto, P. Conception, A. Dejoz, H. Knozinger, F. Melo, M.I. Vazquez, J. Catal. 189 (2000) 147.

89. M.D. Putra, S.M. Al-Zahrani, A.E. Abasaeed, Ind. Eng. Chem. 18 (2012) 1153.

90. M.D. Putra, S.M. Al-Zahrani, A.E. Abasaeed, Catal. Commun. 14 (2011) 107.

91. C. Limberg, Angew. Chem., Int. Ed. 42 (2003) 5932-5954.

92. E.V. Kondratenko, M.Y. Sinev, Appl. Catal. A, 325 (2007) 353.

93. W.A. Goddard III, K. Chenoweth, S. Pudar, A.C.T. van Duin, M.J. Cheng, Top. Catal. 50 (2008) 2.

94. K.Mori, A. Miyamoto, Y. Murakami, J. Phys. Chem. 89 (1985) 4265.

95. F.Gilardoni, A.T. Bell, A. Chakraborty, P. Boulet, J. Phys. Chem. B 104 (2000) 12250.

96. J.G. Eon, R. Olier, J.C. Volta, J. Catal. 145 (1994) 318.

97. M. Witko, K. Hermann, R. Tokrarz, Catal. Today. 50 (1998) 553.

98. K. Alexopoulos, M-F, Reyniers, G. B. Martin, J. Catal. 289 (2012) 127.

99. H. Fu, Z.P. Liu, Z.H. Li, W.N. Wang, K.N. Fan, J. Am. Chem. Soc. 128 (2006) 11114.

100. O.A. Hougen, K.M. Watson, Ind. Eng. Chem., 43 (1943) 529.

101. E.K. Rideal, Proc. Cambridge Phil. Soc. A 178 (1941) 428.

102. D.D. Eley, E.K. Rideal, Proc. Roy. Soc. A 178 (1941) 429.

103. I. Langmuir, Trans. Faraday Soc. 17 (1921) 621.

104. P. Boutry, R. Montarnal, C. R. Acad. Sci. 263C (1966) 1102.

105. G. Thomas, R. Montarnal, P. Boutry, C. R. Acad. Sci. 269C (1969) 283.

106. P. Mars, D.W. Van Krevelen, Chem. Eng. Sci. 3 (1954) 41.

107. K.A. Sheslstad, J. Downie, W.F. Graydon, Can. J. Chem. Eng. 38 (1960) 102.

108. G.C.A. Schuit, L.L. van Reijen, Bull. Soc. Chim. Belges. 67 (1958) 489.

109. G.C.A. Schuit, L.L. van Reijen, Advances in Catalysis 10 (1997) 243.

110. C. Hinshelwood, Kinetics of Chemical Change; Oxford University Press: Oxford. 1940

111. J. Downie, K.A. Sheslstad, W.F. Graydon, Can. J. Chem. Eng. 69 (1965) 457.

112. J.A. Jussola, R.F. Mann, J. Downie, J. Catal. 17 (1970) 103.

113. I.F. Boag, D.W. Bacon, J. Downie, J. Catal. 38 (1975) 375.

114. A. Dinse, S. Khennache, B. Frank, C. Hess, R. Herbert, S. Wrabetz, R. Schlogl, R. Schomacker, J. Mol. Catal. A 307 (2009) 43.

115. M.D. Argyle, K.D. Chen, E. Iglesia, A.T. Bell, J. Phys. Chem. B 109 (2005) 2414.

116. J.A. Montgomery, Jr., M.J. Frisch, J.W. Ochterski, G.A. Petersson, J. Chem. Phys. 110 (1999) 2822.

117. J.W. Ochterski, G.A. Petersson, J.A. Montgomery, Jr., J. Chem. Phys. 104 (1996) 2598.

118. E.K. Pokon, M.D. Liptak, S. Feldgus, G.C. Shields, J. Phys. Chem. A 105 (2001) 10483.

119. J.K. Merle, C.J. Hayes, S.J. Zalyubovsky, B.G. Glover, T.A. Miller, C.M. Hadad, J. Phys. Chem. A 109 (2005) 3637.

120. L. Zhu, J.W. Bozzelli, L.M. Kardos, J. Phys. Chem. A 111 (2007) 6361.

121. J.M. Simmie, G. Black, H.J. Curran, J.P. Hinde, J. Phys. Chem. A 112 (2008) 5010.

122. L.K. Huynh, H.-H. Carstensen, A.M. Dean, J. Phys. Chem. A 114 (2010) 6594.

123. M.J. Frisch, G.W. Trucks, H.B. Schlegel, G.E. Scuseria, M.A. Robb, J.R. Cheeseman, G. Scalmani, V. Barone, B. Mennucci, G.A. Petersson, H. Nakatsuji, M. Caricato, X. Li, H.P. Hratchian, A.F. Izmaylov, J. Bloino, G. Zheng, J.L. Sonnenberg, M. Hada, M. Ehara, K. Toyota, R. Fukuda, J. Hasegawa, M. Ishida, T. Nakajima, Y. Honda, O. Kitao, H. Nakai, T. Vreven, J.A. Montgomery, Jr., J.E. Peralta, F. Ogliaro, M. Bearpark, J.J. Heyd, E. Brothers, K.N. Kudin, V.N. Staroverov, R. Kobayashi, J. Normand, K. Raghavachari, A. Rendell, J.C. Burant, S.S. Iyengar, J. Tomasi, M. Cossi, N. Rega, J.M. Millam, M. Klene, J.E. Knox, J.B. Cross, V. Bakken, C. Adamo, J. Jaramillo, R. Gomperts, R.E. Stratmann, O. Yazyev, A.J. Austin, R. Cammi, C. Pomelli, J.W. Ochterski, R.L. Martin, K. Morokuma, V.G. Zakrzewski, G.A. Voth, P. Salvador, J.J. Dannenberg, S. Dapprich, A.D. Daniels, O. Farkas, J.B. Foresman, J.V. Ortiz, J. Cioslowski, D.J. Fox, Gaussian 09, Revision C.01; Gaussian, Inc., Wallingford CT, 2009.

124. G. Kresse, J. Hafner, Phys. Rev. B 47 (1993) 558.

125. G. Kresse, J. Hafner, Phys. Rev. B 49 (1994) 14251.

126. G. Kresse, J. Furthmuller, Comput. Mat. Sci. 6 (1996) 15.

127. G. Kresse, J. Furthmuller, Phys. Rev. B 54 (1996) 11169.

128. J.P. Perdew, K. Burke, M. Ernzerhof, Phys. Rev. Lett. 77 (1996) 3865.

129. J. Lo, Z.A. Premji, T. Ziegler, P.D. Clark, First-Principles Investigation of Selective Oxidation of Propane on Clean and Sulfided V_2O_5 (010) Surfaces. (Submitted manuscript – Journal of Physical Chemistry) (2013) Calgary, Canada

130. G.E. Herriott, R.E. Eckert, L.F. Albright, AICHe J. 18(1) (1972) 84.

131. F. Cavani, N. Ballarini, A. Cericola, Catal. Today 127 (2007) 113.

132. H.H. Kung, Oxidative Dehydrogenation of Light (C2-C4) Alkanes, in: D.D. Eley, H. Pines, W.O. Haag (Eds.), Advances in Catalysis, Academic Press, New York, 1994, Vol. 40, pp 1-38.

133. E.V. Kondratenko, O. Ovsitser, Catal. Today 142 (2009) 138.

134. M.A. Botavina, G. Martra, Yu.A. Agafonov, N.A. Gaidai, N.V. Nekrasov, D.V. Trushin, S. Coluccia, A.L. Lapidus, Appl. Catal. A 347 (2008) 126.

135. M.E.D. Raymont, Hydrocarb. Process. 54(7) (1975) 139.

136. V. Kaloidas, N. Papayannakos, Chem. Eng. Sci. 44 (1989) 2493.

137. T. Higashihara, K. Saito, H. Yamamura, Bull. Chem. Soc. Jpn. 49(4) (1976) 965.

138. L.M. Al-Shamma, S.A. Naman, Int. J. Hydrogen Energy 14(3) (1989) 173.

139. T. Chivers, J.B. Hyne, C. Lau, Int. J. Hydrogen Energy 5 (1980) 499.

140. B.G. Cox, P.F. Clarke, B.B. Pruden, Int. J. Hydrogen Energy 23(7) (1998) 531.

141. V.E. Kaloidas, N.G. Papayannakas, Int. J. Hydrogen Energy 12(6) (1987) 403.

142. S.K. Layokun, D.H. Slater, Ind. Eng. Chem. Process Des. Dev. 18(2) (1979) 232.

143. M.C. Lin, K.J. Laidier, Can. J. Chem. 44 (1966) 2927.

144. V.R. Choudhary, V.H. Rane, A.M. Rajput, AIChE Journal. 44(10) (1998) 2293.

145. J.W. Falconer, J.H. Knox, Proc. Royal Soc. A. 250 (1959) 493.

146. B.L. Crynes, L.F. Albright, Ind. Eng. Chem. Process Des. Dev. 8(1) (1969) 25.

147. V.I. Savchenko, L.P. Didenko, L.V. Zav'yalova, Kinet. Catal. 37(2) (1996) 151.

148. R.L.C. Bonne, A.D. van Langeveld, J.A. Moulijn, J. Catal. 154 (1995) 115.

149. D. Depeyre, G.F. Flocoteaux, Ind. Eng. Chem. Process Des. Dev. 15 (1976) 291.

150. B.M. Weckhuysen, D.E. Keller, Catal. Today 78 (2003) 25.

151. H.E. Coward, G.W. Jones, Bur. Mines Bull. 279 (1931) 114.

152. Anon. Sulphur, 187 (1986) 1.

153. G. Dupuy, M. Graulier, Inform. Chim., Special Catalyse, 74 (1969) 33

154. C.F. Claus, British Patent 5958 (1883)

155. H. Baehr, Refiner Natural Gas. Manuf., 17 (1938) 237.

156. A. Pieplu, O. Saur, J-C. Lavalley, Catal. Rev. Sci. Eng. 40(4) (1998) 409.

157. I.A. Gargurevich, Ind. Eng. Chem. Res. 44(20) (2005) 7706.

158. Chris Morley, GASEQ chemical equilibrium program. V 0.79 jan 2005. http://www.c.morley.dsl.pipex.com/

159. A.J. Gordon, R.A. Ford, Chemist's Companion - A Handbook of Practical Data, Techniques, and References. John Wiley & Sons. 1972.

160. A.E. Shilov, G.B. Shul'pin, Activation and Catalytic Reactions of Saturated Hydrocarbons in the Presence of Metal Complexes. Springer-Verlag. 2000.

161. J.H. Kolts, Ind. Eng. Chem. Fundam. 25 (1986) 265.

162. M.A. Ghaly, B.L. Crynes, ACS Symp. Ser. 32 (1976) 218-240.

163. V. Marshneva, V. Mokrinskii, Kinet. Katal., 29 (1988) 989.

164. M.Y. Shin, C.M. Nam, D.W. Park, J.S. Chung, Appl. Catal. A. 211 (2001) 213.

Appendix 2.1: Minimum, maximum and average values to show variation between data points for an experiment. (Data from Table 4.8 for an empty tube, 4:2:2 C_3H_8: H_2S:O_2 feed at 20 ms residence time experiment)

	Products, mole/100 moles of feed														Conversion %			Yield % [Selectivity %]								
	N_2	C_3H_8	H_2S	O_2	H_2	C_3H_6	C_2H_4	C_2H_6	CH_4	CO	CO_2	$C_{(s)}$	S_2	H_2O	C_3H_8	O_2	H_2S	C_3H_6	C_2H_4	C_2H_6	CH_4	CO	CO_2	$C_{(s)}$	S_2	H_2O
						T= 923 K																				
Average	33.00	16.88	2.68	1.55	2.15	8.44	5.59	0.26	5.83	2.34	0.17	4.50	7.04	27.72	49.62	90.77	84.01	25.19	11.13	0.51	5.80	2.33	0.17	4.48	84.01	82.74
min		16.24	2.60	1.43	1.91	8.13	5.26	0.23	5.45	2.27	0.17	4.13	6.98	27.44	47.96	89.73	83.44	24.27	10.50	0.46	5.42	2.26	0.17	4.10	83.44	81.93
max		17.43	2.77	1.72	2.44	8.78	5.96	0..29	6.27	2.39	0.18	4.94	7.07	27.90	51.52	91.49	84.47	26.20	11.90	0.57	6.24	2.38	0.18	4.91	84.47	83.29
Average																		[50.8]	[22.4]	[1.03]	[11.67]	[4.7]	[0.35]	[9.06]		
min																		[50.6]	[21.8]	[0.96]	[11.3]	[4.62]	[0.34]	[7.97]		
max																		[50.8]	[23]	[1.11]	[12.11]	[4.76]	[0.35]	[10.3]		
						T= 1023 K																				
Average	33.00	10.74	2.41	0.89	4.25	11.04	8.66	0.53	9.27	2.74	0.17	4.59	7.17	28.65	67.94	94.70	85.61	32.96	17.24	1.06	9.22	2.73	0.17	4.57	85.61	85.52
min		10.04	2.30	0.83	4.18	10.95	8.46	0.52	8.98	2.52	0.15	3.19	7.13	28.49	65.86	94.34	85.14	32.68	16.80	1.04	8.93	2.51	0.15	3.17	85.14	85.05
max		11.44	2.49	0.95	4.33	11.12	8.94	0.55	9.62	2.95	0.19	5.50	7.22	28.93	70.03	95.02	86.28	33.19	17.80	1.10	9.57	2.94	0.19	5.47	86.28	86.37
Average																		[48.5]	[25.4]	[1.56]	[13.57]	[4.01]	[0.24]	[6.7]		
min																		[47.2]	[25.1]	[1.54]	[13.48]	[3.81]	[0.21]	[4.81]		
max																		[50.4]	[25.6]	[1.57]	[13.67]	[4.19]	[0.29]	[7.82]		

Note: Values for $C_{(s)}$ and S_2 and H_2O are calculated from mass balance data and can therefore include a greater amount of variation (error).

Appendix 3.1a $C_3H_8/H_2S/N_2$ Gas Phase Reactions with and without H_2S

Catalyst: empty tube (void) Contact time: 36ms Temperature: 923 K

	Products, mole/100 moles of feed										Conversion %		Yield % [Selectivity %]					
	N_2	C_3H_8	H_2S	H_2	C_3H_6	C_2H_4	C_2H_6	CH_4	$C_{(s)}$	S_2	C_3H_8	H_2S	C_3H_6	C_2H_4	C_2H_6	CH_4	$C_{(s)}$	S_2
					without H_2S													
Feed	66.6	34.2	0.0															
Product	66.6	32.7	0.0	0.5	0.3	0.2	0.0	0.3	2.5	0.0	4	0	1	0	0	0	2	0
													[24]	[9.9]	[0]	[7]	[59]	
					with H_2S													
Feed	60.3	34.9	4.9															
Product	60.3	32.3	4.7	0.5	0.4	0.5	0.0	0.5	5.1	0.1	8	4	1	1	0	0	5	0
													[15]	[13]	[0]	[7]	[65]	

Appendix 3.1b $C_3H_8/H_2S/N_2$ Gas Phase Reactions with and without H_2S

Catalyst: empty tube (void) Contact time: 36ms Temperature: 1023 K

	Products, mole/100 moles of feed										Conversion %		Yield % [Selectivity %]					
	N_2	C_3H_8	H_2S	H_2	C_3H_6	C_2H_4	C_2H_6	CH_4	$C_{(s)}$	S_2	C_3H_8	H_2S	C_3H_6	C_2H_4	C_2H_6	CH_4	$C_{(s)}$	S_2
						without H_2S												
Feed	66.6	34.2	0.0															
Product	66.6	25.1	0.0	4.1	3.5	4.8	0.0	4.6	2.5	0.0	26	0	10 [39]	9 [35]	0 [0]	5 [17]	2 [9]	0
						with H_2S												
Feed	60.3	34.9	4.9															
Product	60.3	19.0	4.7	5.4	5.2	6.1	0.4	6.6	12.5	0.1	46	2	15 [32]	12 [26]	1 [2]	6 [14]	12 [26]	2

Appendix 3.2a $C_3H_8/H_2S/N_2$ Gas Phase Reactions with and without H_2S

Catalyst: crystalline silica Temperature: 923 K Contact time = ~36 ms

	Products, mole/100 moles of feed										Conversion %		Yield % [Selectivity %]					
	N_2	C_3H_8	H_2S	H_2	C_3H_6	C_2H_4	C_2H_6	CH_4	$C_{(s)}$	S_2	C_3H_8	H_2S	C_3H_6	C_2H_4	C_2H_6	CH_4	$C_{(s)}$	S_2
		without H_2S																
Feed	65.3	36.6	0.0															
Product	65.3	34.8	0.0	0.5	0.4	0.4	0.0	0.4	3.1	0.0	5	n/a	1 [22]	1 [14]	0 [0]	0 [7]	3 [57]	0
		with H_2S																
Feed	60.6	35.6	5.0															
Product	60.6	33.7	5.1	1.0	0.9	1.2	0.0	1.2	-0.7	-0.1	5	-1	3 [49]	2 [42]	0 [0]	1 [22]	-1 -[13]	0

Appendix 3.2b $C_3H_8/H_2S/N_2$ Gas Phase Reactions with and without H_2S

Catalyst: crystalline silica Temperature: 1023 K Contact time= ~36 ms

	Products, mole/100 moles of feed										Conversion %		Yield % [Selectivity %]					
	N_2	C_3H_8	H_2S	H_2	C_3H_6	C_2H_4	C_2H_6	CH_4	$C_{(s)}$	S_2	C_3H_8	H_2S	C_3H_6	C_2H_4	C_2H_6	CH_4	$C_{(s)}$	S_2
		without H_2S																
Feed	65.3	36.6	0.0															
Product	65.3	27.1	0.0	4.5	3.5	5.3	0.2	5.3	1.7	0.0	26	n/a	10 [37]	10 [37]	0 [2]	5 [18]	2 [6]	n/a
		with H_2S																
Feed	60.6	35.6	5.0															
Product	60.6	19.2	5.1	6.0	7.1	7.5	0.8	8.2	2.8	-0.1	46	-2	20 [44]	14 [31]	1 [3]	8 [17]	3 [6]	-4

Appendix 3.3a $C_3H_8/H_2S/N_2$ Catalytic Reaction with and without H_2S

Catalyst: 5% Vox/CS Contact time: 40 ms Temperature: 923 K

	Products, mole/100 moles of feed										Conversion %		Yield % [Selectivity %]					
	N_2	C_3H_8	H_2S	H_2	C_3H_6	C_2H_4	C_2H_6	CH_4	$C_{(s)}$	S_2	C_3H_8	H_2S	C_3H_6	C_2H_4	C_2H_6	CH_4	$C_{(s)}$	S_2
			Without H_2S															
Feed	65.3	36.3	0.0															
Product	65.3	34.8	0.0	1.3	0.9	0.6	0.0	0.6	0.2	0.0	4	0	2	1	0	1	0	0
													[58]	[25]	[0]	[13]	[5]	
			With H_2S															
Feed	62.1	35.7	4.7															
Product	62.1	32.7	4.9	2.9	2.3	1.1	0.0	1.1	-1.4	-0.1	8	-7	6	2	0	1	-1	0
													[79]	[24]	[0]	[13]	-[16]	

Appendix 3.3b $C_3H_8/H_2S/N_2$ Catalytic Reaction with and without H_2S

Catalyst: 5% Vox/CS Contact time: 40 ms Temperature: 1023 K

	Products, mole/100 moles of feed										Conversion %		Yield % [Selectivity %]					
	N_2	C_3H_8	H_2S	H_2	C_3H_6	C_2H_4	C_2H_6	CH_4	$C_{(s)}$	S_2	C_3H_8	H_2S	C_3H_6	C_2H_4	C_2H_6	CH_4	$C_{(s)}$	S_2
			Without H_2S															
Feed	65.3	36.3	0.0															
Product	65.3	26.0	0.0	4.5	3.8	5.6	0.0	5.3	3.1	0.0	28	0	11	10	0	5	3	0
													[37]	[36]	[0]	[17]	[10]	
			With H_2S															
Feed	62.1	35.7	4.7															
Product	62.1	18.5	4.9	6.7	7.4	8.0	0.7	9.5	2.5	-0.1	48	-9	21	15	1	9	2	-5
													[43]	[31]	[2.6]	[19]	[5]	

Appendix 3.4a $C_3H_8/H_2S/N_2$ Catalytic Reaction at Various Feed Compositions

Catalyst: 5% VOx/CS Contact time: 35 ms Temperature: 823 K

	Products, mole/100 moles of feed										Conversion %		Yield % [Selectivity %]					
	N_2	C_3H_8	H_2S	H_2	C_3H_6	C_2H_4	C_2H_6	CH_4	$C_{(s)}$	S_2	C_3H_8	H_2S	C_3H_6	C_2H_4	C_2H_6	CH_4	$C_{(s)}$	S_2
			$C_3H_8 : H_2S = 10.41$															
Feed	61.9	35.4	3.4															
Product	61.9	34.2	3.6	1.2	0.9	0.0	0.0	0.05	0.8	-0.1	3	-10	2	0	0	0	1	-6
													[75]	[0]	[0]	[1.3]	[23]	
			$C_3H_8 : H_2S = 4.96$															
Feed	59.9	34.6	7.0															
Product	59.9	33.1	7.3	1.1	0.9	0.0	0.0	0.0	1.9	-0.2	4	-10	2	0	0	0	2	-5
													[58]	[0]	[0]	[0]	[42]	
			$C_3H_8 : H_2S = 3.64$															
Feed	56.4	38.1	10.5															
Product	56.4	34.3	9.4	1.2	1.0	0.0	0.0	0.05	8.2	0.5	10	0	3	0	0	0	7	10
													[27]	[0]	[0]	[0.4]	[72]	

Appendix 3.4b $C_3H_8/H_2S/N_2$ Catalytic Reaction at Various Feed Compositions

Catalyst: 5% VOx/CS Contact time: 35 ms Temperature: 923 K

	Products, mole/100 moles of feed										Conversion %		Yield % [Selectivity %]					
	N_2	C_3H_8	H_2S	H_2	C_3H_6	C_2H_4	C_2H_6	CH_4	$C_{(s)}$	S_2	C_3H_8	H_2S	C_3H_6	C_2H_4	C_2H_6	CH_4	$C_{(s)}$	S_2
			$C_3H_8 : H_2S = 10.41$															
Feed	61.9	35.4	3.4															
Product	61.9	29.9	3.6	2.3	2.0	0.7	0.0	0.7	8.3	0.0	16	-5	6	1	0	1	8	1
													[37]	[8]	[0]	[4]	[50]	
			$C_3H_8 : H_2S = 4.96$															
Feed	59.9	34.6	7.0															
Product	59.9	29.6	7.2	2.9	2.5	0.8	0.0	0.9	4.8	-0.1	14	-11	7	2	0	1	5	-3
													[51]	[11]	[0]	[6]	[32]	
			$C_3H_8 : H_2S = 3.64$															
Feed	56.4	38.1	10.5															
Product	56.4	32.2	11.0	3.5	2.9	0.9	0.0	1.0	5.9	-0.3	15	-4	8	2	0	1	5	-5
													[50]	[11]	[0]	[6]	[34]	

Appendix 3.4c $C_3H_8/H_2S/N_2$ Catalytic Reaction at Various Feed Compositions

Catalyst: 5% VOx/CS Contact time: 35 ms Temperature: 1023 K

	Products, mole/100 moles of feed										Conversion %		Yield % [Selectivity %]					
	N_2	C_3H_8	H_2S	H_2	C_3H_6	C_2H_4	C_2H_6	CH_4	$C_{(s)}$	S_2	C_3H_8	H_2S	C_3H_6	C_2H_4	C_2H_6	CH_4	$C_{(s)}$	S_2
			$C_3H_8 : H_2S = 10.41$															
Feed	61.9	35.4	3.4															
Product	61.9	17.5	3.5	6.0	6.4	7.8	0.9	8.8	8.3	-0.1	51	-11	18 [36]	15 [29]	2 [3]	8 [16]	8 [15]	-4
			$C_3H_8 : H_2S = 4.96$															
Feed	59.9	34.6	7.0															
Product	59.9	15.5	7.2	6.0	7.1	8.8	0.9	9.4	7.2	-0.1	55	-11	20 [37]	17 [31]	2 [3]	9 [16]	7 [13]	-3
			$C_3H_8 : H_2S = 3.64$															
Feed	56.4	38.1	10.5															
Product	56.4	17.0	11.0	7.6	8.5	9.6	0.8	11.1	5.7	-0.3	55	-6	22 [41]	17 [30]	1 [2]	10 [18]	5 [9]	-5

Appendix 3.5a $C_3H_8/H_2S/N_2$ Catalytic Reaction at Various Contact Times

Catalyst: 5% VOx/CS Temperature: 823 K

	Products, mole/100 moles of feed										Conversion %		Yield % [Selectivity %]					
	N_2	C_3H_8	H_2S	H_2	C_3H_6	C_2H_4	C_2H_6	CH_4	$C_{(s)}$	S_2	C_3H_8	H_2S	C_3H_6	C_2H_4	C_2H_6	CH_4	$C_{(s)}$	S_2
			Contact time: 18 ms															
Feed	61.3	34.8	4.9															
Product	61.3	33.3	4.6	0.7	0.5	0.0	0.0	0.0	2.9	0.1	4	-1	1	0	0	0	3	5
													[34]	[0]	[0]	[0]	[66]	
			Contact time: 35 ms															
Feed	61.3	34.8	4.9															
Product	61.3	33.4	4.9	0.7	0.5	0.0	0.0	0.1	2.6	0.0	4	-6	1	0	0	0	2	1
													[34]	[0]	[0]	[3]	[63]	
			Contact time: 158 ms															
Feed	32.3	64.0	8.0															
Product	32.3	56.0	8.2	5.5	4.4	0.0	0.0	0.2	10.8	-0.1	13	-7	7	0	0	0	6	-3
													[55]	[0]	[0]	[0.7]	[45]	

Appendix 3.5b $C_3H_8/H_2S/N_2$ Catalytic Reaction at Various Contact Times

Catalyst: 5% VOx/CS Temperature: 923 K

	Products, mole/100 moles of feed										Conversion %		Yield % [Selectivity %]					
	N_2	C_3H_8	H_2S	H_2	C_3H_6	C_2H_4	C_2H_6	CH_4	$C_{(s)}$	S_2	C_3H_8	H_2S	C_3H_6	C_2H_4	C_2H_6	CH_4	$C_{(s)}$	S_2
			Contact time: 18 ms															
Feed	61.3	34.8	4.9															
Product	61.3	30.7	4.7	1.7	1.6	1.0	0.0	1.0	4.1	0.1	12	-3	5 [40]	2 [17]	0 [0]	1 [9]	4 [34]	4
			Contact time: 35 ms															
Feed	61.3	34.8	4.9															
Product	61.3	29.6	4.9	3.0	2.5	1.2	0.0	1.3	4.4	0.0	15	-7	7 [48]	2 [15]	0 [0]	1 [8]	4 [28]	0
			Contact time: 158 ms															
Feed	32.3	64.0	8.0															
Product	32.3	48.6	8.3	7.4	9.3	1.8	0.3	2.3	12.0	-0.2	24	-9	14 [60]	2 [8]	0 [1]	1 [5]	6 [26]	-4

Appendix 3.5c $C_3H_8/H_2S/N_2$ Catalytic Reaction at Various Contact Times

Catalyst: 5% VOx/CS Temperature: 1023 K

	Products, mole/100 moles of feed										Conversion %		Yield % [Selectivity %]					
	N_2	C_3H_8	H_2S	H_2	C_3H_6	C_2H_4	C_2H_6	CH_4	$C_{(s)}$	S_2	C_3H_8	H_2S	C_3H_6	C_2H_4	C_2H_6	CH_4	$C_{(s)}$	S_2
			Contact time: 18 ms															
Feed	61.3	34.8	4.9															
Product	61.3	15.9	4.4	6.0	6.3	7.7	0.9	9.8	10.6	0.3	54	1	18 [34]	15 [27]	2 [3]	9 [17]	10 [19]	10
			Contact time: 35 ms															
Feed	61.3	34.8	4.9															
Product	61.3	13.9	4.7	6.9	7.1	8.7	1.0	9.6	6.5	0.1	55	-8	21 [38]	17 [31]	2 [3]	9 [17]	6 [11]	4
			Contact time: 158 ms															
Feed	32.3	64.0	8.0															
Product	32.3	25.4	8.6	8.2	14.7	17.5	4.3	20.2	8.2	-0.3	60	-9	23 [38]	18 [30]	4 [7]	11 [17]	4 [7]	-9

Appendix 3.6a $C_3H_8/H_2S/N_2$ Reaction Using Catalysts with Various Amounts of Vanadium

Temperature: 823 K

	Products, mole/100 moles of feed										Conversion %		Yield % [Selectivity %]					
	N_2	C_3H_8	H_2S	H_2	C_3H_6	C_2H_4	C_2H_6	CH_4	$C_{(s)}$	S_2	C_3H_8	H_2S	C_3H_6	C_2H_4	C_2H_6	CH_4	$C_{(s)}$	S_2
	Catalyst: 1%VOx/CS				**Contact time: 42 ms**													
Feed	62.3	35.8	5.1															
Product	62.3	33.4	5.0	1.1	0.9	0.0	0.0	0.2	4.4	0.1	7	3	2	0	0	0	4	3
													[36]	[0]	[0]	[2]	[62]	
	Catalyst: 2.5% VOx/CS				**Contact time: 38 ms**													
Feed	62.3	35.8	5.1															
Product	62.3	34.8	4.7	0.5	0.3	0.0	0.0	0.0	2.2	0.2	3	7	1	0	0	0	2	7
													[29]	[0]	[0]	[0]	[70]	
	Catalyst: 10% VOx/CS				**Contact time: 36 ms**													
Feed	62.3	35.8	5.1															
Product	62.3	34.8	4.7	0.5	0.2	0.0	0.0	0.0	2.5	0.2	3	7	1	0	0	0	2	7
													[19]	[0]	[0]	[1]	[80]	

Appendix 3.6b $C_3H_8/H_2S/N_2$ Reaction Using Catalysts with Various Amounts of Vanadium

Temperature: 923 K

	Products, mole/100 moles of feed										Conversion %		Yield % [Selectivity %]					
	N_2	C_3H_8	H_2S	H_2	C_3H_6	C_2H_4	C_2H_6	CH_4	$C_{(s)}$	S_2	C_3H_8	H_2S	C_3H_6	C_2H_4	C_2H_6	CH_4	$C_{(s)}$	S_2
	Catalyst: 1%VOx/CS				**Contact time: 42 ms**													
Feed	62.3	35.8	5.1															
Product	62.3	29.7	5.0	3.5	3.0	1.3	0.0	1.4	5.4	0.1	17	2	8	2	0	1	5	2
													[49]	[14]	[0]	[8]	[29]	
	Catalyst: 2.5% VOx/CS				**Contact time: 38 ms**													
Feed	62.3	35.8	5.1															
Product	62.3	33.1	4.8	2.3	1.5	0.8	0.0	0.9	0.9	0.2	8	6	4	2	0	1	1	6
													[58]	[20]	[0]	[11]	[11]	
	Catalyst: 10% VOx/CS				**Contact time: 36 ms**													
Feed	62.3	35.8	5.1															
Product	62.3	33.8	4.8	1.4	1.0	0.7	0.0	0.7	0.8	0.1	6	4	3	1	0	1	1	4
													[51]	[23]	[0]	[12]	[14]	

Appendix 3.6c $C_3H_8/H_2S/N_2$ Reaction Using Catalysts with Various Amounts of Vanadium

Temperature: 1023 K

					Products, mole/100 moles of feed						Conversion %		Yield % [Selectivity %]					
	N_2	C_3H_8	H_2S	H_2	C_3H_6	C_2H_4	C_2H_6	CH_4	$C_{(s)}$	S_2	C_3H_8	H_2S	C_3H_6	C_2H_4	C_2H_6	CH_4	$C_{(s)}$	S_2
	Catalyst: 1%VOx/CS				**Contact time: 42 ms**													
Feed	62.3	35.8	5.1															
Product	62.3	15.7	4.7	6.2	6.6	8.1	0.9	8.9	13.6	0.2	56	9	18	15	2	8	13	9
													[33]	[27]	[3]	[15]	[23]	
	Catalyst: 2.5% VOx/CS				**Contact time: 38 ms**													
Feed	62.3	35.8	5.1															
Product	62.3	17.6	4.7	7.0	7.2	7.7	0.7	8.6	7.5	0.1	51	4	20	14	1	8	7	4
													[40]	[28]	[2]	[16]	[14]	
	Catalyst: 10% VOx/CS				**Contact time: 36 ms**													
Feed	62.3	35.8	5.1															
Product	62.3	19.1	4.8	6.7	6.8	7.3	0.6	8.3	5.5	0.1	47	4	19	14	1	8	5	4
													[41]	[29]	[2]	[17]	[11]	

Appendix 4.1 Equilibrium calculations for the reaction of H_2S and O_2, calculated using GASEQ

Feed ratio	Adiabatic T (K)		O_2 conversion		H_2S conversion		H_2 yield		SO_2 yield		S_2 yield		H_2O yield	
$H_2S:O_2$	923°K	1023°K	923°K	1023°K	923°K	1023°K	923°K	1023°K	923°K	1023°K	923°K	1023°K	923°K	1023°K
1:1	2551	2630	99.91	99.84	98.85	98.94	34.80	36.85	67.88	68.79	30.97	30.15	32.03	31.05
2:1	1904	1978	100.00	100.00	93.23	93.97	27.03	29.97	16.88	17.98	76.34	75.99	66.22	64.02
3:1	1603	1673	100.00	100.00	82.25	84.54	22.67	26.04	3.54	4.08	78.70	80.46	89.37	87.76
4:1	1441	1506	100.00	100.00	68.12	71.78	19.80	23.74	0.84	0.98	67.28	70.80	96.63	96.08

Note: total moles in the feed used was 100 moles. N_2 was kept at 60 moles and the other 40 were split according to the ratio used.

Appendix 4.2a Equilibrium calculations for the reaction between C_3H_8 and O_2 at different feed ratios, calculated without allowing $C_{(s)}$ as a product

Feed ratio C_3H_8:O_2	Temperature °K	Feed (moles/100 moles)			Conversion %		Product (moles/100 moles) [Selectivity %]							
		N_2	C_3H_8	O_2	C_3H_8	O_2	C_3H_6	C_2H_4	C_2H_6	CH_4	CO	CO_2	H_2O	H_2
2:1	923	33.00	44.66	22.33	100.00	100.00	0.22 [0.486]	16.09 [24.01]	0.14 [0.21]	56.20 [41.95]	44.66 [33.3]	0.00 [0]	0.00	32.98
4:1	923	33.00	53.10	13.30	99.98	100.00	1.29 [2.428]	26.55 [33.33]	0.45 [0.56]	74.48 [46.76]	26.60 [16.7]	0.00 [0]	0.00	4.77
2:1	1023	33.00	44.66	22.33	100.00	100.00	0.23 [0.515]	18.58 [27.74]	0.12 [0.18]	51.19 [38.21]	44.66 [33.3]	0.00 [0]	0.00	38.00
4:1	1023	33.00	53.10	13.30	99.99	100.00	1.04 [1.963]	28.79 [36.15]	0.36 [0.46]	71.03 [44.59]	26.60 [16.7]	0.00 [0]	0.00	8.30

Note: selectivities are based on carbon, therefore, show product distribution according to % of overall carbon used on that product

Appendix 4.2b Equilibrium calculations for the reaction between C_3H_8 and O_2 at different feed ratios, calculated while allowing $C_{(s)}$ as a product

C_3H_8: O_2 ratio	Temperature °K	Feed (moles/100 moles)			Conversion %		Products (moles/100 moles) [Selectivity %]								
		N_2	C_3H_8	O_2	C_3H_8	O_2	C_3H_6	C_2H_4	C_2H_6	CH_4	CO	CO_2	$C_{(s)}$	H_2O	H_2
2-1	923	33.00	44.66	22.33	100.00	100.00	0.00 [2E-08]	0.00 [1E-04]	0.00 [0]	7.51 [5.6]	35.23 [26.3]	1.73 [1.29]	89.52 [66.82]	5.98	157.64
4-1	923	33.00	53.10	13.30	100.00	100.00	0.00 [1E-08]	0.00 [5E-05]	0.00 [0]	23.13 [14.5]	11.79 [7.4]	1.74 [1.09]	122.63 [76.98]	11.33	154.81
2-1	1023	33.00	44.66	22.33	100.00	100.00	0.00 [2E-08]	0.00 [1E-04]	0.00 [0]	5.51 [4.11]	38.75 [28.9]	1.03 [0.77]	88.70 [66.2]	3.86	163.77
4-1	1023	33.00	53.10	13.30	100.00	100.00	0.00 [2E-08]	0.00 [7E-05]	0.00 [0]	18.64 [11.7]	14.78 [9.28]	1.42 [0.89]	124.46 [78.13]	8.98	166.13

Note: selectivities are based on carbon, therefore showing product distribution according to % of overall carbon used on that product

Appendix 4.3a Equilibrium calculations for the reaction between C_3H_8, H_2S and O_2 at different feed ratios, calculated without allowing $C_{(s)}$ as a product

Feed ratio C_3H_8:H_2S:O_2	Temperature (°K)		Feed, mole/100 moles of feed				Conversion %			Products, mole/100 moles of feed [Selectivity %]											
	Initial	Adiabatic	N_2	C_3H_8	H_2S	O_2	C_3H_8	O_2	H_2S	C_3H_6	C_2H_4	C_2H_6	CH_4	CO	CO_2	CS_2	COS	SO_2	S_2	H_2O	H_2
4:2:1	923	1133.3	33.00	38.29	19.14	9.57	100.00	100.00	95.27	0.15 [0.39]	6.96 [12.11]	0.20 [0.36]	71.85 [62.55]	19.10 [16.6]	4.89E-05 [4E-05]	9.10 [31.67]	0.04 [0.15]	1.4E-16	5.6E-04	4.3E-02	12.71
4:2:2	923	1247.9	33.00	33.50	16.75	16.75	100.00	100.00	87.52	0.03 [0.1]	3.89 [7.75]	0.08 [0.15]	51.66 [51.4]	33.44 [33.3]	1.18E-04 [1E-04]	7.30 [29.05]	0.06 [0.24]	4.1E-15	2.1E-03	2.0E-04	37.22
8:3:1	923	945.3	13.42	60.56	18.58	6.76	99.93	100.00	99.63	2.90 [4.79]	23.33 [25.71]	1.03 [1.14]	99.76 [54.95]	13.49 [7.43]	2.30E-05 [1E-05]	9.24 [20.36]	0.03 [0.07]	1.4E-19	1.2E-05	9.2E-07	1.00
4:2:1	1023	1180.7	33.00	38.29	19.14	9.57	100.00	100.00	95.15	0.17 [0.45]	9.03 [15.72]	0.19 [0.33]	67.67 [58.91]	19.11 [16.6]	2.94E-05 [3E-05]	9.09 [31.65]	0.03 [0.12]	1.4E-16	7.2E-04	3.4E-02	16.87
4:2:2	1023	1292.2	33.00	33.50	16.75	16.75	100.00	100.00	89.58	0.05 [0.15]	5.65 [11.25]	0.08 [0.15]	47.92 [47.68]	33.45 [33.3]	6.55E-05 [7E-05]	7.48 [29.76]	0.05 [0.18]	2.5E-15	2.2E-03	1.4E-04	41.49
8:3:1	1023	1025.2	13.42	60.56	18.58	6.76	99.96	100.00	99.23	1.96 [3.24]	26.27 [28.93]	0.76 [0.84]	98.20 [54.07]	13.50 [7.43]	1.31E-05 [7E-06]	9.21 [20.28]	0.02 [0.05]	6.1E-19	4.1E-05	2.0E-06	2.73

Note: selectivities are based on carbon, therefore showing product distribution according to % of overall carbon used on that product

Appendix 4.3b Equilibrium calculations for the reaction between C_3H_8, H_2S and O_2 at different feed ratios, calculated while allowing $C_{(s)}$ as a product

Feed Ratio C_3H_8:H_2S:O_2	Temperature (°K)		Feed, mole/100 moles of feed				Conversion %			Products, mole/100 moles of feed [Selectivity %]												
	Initial	Adiabatic	N_2	C_3H_8	H_2S	O_2	C_3H_8	O_2	H_2S	C_3H_6	C_2H_4	C_2H_6	CH_4	CO	CO_2	CS_2	COS	$C_{(s)}$	SO_2	S_2	H_2	H_2O
4:2:1	923	919	33.00	38.29	19.14	9.57	100.00	100.00	0.24	0.00 [9.9E-09]	0.00 [4E-05]	0.00 [3E-04]	16.07 [13.99]	8.44 [7.35]	1.27 [1.11]	0.00 [0.001]	0.05 [0.16]	89.05 [77.52]	1.1E-09	4.4E-05	112.96	8.11
4:2:2	923	1016.8	33.00	33.50	16.75	16.75	100.00	100.00	0.72	0.00 [1.2E-08]	0.00 [9E-05]	0.00 [1E-04]	5.54 [5.514]	26.06 [25.9]	1.36 [1.36]	0.00 [0.009]	0.12 [0.46]	67.42 [67.08]	4.4E-09	3.0E-04	118.44	4.60
8:3:1	923	860.5	13.42	60.56	18.58	6.76	100.00	100.00	0.06	0.00 [8.6E-09]	0.00 [3E-05]	0.00 [7E-04]	46.50 [25.59]	2.80 [1.54]	0.56 [0.31]	0.00 [1E-04]	0.01 [0.03]	131.81 [72.55]	1.2E-10	6.5E-06	139.66	9.60
4:2:1	1023	949.2	33.00	38.29	19.14	9.57	100.00	100.00	0.29	0.00 [1.2E-08]	0.00 [6E-05]	0.00 [2E-04]	12.55 [10.93]	10.86 [9.45]	1.00 [0.87]	0.00 [0.002]	0.05 [0.19]	90.40 [78.7]	1.3E-09	3.0E-04	121.88	6.22
4:2:2	1023	1056.6	33.00	33.50	16.75	16.75	100.00	100.00	0.80	0.00 [1.3E-08]	0.00 [0.0001]	0.00 [7E-05]	3.95 [3.93]	28.97 [28.8]	0.77 [0.77]	0.00 [0.019]	0.12 [0.49]	66.67 [66.34]	4.2E-09	6.3E-04	123.38	2.85
8:3:1	1023	887.9	13.42	60.56	18.58	6.76	100.00	100.00	0.09	0.00 [1.1E-08]	0.00 [4E-05]	0.00 [6E-04]	38.54 [21.21]	4.06 [2.23]	0.54 [0.29]	0.00 [2E-04]	0.02 [0.03]	138.53 [76.25]	1.8E-10	1.2E-05	156.80	8.37

Note: selectivities are based on carbon, therefore showing product distribution according to % of overall carbon used on that product

Appendix 4.4a $C_3H_8/O_2/N_2$ Gas Phase Reactions at Various Feed Ratios

Reactor: empty (void space) Residence time: 20 ms Temperature: 923 K

	Products, mole/100 moles of feed												Conversion %		Yield % [Selectivity %]							
	N_2	C_3H_8	O_2	H_2	C_3H_6	C_2H_4	C_2H_6	CH_4	CO	CO_2	$C_{(s)}$	H_2O	C_3H_8	O_2	C_3H_6	C_2H_4	C_2H_6	CH_4	CO	CO_2	$C_{(s)}$	H_2O
		Feed ratio: 4:1																				
Feed	33.0	53.1	13.3																			
Product	33.0	43.1	10.3	0.7	1.3	2.4	0.0	1.6	0.4	0.5	18.6	4.7	19	23	2	3	0	1	0	0	12	18
															[13]	[17]	[0]	[5]	[1]	[2]		
		Feed ratio: 2:1																				
Feed	33.0	44.7	22.3																			
Product	33.0	28.5	15.7	1.7	3.5	5.1	0.2	3.7	1.7	0.4	21.7	10.9	36	30	8	8	0	3	1	0	16	24
															[21]	[20]	[1]	[7]	[3]	[1]		

Appendix 4.4b $C_3H_8/O_2/N_2$ Gas Phase Reactions at Various Feed Ratios

Reactor: empty (void space) Residence time: 20 ms Temperature: 1023 K

	Products, mole/100 moles of feed												Conversion %		Yield % [Selectivity %]							
	N_2	C_3H_8	O_2	H_2	C_3H_6	C_2H_4	C_2H_6	CH_4	CO	CO_2	$C_{(s)}$	H_2O	C_3H_8	O_2	C_3H_6	C_2H_4	C_2H_6	CH_4	CO	CO_2	$C_{(s)}$	H_2O
		Feed ratio: 4:1																				
Feed	33.0	53.1	13.3																			
Product	33.0	26.7	2.3	5.7	5.4	10.6	0.7	9.0	5.1	1.5	25.0	13.9	50	83	10	13	1	6	3	1	16	52
															[21]	[27]	[2]	[11]	[6]	[2]		
		Feed ratio: 2:1																				
Feed	33.0	44.7	22.3																			
Product	33.0	12.6	3.9	6.7	5.8	13.9	0.9	11.5	10.1	2.2	25.6	22.2	72	82	13	21	1	9	8	2	19	50
															[18]	[29]	[2]	[12]	[10]	[2]		

Appendix 4.5a $C_3H_8/H_2S/O_2/N_2$ Gas Phase Reactions with and without H_2S

Reactor: Empty (void space) Contact time: 20 ms Temperature: 923 K

	Products, mole/100 moles of feed														Conversion %			Yield % [Selectivity %]								
	N_2	C_3H_8	H_2S	O_2	H_2	C_3H_6	C_2H_4	C_2H_6	CH_4	CO	CO_2	$C_{(s)}$	S_2	H_2O	C_3H_8	O_2	H_2S	C_3H_6	C_2H_4	C_2H_6	CH_4	CO	CO_2	$C_{(s)}$	S_2	H_2O
		Feed ratio: 4:1 (C_3H_8: O_2)																								
Feed	33.0	53.1	0.0	13.3																						
Product	33.0	43.1	0.0	10.3	0.7	1.3	2.4	0.0	1.6	0.4	0.5	18.6	0.0	4.7	19	23	0	2	3	0	1	0	0	12	0	18
																		[13]	[17]	[0]	[5]	[1]	[2]			
		Feed ratio: 4:2:1 (C_3H_8: H_2S: O_2)																								
Feed	33.0	38.3	19.1	9.6																						
Product	33.0	23.9	7.9	1.9	1.9	5.1	4.5	0.2	5.0	1.2	0.0	12.4	5.6	14.2	38	80	59	13	8	0	4	1	0	11	59	74
																		[35]	[21]	[1]	[11]	[3]	[0]			

Appendix 4.5b $C_3H_8/H_2S/O_2/N_2$ Gas Phase Reactions with and without H_2S

Reactor: Empty (void space) Contact time: 20 ms Temperature: 973 K

	Products, mole/100 moles of feed														Conversion %			Yield % [Selectivity %]								
	N_2	C_3H_8	H_2S	O_2	H_2	C_3H_6	C_2H_4	C_2H_6	CH_4	CO	CO_2	$C_{(s)}$	S_2	H_2O	C_3H_8	O_2	H_2S	C_3H_6	C_2H_4	C_2H_6	CH_4	CO	CO_2	$C_{(s)}$	S_2	H_2O
		Feed ratio: 4:1 (C_3H_8: O_2)																								
Feed	33.0	53.1	0.0	13.3																						
Product	33.0	33.5	0.0	5.6	2.9	4.2	7.0	0.3	5.6	2.2	0.8	22.9	0.0	11.7	37	58	0	8 [22]	9 [24]	0 [1]	4 [9]	1 [4]	0 [1]	14	0	44
		Feed ratio: 4:2:1 (C_3H_8: H_2S: O_2)																								
Feed	33.0	38.3	19.1	9.6																						
Product	33.0	19.3	8.0	1.4	3.2	6.7	6.8	0.3	7.5	1.6	0.0	13.5	5.6	14.6	50	85	58	18 [35]	12 [24]	1 [1]	6 [13]	1 [3]	0 [0]	12	58	76

Appendix 4.5c $C_3H_8/H_2S/O_2/N_2$ Gas Phase Reactions with and without H_2S

Reactor: Empty (void space) Contact time: 20 ms Temperature: 1023 K

	Products, mole/100 moles of feed														Conversion %			Yield % [Selectivity %]								
	N_2	C_3H_8	H_2S	O_2	H_2	C_3H_6	C_2H_4	C_2H_6	CH_4	CO	CO_2	$C_{(s)}$	S_2	H_2O	C_3H_8	O_2	H_2S	C_3H_6	C_2H_4	C_2H_6	CH_4	CO	CO_2	$C_{(s)}$	S_2	H_2O
		Feed ratio: 4:1 (C_3H_8: O_2)																							
Feed	33.0	53.1	0.0	13.3																					
Product	33.0	26.7	0.0	2.3	5.7	5.4	10.6	0.7	9.0	5.1	1.5	25.0	0.0	13.9	50	83	0	10 [21]	13 [27]	1 [2]	6 [11]	3 [6]	1 [2]	16	0	52
		Feed ratio: 4:2:1 (C_3H_8: H_2S: O_2)																							
Feed	33.0	38.3	19.1	9.6																					
Product	33.0	14.5	7.6	0.8	4.6	8.9	8.9	0.5	9.8	1.8	0.1	14.2	5.7	15.7	62	92	60	23 [37]	15 [25]	1 [1]	9 [14]	2 [2]	0 [0]	12	60	82

Appendix 4.6a $C_3H_8/H_2S/O_2/N_2$ Gas Phase Reactions with and without H_2S

Reactor: Empty (void space) Contact time: 20 ms Temperature: 923 K

	Products, mole/100 moles of feed														Conversion %			Yield % [Selectivity %]								
	N_2	C_3H_8	H_2S	O_2	H_2	C_3H_6	C_2H_4	C_2H_6	CH_4	CO	CO_2	$C_{(s)}$	S_2	H_2O	C_3H_8	O_2	H_2S	C_3H_6	C_2H_4	C_2H_6	CH_4	CO	CO_2	$C_{(s)}$	S_2	H_2O
		Feed ratio: 2:1 (C_3H_8: O_2)																								
Feed	33.0	44.7	0.0	22.3																						
Product	33.0	28.5	0.0	21.7	1.7	3.5	5.1	0.2	3.7	1.7	0.4	21.7	0.0	10.9	36	30	0	8	8	0	3	1	0	16	0	24
																		[21]	[20]	[1]	[7]	[3]	[1]	[47]		
		Feed ratio: 4:2:2 (C_3H_8: H_2S: O_2)																								
Feed	33.0	33.5	16.8	16.8																						
Product	33.0	16.9	2.7	4.5	2.2	8.4	5.6	0.3	5.8	2.3	0.2	4.5	7.0	27.7	50	91	84	25	11	1	6	2	0	4	84	83
																		[51]	[22]	[1]	[12]	[5]	[0]	[9]		

Appendix 4.6b $C_3H_8/H_2S/O_2/N_2$ Gas Phase Reactions with and without H_2S

Reactor: Empty (void space) Contact time: 20 ms Temperature: 973 K

	Products, mole/100 moles of feed														Conversion %			Yield % [Selectivity %]								
	N_2	C_3H_8	H_2S	O_2	H_2	C_3H_6	C_2H_4	C_2H_6	CH_4	CO	CO_2	$C_{(s)}$	S_2	H_2O	C_3H_8	O_2	H_2S	C_3H_6	C_2H_4	C_2H_6	CH_4	CO	CO_2	$C_{(s)}$	S_2	H_2O
		Feed ratio: 2:1 (C_3H_8: O_2)																								
Feed	33.0	44.7	0.0	22.3																						
Product	33.0	19.0	0.0	23.8	5.6	5.4	9.6	0.5	7.6	7.7	1.8	23.8	0.0	19.7	58	70	0	12	14	1	6	6	1	18	0	44
																		[21]	[25]	[1]	[10]	[10]	[2]	[31]		
		Feed ratio: 4:2:2 (C_3H_8: H_2S: O_2)																								
Feed	33.0	33.5	16.8	16.8																						
Product	33.0	13.2	2.9	5.1	3.2	9.7	7.3	0.4	7.8	2.9	0.2	5.1	6.9	27.9	61	93	83	29	15	1	8	3	0	5	83	83
																		[48]	[24]	[1]	[13]	[5]	[0]	[8]		

Appendix 4.6c $C_3H_8/H_2S/O_2/N_2$ Gas Phase Reactions with and without H_2S

Reactor: Empty (void space) Contact time: 20 ms Temperature: 1023 K

	Products, mole/100 moles of feed														Conversion %			Yield % [Selectivity %]								
	N_2	C_3H_8	H_2S	O_2	H_2	C_3H_6	C_2H_4	C_2H_6	CH_4	CO	CO_2	$C_{(s)}$	S_2	H_2O	C_3H_8	O_2	H_2S	C_3H_6	C_2H_4	C_2H_6	CH_4	CO	CO_2	$C_{(s)}$	S_2	H_2O
	Feed ratio: 2:1 (C_3H_8: O_2)																									
Feed	33.0	44.7	0.0	22.3																						
Product	33.0	12.6	0.0	25.6	6.7	5.8	13.9	0.9	11.5	10.1	2.2	25.6	0.0	22.2	72	82	0	13	21	1	9	8	2	19	0	50
																		[18]	[29]	[2]	[12]	[10]	[2]	[27]		
	Feed ratio: 4:2:2 (C_3H_8: H_2S: O_2)																									
Feed	33.0	33.5	16.8	16.8																						
Product	33.0	10.7	2.4	4.6	4.3	11.0	8.7	0.5	9.3	2.7	0.2	4.6	7.2	28.6	68	95	86	33	17	1	9	3	0	5	86	86
																		[49]	[25]	[2]	[14]	[4]	[0]	[7]		

Appendix 4.7a $C_3H_8/H_2S/O_2/N_2$ Gas Phase Reactions: Comparisons Between an Empty Reactor and a Reactor Containing Quartz Chips

Feed ratio: 4:2:2: (C_3H_8: H_2S: O_2) Contact time: 20 ms Temperature: 923 K

	Products, mole/100 moles of feed														Conversion %			Yield % [Selectivity %]								
	N_2	C_3H_8	H_2S	O_2	H_2	C_3H_6	C_2H_4	C_2H_6	CH_4	CO	CO_2	$C_{(s)}$	S_2	H_2O	C_3H_8	O_2	H_2S	C_3H_6	C_2H_4	C_2H_6	CH_4	CO	CO_2	$C_{(s)}$	S_2	H_2O
		empty tube																								
Feed	33.0	33.5	16.8	16.8																						
Product	33.0	16.9	2.7	1.6	2.2	8.4	5.6	0.3	5.8	2.3	0.2	4.5	7.0	27.7	50	91	84	25 [51]	11 [22]	1 [1]	6 [12]	2 [5]	0 [0]	4	84	83
		quartz chips																								
Feed	33.0	33.5	16.8	16.8																						
Product	33.0	14.4	3.9	3.3	3.3	9.1	7.0	0.4	7.8	2.8	0.2	4.3	6.4	23.8	57	80	77	27 [48]	14 [24]	1 [1]	8 [14]	3 [5]	0 [0]	4	77	71

Appendix 4.7b $C_3H_8/H_2S/O_2/N_2$ Gas Phase Reactions: Comparisons Between an Empty Reactor and a Reactor Containing Quartz Chips

Feed ratio: 4:2:2: (C_3H_8: H_2S: O_2) Contact time: 20 ms Temperature: 1023 K

	Products, mole/100 moles of feed														Conversion %			Yield % [Selectivity %]								
	N_2	C_3H_8	H_2S	O_2	H_2	C_3H_6	C_2H_4	C_2H_6	CH_4	CO	CO_2	$C_{(s)}$	S_2	H_2O	C_3H_8	O_2	H_2S	C_3H_6	C_2H_4	C_2H_6	CH_4	CO	CO_2	$C_{(s)}$	S_2	H_2O
		empty tube																								
Feed	33.0	33.5	16.8	16.8																						
Product	33.0	10.7	2.4	0.9	4.3	11.0	8.7	0.5	9.3	2.7	0.2	4.6	7.2	28.6	68	95	86	33	17	1	9	3	0	5	86	86
																		[49]	[25]	[2]	[14]	[4]	[0]			
		quartz chips																								
Feed	33.0	33.5	16.8	16.8																						
Product	33.0	8.7	4.0	1.9	5.2	11.3	9.5	0.6	10.3	3.3	0.4	6.3	6.4	25.7	74	89	76	34	19	1	10	3	0	6	76	77
																		[46]	[25]	[2]	[14]	[4]	[1]			

Appendix 4.8a $C_3H_8/H_2S/O_2/N_2$ Gas Phase Reactions with and without H_2S

Catalyst: Quartz chips Residence time: 5 ms Temperature: 923 K

	Products, mole/100 moles of feed														Conversion %			Yield % [Selectivity %]								
	N_2	C_3H_8	H_2S	O_2	H_2	C_3H_6	C_2H_4	C_2H_6	CH_4	CO	CO_2	$C_{(s)}$	S_2	H_2O	C_3H_8	O_2	H_2S	C_3H_6	C_2H_4	C_2H_6	CH_4	CO	CO_2	$C_{(s)}$	S_2	H_2O
		Feed ratio: 4:1 (C_3H_8: O_2)																							
Feed	33.0	53.1	0.0	13.3																					
Product	33.0	18.1	0.0	2.6	3.5	5.5	10.0	0.7	7.3	4.6	0.2	54.8	0.0	16.5	66	80	0	10	12	1	5	3	0	34	0	62
																		[16]	[19]	[1]	[7]	[4]	[0]			
		Feed ratio: 4:2:1 (C_3H_8: H_2S: O_2)																							
Feed	33.0	38.3	19.1	9.6																					
Product	33.0	21.2	8.7	2.1	2.8	5.9	6.2	0.3	6.9	1.4	0.0	12.3	5.2	13.6	45	79	55	15	11	1	6	1	0	11	55	71
																		[34]	[24]	[1]	[13]	[3]	[0]			

Appendix 4.8b $C_3H_8/H_2S/O_2/N_2$ Gas Phase Reactions with and without H_2S

Catalyst: Quartz chips Residence time: 5 ms Temperature: 973 K

	Products, mole/100 moles of feed														Conversion %			Yield % [Selectivity %]								
	N_2	C_3H_8	H_2S	O_2	H_2	C_3H_6	C_2H_4	C_2H_6	CH_4	CO	CO_2	$C_{(s)}$	S_2	H_2O	C_3H_8	O_2	H_2S	C_3H_6	C_2H_4	C_2H_6	CH_4	CO	CO_2	$C_{(s)}$	S_2	H_2O
		Feed ratio: 4:1 (C_3H_8: O_2)																								
Feed	33.0	53.1	0.0	13.3																						
Product	33.0	14.6	0.0	1.7	4.7	6.1	12.4	1.0	9.5	5.7	0.1	55.2	0.0	17.3	72	87	0	11	16	1	6	4	<1	35	0	65
																		[16]	[21]	[2]	[8]	[5]	[<1]			
		Feed ratio: 4:2:1 (C_3H_8: H_2S: O_2)																								
Feed	33.0	38.3	19.1	9.6																						
Product	33.0	16.3	8.8	1.8	4.2	7.6	8.2	0.5	9.2	1.8	0.0	14.7	5.1	13.8	57	82	54	20	14	1	8	2	<1	13	54	72
																		[35]	[25]	[1]	[14]	[3]	[<1]			

Appendix 4.8c $C_3H_8/H_2S/O_2/N_2$ Gas Phase Reactions with and without H_2S

Catalyst: Quartz chips Residence time: 5 ms Temperature: 1023 K

	Products, mole/100 moles of feed														Conversion %			Yield % [Selectivity %]								
	N_2	C_3H_8	H_2S	O_2	H_2	C_3H_6	C_2H_4	C_2H_6	CH_4	CO	CO_2	$C_{(s)}$	S_2	H_2O	C_3H_8	O_2	H_2S	C_3H_6	C_2H_4	C_2H_6	CH_4	CO	CO_2	$C_{(s)}$	S_2	H_2O
		Feed ratio: 4:1 (C_3H_8: O_2)																							
Feed	33.0	53.1	0.0	13.3																					
Product	33.0	13.2	0.0	1.8	6.1	6.6	15.1	1.0	12.3	6.3	0.2	49.0	0.0	16.4	75	87	0	12	19	1	8	4	<1	31	0	62
																		[17]	[25]	[2]	[10]	[5]	[<1]			
		Feed ratio: 4:2:1 (C_3H_8: H_2S: O_2)																							
Feed	33.0	38.3	19.1	9.6																					
Product	33.0	11.1	8.7	1.4	5.8	9.9	10.7	0.7	12.1	2.1	0.2	14.5	5.2	13.8	71	86	54	26	19	1	11	2	<1	13	54	72
																		[37]	[26]	[2]	[15]	[3]	[<1]			

Appendix 4.9a $C_3H_8/H_2S/O_2/N_2$ Gas Phase Reactions with and without H_2S

Catalyst: Quartz chips Residence time: 10 ms Temperature: 923 K

	Products, mole/100 moles of feed														Conversion %			Yield % [Selectivity %]								
	N_2	C_3H_8	H_2S	O_2	H_2	C_3H_6	C_2H_4	C_2H_6	CH_4	CO	CO_2	$C_{(s)}$	S_2	H_2O	C_3H_8	O_2	H_2S	C_3H_6	C_2H_4	C_2H_6	CH_4	CO	CO_2	$C_{(s)}$	S_2	H_2O
	Feed ratio: 2:1 (C_3H_8: O_2)																								
Feed	33.0	44.7	0.0	22.3																					
Product	33.0	16.9	0.0	6.5	4.8	6.6	13.5	0.9	9.7	7.4	0.3	17.2	0.0	23.8	62	71	0	15	20	1	7	6	<1	13	0	53
																		[24]	[32]	[2]	[12]	[9]	[<1]	[21]		
	Feed ratio: 4:2:2 (C_3H_8: H_2S: O_2)																								
Feed	33.0	33.5	16.8	16.8																					
Product	33.0	13.6	4.2	2.8	3.5	10.0	6.9	0.3	7.5	2.5	0.1	-3.0	6.3	25.2	60	83	75	30	14	1	7	3	<1	-3	75	75
																		[50]	[23]	[1]	[13]	[4]	[<1]	-[5]		

Appendix 4.9b $C_3H_8/H_2S/O_2/N_2$ Gas Phase Reactions with and without H_2S

Catalyst: Quartz chips Residence time: 10 ms Temperature: 1023 K

	Products, mole/100 moles of feed														Conversion %			Yield % [Selectivity %]								
	N_2	C_3H_8	H_2S	O_2	H_2	C_3H_6	C_2H_4	C_2H_6	CH_4	CO	CO_2	$C_{(s)}$	S_2	H_2O	C_3H_8	O_2	H_2S	C_3H_6	C_2H_4	C_2H_6	CH_4	CO	CO_2	$C_{(s)}$	S_2	H_2O
	Feed ratio: 2:1 (C_3H_8: O_2)																									
Feed	33.0	44.7	0.0	22.3																						
Product	0.0	8.8	0.0	4.2	7.2	6.5	18.7	1.1	15.9	10.9	0.6	20.9	0.0	24.1	80	81	0	15	28	2	12	8	0	16	0	54
																		[18]	[35]	[2]	[15]	[10]	[1]	[19]		
	Feed ratio: 4:2:2 (C_3H_8: H_2S: O_2)																									
Feed	33.0	33.5	16.8	16.8																						
Product	0.0	7.6	6.6	1.6	5.1	12.1	9.4	0.6	10.1	2.9	0.5	-2.6	5.1	26.5	77	91	61	36	19	1	10	3	0	-3	61	79
																		[47]	[24]	[1]	[13]	[4]	[1]	-[3]		

Appendix 4.10a $C_3H_8/H_2S/O_2/N_2$ Gas Phase Reactions at Various Contact Times

Catalyst: Crystalline silica Feed ratio: 8:4:1 (C_3H_8: H_2S: O_2) Temperature: 923 K

	Products, mole/100 moles of feed														Conversion %			Yield % [Selectivity %]								
	N_2	C_3H_8	H_2S	O_2	H_2	C_3H_6	C_2H_4	C_2H_6	CH_4	CO	CO_2	$C_{(s)}$	S_2	H_2O	C_3H_8	O_2	H_2S	C_3H_6	C_2H_4	C_2H_6	CH_4	CO	CO_2	$C_{(s)}$	S_2	H_2O
		Contact time: 12 ms																								
Feed	20.5	58.1	16.3	8.5																						
Product	20.5	51.5	15.5	0.4	2.2	3.4	3.7	0.0	3.8	0.8	1.5	-3.8	0.4	12.2	11	95	7	6	4	0	2	0	1	-2	0	72
																		[56]	[40]	[0]	[21]	[5]	[8]			
		Contact time: 60 ms																								
Feed	20.5	58.1	16.3	8.5																						
Product	20.5	46.7	15.3	0.7	2.6	4.9	4.3	0.0	4.5	0.6	1.3	4.9	0.5	12.1	20	92	6	8	5	0	3	0	1	3	1	71
																		[42]	[25]	[0]	[13]	[2]	[5]			
		Contact time: 120 ms																								
Feed	20.5	58.1	16.3	8.5																						
Product	20.5	45.2	15.5	0.2	2.3	5.4	4.1	0.0	4.3	0.6	0.7	8.9	0.4	14.4	22	98	5	9	5	0	2	0	0	5	0	85
																		[42]	[21]	[0]	[11]	[2]	[2]			

Appendix 4.10b $C_3H_8/H_2S/O_2/N_2$ Gas Phase Reactions at Various Contact Times

Catalyst: Crystalline silica Feed ratio: 8:4:1 (C_3H_8: H_2S: O_2) Temperature: 1023 K

	Products, mole/100 moles of feed														Conversion %			Yield % [Selectivity %]							
	N_2	C_3H_8	H_2S	O_2	H_2	C_3H_6	C_2H_4	C_2H_6	CH_4	CO	CO_2	$C_{(s)}$	S_2	H_2O	C_3H_8	O_2	H_2S	C_3H_6	C_2H_4	C_2H_6	CH_4	CO	CO_2	$C_{(s)}$	S_2	H_2O
		Contact time: 12 ms																							
Feed	20.5	58.1	16.3	8.5																					
Product	20.5	14.5	16.0	0.6	7.7	16.4	20.9	2.2	24.3	0.5	1.9	8.3	0.2	11.4	75	93	4	28	24	3	14	0	1	5	2	67
																		[38]	[32]	[3]	[19]	[0]	[1.5]			
		Contact time: 60 ms																							
Feed	20.5	58.1	16.3	8.5																					
Product	20.5	14.5	15.0	0.8	7.3	14.8	18.8	2.0	21.7	0.4	1.7	21.2	0.6	11.3	75	90	5	26	22	2	12	0	1	12	8	66
																		[34]	[29]	[3]	[17]	[0]	[1.3]			
		Contact time: 120 ms																							
Feed	20.5	58.1	16.3	8.5																					
Product	20.5	14.6	13.9	0.2	7.9	13.8	16.4	1.8	19.0	0.5	0.5	32.7	1.2	14.4	75	98	14	24	19	2	11	0	0	19	14	84
																		[32]	[25]	[3]	[15]	[0]	[0.3]			

Appendix 4.11 Reaction of C_3H_8, H_2S and O_2 over a catalyst bed

Catalyst: 1% VO_x/CS Feed ratio: 4:2:1 (C_3H_8: H_2S: O_2) Contact time: 36 ms

	Products, mole/100 moles of feed														Conversion %			Yield % [Selectivity %]								
	N_2	C_3H_8	H_2S	O_2	H_2	C_3H_6	C_2H_4	C_2H_6	CH_4	CO	CO_2	$C_{(s)}$	S_2	H_2O	C_3H_8	O_2	H_2S	C_3H_6	C_2H_4	C_2H_6	CH_4	CO	CO_2	$C_{(s)}$	S_2	H_2O
						T= 973 K																				
Feed	11.6	58.5	17.7	12.9																						
Product	11.6	41.9	11.4	0.2	4.2	8.3	6.9	0.4	6.8	1.3	0.5	2.0	3.2	23.2	28	99	36	14	8	<1	4	1	<1	1	36	90
																		[50]	[29]	[2]	[14]	[2]	[1]	[2]		
						T= 1023 K																				
Feed	11.6	58.5	17.7	12.9																						
Product	11.6	32.4	11.3	0.2	6.4	12.9	12.1	0.9	12.6	0.8	0.2	0.2	3.2	24.1	45	98	36	22	14	1	7	<1	<1	<1	36	94
																		[49]	[31]	[2]	[16]	[1]	[<1]	[<1]		
						T= 1073 K																				
Feed	11.6	58.5	17.7	12.9																						
Product	0.0	14.0	11.2	0.2	9.3	19.7	19.9	1.7	21.7	1.0	0.2	8.2	3.3	24.0	76	98	37	34	23	2	12	1	<1	5	37	93
																		[44]	[30]	[3]	[16]	[1]	[<1]	[6]		

Appendix 4.12 Lower temperature reactions over an inert versus a catalyst bed, with and without H_2S

Contact time: 20 ms

	Temp K	Products, mole/100 moles of feed														Conversion %			Yield % [Selectivity %]								
		N_2	C_3H_8	H_2S	O_2	H_2	C_3H_6	C_2H_4	C_2H_6	CH_4	CO	CO_2	$C_{(s)}$	S_2	H_2O	C_3H_8	O_2	H_2S	C_3H_6	C_2H_4	C_2H_6	CH_4	CO	CO_2	$C_{(s)}$	S_2	H_2O
			Crystalline silica - without H_2S																								
Feed		33.0	44.7	0.0	22.3																						
Product	823	33.0	41.3	0.0	9.9	0.2	0.0	0.02	0.0	0.05	0.0	0.0	9.9	0.00	1.1	7	2	0	0.00	0.03	0.00	0.04	0.00	0.00	7.39	0.00	2.36
																			[0]	[0.4]	[0]	[0.5]	[0]	[0]	[99]		
Feed		33.0	44.7	0.0	22.3																						
Product	873	33.0	39.0	0.0	10.7	0.3	1.1	1.1	0.0	0.7	0.3	0.01	10.7	0.0	3.2	13	12	0	2.36	1.61	0.00	0.49	0.22	0.01	8.02	0.00	7.23
																			[18.5]	[13]	[0]	[3.8]	[1.71]	[0]	[63]		
			1% VO_x/CS - without H_2S																								
Feed		33.0	44.7	0.0	22.3																						
Product	823	33.0	39.2	0.0	15.1	0.4	0.3	0.02	0.0	0.04	0.0	0.1	15.1	0.0	1.1	12	3	0	0.72	0.03	0.00	0.03	0.00	0.09	11.28	0.00	2.40
																			[6.05]	[0.3]	[0]	[0.2]	[0]	[0.7]	[93]		
Feed		33.0	44.7	0.0	22.3																						
Product	873	33.0	34.8	0.0	17.4	0.2	2.4	1.5	0.03	0.9	0.7	0.4	17.4	0.0	4.4	22	18	0	5.44	2.23	0.05	0.66	0.51	0.27	13.02	0.00	9.87
																			[24.4]	[9.9]	[0.2]	[2.9]	[2.27]	[1.2]	[59]		
			1% VO_x/CS - with H_2S																								
Feed		33.0	33.5	16.8	16.8																						
Product	823	33.0	28.1	5.8	2.5	0.3	4.7	0.7	0.0	0.4	0.7	0.1	-0.6	5.5	18.4	16	85	65	14.08	1.48	0.00	0.35	0.70	0.13	-0.63	65.36	54.86
																			[87.5]	[9.2]	[0]	[2.2]	[4.32]	[0.8]	-[4]		

Appendix 4.13 $C_3H_8/O_2/N_2$ Reaction over a catalyst with and without H_2S

Catalyst: 1% VO_x/CS Contact time: 35 ms

	Temp K	Products, mole/100 moles of feed														Conversion %			Yield % [Selectivity %]								
		N_2	C_3H_8	H_2S	O_2	H_2	C_3H_6	C_2H_4	C_2H_6	CH_4	CO	CO_2	$C_{(s)}$	S_2	H_2O	C_3H_8	O_2	H_2S	C_3H_6	C_2H_4	C_2H_6	CH_4	CO	CO_2	$C_{(s)}$	S_2	H_2O
			Without H_2S																								
Feed		10.7	72.8	0.0	20.4																						
Product	923	10.7	52.9	0.0	0.6	6.1	3.9	6.0	0.4	5.9	4.9	7.5	16.7	0.0	19.3	27	97	0	5	6	<1	3	2	3	8	0	47
																			[20]	[20]	[1.4]	[10]	[9]	[13]	[27]		
Feed		10.7	72.8	0.0	20.4																						
Product	1023	10.7	31.8	0.0	0.5	7.3	8.9	16.9	1.1	17.9	9.8	4.6	28.2	0.0	19.5	56	98	0	12	15	1	8	4	2	13	0	48
																			[22]	[27]	[1.8]	[15]	[8]	[4]	[23]		
			With H_2S																								
Feed		11.6	58.5	17.7	12.9																						
Product	1023	11.6	32.4	11.3	0.2	6.4	12.9	12.1	0.9	12.6	0.8	0.2	0.2	3.2	24.1	45	98	36	22	14	1	7	<1	<1	<1	36	94
																			[49]	[31]	[2.2]	[16]	[1]	[<1]	[<1]		
Feed		11.6	58.5	17.7	12.9																						
Product	1073	0.0	14.0	11.2	0.2	9.3	19.7	19.9	1.7	21.7	1.0	0.2	8.2	3.3	24.0	76	98	37	34	23	2	12	1	<1	5	37	93
																			[44]	[30]	[2.6]	[16]	[1]	[<1]	[6.1]		

Appendix 4.14a $C_3H_8/O_2/N_2$ Reactions using Catalysts with Varying Amounts of Vanadium

Feed ratio: 4:1 (C_3H_8: O_2) Contact time: ≈25 ms Temperature: 923 K

	Products, mole/100 moles of feed												Conversion %		Yield % [Selectivity %]							
	N_2	C_3H_8	O_2	H_2	C_3H_6	C_2H_4	C_2H_6	CH_4	CO	CO_2	$C_{(s)}$	H_2O	C_3H_8	O_2	C_3H_6	C_2H_4	C_2H_6	CH_4	CO	CO_2	$C_{(s)}$	H_2O
		1% VOx/CS																				
Feed	10.7	72.8	20.4																			
Product	10.7	52.9	0.6	6.1	3.9	6.0	0.4	5.9	4.9	7.5	16.7	19.3	27	97	5	6	0	3	2	3	8	47
															[20]	[20]	[1]	[10]	[9]	[13]		
		2.5%Vox/CS																				
Feed	17.8	64.7	18.3																			
Product	17.8	38.8	0.9	4.3	4.9	8.7	0.5	7.5	2.6	5.8	28.6	20.5	40	95	8	9	1	4	1	3	15	56
															[19]	[22]	[1]	[10]	[3]	[7]		
		5%Vox/CS																				
Feed	12.3	70.9	19.0																			
Product	12.3	36.0	3.8	4.3	4.9	10.4	0.6	9.1	3.9	3.6	51.3	19.2	49	80	7	10	1	4	2	2	24	51
															[14]	[20]	[1]	[9]	[4]	[3]		

Appendix 4.14b $C_3H_8/O_2/N_2$ Reactions using Catalysts with Varying Amounts of Vanadium

Feed ratio: 4:1 (C_3H_8: O_2) Contact time: ≈25 ms Temperature: 1023 K

	Products, mole/100 moles of feed												Conversion %		Yield % [Selectivity %]							
	N_2	C_3H_8	O_2	H_2	C_3H_6	C_2H_4	C_2H_6	CH_4	CO	CO_2	$C_{(s)}$	H_2O	C_3H_8	O_2	C_3H_6	C_2H_4	C_2H_6	CH_4	CO	CO_2	$C_{(s)}$	H_2O
		1% VOx/CS																				
Feed	10.7	72.8	20.4																			
Product	10.7	31.8	0.5	7.3	8.9	16.9	1.1	17.9	9.8	4.6	28.2	19.5	56	98	12	15	1	8	4	2	13	48
															[22]	[27]	[2]	[15]	[8]	[4]		
		2.5%Vox/CS																				
Feed	17.8	64.7	18.3																			
Product	17.8	21.7	0.2	7.4	7.2	19.8	1.5	18.4	6.1	3.9	36.7	22.2	66	99	11	20	2	9	3	2	19	61
															[17]	[31]	[2]	[14]	[5]	[3]		
		5%Vox/CS																				
Feed	12.3	70.9	19.0																			
Product	12.3	22.8	0.9	8.6	10.2	22.8	1.4	21.0	6.7	4.2	33.1	21.0	68	95	14	21	1	10	3	2	6	55
															[21]	[32]	[2]	[15]	[5]	[3]		

Appendix 4.15a $C_3H_8/H_2S/O_2/N_2$ Reaction using Catalysts with Varying Amounts of Vanadium

Feed ratio: 4:2:1 (C_3H_8: H_2S: O_2) Contact time: 23-30 ms Temperature: 923 K

	Products, mole/100 moles of feed														Conversion %			Yield % [Selectivity %]								
	N_2	C_3H_8	H_2S	O_2	H_2	C_3H_6	C_2H_4	C_2H_6	CH_4	CO	CO_2	$C_{(s)}$	S_2	H_2O	C_3H_8	O_2	H_2S	C_3H_6	C_2H_4	C_2H_6	CH_4	CO	CO_2	$C_{(s)}$	S_2	H_2O
		1% Vox/CS					**Contact time: 30 ms**																			
Feed	11.9	58.5	17.7	12.9																						
Product	11.9	50.8	16.8	0.1	1.4	3.8	2.3	0.1	1.8	1.9	4.2	-0.9	0.5	15.2	13	99	5	7 [53]	3 [20]	0 [1]	1 [8]	1 [9]	2 [20]	-1	5	59
		5% Vox/CS					**Contact time: 25 ms**																			
Feed	20.6	53.0	14.7	15.6																						
Product	20.6	36.8	12.4	0.3	5.6	3.6	5.4	0.1	5.9	2.6	4.1	14.2	1.2	17.9	31	98	6	7 [23]	7 [23]	0 [0]	4 [12]	2 [5]	3 [9]	9	1	58
		10% Vox/CS					**Contact time: 25 ms**																			
Feed	20.2	53.2	14.9	15.0																						
Product	20.2	36.1	12.2	0.2	4.9	3.8	5.0	0.1	5.1	2.0	4.0	18.6	1.3	17.9	32	99	8	7 [22]	6 [20]	0 [0]	3 [10]	1 [4]	2 [8]	12	1	60

Appendix 4.15b $C_3H_8/H_2S/O_2/N_2$ Reaction using Catalysts with Varying Amounts of Vanadium

Feed ratio: 4:2:1 (C_3H_8: H_2S: O_2) Contact time: 25-30 ms Temperature: 1023 K

	Products, mole/100 moles of feed														Conversion %			Yield % [Selectivity %]								
	N_2	C_3H_8	H_2S	O_2	H_2	C_3H_6	C_2H_4	C_2H_6	CH_4	CO	CO_2	$C_{(s)}$	S_2	H_2O	C_3H_8	O_2	H_2S	C_3H_6	C_2H_4	C_2H_6	CH_4	CO	CO_2	$C_{(s)}$	S_2	H_2O
		1% Vox/CS				**Contact time: 30 ms**																				
Feed	11.9	58.5	17.7	12.9																						
Product	11.9	33.4	15.9	0.1	5.6	11.9	10.5	0.6	10.2	2.2	1.5	3.5	0.9	20.3	43	99	10	20 [47]	12 [28]	1 [2]	6 [14]	1 [3]	1 [2]	2	10	79
		2.5%Vox/CS				**Contact time: 25 ms**																				
Feed	21.1	52.1	15.3	13.1																						
Product	21.1	24.2	13.7	0.2	7.0	9.9	13.6	1.1	13.5	2.1	2.2	6.9	0.8	19.4	54	99	10	19 [35]	17 [33]	1 [3]	9 [16]	1 [2]	1 [3]	4	10	74
		10% Vox/CS				**Contact time: 25 ms**																				
Feed	20.2	53.2	14.9	15.0																						
Product	20.2	11.1	12.9	0.3	7.4	13.7	17.7	1.7	19.9	1.6	3.5	21.5	1.0	19.3	79	98	14	26 [32]	22 [28]	2 [3]	12 [16]	1 [1]	2 [3]	13	13	64

Appendix 4.16a $C_3H_8/H_2S/O_2/N_2$ Catalytic Reactions with Varying Feed Compositions

Catalyst: 2.5% VOx/CS Contact time: 22 ms Temperature: 923 K

	Products, mole/100 moles of feed														Conversion %			Yield % [Selectivity %]								
	N_2	C_3H_8	H_2S	O_2	H_2	C_3H_6	C_2H_4	C_2H_6	CH_4	CO	CO_2	$C_{(s)}$	S_2	H_2O	C_3H_8	O_2	H_2S	C_3H_6	C_2H_4	C_2H_6	CH_4	CO	CO_2	$C_{(s)}$	S_2	H_2O
			Feed ratio: 7:2:1 (C_3H_8: H_2S: O_2)																							
Feed	20.8	58.5	16.2	7.5																						
Product	20.8	42.2	15.6	0.3	0.8	4.3	1.6	0.0	1.5	0.3	0.0	31.1	0.3	14.2	28	96	4	7	2	0	1	<1	0	18	0	94
																		[27]	[6]	[0]	[3]	[1]	[0]			
			Feed ratio: 4:1:1 (C_3H_8: H_2S: O_2)																							
Feed	21.1	52.1	15.3	13.1																						
Product	21.1	28.8	12.0	0.4	2.1	5.7	4.7	0.2	4.2	1.4	1.0	36.3	1.6	21.9	45	97	22	11	6	<1	3	1	1	23	2	83
																		[25]	[14]	[1]	[6]	[2]	[1]			

Appendix 4.16b $C_3H_8/H_2S/O_2/N_2$ Catalytic Reactions with Varying Feed Compositions

Catalyst: 2.5% VOx/CS Contact time: 22 ms Temperature: 1023 K

	Products, mole/100 moles of feed														Conversion %			Yield % [Selectivity %]								
	N_2	C_3H_8	H_2S	O_2	H_2	C_3H_6	C_2H_4	C_2H_6	CH_4	CO	CO_2	$C_{(s)}$	S_2	H_2O	C_3H_8	O_2	H_2S	C_3H_6	C_2H_4	C_2H_6	CH_4	CO	CO_2	$C_{(s)}$	S_2	H_2O
			Feed ratio: 7:2:1 (C_3H_8: H_2S: O_2)																							
Feed	20.8	58.5	16.2	7.5																						
Product	20.8	31.0	15.6	0.4	6.2	11.0	11.0	0.8	11.8	0.4	0.0	13.8	0.3	14.0	47	95	4	19	13	1	7	<1	0	8	4	93
																		[40]	[27]	[2]	[14]	[0]	[0]			
			Feed ratio: 4:1:1 (C_3H_8: H_2S: O_2)																							
Feed	21.1	52.1	15.3	13.1																						
Product	21.1	24.2	13.7	0.2	7.0	9.9	13.6	1.1	13.5	2.1	2.2	6.9	0.8	19.4	54	99	10	19	17	1	9	1	1	4	10	74
																		[35]	[33]	[3]	[16]	[2]	[3]			

Appendix 4.17a Effect of contact time on the H_2S assisted ODH of C_3H_8 over a 2.5% VOx/CS catalyst

Catalyst: 2.5% VOx/CS Feed ratio: 7:2:1 (C_3H_8: H_2S: O_2) Temperature: 923 K

	Products, mole/100 moles of feed														Conversion %			Yield % [Selectivity %]							
	N_2	C_3H_8	H_2S	O_2	H_2	C_3H_6	C_2H_4	C_2H_6	CH_4	CO	CO_2	$C_{(s)}$	S_2	H_2O	C_3H_8	O_2	H_2S	C_3H_6	C_2H_4	C_2H_6	CH_4	CO	CO_2	$C_{(s)}$	S_2	H_2O
	Contact time: 12 ms																								
Feed	22.6	56.6	16.1	7.7																					
Product	22.6	47.6	15.6	0.2	2.7	4.1	4.5	0.2	4.5	0.7	0.2	-1.2	0.3	13.7	16	97	4	7	5	<1	3	<1	<1	-1	0	89
																		[46]	[33]	[1]	[17]	[2]	[1]	-[7]		
	Contact time: 60 ms																								
Feed	22.6	56.6	16.1	7.7																					
Product	22.6	36.7	16.1	0.5	4.0	4.6	4.4	0.2	4.5	1.2	0.4	30.5	0.0	12.3	35	93	0	8	5	<1	3	1	<1	18	0	80
																		[23]	[15]	[1]	[8]	[2]	[1]	[48]		
	Contact time: 100 ms																								
Feed	22.6	56.6	16.1	7.7																					
Product	22.6	26.4	15.8	1.0	5.1	5.2	3.9	0.4	4.4	1.8	0.5	49.5	0.2	10.6	53	88	2	10	5	1	3	1	<1	31	0	69
																		[18]	[9]	[1]	[5]	[2]	[1]	[58]		

Appendix 4.17b Effect of contact time on the H_2S assisted ODH of C_3H_8 over a 2.5% VOx/CS catalyst

Catalyst: 2.5% VOx/CS Feed ratio: 7:2:1 (C_3H_8: H_2S: O_2) Temperature: 1023 K

	Products, mole/100 moles of feed														Conversion %			Yield % [Selectivity %]								
	N_2	C_3H_8	H_2S	O_2	H_2	C_3H_6	C_2H_4	C_2H_6	CH_4	CO	CO_2	$C_{(s)}$	S_2	H_2O	C_3H_8	O_2	H_2S	C_3H_6	C_2H_4	C_2H_6	CH_4	CO	CO_2	$C_{(s)}$	S_2	H_2O
		Contact time: 12 ms																								
Feed	22.6	56.6	16.1	7.7																						
Product	22.6	13.7	17.0	0.3	8.5	15.7	22.4	2.4	30.9	0.3	2.1	4.3	-0.4	10.2	76	96	-5	27	25	3	18	<1	1	2	-5	67
																		[36]	[34]	[4]	[23]	[<1]	[2]	[3]		
		Contact time: 60 ms																								
Feed	22.6	56.6	16.1	7.7																						
Product	22.6	9.3	16.4	1.3	8.3	14.5	20.5	2.1	23.4	0.4	2.2	31.5	-0.1	8.0	84	83	-2	25	24	2	13	<1	1	18	-2	52
																		[30]	[28]	[3]	[16]	[<1]	[2]	[22]		
		Contact time: 100 ms																								
Feed	22.6	56.6	16.1	7.7																						
Product	22.6	8.9	15.0	1.4	7.4	8.4	18.3	1.9	21.1	0.3	1.6	44.3	0.6	9.1	84	82	7	16	23	2	13	<1	1	28	7	59
																		[19]	[27]	[3]	[16]	[<1]	[1]	[33]		

Appendix 5.1a: Product distribution, as calculated by equilibrium calculations, of the reaction between C_4H_{10} and S_2, without allowing $C_{(s)}$ in the products

	Products, mole/100 moles of feed													Conversion %		Yield % [Selectivity %]							
	N_2	n-C_4H_{10}	H_2S	S_2	H_2	1-C_4H_8	C_3H_6	C_3H_8	C_2H_4	C_2H_6	CH_4	CS	CS_2	C_4H_{10}	S_2	1-C_4H_8	C_3H_6	C_3H_8	C_2H_4	C_2H_6	CH_4	CS	CS_2
							T= 923°K																
Feed	27.97	50.25		6.45																			
Product	27.97	0.38	5.5E-04	7.1E-09	2.4E-03	17.18	15.60	0.75	8.45	2.44	53.05	3.4E-08	6.45	99.24	100.00	34.20	23.29	1.12	8.41	2.43	26.39	1.7E-08	3.21
																[34.46]	[23.47]	[1.13]	[8.47]	[2.44]	[26.6]	[2E-08]	[3.23]
							T= 1023°K																
Feed	27.97	50.25		6.45																			
Product	27.97	0.11	1.2E-03	3.8E-08	1.1E-02	11.97	17.12	0.38	17.77	1.92	54.26	7.8E-07	6.45	99.78	100.00	23.82	25.55	0.57	17.68	1.91	26.99	3.9E-07	3.21
																[23.88]	[25.61]	[0.57]	[17.72]	[1.91]	[27.1]	[4E-07]	[3.22]

Appendix 5.1b: Product distribution, as calculated by equilibrium calculations, of the reaction between C_4H_{10} and O_2, without allowing $C_{(s)}$ in the products

	Products, mole/100 moles of feed													Conversion %		Yield % [Selectivity %]							
	N_2	n-C_4H_{10}	O_2	H_2	1-C_4H_8	C_3H_6	C_3H_8	C_2H_4	C_2H_6	CH_4	CO	CO_2	H_2O	C_4H_{10}	O_2	1-C_4H_8	C_3H_6	C_3H_8	C_2H_4	C_2H_6	CH_4	CO	CO_2	H_2O
						T= 923°K																		
Feed	27.97	50.25	6.45																				
Product	27.97	0.06	1.4E-38	0.03	7.99	15.09	0.27	22.61	1.78	61.01	12.90	5.2E-05	2.0E-08	99.89	100.00	15.90	22.53	0.41	22.50	1.77	30.35	6.42	2.6E-05	1.6E-07
																[15.9]	[22.55]	[0.41]	[22.52]	[1.77]	[30.4]	[6.43]	[3E-05]	
						T= 1023°K																		
Feed	27.97	50.25	6.45																				
Product	27.97	0.02	2.8E-36	0.09	4.53	12.83	0.14	33.37	1.37	61.53	12.90	2.0E-05	4.0E-08	99.96	100.00	9.01	19.14	0.21	33.20	1.37	30.61	6.42	9.7E-06	3.1E-07
																[9.01]	[19.15]	[0.21]	[33.21]	[1.37]	[30.6]	[6.42]	[1E-05]	

Appendix 5.2a: Product distribution, as calculated by equilibrium calculations, of the reaction between C_4H_{10} and S_2, with $C_{(s)}$ in the products

	Products, mole/100 moles of feed													Conversion %		Yield % [Selectivity %]								
	N_2	n-C_4H_{10}	H_2S	S_2	H_2	1-C_4H_8	C_3H_6	C_3H_8	C_2H_4	C_2H_6	CH_4	CS	CS_2	$C_{(s)}$	C_4H_{10}	S_2	1-C_4H_8	C_3H_6	C_3H_8	C_2H_4	C_2H_6	CH_4	CS	CS_2	$C_{(s)}$
								T= 923°K																	
Feed	27.97	50.25		6.45																					
Product	27.97	0.00	1.3E+01	1.1E-06	1.1E+02	6.5E-13	3.0E-09	5.3E-08	1.2E-05	8.3E-04	63.19	1.3E-11	1.2E-05	1.4E+02	100	100	1.3E-12	4.5E-09	7.9E-08	1.2E-05	8.3E-04	31.44	6.5E-12	5.9E-06	6.9E+01
																	[1E-12]	[4E-09]	[8E-08]	[1E-05]	[8E-04]	[31.4]	[7E-12]	[0]	[68.56]
								T= 1023°K																	
Feed	27.97	50.25		6.45																					
Product	27.97	0.00	1.3E+01	2.2E-06	1.3E+02	9.9E-13	4.6E-09	4.6E-08	2.0E-05	7.3E-04	52.97	5.8E-11	2.2E-05	1.5E+02	100	100	2.0E-12	6.9E-09	6.9E-08	2.0E-05	7.2E-04	26.35	2.9E-11	1.1E-05	7.4E+01
																	[2E-12]	[7E-09]	[7E-08]	[2E-05]	[7E-04]	[26.4]	[3E-11]	[0]	[73.65]

Appendix 5.2b: Product distribution, as calculated by equilibrium calculations, of the reaction between C_4H_{10} and O_2, with $C_{(s)}$ in the products

	Products, mole/100 moles of feed														Conversion %		Yield % [Selectivity %]									
	N_2	n-C_4H_{10}	O_2	H_2	1-C_4H_8	C_3H_6	C_3H_8	C_2H_4	C_2H_6	CH_4	CO	CO_2	H_2O	C(s)	C_4H_{10}	O_2	1-C_4H_8	C_3H_6	C_3H_8	C_2H_4	C_2H_6	CH_4	CO	CO_2	C(s)	H_2O
						T= 923°K																				
Feed	27.97	50.25	6.45																							
Product	27.97	0.00	3.7E-25	141.66	1.1E-12	5.4E-09	4.4E-08	2.4E-05	7.0E-04	50.09	2.52	4.9E-01	9.4E+00	1.5E+02	100	100	2.3E-12	8.0E-09	6.6E-08	2.4E-05	6.9E-04	24.92	1.25	2.4E-01	7.4E+01	7.3E+01
																	2.3E-12	8.0E-09	6.6E-08	2.4E-05	6.9E-04	[24.9]	[1.25]	[0.244]	[73.58]	
						T= 1023°K																				
Feed	27.97	50.25	6.45																							
Product	27.97	0.00	2.1E-24	159.96	1.5E-12	7.2E-09	3.6E-08	3.5E-05	5.9E-04	41.52	3.70	4.8E-01	8.2E+00	1.6E+02	100	100	3.0E-12	1.1E-08	5.4E-08	3.5E-05	5.8E-04	20.66	1.84	2.4E-01	7.7E+01	6.4E+01
																	3.0E-12	1.1E-08	5.4E-08	3.5E-05	5.8E-04	[20.7]	[1.84]	[0.238]	[77.26]	

Appendix 5.3a: Product distribution, as calculated by equilibrium calculations, of the reaction between C_4H_{10}, H_2S and O_2, with $C_{(s)}$ in the products

	Products, mole/100 moles of feed																Conversion %			Yield % [Selectivity %]											
	N_2	C_4H_{10}	H_2S	O_2	H_2	C_3H_6	C_2H_4	C_2H_6	CH_4	CO	CO_2	CS_2	COS	$C_{(s)}$	SO_2	S_2	H_2O	C_4H_{10}	O_2	H_2S	C_4H_8	C_3H_6	C_2H_4	C_2H_6	CH_4	CO	CO_2	CS_2	COS	$C_{(s)}$	SO_2	S_2	H_2O
						T= 923°K																											
Feed	27.97	50.25	15.53	6.45																													
Product	27.97	2.8E-12	15.52	3.3E-25	143.24	4.8E-09	2.3E-05	6.5E-04	49.32	2.53	0.49	3.8E-05	0.01	148.64	8.0E-11	3.9E-06	9.37	100.00	100.00	0.06	2.0E-12	7.2E-09	2.2E-05	6.5E-04	24.54	1.26	0.25	0.00	0.02	73.95	5.2E-10	5.0E-05	72.64
																					[2E-12]	[7E-09]	[2E-05]	[6E-04]	[24.54]	[1.26]	[0.25]	[8E-05]	[0.02]	[73.95]			
						T= 1023°K																											
Feed	27.97	50.25	15.53	6.45																													
Product	27.97	2.1E-12	15.52	2.0E-24	162.23	6.6E-09	3.3E-05	5.4E-04	40.44	3.78	0.48	6.7E-05	0.01	156.28	1.2E-10	7.3E-06	8.14	100.00	100.00	0.08	2.6E-12	9.8E-09	3.3E-05	5.4E-04	20.12	1.88	0.24	0.00	0.02	77.75	7.8E-10	9.3E-05	63.14
																					[3E-12]	[1E-08]	[3E-05]	[5E-04]	[20.12]	[1.88]	[0.24]	[1E-04]	[0.02]	[77.75]			

Appendix 5.3b: Product distribution, as calculated by equilibrium calculations, of the reaction between C_4H_{10}, H_2S and O_2, without $C_{(s)}$ in the products

	Products, mole/100 moles of feed															Conversion %			Yield % [Selectivity %]											
	N_2	C_4H_{10}	H_2S	O_2	H_2	C_3H_6	C_2H_4	C_2H_6	CH_4	CO	CO_2	CS_2	COS	SO_2	S_2	H_2O	C_4H_{10}	O_2	H_2S	C_4H_8	C_3H_6	C_2H_4	C_2H_6	CH_4	CO	CO_2	CS_2	COS	$C_{(s)}$	SO_2	S_2	H_2O
						T= 923°K																										
Feed	27.97	50.25	15.53	6.45																												
Product	27.97	0.02	0.01	0.00	0.11	9.43	25.65	1.71	84.41	12.87	0.00	7.74	0.03	1.7E-21	5.9E-07	8.2E-08	99.96	100.00	99.94	6.15	14.08	25.52	1.70	42.00	6.40	0.00	15.41	0.07	73.95	1.1E-20	7.6E-06	6.4E-07
																				[6.16]	[14.08]	[25.53]	[1.7]	[42.01]	[6.4]	[2E-05]	[15.42]	[0.07]	[73.98]			
						T= 1023°K																										
Feed	27.97	50.25	15.53	6.45																												
Product	0.00	0.01	0.02	0.00	0.39	6.70	33.65	1.24	84.69	12.88	0.00	7.74	0.02	9.4E-21	2.7E-06	2.0E-07	99.99	100.00	99.87	2.75	10.00	33.48	1.23	42.13	6.41	0.00	15.41	0.04	77.75	6.1E-20	3.5E-05	1.5E-06
																				[2.75]	[10.01]	[33.49]	[1.23]	[42.14]	[6.41]	[7E-06]	[15.41]	[0.04]	[77.76]			

Appendix 5.4a $n\text{-}C_4H_{10}/O_2/N_2$ gas phase reaction with and without H_2S

Catalyst: Crystalline Silica (inert) Contact time: 8 ms Temperature: 923°K

	Products, mole/100 moles of feed																	Conversion %			Yield % [Selectivity %]											
	N_2	$n\text{-}C_4H_{10}$	H_2S	O_2	H_2	$1\text{-}C_4H_8$	$2\text{-}C_4H_8$	C_3H_6	C_3H_8	C_2H_4	C_2H_6	CH_4	CO	CO_2	$C_{(s)}$	S_2	H_2O	C_4H_{10}	O_2	H_2S	$1\text{-}C_4H_8$	$2\text{-}C_4H_8$	C_3H_6	C_3H_8	C_2H_4	C_2H_6	CH_4	CO	CO_2	$C_{(s)}$	S_2	H_2O
	Without H_2S																															
Feed	17.8	73.5	0.0	16.7																												
Product	17.8	59.2	0.0	0.1	3.1	1.5	0.2	3.5	0.1	5.1	1.1	4.6	1.7	5.6	15.6	0.0	20.3	19	99	n/a	2	0	4	<1	3	1	2	1	2	5	0	61
																					[10]	[1]	[18]	{<1]	[18]	[4]	[8]	[3]	[10]	[27]		
	With H_2S																															
Feed	28.0	50.2	15.5	6.4																												
Product	28.0	37.9	11.0	0.6	0.3	2.4	1.0	5.2	0.0	2.2	1.3	5.2	0.1	0.1	8.0	2.3	11.3	25	90	29	5	2	8	0	2	1	3	<1	<1	4	2	88
																					[20]	[8]	[32]	[0]	[9]	[5]	[10]	[<1]	[<1]	[16]		

Appendix 5.4b $n\text{-}C_4H_{10}/O_2/N_2$ gas phase reaction with and without H_2S

Catalyst: Crystalline Silica (inert) Contact time: 6 ms Temperature: 1023°K

	Products, mole/100 moles of feed																	Conversion %			Yield % [Selectivity %]											
	N_2	$n\text{-}C_4H_{10}$	H_2S	O_2	H_2	$1\text{-}C_4H_8$	$2\text{-}C_4H_8$	C_3H_6	C_3H_8	C_2H_4	C_2H_6	CH_4	CO	CO_2	$C_{(s)}$	S_2	H_2O	C_4H_{10}	O_2	H_2S	$1\text{-}C_4H_8$	$2\text{-}C_4H_8$	C_3H_6	C_3H_8	C_2H_4	C_2H_6	CH_4	CO	CO_2	$C_{(s)}$	S_2	H_2O
	Without H_2S																															
Feed	17.8	73.5	0.0	16.7																												
Product	17.8	50.9	0.0	0.2	5.1	3.5	0.3	7.7	0.2	10.8	2.0	10.2	2.0	6.0	7.6	0.0	6.4	31	99	n/a	5	0	8	0	7	1	3	1	2	3	n/a	19
																					[16]	[<1]	[25]	[0.6]	[24]	[4]	[11]	[2]	[7]	[8]		
	With H_2S																															
Feed	28.0	50.2	15.5	6.4																												
Product	28.0	11.9	11.8	0.3	3.4	3.7	1.1	20.5	0.0	9.4	6.7	23.8	0.3	0.8	15.7	1.9	10.3	76	95	24	7	2	31	0	9	7	12	0	0	8	24	80
																					[10]	[3]	[40]	[0]	[12]	[9]	[15]	[0]	[1]	[10]		

Appendix 5.5 $n\text{-}C_4H_{10}/H_2S/O_2/N_2$ gas phase reaction at varying contact times Catalyst: Crystalline Silica (inert)

	Temp °K	Products, mole/100 moles of feed																Conversion %			Yield % [Selectivity %]										
		N_2	$n\text{-}C_4H_{10}$	H_2S	O_2	H_2	$1\text{-}C_4H_8$	$2\text{-}C_4H_8$	C_3H_6	C_3H_8	C_2H_4	C_2H_6	CH_4	CO	CO_2	$C_{(s)}$	S_2	H_2O	C_4H_{10}	O_2	H_2S	$1\text{-}C_4H_8$	$2\text{-}C_4H_8$	C_3H_6	C_3H_8	C_2H_4	C_2H_6	CH_4	CO	CO_2	$C_{(s)}$	H_2O
Feed		28.0	50.2	15.5	6.4																										
8 ms	923	28.0	37.9	11.0	0.6	0.3	2.4	1.0	5.2	0.0	2.2	1.3	5.2	0.1	0.1	8.0	2.3	11.3	25	90	29	5	2	8	0	2	1	3	<1	<1	4	88
																						[20]	[8]	[32]	[0]	[9]	[5]	[10]	[<1]	[<1]	[16]	
Feed		30.0	52.5	13.6	6.0																										
27 ms	923	30.0	34.2	12.1	0.4	0.6	5.3	0.5	8.7	0.0	3.5	2.6	9.2	0.5	0.6	1.3	0.8	9.2	35	93	14	10	1	12	0	3	2	4	<1	<1	1	77
																						[29]	[3]	[36]	[0]	[10]	[7]	[13]	[1]	[1]	[2]	
Feed		28.0	50.2	15.5	6.4																										
8 ms	1023	28.0	11.9	11.8	0.3	3.4	3.7	1.1	20.5	0.0	9.4	6.7	23.8	0.3	0.8	15.7	1.9	10.3	76	95	24	7	2	31	0	9	7	12	0	0	8	80
																						[10]	[3]	[40]	[0]	[12]	[9]	[15]	[0]	[1]	[10]	
Feed		30.0	52.5	13.6	6.0																										
27 ms	1023	30.0	10.3	12.1	0.6	3.1	4.1	0.9	23.9	0.3	11.3	7.9	28.4	0.6	1.0	7.9	0.7	8.0	80	90	10	8	2	34	0	11	8	14	0	0	4	67
																						[10]	[2]	[42]	[1]	[13]	[9]	[17]	[0]	[1]	[5]	

Appendix 5.6a $C_4H_{10}/H_2S/O_2/N_2$ Reaction with and without a catalyst

Feed ratio: 8:2.5:1 (C_4H_{10}: H_2S: O_2) Contact time: 8 ms Temperature: 923 K

	Products, mole/100 moles of feed																	Conversion %			Yield % [Selectivity %]											
	N_2	n-C_4H_{10}	H_2S	O_2	H_2	1-C_4H_8	2-C_4H_8	C_3H_6	C_3H_8	C_2H_4	C_2H_6	CH_4	CO	CO_2	$C_{(s)}$	S_2	H_2O	C_4H_{10}	O_2	H_2S	1-C_4H_8	2-C_4H_8	C_3H_6	C_3H_8	C_2H_4	C_2H_6	CH_4	CO	CO_2	$C_{(s)}$	S_2	H_2O
	Catalyst: Crystalline silica (inert)																															
Feed	25.9	50.8	15.5	6.4																												
Product	25.9	35.1	9.8	0.6	0.3	4.7	0.6	4.7	0.0	1.9	1.1	4.6	0.1	0.0	16.4	2.9	11.6	31	91	37	9	1	7	0	2	1	2	,1	<1	8	3	90
																					[30]	[4]	[22]	[0]	[6]	[4]	[7]	[<1]	[<1]	[26]		
	Catalyst: 5% VOx/CS																															
Feed	60.7	32.0	7.8	3.8																												
Product	60.7	22.2	6.7	0.5	0.1	4.6	0.7	4.0	0.0	1.8	0.9	3.9	0.2	0.1	-3.3	0.5	5.6	31	87	13	14	2	9	0	3	1	3	<1	<1	-3	1	75
																					[47]	[7]	[30]	[0]	[9]	[5]	[10]	[<1]	[<1]	-[9]		

Appendix 5.6b $C_4H_{10}/H_2S/O_2/N_2$ Reaction with and without a catalyst

Feed ratio: 8:2.5:1 (C_4H_{10}: H_2S: O_2) Contact time: 8 ms Temperature: 1023 K

	Products, mole/100 moles of feed																	Conversion %			Yield % [Selectivity %]											
	N_2	n-C_4H_{10}	H_2S	O_2	H_2	1-C_4H_8	2-C_4H_8	C_3H_6	C_3H_8	C_2H_4	C_2H_6	CH_4	CO	CO_2	$C_{(s)}$	S_2	H_2O	C_4H_{10}	O_2	H_2S	1-C_4H_8	2-C_4H_8	C_3H_6	C_3H_8	C_2H_4	C_2H_6	CH_4	CO	CO_2	$C_{(s)}$	S_2	H_2O
	Catalyst: Crystalline silica (inert)																															
Feed	25.9	50.8	15.5	6.4																												
Product	25.9	12.5	10.6	0.3	3.0	3.4	0.8	18.4	0.0	8.4	6.2	21.3	0.3	0.8	29.7	2.5	10.5	75	96	32	7	2	27	0	8	6	10	<1	<1	15	32	82
																					[9]	[2]	[36]	[0]	[11]	[8]	[14]	[<1]	[<1]	[19]		
	Catalyst: 5% VOx/CS																															
Feed	60.7	32.0	7.8	3.8																												
Product	60.7	7.7	7.5	0.4	2.1	2.6	0.6	13.3	0.0	6.6	4.2	15.3	0.3	1.0	6.2	0.1	4.2	76	89	2	8	2	31	0	10	7	12	<1	1	5	3	56
																					[11]	[3]	[41]	[0]	[14]	[9]	[16]	[<1]	[1]	[6]		

Appendix 5.7a $C_4H_{10}/H_2S/O_2/N_2$ Reaction with and without a catalyst

Feed ratio: 8:2:1 (C_4H_{10}: H_2S: O_2) Contact time: 27 ms Temperature: 923 K

	Products, mole/100 moles of feed																	Conversion %			Yield % [Selectivity %]											
	N_2	n-C_4H_{10}	H_2S	O_2	H_2	1-C_4H_8	2-C_4H_8	C_3H_6	C_3H_8	C_2H_4	C_2H_6	CH_4	CO	CO_2	$C_{(s)}$	S_2	H_2O	C_4H_{10}	O_2	H_2S	1-C_4H_8	2-C_4H_8	C_3H_6	C_3H_8	C_2H_4	C_2H_6	CH_4	CO	CO_2	$C_{(s)}$	S_2	H_2O
	Catalyst: Crystalline silica (inert)																															
Feed	30.0	52.5	13.6	6.0																												
Product	30.0	34.2	12.1	0.4	0.6	5.3	0.5	8.7	0.0	3.5	2.6	9.2	0.5	0.6	1.3	0.8	9.2	35	93	14	10	1	12	0	3	2	4	<1	<1	1	1	77
																					[28.91]	[3]	[35.8]	[0]	[10]	[7]	[12.5]	[1]	[1]	[2]		
	Catalyst: 2.5% VOx/CS																															
Feed	30.0	52.5	13.6	6.0																												
Product	30.0	35.9	11.6	0.8	0.7	5.7	0.8	9.7	0.0	4.1	2.6	10.9	0.5	0.9	0.0	1.0	8.1	39	87	15	11	2	14	0	4	2	5	<1	<1	<1	1	68
																					[28.34]	[4]	[35.9]	[0]	[10]	[7]	[13.4]	[1]	[1]	[<1]		

Appendix 5.7b $C_4H_{10}/H_2S/O_2/N_2$ Reaction with and without a catalyst

Feed ratio: 8:2:1 (C_4H_{10}: H_2S: O_2) Contact time: 27 ms Temperature: 1023 K

	Products, mole/100 moles of feed																	Conversion %			Yield % [Selectivity %]											
	N_2	n-C_4H_{10}	H_2S	O_2	H_2	1-C_4H_8	2-C_4H_8	C_3H_6	C_3H_8	C_2H_4	C_2H_6	CH_4	CO	CO_2	$C_{(s)}$	S_2	H_2O	C_4H_{10}	O_2	H_2S	1-C_4H_8	2-C_4H_8	C_3H_6	C_3H_8	C_2H_4	C_2H_6	CH_4	CO	CO_2	$C_{(s)}$	S_2	H_2O
	Catalyst: Crystalline Silica (inert)																															
Feed	30.0	52.5	13.6	6.0																												
Product	30.0	10.3	12.1	0.6	3.1	4.1	0.9	23.9	0.3	11.3	7.9	28.4	0.6	1.0	7.9	0.7	8.0	80	90	10	8	2	34	<1	11	8	14	<1	<1	4	11	67
																					[10]	[2]	[42]	[<1]	[13]	[9]	[17]	[<1]	[<1]	[5]		
	Catalyst: 2.5% VOx/CS																															
Feed	30.0	52.5	13.6	6.0																												
Product	30.0	7.1	12.9	0.4	3.6	3.7	1.3	26.8	0.1	12.8	8.6	31.5	0.5	1.9	4.3	0.4	6.9	86	93	5	7	2	38	<1	12	8	15	0	1	2	5	57
																					[8]	[3]	[44]	[<1]	[14]	[10]	[17]	[0.3]	[1]	[2]		

Appendix 5.8a $C_4H_{10}/H_2S/O_2/N_2$ Catalytic Reaction with and without H_2S

Catalyst: 5% VOx/CS Contact time: 14 ms Temperature: 923 K

	Products, mole/100 moles of feed																	Conversion %			Yield % [Selectivity %]												
	N_2	n-C_4H_{10}	H_2S	O_2	H_2	1-C_4H_8	2-C_4H_8	C_3H_6	C_3H_8	C_2H_4	C_2H_6	CH_4	CO	CO_2	$C_{(s)}$	S_2	H_2O	C_4H_{10}	O_2	H_2S	1-C_4H_8	2-C_4H_8	C_3H_6	C_3H_8	C_2H_4	C_2H_6	CH_4	CO	CO_2	$C_{(s)}$	S_2	H_2O
		Without H_2S																														
Feed	19.5	61.9	0.0	15.9																												
Product	19.5	44.0	0.0	4.2	2.5	5.5	0.3	6.5	0.3	5.9	1.4	7.5	0.3	0.2	5.8	0.0	22.5	29	74	n/a	9	1	8	<1	5	1	3	<1	<1	2	0	71
																					[30]	[2]	[27]	[1]	[17]	[4]	[10]	[<1]	[<1]	[8]		
		With H_2S																														
Feed	19.9	54.9	11.1	10.1																												
Product	19.9	36.0	6.0	2.0	0.9	8.9	1.2	6.6	0.0	4.3	2.0	9.0	0.3	0.0	-7.0	2.5	15.4	34	80	27	16	2	9	0	4	2	4	<1	0	-3	46	76
																					[47]	[6]	[26]	[0]	[11]	[5]	[12]	[<1]	[0]	-[9]		

Appendix 5.8b $C_4H_{10}/H_2S/O_2/N_2$ Catalytic Reaction with and without H_2S

Catalyst: 5% VOx/CS Contact time: 14 ms Temperature: 1023 K

	Products, mole/100 moles of feed																	Conversion %			Yield % [Selectivity %]												
	N_2	n-C_4H_{10}	H_2S	O_2	H_2	1-C_4H_8	2-C_4H_8	C_3H_6	C_3H_8	C_2H_4	C_2H_6	CH_4	CO	CO_2	$C_{(s)}$	S_2	H_2O	C_4H_{10}	O_2	H_2S	1-C_4H_8	2-C_4H_8	C_3H_6	C_3H_8	C_2H_4	C_2H_6	CH_4	CO	CO_2	$C_{(s)}$	S_2	H_2O
		Without H_2S																														
Feed	19.5	61.9	0.0	15.9																												
Product	19.5	26.8	0.0	1.9	9.6	9.9	0.7	10.8	0.2	15.4	2.8	15.2	0.8	0.9	11.3	0.0	23.2	57	88	0	16	1	13	<1	12	2	6	<1	<1	5	0	73
																					[29]	[2]	[23]	[<1]	[22]	[4]	[11]	[1]	[1]	[8]		
		With H_2S																														
Feed	19.9	54.9	11.1	10.1																												
Product	19.9	6.1	9.0	2.1	5.1	4.2	1.2	23.9	0.1	16.2	8.8	34.6	1.1	2.5	13.2	1.1	9.9	90	79	19	8	2	33	<1	15	8	16	<1	1	6	19	49
																					[9]	[3]	[36]	[<1]	[16]	[9]	[18]	[1]	[1]	[7]		

Appendix 5.9a $C_4H_{10}/H_2S/O_2/N_2$ Reaction over catalysts containing differing amounts of vanadium oxide

Feed ratio: 8:2.5:1 (C_4H_{10}: H_2S: O_2) Contact time: 8 ms Temperature: 923 K

	Products, mole/100 moles of feed																	Conversion %			Yield % [Selectivity %]												
	N_2	n-C_4H_{10}	H_2S	O_2	H_2	1-C_4H_8	2-C_4H_8	C_3H_6	C_3H_8	C_2H_4	C_2H_6	CH_4	CO	CO_2	$C_{(s)}$	S_2	H_2O	C_4H_{10}	O_2	H_2S	1-C_4H_8	2-C_4H_8	C_3H_6	C_3H_8	C_2H_4	C_2H_6	CH_4	CO	CO_2	$C_{(s)}$	S_2	H_2O
		Catalyst: 2.5% VOx/CS																															
Feed	61.1	28.2	7.8	3.4																													
Product	61.1	19.3	6.8	0.4	0.4	3.6	0.4	4.3	0.0	1.9	0.9	4.0	0.2	0.2	-2.8	0.5	5.6	32	90	13	13	1	11	0	3	2	4	0	0	-3	13	81	
																					[40]	[4]	[36]	[0]	[11]	[5]	[11]	[1]	[<1]	-[8]			
		Catalyst: 5% VOx/CS																															
Feed	60.7	32.0	7.8	3.8																													
Product	60.7	22.2	6.7	0.5	0.1	4.6	0.7	4.0	0.0	1.8	0.9	3.9	0.2	0.1	-3.3	0.5	5.6	31	87	13	14	2	9	0	3	1	3	0	0	-3	1	75	
																					[47]	[7]	[30]	[0]	[9]	[5]	[10]	[1]	[<1]	-[9]			

Appendix 5.9b $C_4H_{10}/H_2S/O_2/N_2$ Reaction over catalysts containing differing amounts of vanadium oxide

Feed ratio: 8:2.5:1 (C_4H_{10}: H_2S: O_2) Contact time: 8 ms Temperature: 1023 K

	Products, mole/100 moles of feed																	Conversion %			Yield % [Selectivity %]												
	N_2	n-C_4H_{10}	H_2S	O_2	H_2	1-C_4H_8	2-C_4H_8	C_3H_6	C_3H_8	C_2H_4	C_2H_6	CH_4	CO	CO_2	$C_{(s)}$	S_2	H_2O	C_4H_{10}	O_2	H_2S	1-C_4H_8	2-C_4H_8	C_3H_6	C_3H_8	C_2H_4	C_2H_6	CH_4	CO	CO_2	$C_{(s)}$	S_2	H_2O
		Catalyst: 2.5% VOx/CS																															
Feed	61.1	28.2	7.8	3.4																													
Product	61.1	4.9	7.7	0.3	2.0	1.9	0.5	13.4	0.0	7.0	4.1	15.8	0.2	0.8	3.8	0.1	4.4	82	2	91	7	2	36	<1	12	7	14	<1	<1	3	2	65	
																					[8]	[2]	[43]	[<1]	[15]	[9]	[17]	<1]	[1]	[4]			
		Catalyst: 5% VOx/CS																															
Feed	60.7	32.0	7.8	3.8																													
Product	60.7	7.7	7.5	0.4	2.1	2.6	0.6	13.3	0.0	6.6	4.2	15.3	0.3	1.0	6.2	0.1	4.2	76	89	2	8	2	31	0	10	7	12	<1	1	5	3	56	
																					[11]	[3]	[41]	[0]	[14]	[9]	[16]	[<1]	[1.3]	[6]			

Appendix 5.10a C_4H_{10}/N_2 Pyrolysis Reaction and the effect of adding H_2S

Catalyst: Crystalline Silica (inert) Contact time: 36 ms Temperature: 923 K

	Products, mole/100 moles of													Conversion %		Yield % [Selectivity %]								
	N_2	n-C_4H_{10}	H_2S	H_2	1-C_4H_8	2-C_4H_8	C_3H_6	C_3H_8	C_2H_4	C_2H_6	CH_4	$C_{(s)}$	S_2	C_4H_{10}	H_2S	1-C_4H_8	2-C_4H_8	C_3H_6	C_3H_8	C_2H_4	C_2H_6	CH_4	$C_{(s)}$	S_2
		Without H_2S																						
Feed	79.0	23.5	0.0																					
Product	79.0	20.5	0.0	0.4	0.3	0.0	0.8	0.0	0.7	0.2	0.8	5.7	0.0	13	0	1 [10]	0 [0]	2 [20]	0 [0]	2 [12]	0 [3]	1 [7]	6 [48]	0
		With H_2S																						
Feed	66.6	29.1	4.9																					
Product	66.6	22.6	4.9	0.4	0.6	0.1	4.0	0.0	1.4	1.3	4.3	1.3	0.0	25	1	2 [9]	0 [1]	10 [42]	0 [0]	2 [10]	2 [9]	4 [15]	1 [5]	<1

Appendix 5.10b C_4H_{10}/N_2 Pyrolysis Reaction and the effect of adding H_2S

Catalyst: Crystalline Silica (inert) Contact time: 36 ms Temperature: 1023 K

	Products, mole/100 moles of fee													Conversion %		Yield % [Selectivity %]								
	N_2	n-C_4H_{10}	H_2S	H_2	1-C_4H_8	2-C_4H_8	C_3H_6	C_3H_8	C_2H_4	C_2H_6	CH_4	$C_{(s)}$	S_2	C_4H_{10}	H_2S	1-C_4H_8	2-C_4H_8	C_3H_6	C_3H_8	C_2H_4	C_2H_6	CH_4	$C_{(s)}$	S_2
		Without H_2S																						
Feed	79.0	23.5	0.0																					
Product	79.0	12.5	0.0	3.0	3.2	0.0	4.4	0.1	6.6	0.8	6.0	-4.1	0.0	47	0	14 [29]	1 [2]	14 [30]	<1 [1]	14 [30]	2 [4]	6 [14]	-4 -[9]	0
		With H_2S																						
Feed	66.6	29.1	4.9																					
Product	66.6	6.7	5.0	2.8	2.5	0.5	13.7	0.0	7.8	4.2	16.8	-3.8	0.0	74	-1	9 [12]	2 [2]	35 [48]	<1 [<1]	13 [18]	7 [10]	14 [20]	-3 -[4]	-1

Appendix 5.11a C_4H_{10}/N_2 Pyrolysis Reaction and the effect of adding H_2S

Catalyst: 5% VOx/CS Contact time: 36 ms Temperature: 923 K

	Products, mole/100 moles of feed													Conversion %		Yield % [Selectivity %]								
	N_2	n-C_4H_{10}	H_2S	H_2	1-C_4H_8	2-C_4H_8	C_3H_6	C_3H_8	C_2H_4	C_2H_6	CH_4	$C_{(s)}$	S_2	C_4H_{10}	H_2S	1-C_4H_8	2-C_4H_8	C_3H_6	C_3H_8	C_2H_4	C_2H_6	CH_4	$C_{(s)}$	S_2
		Without H_2S																						
Feed	72.1	28.2	0.0																					
Product	72.1	24.8	0.0	1.4	1.5	0.2	0.7	0.5	0.6	0.0	0.7	1.5	0.0	12	0	5	1	2	1	1	0	1	1	n/a
																[43]	[7]	[15]	[10]	[9]	[0]	[5]	[11]	
		With H_2S																						
Feed	69.2	24.2	5.7																					
Product	69.2	18.4	5.5	0.1	0.6	0.0	2.6	0.0	0.8	0.9	2.7	7.1	0.1	24	3	2	0	8	0	2	2	3	7	3
																[10]	[0]	[33]	[0]	[7]	[7]	[12]	[31]	

Appendix 5.11b C_4H_{10}/N_2 Pyrolysis Reaction and the effect of adding H_2S

Catalyst: 5% VOx/CS Contact time: 36 ms Temperature: 1023 K

	Products, mole/100 moles of feed													Conversion %		Yield % [Selectivity %]								
	N_2	n-C_4H_{10}	H_2S	H_2	1-C_4H_8	2-C_4H_8	C_3H_6	C_3H_8	C_2H_4	C_2H_6	CH_4	$C_{(s)}$	S_2	C_4H_{10}	H_2S	1-C_4H_8	2-C_4H_8	C_3H_6	C_3H_8	C_2H_4	C_2H_6	CH_4	$C_{(s)}$	S_2
		Without H_2S																						
Feed	72.1	28.2	0.0																					
Product	72.1	14.6	0.0	3.8	3.5	0.0	5.6	0.0	8.0	1.1	7.5	-2.2	0.0	48	0	12	0	15	0	14	2	7	-2	n/a
																[26]	[0]	[31]	[0]	[30]	[4]	[14]	-[4]	
		With H_2S																						
Feed	69.2	24.2	5.7																					
Product	69.2	6.3	5.5	1.7	2.1	0.4	10.4	0.0	5.3	3.3	12.1	1.2	0.1	74	1	9	2	32	0	11	7	12	1	1
																[12]	[2]	[44]	[0]	[15]	[9]	[17]	[2]	

Appendix 5.12a: Comparison of the reaction of propane and butane mixtures in the gas phase and over a catalyst bed.

Temperature: 923 K Feed ratio: 20:3:2 (C_3+C_4: H_2S: O_2) Contact time: 12 ms

	Products, mole/100 moles of feed																		Conversion %					Yield % [Selectivity %]										
	N_2	C_3H_8	C_4H_{10}	H_2S	O_2	H_2	1-C_4H_8	2-C_4H_8	C_3H_6	C_2H_4	C_2H_6	CH_4	CO	CO_2	$C_{(s)}$	SO_2	S_2	H_2O	C_3H_8	C_4H_{10}	C_3+C_4	O_2	H_2S	1-C_4H_8	2-C_4H_8	C_3H_6	C_2H_4	C_2H_6	CH_4	CO	CO_2	$C_{(s)}$	S_2	H_2O
Catalyst: CS																																	
Feed	12.7	14.1	59.6	9.6	6.2																												
Product	12.7	10.5	47.3	7.7	1.7	0.5	4.3	0.5	5.3	2.6	1.1	5.3	0.2	0.0	11.8	1.2	0.4	8.9	25	21	21	73	20	6	1	6	2	1	2	<1	0	4	<1	71
																								[28]	[4]	[27]	[9]	[4]	[9]	[<1]	[0]	[20]		
Catalyst: 2.5% VO_x/CS																																	
Feed	12.9	14.3	58.0	9.3	7.4																												
Product	12.9	8.7	33.6	5.6	1.0	1.0	5.2	0.5	5.2	2.4	1.2	5.5	0.4	1.8	27.0	0.0	1.9	8.8	14	30	29	87	40	7	1	6	2	1	2	<1	1	10	2	60
																								[26]	[3]	[19]	[6]	[3]	[7]	[<1]	[2]	[34]		

Appendix 5.12b: Comparison of the reaction of propane and butane mixtures in the gas phase and over a catalyst bed.

Temperature: 1023 K Feed ratio: 20:3:2 (C_3+C_4: H_2S: O_2) Contact time: 12 ms

	Products, mole/100 moles of feed																		Conversion %					Yield % [Selectivity %]										
	N_2	C_3H_8	C_4H_{10}	H_2S	O_2	H_2	1-C_4H_8	2-C_4H_8	C_3H_6	C_2H_4	C_2H_6	CH_4	CO	CO_2	$C_{(s)}$	SO_2	S_2	H_2O	C_3H_8	C_4H_{10}	C_3+C_4	O_2	H_2S	1-C_4H_8	2-C_4H_8	C_3H_6	C_2H_4	C_2H_6	CH_4	CO	CO_2	$C_{(s)}$	S_2	H_2O
Catalyst: CS																																	
Feed	12.7	14.1	59.6	9.6	6.2																												
Product	12.7	6.6	19.2	9.5	1.0	5.5	5.2	0.9	25.4	16.0	8.6	33.0	0.4	1.9	-0.5	1.1	-0.5	6.3	53	68	66	84	1	7	1	27	11	6	12	<1	1	0	-10	51
																								[11]	[2]	[41]	[17]	[9]	[18]	[<1]	[1]	[0]		
Catalyst: 2.5% VOx/CS																																	
Feed	12.9	14.3	58.0	9.3	7.4																												
Product	12.9	4.3	10.5	4.3	1.2	6.0	5.2	0.9	24.2	16.1	8.4	33.2	0.5	2.0	20.3	0.0	2.5	7.6	70	72	72	83	54	7	1	26	12	6	12	<1	1	7	54	52
																								[10]	[2]	[36]	[16]	[8]	[16]	[<1]	[1]	[10]		

Appendix 6.1a: Potential energy surface for the reaction between i-C_4H_9• + O_2

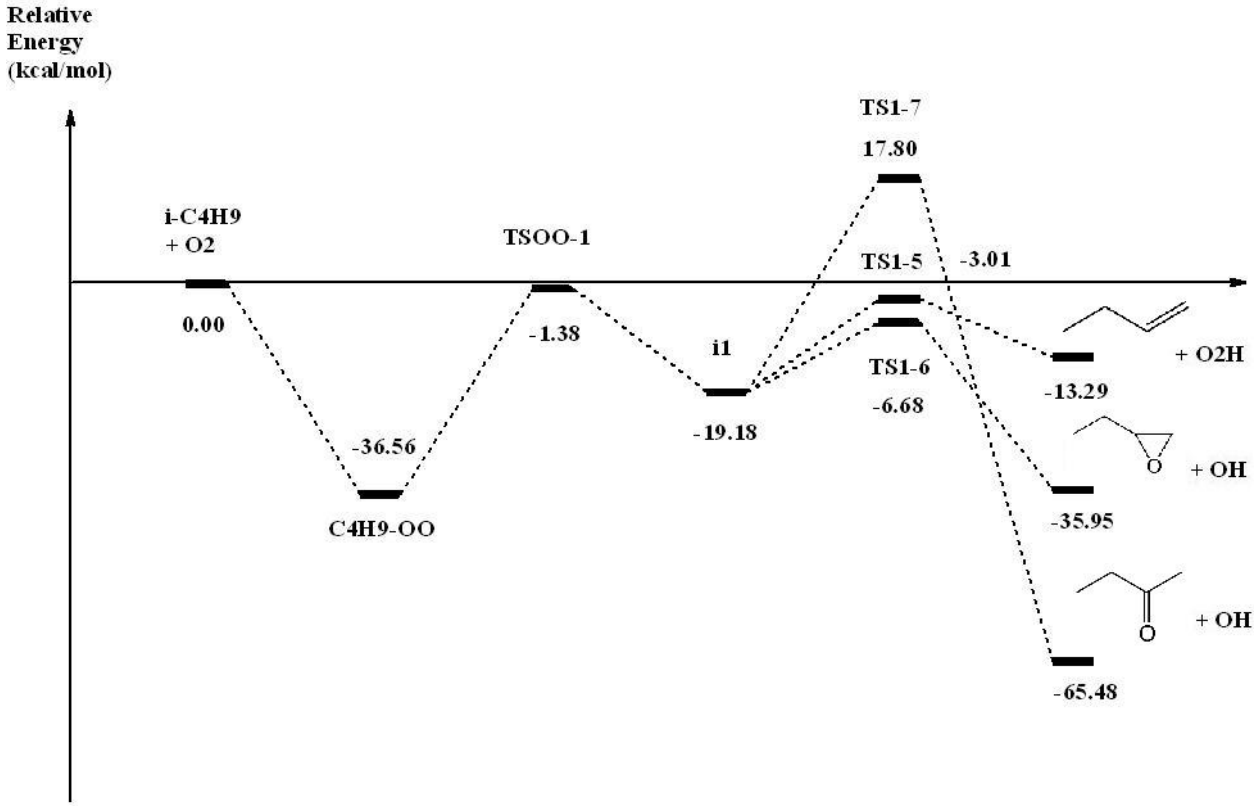

Appendix 6.1b: Potential energy surface for the reaction between i-C_4H_9• + O_2

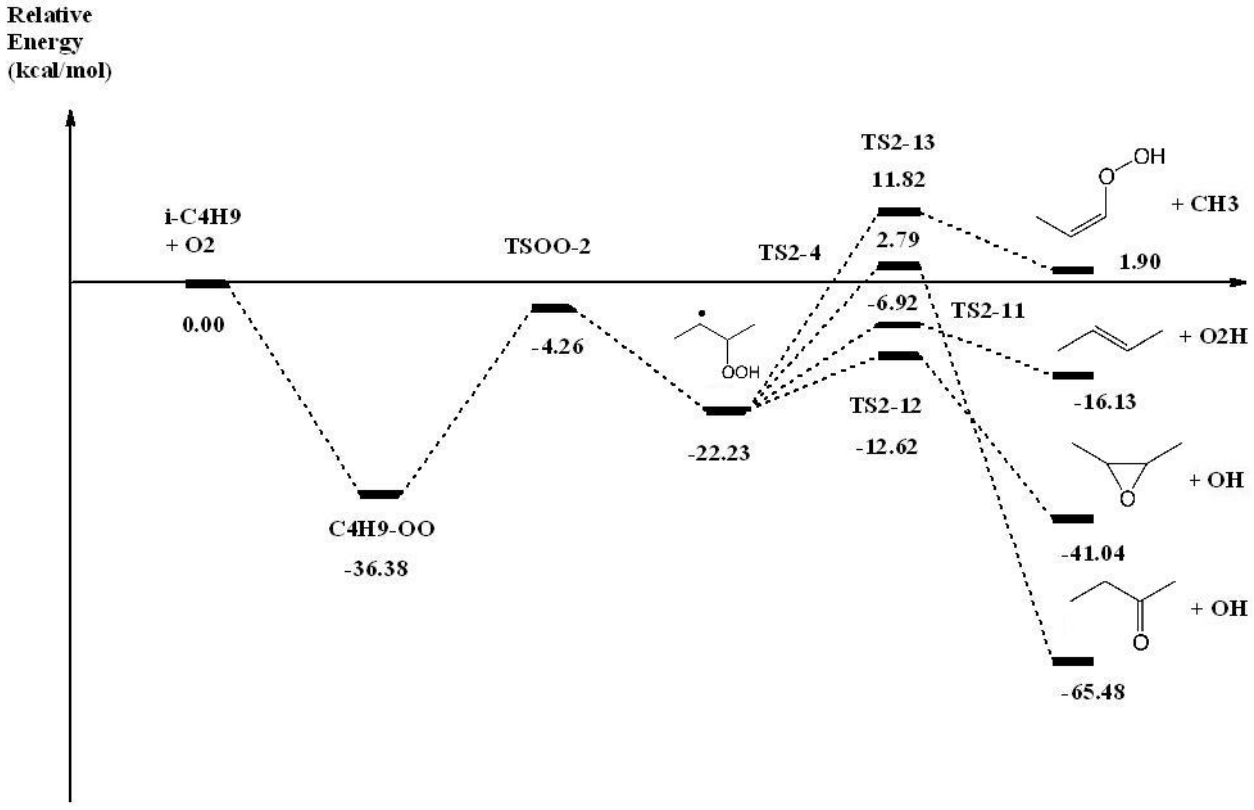

Appendix 6.1c: Potential energy surface for the reaction between i-C_4H_9• + O_2

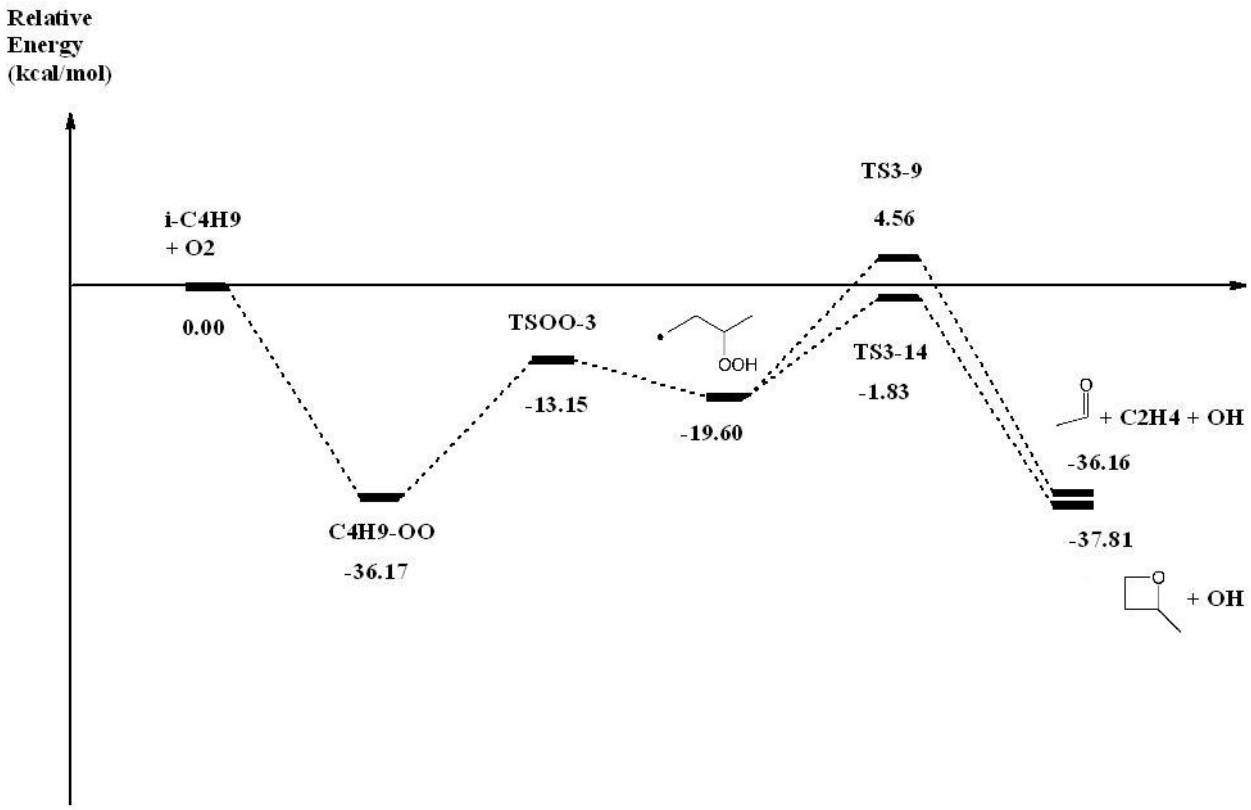

Note: The calculations as well as the rest of the energy profiles shown in this chapter were carried out by Dr J. Lo (Alberta Sulphur Research Ltd) using the CBS-QB3 method which is good for predicting thermodynamic quantities such as reaction energies. The mean absolute deviation (MAD) of this method from experimental values is usually about 1-1.5 kcal/mol.

Appendix 6.2a: Potential energy surface for the reaction between i-C_4H_9• + S_2

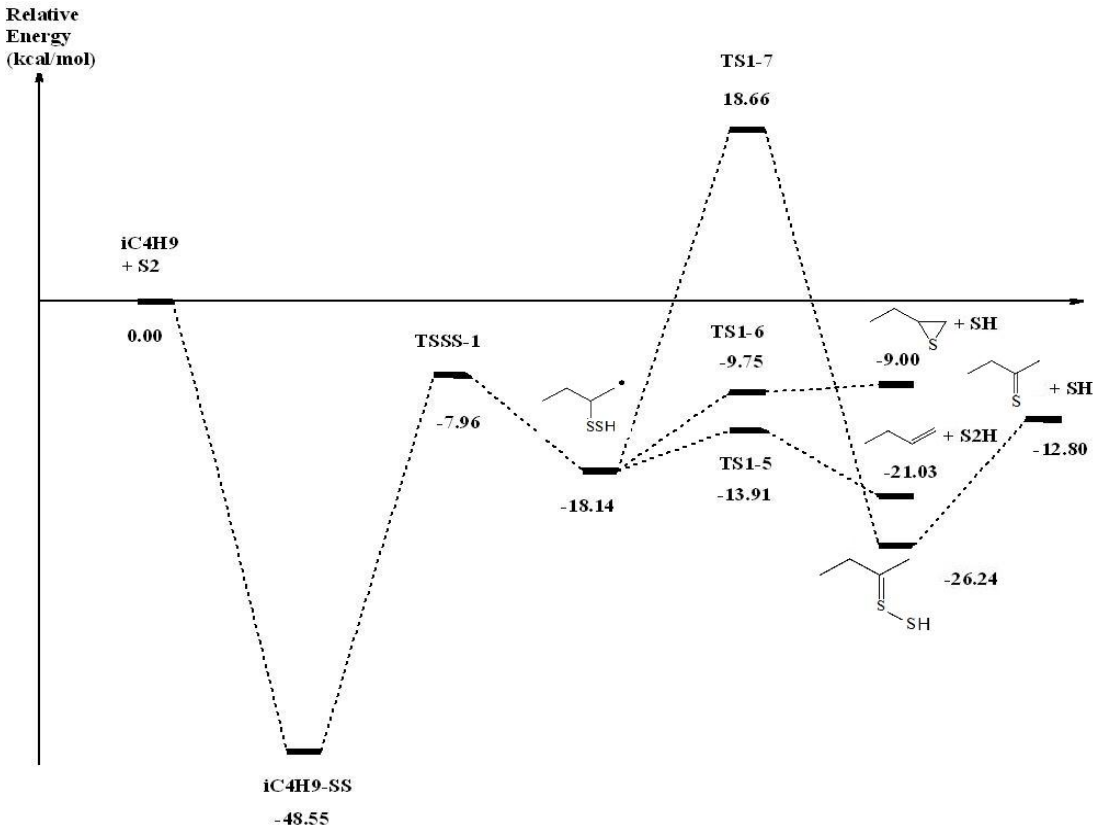

Appendix 6.2b: Potential energy surface for the reaction between i-C_4H_9• + S_2

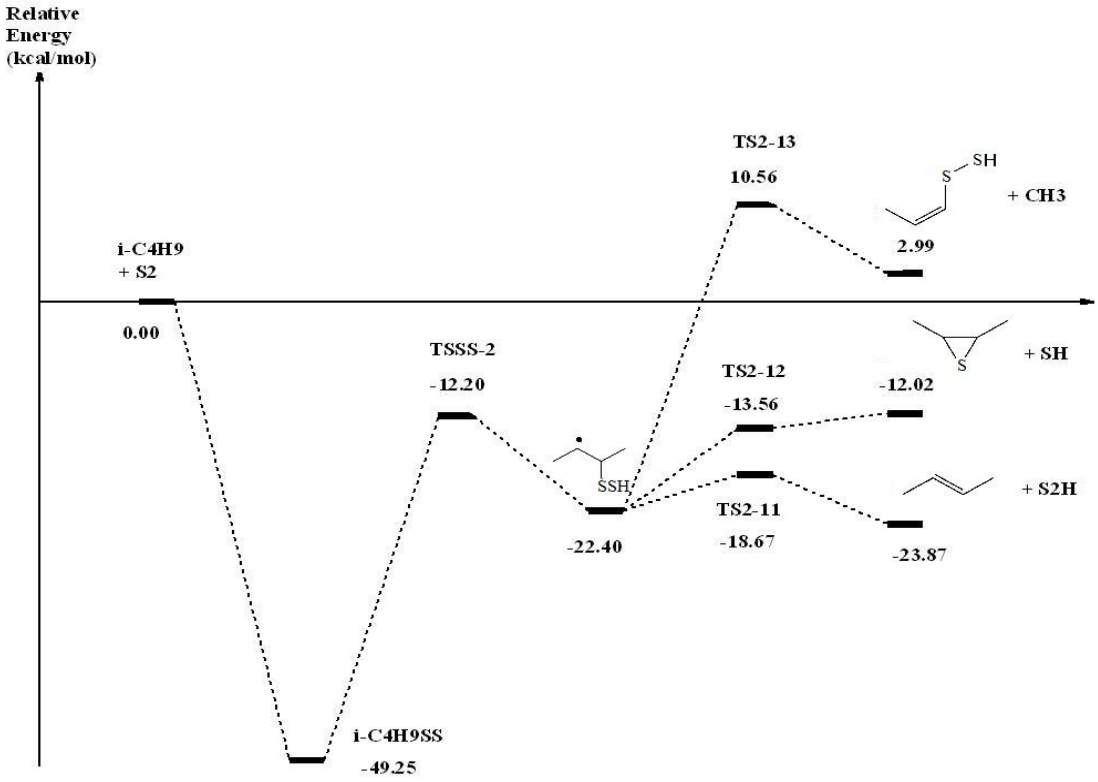

Appendix 6.2c: Potential energy surface for the reaction between i-C_4H_9• + S_2

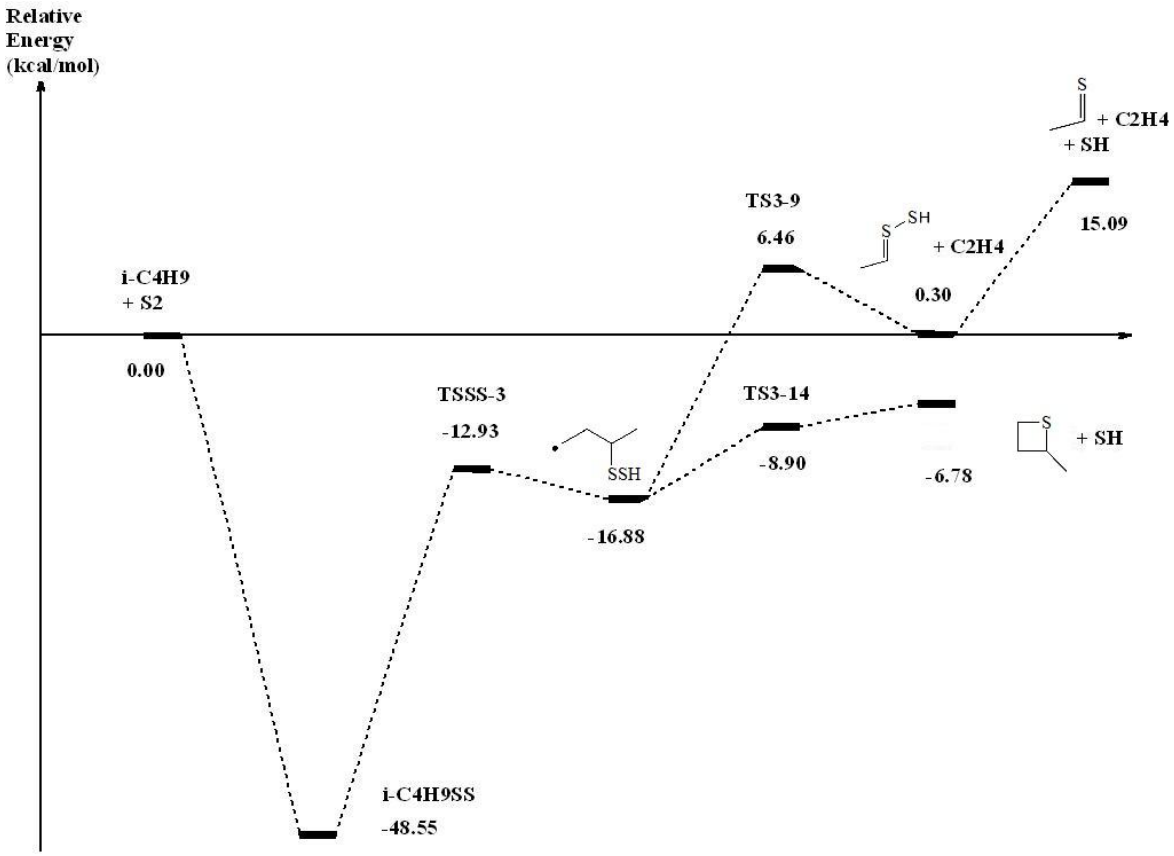

Appendix 6.3a: Potential energy surface for the reaction between n-C_4H_9• + O_2

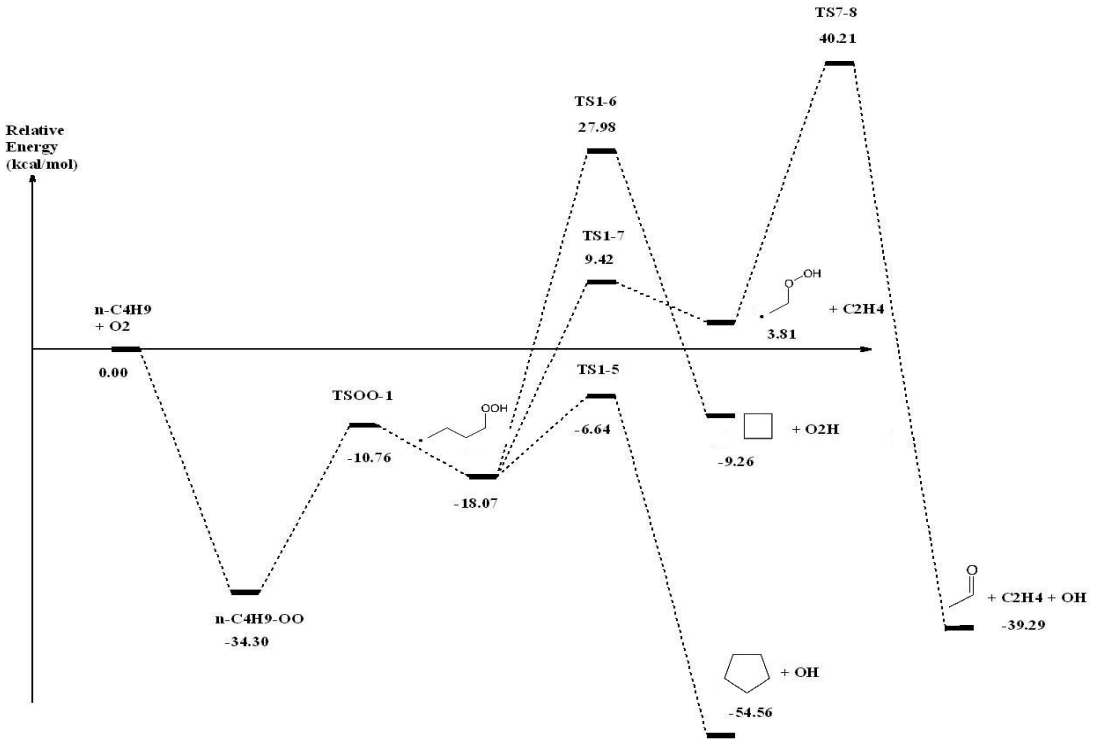

Appendix 6.3b: Potential energy surface for the reaction between n-C_4H_9• + O_2

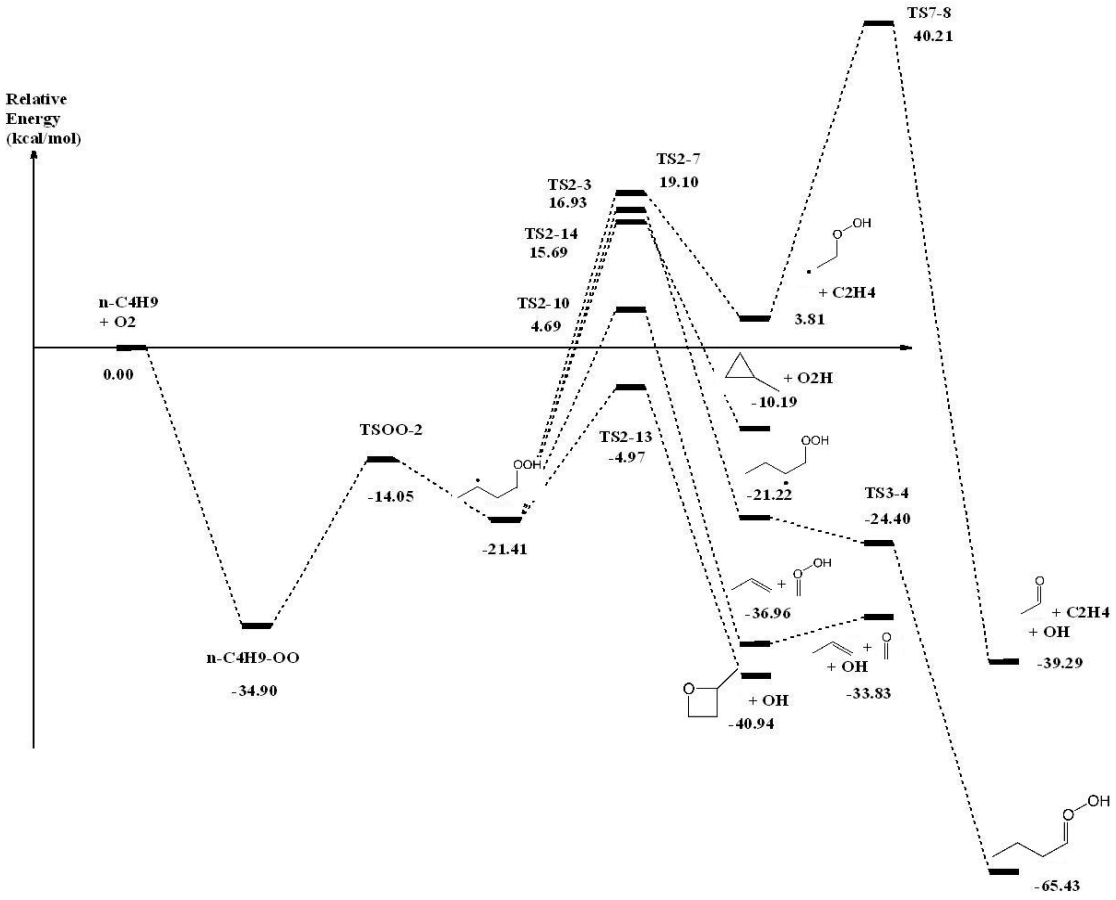

Appendix 6.3c: Potential energy surface for the reaction between n-C_4H_9• + O_2

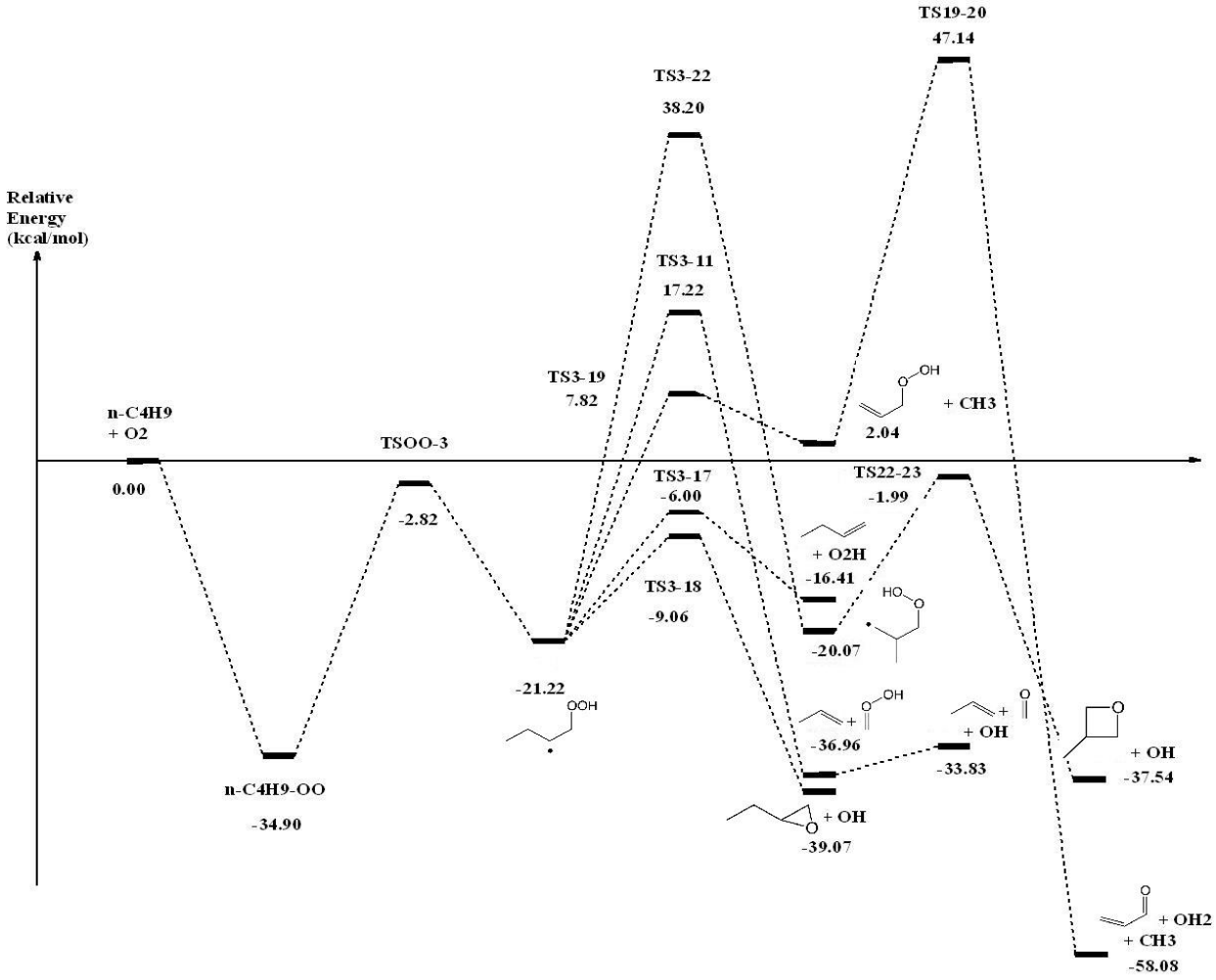

Appendix 6.3d: Potential energy surface for the reaction between n-C_4H_9• + O_2

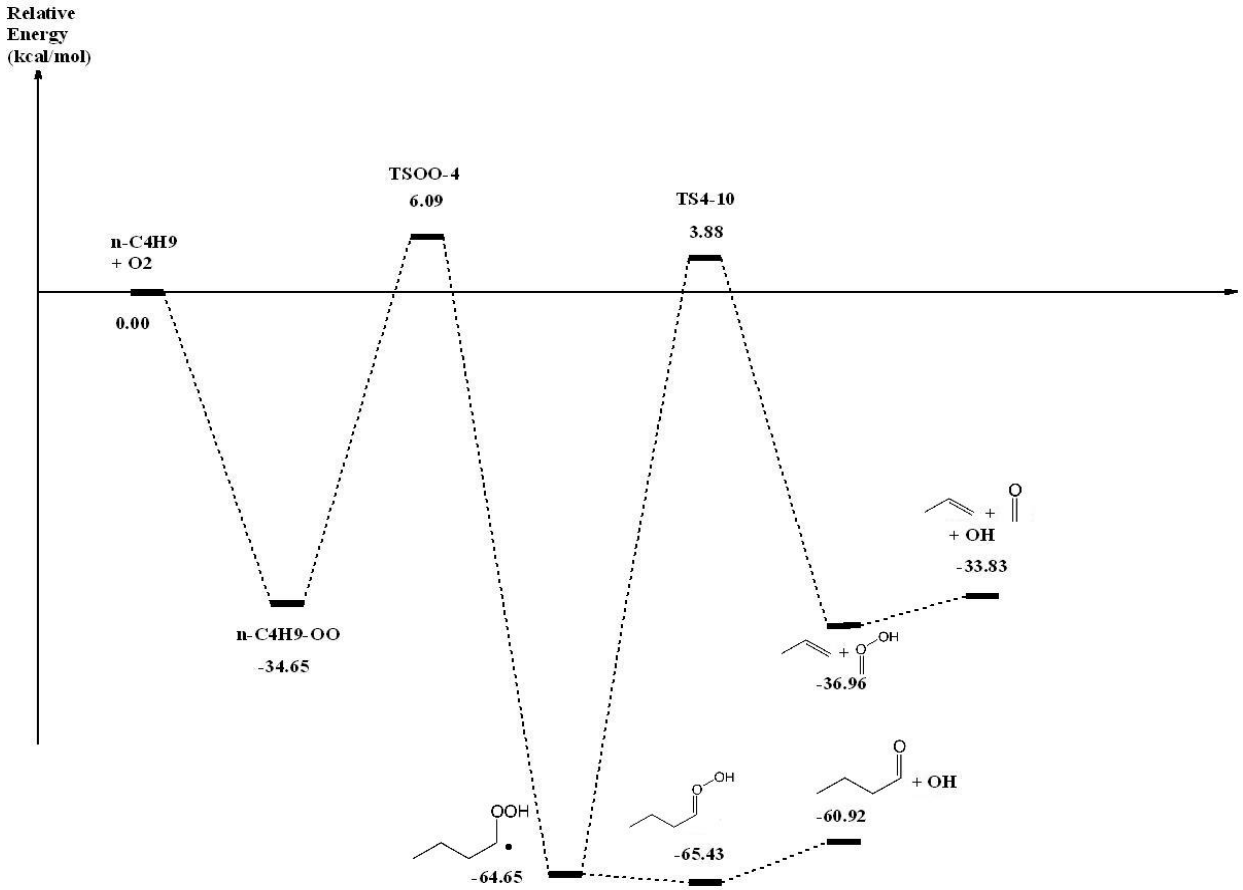

Appendix 6.4a: Potential energy surface for the reaction between n-C_4H_9• + S_2

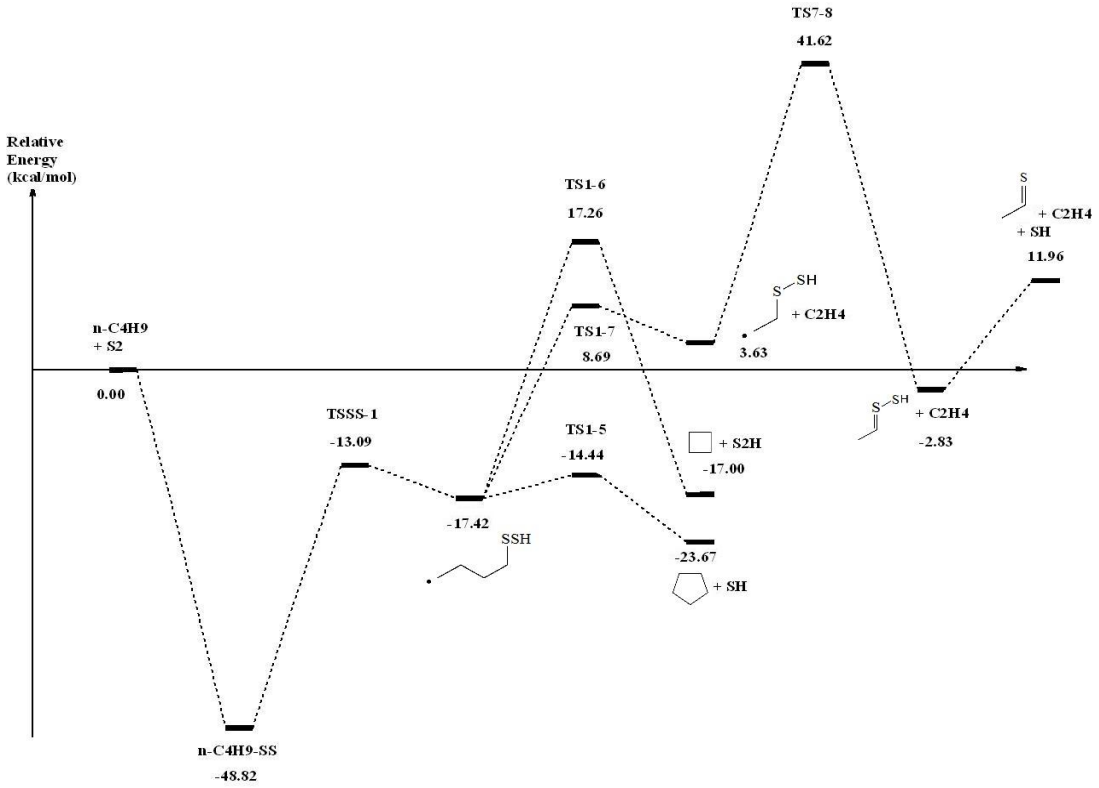

Appendix 6.4b: Potential energy surface for the reaction between n-C_4H_9• + S_2

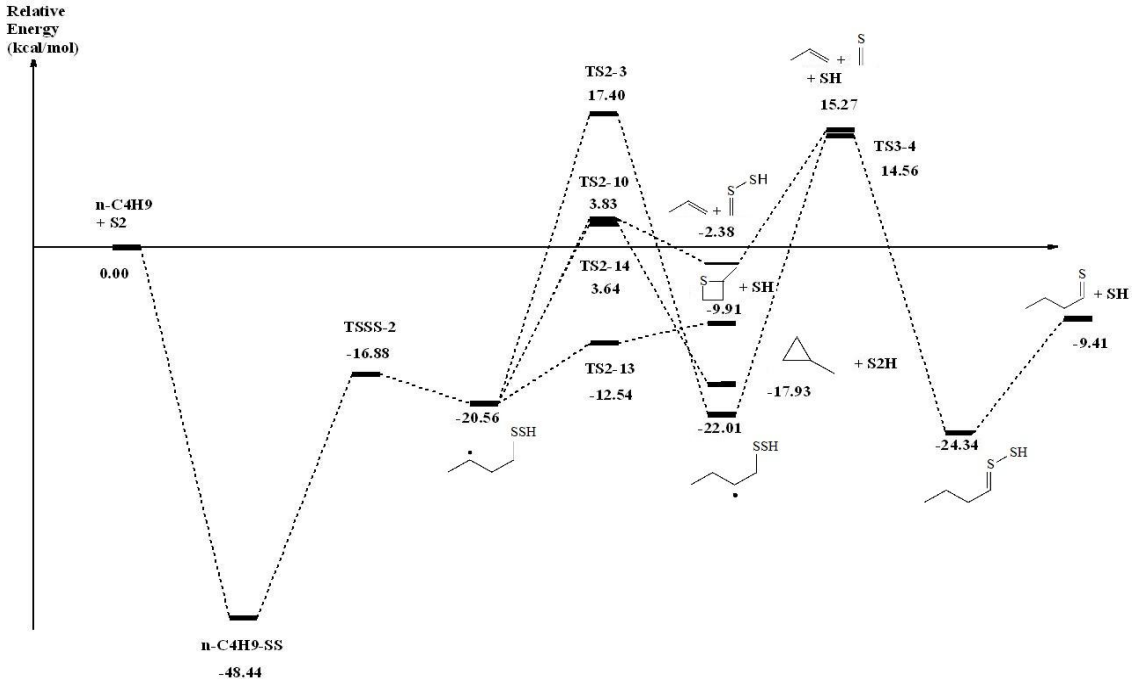

Appendix 6.4c: Potential energy surface for the reaction between n-C_4H_9• + S_2

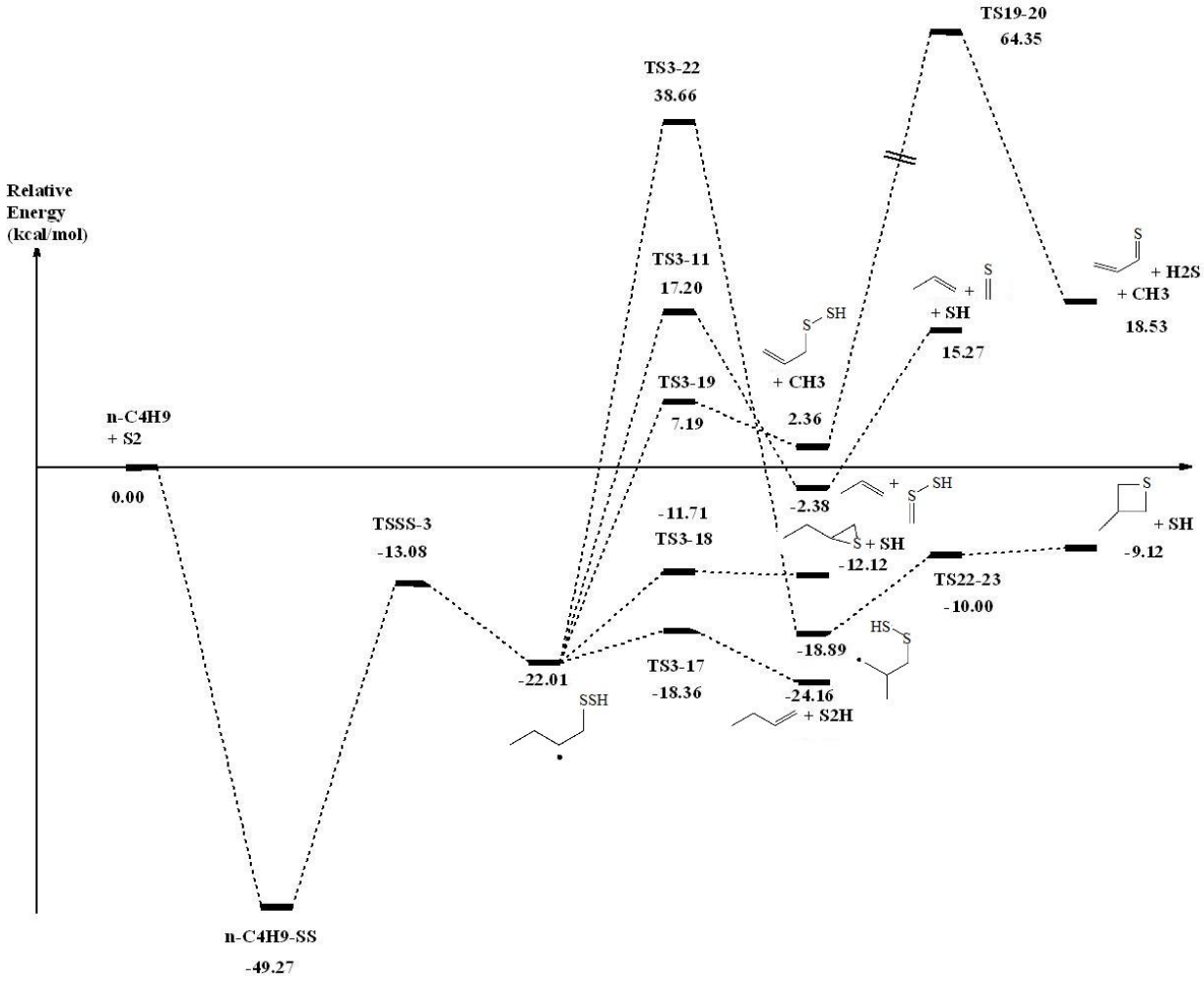

Appendix 6.4d: Potential energy surface for the reaction between n-C_4H_9• + S_2

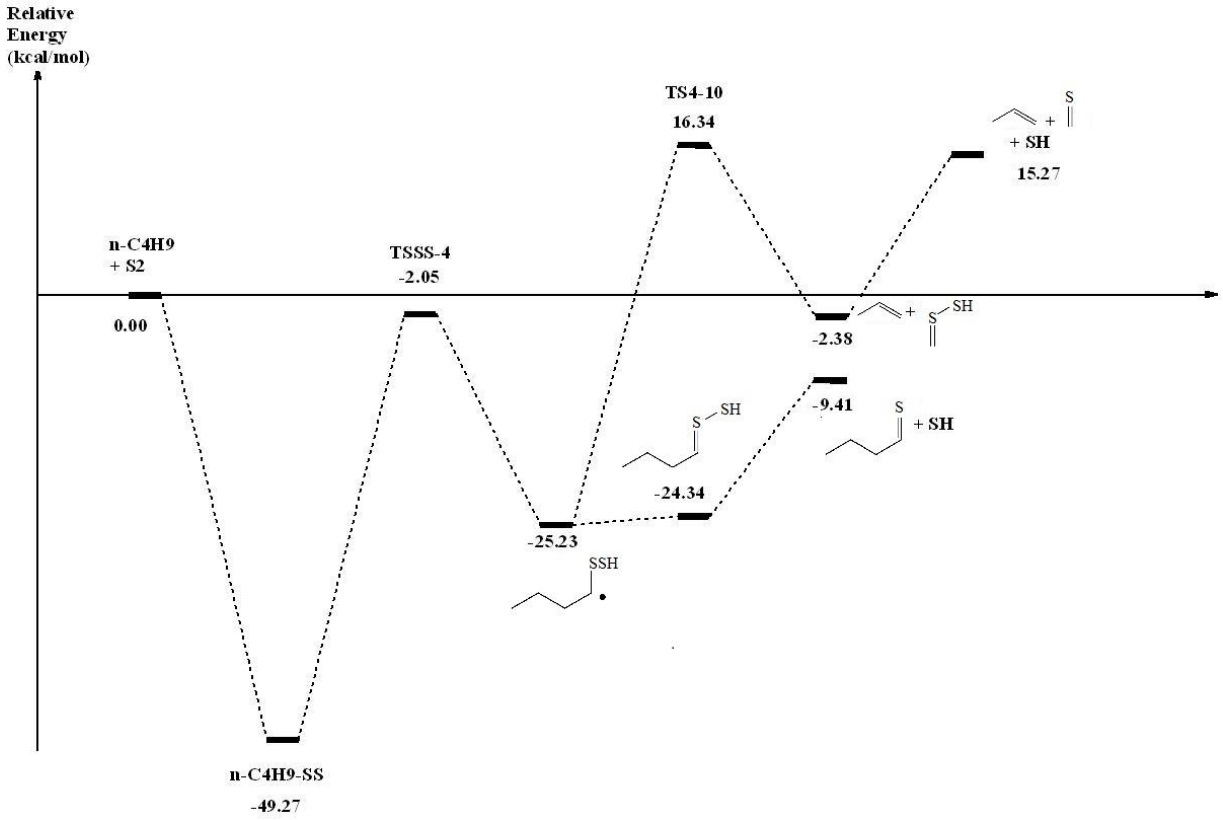

Appendix 6.5a: Structure of transition states as labelled in the potential energy surfaces in Figure 6.8.

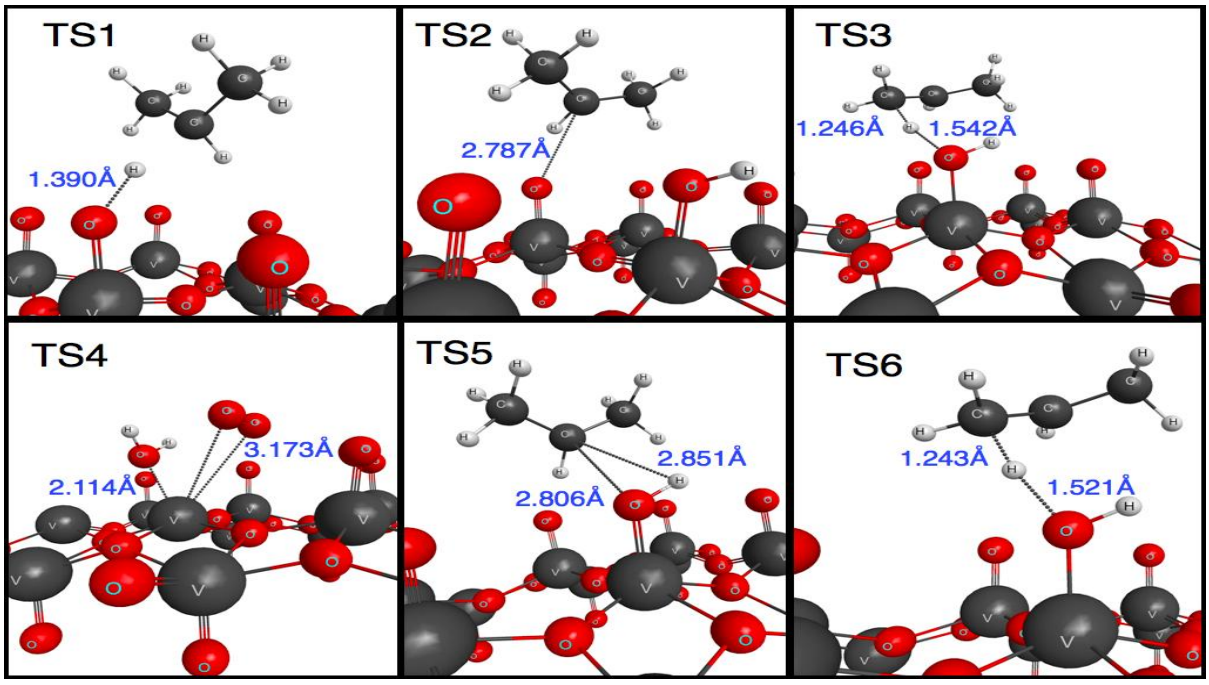

Appendix 6.5b: Structure of transition states as labelled in the potential energy surfaces in Figure 6.9.

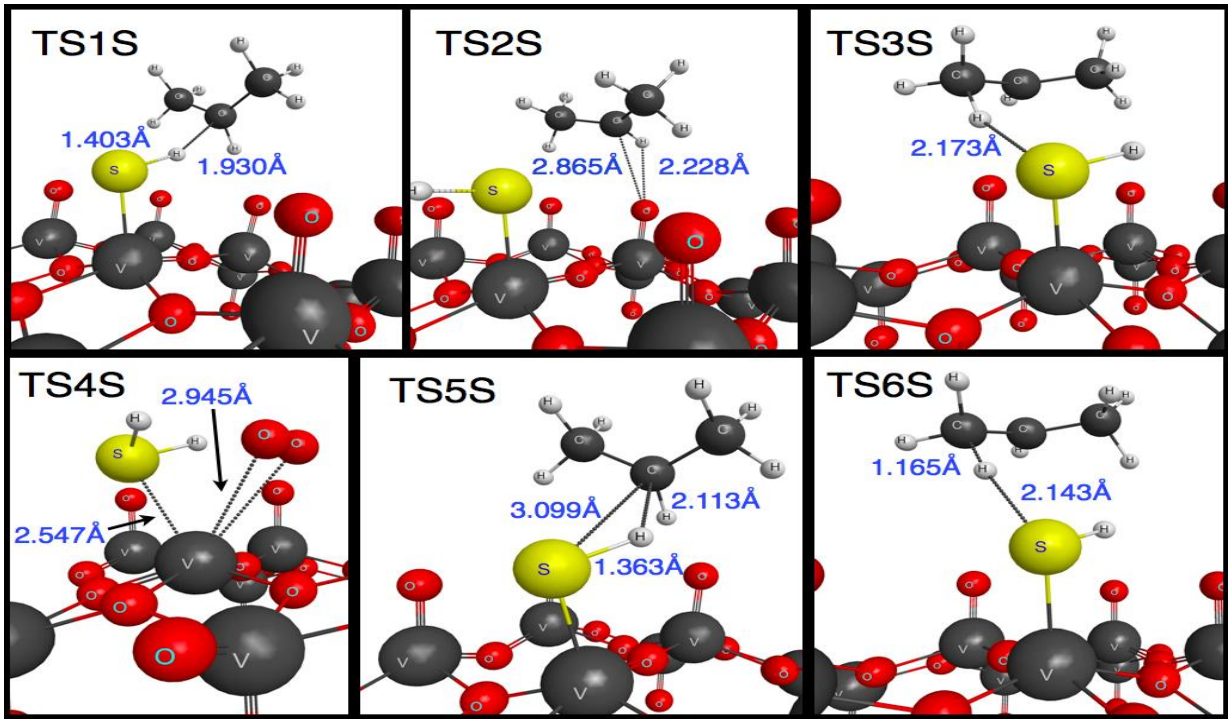

Appendix 6.5c: Mechanism of phase 1 of the ODH of propane on a vanadyl site and structures of species as labelled in the potential energy surfaces in Figures 6.8 and 6.9.